Long-lasting effects of operant conditioning and cocaine on D1 pyramidal neurons in prefrontal cortex and on the D1 and D2 striatal neurons mRNAs

Enrica Montalban

Thèse de doctorat de l'Université Pierre et Marie Curie

Ecole doctorale Cerveau Cognition Comportement

Long-lasting effects of operant conditioning and cocaine on D1 pyramidal neurons in prefrontal cortex and on the D1 and D2 striatal neurons mRNAs

Présentée par

Enrica Montalban

Pour obtenir le grade de

Docteur de l'Université Pierre et Marie Curie

Soutenue le 22 septembre 2016

Devant le jury composé de

Dr. Jocelyne CABOCHE :	Présidente
Dr. Michael R KREUTZ :	Rapporteur
Dr. Miguel Angel MARTIN SANCHEZ :	Rapporteur
Dr. Alban de KERCHOVE D'EXAERDE:	Examinateur
Dr. Emmanuel VALJENT	Examinateur
Dr. Jean-Antoine GIRAULT	Directeur de thèse

- Acknowledgments -

Dear Jean-Antoine, it has been a long but instructive journey untill here. I should insert another long table to list all the reasons that I have to thank you. Thanks for the possibility of joining our lab. Thanks for having "obliged" me to discuss every single experiment that I thought to do. I learned the importance of having a clear idea of what you wish to do, as well as the importance of knowing how to defend it. I also learned how fundamental is to be rigorous and so to be patient. The work that you did on me during these 4 years, and the work that you have done for my thesis in this last month is unvaluable. Even if there is always something new to learn to do this job properly, I'm sure that now I have the good imprinting for the future. Thank you.

Cher Denis, thank you, thank you for having found always the time to discuss and give me real precious advises. Thank you very much for being always direct in the comments on my work as well as on my experiments. Not less important, I really have to thank you for being always that kind, generous, and accessible in the everyday lab life.

I would like to thank, Paul Grennegard. The collaboration with the Greengard's lab was foundamental to realizationon of my thesis work. Thank you as well for having supported me, and make me feel as part of the lab.

I would like to thank all the members of my thesis comeetee, Jocelyne Caboche, Alban de Kerchove, Emmanuel Valjent, Miquel Martinez, and Michael Kreutz for accepting to my jury and to rewiev my work.

Michael Kreutz, I really have several reasons to thank you. First thank you for being part of my thesis commetee, thank you for the scientific and personal adivices that you gave me during the last years, and most of all thank you and Christina Spilker for the amazing work that you did with the NPLAST. You really took care of us, and it has been a unique, formative, challenging, and excellent experience. Thank you.

Dear Miquel Martinez, thank you for having accept to be part of my thesis, thank you for your patience, and most of all, for all the help that you an Emmanuel gave me in setting up the operant protocol. You can see now how important was for my work.

#5thfloor. Lieng je commence par toi, parfois trouver une langue commun n'a pas été facile, mais on y est arrivés. Merci pour avoir essayé et réussi a te mettre sur ma longueur d'onde et pour le soutien et surtout pour tout ce que on a produit ensemble. Sophie, t'es mon daily rappel au calme. Comment te remercier pour ça ? Merci aussi pour ton amitié sincère et pour ta confiance. Moshi moshi Yuki, when you arrived « madreusement » you found me a bit stressed but we made a good team! Thank for having brought a little japanise organization in my lab-life, the help and the good time. Yukari, welcome on board, you'll be amazing, I know it already! Merci Nico, merci pour tes conseils, ta

délicatesse et ton amitié, tu sais très bien à quel niveau elle est importante pour moi. Gress, merci Gress pour tes précieux conseils et pour toutes les fois où nous avons parlé de littérature. Un jour tu m'as dis « ah si on pouvait parler toujours de Dante » ; on ne peut pas mais si tu savais quel bonheur discuter avec toi ! Assu, Alb, Renata, s'il y a quelqu'un qui m'a aidé, fait grandir, été de support inconditionnel pendant tout ce trajet, c'est vous. Je vous estime mes amis.

Grazie mia cara famiglia. Se son stata sempre certa di questo lungo percorso è solo grazie a voi. L'educazione che mi avete dato, con i suoi principi di rispetto e di impegno è ancora ciò di cui vado più fiera.

Grazie Bruschi, abbiamo cominciato insieme e finiamo insieme, è stato bello e daje forte!
Gli amici della piccolina, se se proprio con voi due ce l'ho. We performed un'amicizia talmente fondamentale a tutto questo! Grazie!

Mameli e Marinella, vado corta, grazie per l'aiuto il sostegno e per i vostri occhi attenti. Mameli, fattelo dire a che punto sei sempre stato di ispirazione. And thanks the Mameli's Salva, Anna, Kri and Frank. Love you guys, the time with you has been amazing.

Angela, compagna di avventure, mia amica sincera, le notti a scrivere insieme, irripagabili, come lo è la tua generosità e quella del Sindaco !!! Come lo è quella della mia bella Vale, arrivata nel momento più inteso, tra le più presenti in questo momento, grazie di tutto il sostegno Vale.

Martin, quel bonheur ce Martin ! merci pour ? Attends, je commence la liste : soirée écriture, balades nocturnes, soutiens, relectures… et ah ouuuuais, amitié. T'es genial Martin, Love you !

Jean-Pierre merci pour tous les moments d'éternel retour, le boulot, les nuits blanches, ton amitié, merci pour être ici aujourd'hui. Et avec toi je remercie aussi mes deux meilleures copines, Manue et Karima. Pour vos soutiens et générosité sans limites, pour vos âmes gentils… Ah mes belles, j'ai une dernier question : mais qu'est-ce que c'est ça??

Carmen and Mesh, this frienship with you, is clearly one of the most important achivment of Paris. I love you girls, thank you for all you gave me and all you are.

Benoit, à toi mes derniers mots. Merci Benoit, pour cette amitié qui m'est si chère, pour tout ce qu'on a attendu ensemble. Je n'irai pas plus lointaine, tu sais déjà tout ce qu'il faut savoir.

- Summary -

Dopamine (DA) controls movement execution, action selection, and incentive learning by regulating the activity and plasticity of corticostriatal transmission. Long-term modifications require changes in gene transcription. The aim of this work is to study the changes in transcriptions following an operant learning protocol or mimicking stimulation of the reward system with cocaine.

The largest neuronal population of the striatum is comprised of medium-size spiny striatal projection neurons (SPNs), which can be divided into two different populations based on the expression of the D1 or D2 DA receptor. Although these two populations share many morphological characteristics and functional properties, they participate in distinct pathways, the direct pathway for D1-SPNs and indirect pathway for D2-SPNs, which have opposite functional effects on their target regions. Therefore it is crucial to distinguish responses in the two populations.

To do so, we used transgenic mice that express a tagged ribosomal protein (L10a-EGFP) under control of the D1 or D2 receptor promoter to isolate currently translated mRNA and nuclei from each population of SPNs, as well as from D1 pyramidal neurons of the prefrontal cortex. following passive stimulation of the reward system (chronic treatment with cocaine) and active recruitment of the reward system (operant learning for food). For the latter, we developed an operant conditioning protocol in which mildly food-deprived mice learned to nose poke to obtain either regular food or highly palatable food. The results in trained mice were compared to yoked controls which receive the same food but non-contingently.

The first part of this work was dedicated to the comparison of the basal gene expression in the different neuronal populations characterized by the expression of D1 or D2 receptors and their regional localization in the ventral striatum (nucleus accumbens), dorsal striatum, or prefrontal cortex. We thus identified several hundreds of differentially expressed mRNA which provide a precise characterization of the cellular and regional differences in dopaminoceptive neurons.

In the second part, we characterized the changes induced in each neuronal population by a 1-week exposure to cocaine. In the third part, the pattern of gene alterations in each condition and neuronal population are currently being analyzed and compared to other parameters including morphological alteration of spines.

BAC	Bacterial artificial chromosome
BACTRAP	Bacterial artificial chromosome translating ribosome affinity purification
cAMP	Cyclic AMP
CBR1	Cannabinoid receptor 1
cCOC	Chronic cocaine
cSAL	Chronic saline
D1R	Dopamine receptor 1
D2R	Dopamine receptor 2
DA	Dopamine
DS	Dorsal striatum
FACS	Fluorescence activated sorting
GABA	Gamma-Aminobutyric acid
GAD67	Glutamate decarboxilase
GPe	Globus pallidus external
GPi	Globus pallidus internal
LCM	Laser capture microdissection
LHA	Lateral hypothalamus
MCH	Melanin concentrating hormone
mHP	Master highly palliatable
MSH	Melanocortin 1
MSN	Medium sized spiny neurons
mST	Master standard
NAc	Nucleus accumbens
Ncdn	Neurochondrin
NMDA	N-Methyl-D-Aspartate
ORX	Orexin
PFC	Prefrontal cortex
PGE2	Prostaglandin E2
PKA	Protein Kinase A
PYR	Pyramidal
RT-PCR	Real-Time Polymerase Chain reaction
SEQ	Sequencing

SNc	Substantia nigra pars compacta
SNr	Substantia nigra pars reticulata
SPN	Spiny projection neurons
STN	Subthalamic nucleus
WT	Wild-Type
yHP	Yoked highly palatable
yST	Yoked standard

- Bibliographic introduction -

- Chapter 1 -

The Dopamine Signalling

1.1 Dopamine

Dopamine (DA) is a molecule that belongs to the catecholamine family and plays important roles in the brain as well as in rest of the body. In the nervous system, DA acts as neurotransmitter by regulating the activation of the dopamine receptors, and affecting the neural plasticity of several types of neurons. Dopamine signalling within its different circuit is associated with key mechanisms such as locomotor activity or goal-directed behaviours. The main dopaminergic cell groups are located in ventral mesencephalic tegmentum and project to the more anterior part of the brain via the medial forebrain bundle. Based on the localisation of the dopaminergic cells it is possible to distinguish two principal populations of DA neurons that form a gradient of projections to different areas of the brain: the DA cells of the substantia nigra *pars compacta* (SNc, A9) that principally project to the striatum via the nigro-striatal system, and the DA cells in the ventral tegmental area (VTA, A10) that project to the nucleus accumbens (NAc) and olfactory tubercle by the mesolimbic system, and to the amygdala, hippocampus and prefrontal cortex (PFC) via mesocortical system. The different dopaminergic projections are implicated in the regulation of different mechanisms that are completely dependent of the receiving area. The nigrostriatal circuit (A9>A10) has been traditionally implicated in the regulation of motor function (Graybiel et al. 1994)(Graybiel et al. 1994) and its deregulation results in motor-related disease such as Parkinson's disease (PD). The mesolimbic circuit (A10>A9) is associated with goal directed behaviours (Wise & Rompre 1989) and motivation, and high jacking this system results in different forms of addiction. Finally the mesocortical circuit is mostly associated with higher cognitive functions such as learning and memory. A third of group of DA cells is found at the level of the hypothalamus. The cells in this area project to the pituitary gland where DA inhibits the prolactin secretion, and this circuit is associated with important process such as pregnancy or nurturing behaviour. This pathway hasn't been investigated in the present work; therefore it will be not further discussed.

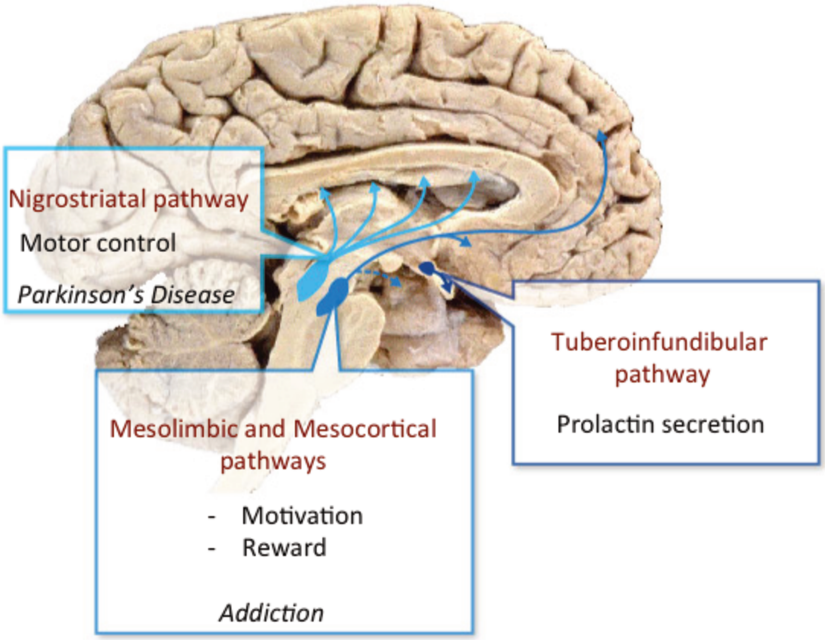

Figure 1: **Schematic representation of the nigrostriatal, mesocorticolimbic and tuberoinfundibular circuits.** The nigrostriatal pathway transmits dopamine from the SNc to the dorsal striatum. Mesocorticolimbic projections are divided in the mesolimbic pathway that transmits dopamine from the VTA to the nucleus accumbens, and the mesocortical pathway, implicated in the DA transmission from the VTA to the frontal cortex. DA cells from the tuberoinfundibular pathway arises the hypothalamus and project to the pituitary gland.

1.2.1 Dopamine receptors

The DA's actions are mediated by 5 different subtypes of DA receptors: D1, D2, D3, D4 and D5. All these receptors are G-protein coupled (GPCRs) referred to as metabotropic receptors. The first DA receptors where identified in in 1971 (Kebabian & Greengard 1971). Spano and collaborators discovered two different subtypes of receptors that were lately classified in D1 or D2 depending on their capacity of activate or inhibits the adenylyl cyclase (AC) (Spano et al. 1978; Stoof & Kebabian 1981). AC is the enzyme converting adenosine triphosphate (ATP) into cyclic adenylate monophosphate (cAMP). The principal adenylyl cyclase isoform in the striatum is AC5 (Lee et al. 2002).

The stimulatory (for D1) or inhibitory (for D2) activity of the dopamine receptors is associated with the expression of one of the two different Gα subunits: the

stimulatory ($G\alpha_s$) or inhibitory ($G\alpha_i$) subunit. In striatal neurons, the stimulatory subunit is the Gα-olf isoform (Hervé et al. 1993; Zhuang et al. 2000; Corvol et al. 2001). Gα-olf mediates the coupling of D1 receptors to the AC and is coded by an independent gene (Corvol et al. 2001). The activation of the receptor via DA stimulation results in the detachment of the Gα subunit from the β and γ subunits. Gαs/olf exerts a positive effect on AC and leads to production of cAMP, whereas Gαi/o inhibits AC and decreases cAMP production (Albert et al. 1990). In the striatum, the activation of D1Rs leads to the Golf-mediated stimulation of adenylyl cyclase. Adenylyl cyclase catalyzes the conversion of ATP to cAMP, which binds to the regulatory subunits of the PKA holoenzyme to disinhibit the catalytic subunits. The activation of cAMP signalling promotes transmission trough the α-amino-3-hydroxyl-5-methyl-4-isoxazole-propionate (AMPA) and *N*-methyl-D-aspartate (NMDA) glutamate receptors (Surmeier et al. 1995; Blank et al. 1997; Snyder et al. 1998). The final output of D1R activation is to elevate the ability of sustained release of glutamate to promote the excitability of the neurons carrying the D1 receptor (Surmeier et al., 2007). In striatal neurons, cAMP is degraded by several phosphodiesterases, including PDE1B and PDE10A, which are highly enriched in medium -sized spiny neurons (Fujishige et al. 1999; Polli & Kincaid 1994) where they play key role in regulating cAMP signalling (Nishi et al. 2008). As mentioned above, the action of the activation of the D2R is coupled with the Gi/o-mediated inhibition of adenylyl cyclase, which decreases cAMP synthesis (Stoof & Kebabian 1981). The decrease of cAMP synthesis will in turn affect the PKA substrates phosphorylation. In addition D2R activation is able to regulate the L-type Ca^{2+} currents trough Ca^{2+} channels (Hernandez-Lopez et al. 2000) and activate K^+ channels (Wickman et al. 1994; Kuzhikandathil et al. 1998; Hopf et al. 2003). The coordinated modulation of ion channels exerted by D2R via activation of Gi/o protein leads to a reduced responsiveness of MSNs to glutamate, and therefore reduced excitability (Surmeier 2007).

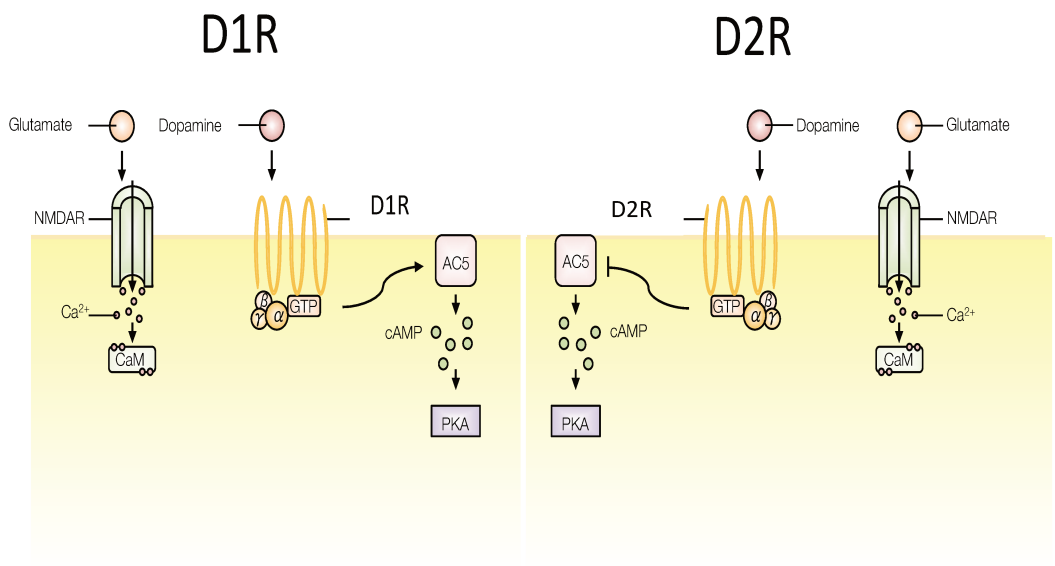

Figure 2: **DA Signalling through D1 and D2 striatal receptor.** DA acts in a bidirectional manner whereby it exerts stimulatory biochemical effects via D1 receptors and inhibitory biochemical effects via D2 receptors. D1 receptors activate adenylyl cyclase AC5 through $G\alpha_{i/o}$, consequently activating PKA. D2 receptors inhibit AC5 through $G\alpha_{i/o}$ thereby inhibiting PKA.

Distribution of the DA receptors

Several studies have shown an enrichment of D1 and D2 receptor with the striatum. In addition, mRNAs from D1Rs have been detected in the prefrontal cortex (PFC) and limbic system, hypothalamus, and thalamus (Dearry *et al.*, 1990; Fremeau *et al.*, 1991; Weiner *et al.*, 1991). D5Rs are concentrated in the hippocampus and entorhinal cortex with very low expression in the striatum.

D2R are expressed in the olfactory tubercle, SNc and in the VTA, where they are expressed by dopaminergic neurons (Meador-Woodruff et al., 1989; Weiner et al., 1991). In SPNs D1 and D2 receptors are mostly expressed post-synaptically on both dendrites and spines (Huang et al., 1992; Levey et al., 1993).). D2Rs are also found in axons terminals forming symmetrical, rather than asymmetrical synapses (Hersch et al., 1995). D2Rs have a high affinity for DA and are tonically activated by low basal concentrations of DA in the extracellular space, whereas D1Rs are thought to be stimulated following burst firing of DA neurons which is more efficient to release DA (Grace, 1991). Importantly, D2Rs can be also detected at the pre-synaptic level

on dopaminergic nerve terminals, where they are involved in the regulation of the DA synthesis and release (Jaber et al., 1996).

- Chapter 2 -

The Basal Ganglia

2.1 Anatomy of the basal ganglia

The basal ganglia (BG) are a set of interconnected deep forebrain nuclei that comprise the striatum and the pallidum. The subthalamic nucleus, in the diencephalon, and the substantia nigra in the mesencephalon are often included in the generic term basal ganglia because of their strong anatomical and functional association. The main structure is the striatum, classically divided in "neostriatum", to date often simply termed "the striatum", and "paleostriatum", a term not frequently used, and referred to as the pallidum or globus pallidus. It should be emphasized that the gross anatomical divisions present some differences between species, especially between the order of primates and that of rodents: in primates (and many other mammals) the dorsal striatum is divided by the fibers of the internal capsule into caudate nucleus and putamen, whereas these two structures form only one in rodents (caudate-putamen). In rodents the internal (medial) globus pallidus is referred to as the entopenduncular nucleus.

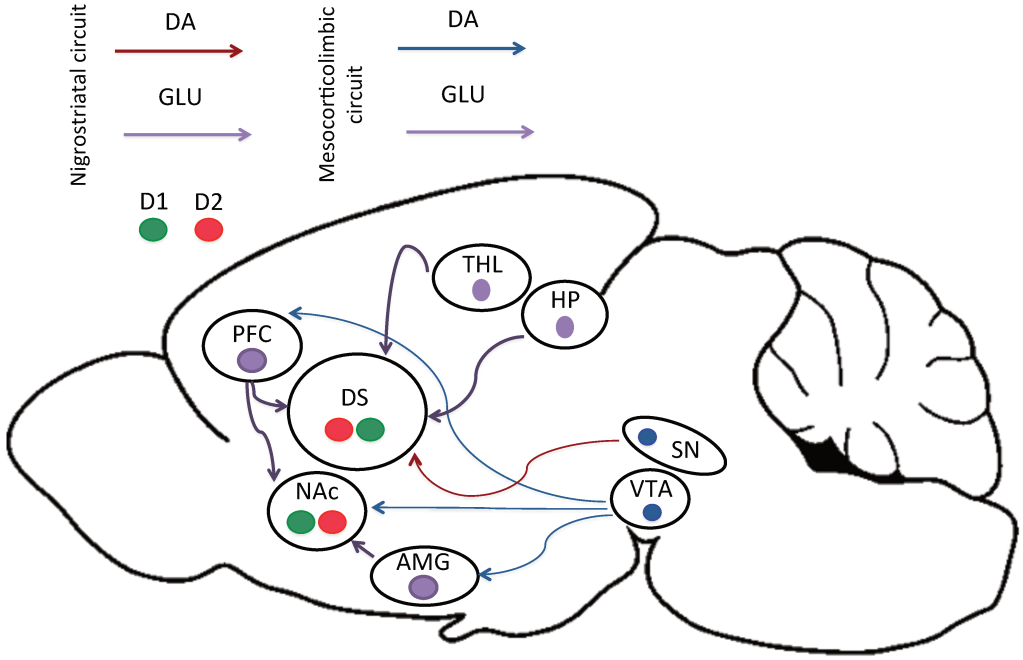

Figure 3: **Schematic representation of the mesocorticolimbic and nigrostriatal dopamine projections in the mouse brain.** The major dopamine projections are shown in brown and blue. The substantia nigra (SN) neurons project primarily to the dorsal striatum (DS,) while the ventro tegmental area (VTA) neurons project primarily to the nucleus accumbens (NAc), the prefrontal cortex (PFC) and the amygdala (AMG). In purple are shown the glutamatergic afferences to the striatum.

The most widely accepted model of basal ganglia circuit function is based on the segregation of information processing into direct and indirect pathways. The direct pathway is composed of striatal D1 GABAergic neurons, also referred as striatonigral neurons, projecting directly to the internal globus pallidus (GPi) and the substantia nigra pas reticulata (SNr), making synpatic contact with the GABAergic output neurons of this structure. The indirect pathway is also composed of GABAergic neurons, referred as striatopallidal or D2 neurons. However, the corticostriatal information is transmitted indirectly to the output nuclei via the external globus pallidus (GPe) and the subthalamic nucleus (STN). GPe neurons innervate the glutamatergic neurons of the STN first, which then innervate the GABAergic output neurons in the GPi/SNr. This flow of transmission is described as two parallel cortex-basal ganglia-thalamus-cortex loops that diverge within the striatum and are differentially modulated by dopamine (Haber et al. 2000; Alexander et al. 1986; Joel & Weiner 1994) as schematized in the following figure.

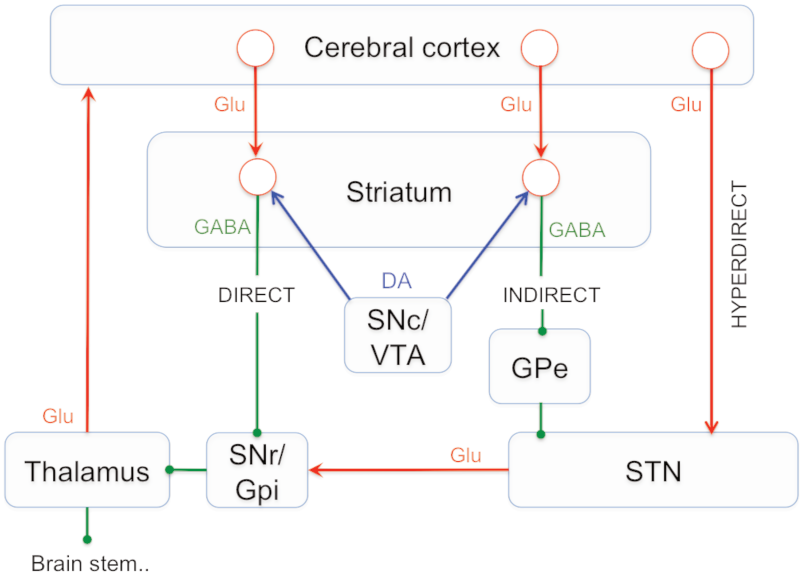

Figure 4: **Schematic wiring diagram of the BG**. SPNs receive excitatory glutamatergic inputs (red) from cerebral cortex and thalamus (not shown in diagram) and a modulatory dopaminergic input (blue) from the SNc and VTA. DA activates the striatonigral pathway and inhibits the striatopallidal pathway. These opposite regulations control the disinhibition of thalamo-cortical glutamatergic neurons and promote motor activity. Abbreviations: DA: dopamine; Glu: glutamate; SNT: subthalamic nucleus; GPe: external globus pallidus; Gpi: internal globul pallidus; SNr: subtantia nigra reticulata; SNc: subtantia nigra pars compacta; VTA: ventral tegmantal area

2.2 The striatum

The striatum is the main recipient of afferents of the basal ganglia. The term striatum refers to its striped appearance produced by the abundant fiber bundles that pass through it. Although the striatum is a complicated and heterogeneous structure, in mice, it is possible to define a gross division of this structure in two sub-regions that correspond to the DS and the ventral striatum that includes NAc and olfactory tuberculum. In primates the presence of the internal capsule allows an additional separation of the DS into two additional components the caudate nucleus, being the main target of the prefrontal cortex inputs, and the putamen that is mostly targeted by sensorimotor and motor cortices. This separation is not found in rodents, even though it is possible to find a regional distribution of the inputs coming from the afferent regions. In rodents the dorsal striatum is also referred to as the caudate-putamen (CP) and can be further sub-divided in dorsomedial and dorsolateral striatum. The NAc can be subdivided in two main sub-regions: the core and the shell (Alheid & Heimer 1988; Voorn et al. 2004). While the core was proposed to be closely related to the DS in terms of connections and functions, the shell is considered to be related to the extended amygdala. The shell itself is highly heterogeneous (Gangarossa et al. 2013). The dorso-ventral division was initially based on the differences in the afferent connections received by these two striatal regions, since DS and NAc are histologically indistinguishable. Important functional differences arise from these afferent connections from the other brain areas. The DS receives a massive excitatory glutamatergic input from most cortical regions and the thalamus, as well as a DA input from the SNc (Kitai et al., 1976, Donoghue and Herkenham, 1986; Nakano, 2000; Herrero et al., 2002). On the other hand the ventral striatum mainly receive DA innervation from the ventral tegmental area as well as glutamatergic input from limbic cortices, amygdala and thalamic nuclei.

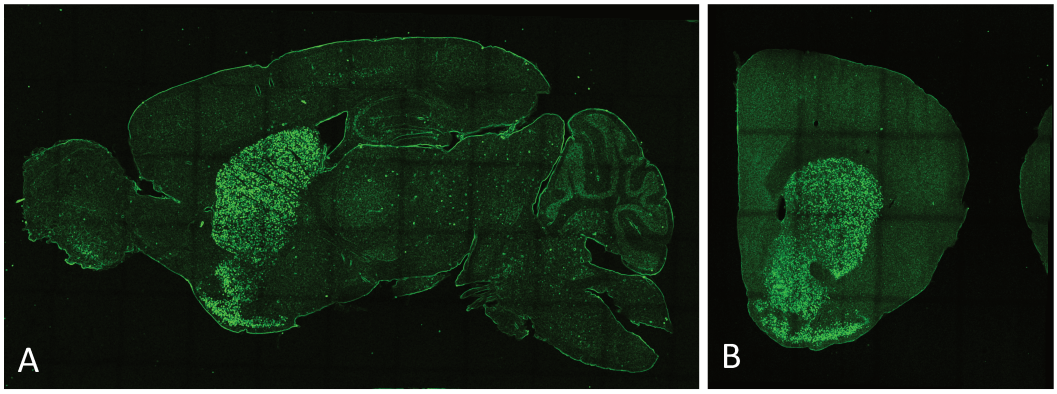

Figure 5: **Striatum A.** sagittal and **B.** coronal confocal sections from Drd2a::EGFP-L10 showing the localization of the striatum in mouse brain. Staining: GFP (Montalban E., this thesis).

2.2.1 Anatomy of the striatum

Inputs to the striatum

Even if the mouse striatum lacks a precise boundary between DS and NAc, it is possible to define functional zones by mapping the sources of the afferent regions. It is important to notice that none of the afferents to the striatum distribute exclusively to the dorsal part or the ventral part of the structure. Different studies on striatal connections pointed out the existence of a dorsomedial to ventrolateral gradient of projections from cortical, thalamic and amygdaloid areas (Voorn et al. 2004).

The dorsal projections are predominantly motor-related while the ventromedial part collects more limbic innervation. The inputs to the striatum can be divided in two main categories: glutamatergic inputs and dopaminergic inputs.

Organization of glutamatergic projection to the striatum

The principal glutamate input to the striatum are represented by the afferents from cortex, thalamus, hippocampus and amygdala. The cerebral cortex provides a massive input to the striatum being a source of corticostriatal fibers. The cortical and thalamic inputs to the striatum are strictly topographically organised in a

dorsomedial to dorsoventral gradient. While the dorsolateral striatum collects projections from the sensorimotor cortical areas, the ventromedial part of the striatum receives a massive innervations from the prelimbic and infralimbic prefontal cortex (Berendse et al. 1992). Amygdala and hippocampus, as the cortical area connect to the striatum. In general, the dorsal striatum collects projections from the neurons located in the dorsal part of the hippocampus while the more ventral neurons in the hippocampus form a major input in the ventral part of the striatum (Groenewegen et al. 1999). The same pattern of projections is maintained for the amygdaloid nuclei: the rostral basal nuclei of the amygdala project to the more lateral striatum and are linked to associative functions, whereas the caudal basal nuclei that associate with viscerolimbic functions target the ventral part of the striatum. The same type of gradient is maintained at the level of the thalamic connections: while the motor associated posterior-lateral intralaminar thalamic nuclei mostly connect with the dorsolateral part of the striatum, the paraventricular nucleus, located more ventrally in the thalamic complex innervates predominantly the NAc.

Organization of the dopaminergic projections to the striatum

DA is the principal modulatory neurotransmitter that is released in the striatum. The main dopaminergic cell groups are located in the midbrain and project in a topographic fashion (Beckstead et al. 1979; Mattiace et al. n.d. 1979). The dorsal lateral striatum mostly collects the projections coming from two distinct populations of DA cells: the DA neurons that originate in the retrorubral area (A8), and the DA cells of SNc (A9) that project to a more intermediary part of the striatum via the nigro-striatal system. Ventromedial striatum and NAc are mostly reached by the DA cells located in the VTA (A10). (Guyenet & Aghajanian 1978; Beckstead et al. 1979; Veening et al. 1980; Albanese & Minciacchi 1983; Gerfen et al. 1987).

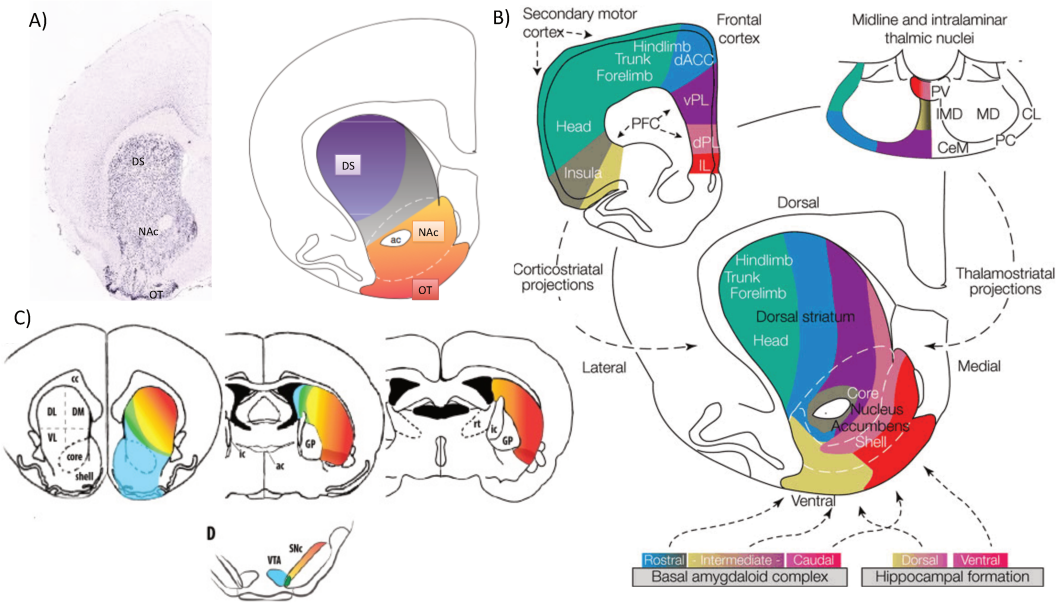

Figure 6: **Anatomical part of the striatum**: **A-** Coronal half-section of the mouse forebrain (Allen Brain Atlas, drd1 in situ hybridization) and diagram showing the striatum, consisting of the dorsal striatum (DS), the nucleus accumbens (NAc) and the striatal elements of the olfactory tubercle (OT). **B-C** Schematic representation of the topographical arrangement of the glutamatergic (**B**) and dopaminergic (**C**) afferents to the striatum. Each colour represents a distinct functional area of the brain converging to the striatum. Green: somatosensory and motor function, blue-purple: higher associative function; pink and red: viscerolimbic function, yellow: polymodal sensory and cognitive function. Abbreviations: PFC, Frontal Cortex: ACd, dorsal anterior cingulate; AId, dorsal agranular insular; AIv, ventral agranular insular, IL, infralimbic; PLd, dorsal prelimbic; PLv, ventral prelimbic; SMC, sensorimotor. Thalamic nuclei: CeM, central medial; CL, central lateral; IMD, intermediodorsal; MD, mediodorsal; PC, paracentral; PV, paraventricular. Amygdaloid nuclei: BLa, anterior basolateral; BLp, posterior basolateral; BMa, anterior basomedial; BMp, posterior basomedial; CeC, capsular central. (Voorn et al. 2004) **C**. Topographical arrangement of the DA projection to the striatum. The different colours represent the distribution of the DA projections originating from the different cell groups in the midbrain from more ventral location (blue) to more lateral (red). The dark red represent the projections from A8 (not represented in the figure). Abbreviations: ac: anterior commissure; cc. corpus callosum; DL, DM: dorsolateral and dorsomedial striatum; GP: globus pallidus; ic: internal capsule; rt, reticular nucleus of the thalamus; SNc, substantia nigra pars compacta, VL, ventrolateral dorsal striatum, SNc: substantia nigra pars compacta,. VTA: ventro tegmental area. (Cenci et al. 2015; Voorn et al. 2004)

The patch/matrix organization in the striatum

The striatum in organized into two anatomically distinct compartments called patches (striosomes) and matrix (extratriosome) (Pert et al. 1976; Graybiel & Ragsdale 1978) .

The very first study suggesting an histological compartmentalization in the striatum dates back to 1976, when Pert and collaborators showed a patchy distribution of the μ-opiate receptors in a matrix characterized by a lower receptor density (Pert et al. 1976; Herkenham & Pert 1981) (Pert et al. 1976; Kent et al. 1981). In general, differential staining pattern are used for visualizing the patch matrix organization, for example the acetylcholinesterase staining as well as calbindin immunoreactivity, is poorer in patches than in the matrix while dopamine transporter (DAT), and Nr4a1 (nuclear receptor subfamily 4, group A, member 1) staining are higher in the patches (Graybiel & Ragsdale 1978; Holt et al. 1997; Prensa et al. 1999; Gerfen n.d.; Davis & Puhl 2011; Jill R Crittenden & Graybiel 2011). The matrix compartment represents approximately 85% of the striatum (Johnston et al., 1990 and Mikula et al., 2009) and the striosomal compartment comprises the 15% of the striatum and is associated with limbic circuits (Eblen & Graybiel 1995; Gerfen n.d.; Kincaid & Wilson 1996) However, as shown in the work of Davis and Puhl in 2011 these ratios can vary across the striatum (Davis & Puhl 2011).

Patches and matrix features

Patches and matrix differ from each other in several ways, including neurotransmitter enrichment (Graybiel & Ragsdale 1978; Holt et al. 1997) connectivity (Gerfen et al. 1987; Gerfen 1989), neuronal organization, development (van der Kooy & Fishell 1987; Graybiel & Hickey 1982; Liu & Graybiel 1992), and gene expression (Moratalla et al. 1992; Grande et al. 2004)

The patch matrix organization during the development: the DA innervation in patches within the striatum can be observed already at the early stages of the post-

natal development (Tennyson et al. 1972). The neurons that are first innervated in the striatum are known as "dopamine island" and mostly receive innervations from the substantia nigra(Olson et al. 1972; Moon Edley & Herkenham 1984; van der Kooy & Fishell 1987). The patches neurons of striatum will develop earlier than most matrix neurons that are born later in the embryogenesis.

Organization of the patch-matrix connectivity: the glutamatergic projections to the striatum differentially innervates patch and matrix in the striatum: while the patches receive mostly the innervation from the limbic circuit (orbitofrontal, anterior cingulate, and insular cortices) (Graybiel & Ragsdale 1978), the projections from the other neocortical areas such as somatosensory, motor, and association cortices terminate mainly in the matrix (Ragsdale & Graybiel 1990; Flaherty & Graybiel 1994; Eblen & Graybiel 1995; Kincaid & Wilson 1996; Lévesque & Parent n.d.). The glutamatergic inputs can terminate on dendritic shafts or spines (Lacey et al. 2005; Raju et al. 2006), however, the inputs on the shaft are mainly enriched in the matrix (Fujiyama et al. 2006; Raju et al. 2006). According to the classical view of the patch-matrix afferents, the inputs from the thalamic nuclei are denser in the matrix (Fujiyama et al. 2006). However, lately it has been shown that the intralaminar thalamic nuclei mainly target the matrix, whereas the midline thalamic nuclei target preferentially the patches (Unzai et al. 2015). DA projections, like the glutamatergic inputs, differentially target the patches and the matrix. While neurons originating from the SNc preferentially target the patch compartment, the cells originating from VTA, lateral SNc and retrobrural area principally connect to the matrix (Gerfen et al. 1987). Given this difference in innervation, a recent work compared the release of DA in the striosome and matrix compartments using fast-scan cyclic voltammetry in Nr4a1-eGFP transgenic mice. In particular in the DS, dopamine release in striosomes was less than in the matrix, while the opposite way was observed in the ventral striatum. Salinas and collaborators also found that cocaine administration enhanced the DA levels more in the patches than in matrix regions (Salinas et al. 2016)

Lastly, concerning the projections arising from the striatum, the matrix compartment preferentially targets the GP and the SNr, while patches synapse preferentially with the SNc (Kawaguchi et al. 1990; Giménez-Amaya & Graybiel 1991; Lévesque & Parent n.d.; Chuhma et al. 2011). According to this scheme of projections, it can be argue that the striatal projection neurons in the striosomes may

have a role in regulating the release of dopamine in the striatum (Fujiyama et al. 2011; Gerfen et al. 1987; Watabe-Uchida et al. 2012)

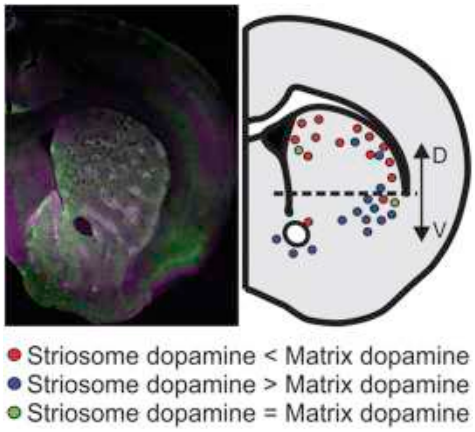

Figure 7: **The different release of DA in the patch and matrix compartments of the striatum. A**. Coronal section from Nr4a1-eGFPmice stained with an antibody against the μ-opiate receptors. **B** Scheme of the dorso ventral release of DA in the patch and the matrix

Differential gene expression in patch and matrix compartments: the different profiles of gene expression in the patch and the matrix represent another useful criterion to distinguish those two compartments. More than 60 genes are reported to have a specific enrichment in striosome or matrix (reviewed in (Jill R. Crittenden & Graybiel 2011)). Already in 1992 it has been shown that the administration of different drugs can regulate the gene expression in matrix and patch in different fashion. For example, amphetamine and a neuroleptic are able to specifically induce different profiles of expression of immediate early genes (IEG) in the patches or the matrix (Grande et al. 2004; Moratalla et al. 1992; Saka et al. 1999; Adams et al. 2003; Miura et al. 2007).

2.2.2. Neuronal composition of the striatum

In the striatum, the DA afferents originating from the midbrain mostly innervate two populations of GABAergic neurons named medium sized spiny neurons (MSNs) or striatal projection neurons (SPNs). In the rat SPNs represent up to 97.7 % of the striatal neuronal population (Rymar et al. 2004), the remaining 2.3 % being mostly GABAergic and cholinergic interneurons (Kreitzer 2009; Tepper et al. 2010). SPNs are GABAergic neurons characterized by a large and extensive dendritic tree, and a medium sized body of 10-20 µm in diameter (Kawaguchi et al. 1990).

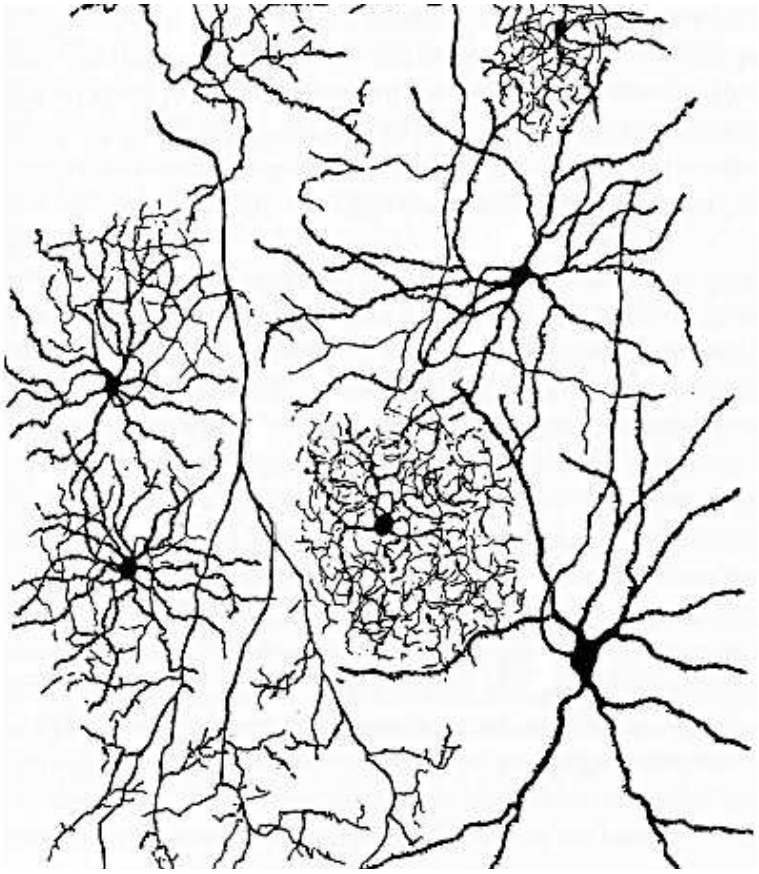

Figure 8: **Different populations of striatal neurons.** Different types of striatal cells described by Ramón y Cajal (Ramón y Cajal, 1911).

Striatal GABAergic interneurons

The striatal GABAergic interneurons represent roughly 2-3% of the interneurons in the striatum, and were firstly identified in 1979 as non-spiny neurons stained for glutamic acid decarboxylase 67 (GAD67) (Ribak et al. 1979; Bolam et al. 1985). Five different classes of interneurons are identifiable on the basis of the combination of markers that they express (Kawaguchi 1993; Kawaguchi et al. 1997)

Somatostatin-positive interneurons. The somatostatin-containing interneurons are medium sized aspiny cells of 12-25 μm in diameter. This class of interneurons is positive for somatostatin, neuropeptide Y, and nitric oxide synthase.

Compared to the other classes of interneurons, their axonal arborizations are less dense within the region of the dendritic field, although they extend over longer distances within the striatum (Kawaguchi 1993). The somatostatin-containing interneurons collect projections from GP, SN and cortex (Kubota et al. 1993; Bevan et al. 1998), are located in both patch and matrix but innervate mainly the striatal matrix. From an electrophysiological point of view, these neurons are characterized by low threshold spikes (LTS) and a prolonged calcium dependent plateau potential (Kawaguchi, 1993). The activation of these cells results in the production of inhibitory postsynaptic currents in the SPNs, and their capacity to release nitric oxide has been proposed as possible regulators of the corticostriatal synaptic plasticity (Centonze et al. 2003)

Parvalbumin positive neurons. Parvalbumin-positive interneurons have been identified in the striatal tissue by their specific content in the calcium binding protein parvalbumin (Kita et al. 1990; Gerfen et al. 1985) and are cells of 16–18 μm in diameter that give rise to aspiny dendrites that branch modestly in the striatum. Paravalbumin neurons receive projections from cortex, thalamus and globus pallidus (Gerfen et al. 1985; Bevan et al. 1998; Luk & Sadikot 2001) and mostly project to the SPNs (Kita 1993; Bennett & Bolam 1994; Kubota & Kawaguchi 2000) on which they exert a strong inhibition through multiple perisomatic synapses. Paravalbumin interneurons are themselves electrotonically coupled through gap junctions (Koós & Tepper 1999; Koos et al. 2004; Kita et al. 1990). Due to their electrophysiological

properties, the paravalbumin interneurons are commonly referred to as fast-spiking interneurons (FSIs). Compared to SPNs, parvalbumin interneurons present a lower threshold of activation (Koós & Tepper 1999)

Calretinin-positive interneurons. The calretinin-positive interneurons are GABAergic interneuron, relatively sparse in the caudal striatum (Bennett & Bolam 1993) that express the calcium binding protein calretinin. The calretinin interneurons are characterized by medium-sized cell bodies and few non-spiny dendrites, and exert a powerful monosynaptic inhibition on the SPNs. Although the electrophysiological profile of those neurons is not fully described yet, they share some of the characteristics of the PLTS neurons (Kawaguchi, 1993), such as their fired prominent LTSs (Petryszyn et al. 2014).

NPY-neurogliaform (NGF) interneurons. The NPY-neurogliaform interneurons are GABAergic interneurons of 13 μm in diameter that have been firstly identified in 2011. NPY-NGF interneurons differ in several features from the somatostatin interneurons. Contrary to the NPY-PLTS interneurons, NPY-NGF neurons are characterized by a dense, compact, highly branched dendritic and local axonal arborizations. Furthermore, NPY-neurogliaform interneurons exhibit a lower input resistance and hyperpolarized membrane potential, as well as the lack of depolarizations plateau or low-threshold spikes. Also, contrary to the NPY-PLST, NPY-NGF interneurons do not react to immunostaining for somatostatin or NOS. The major target of NPY-NGF are the SPNs on which are able to exert a slow GABA(A) receptor-mediated IPSC (Ibáñez-Sandoval et al. 2011).

Late-spiking (LS) neuropeptide-Y (NPY)-negative neurogliaform (NGF) and LTS-lke interneurons. Those two last populations of neurons are both reacting to the 5HT3a marker and were both described by Muñoz-Manchado et al in 2016 (Muñoz-Manchado et al. 2016). Although those cells do not show striking electrophysiological difference they mainly differ one from the other in their pharmacological responses: LTS-like cells are characterized by a robust response to nicotine administration, while NPY-NGF-5HT3 cells type shows little or no response.

Striatal cholinergic interneurons

The cholinergic interneurons in the striatum were firstly identified in the late 1800s by Kolliker by using the Golgi staining. In the beginning those giant cells, were wrongly identified as projection neurons. Cholinergic interneurons are easily identifiable by the presence of the choline acetyltransferase enzyme (ChAT), and from their cell body of 40 μm. ChAT interneurons are often referred as tonically active neurons (TANs) based on their slow and regular firing characterized by a long action potential and slow spike after the phase of hyperpolarization. ChAT interneurons receive excitatory input from the cortex and the thalamus as well as DA inputs form SN and GABAergic inhibition from SPNs. Although they represent a minor fraction of the striatal neurons (1-2%), the synchronic activation of this population provides a tight control of the striatal input via the generation of large inhibitory currents within the striatum. Even if few in number, the ChAT interneurons have an enormous and dense dendritic arborisation that account for the fact that they represent the neurons with the higher level of expression of Ach acetylcholine and ChAT (Macintosh 1941; HEBB 1957). The major targets of the cholinergic interneurons are the SPNs. The ChAT neurons are able to drive an inhibitory response on the SPNs in different fashions. A direct regulation consists in a direct synaptic contact onto distal dendrites and dendritic spine necks of the SPNs (Bolam et al. 1984). A second, indirect, regulation on SPNs is provided by a previous excitatory synaptic input onto the nicotinic synapses on GABAergic interneurons (English et al. 2012). Importantly, due to the high density of their arborisation, and their exact position within the striatum, cholinergic axon terminals can also exert influence via volume transmission (Koós & Tepper 2002; Descarries et al. 1997), (Zhou et al. 2001). Lastly, several recent studies have pointed out that the nigrostriatal DA terminals are good candidates of being activated by the cholinergic neurons (Cachope, Mateo, Brian N. Mathur, et al. 2012; Exley & Cragg 2008; Threlfell et al. 2012; Zhou et al. 2001). In particular it has been shown that the optogenetic stimulation of the cholinergic neurons is able to induce the DA release in the striatum (Cachope, Mateo, Brian N Mathur, et al. 2012). Based on these evidences, recently, Nelson and colleagues suggestsed that the cholinergic interneurons are able to exert a neuromodulatory control of the striatal output by controlling the DA signaling (Nelson et al. 2014)

Medium sized spiny striatal projection neurons (SPNs)

Spiny neurons receive DA inputs from the SNc at the base of the dendrites spines via symmetric synapses. The DA input to the SPNs represent the 13% of the total number of synapses. The thalamic and cortical inputs represent roughly 80% of the synapses in the striatum and are mainly taking place at the level of the tips of the spines (Freund et al. 1986; Smith et al. 1994; Hanley & Bolam 1997). It has been estimated that each SPN receives from 5 to 10 thousand excitatory inputs. The convergent action of several inputs is necessary to trigger the activation of a single neuron. Importantly, SPNs are able to make synaptic symmetric contacts with cholinergic interneurons in the striatum itself, and with serotoninergic projections from the raphe (Izzo & Bolam 1988; Soghomonian et al. 1989). Lastly, SPNs receive a major inhibitory input from the striatal cholinergic and GABAergic interneurons and from the collateral SPNs (Wilson 2007). Importantly, SPNs are really sensitive to the inhibition acted by interneurons. The combination of the weak signal transferred from the thalamo-cortical synapses, the strong inhibitory signal due to interneurons, and of the conductance properties of the SPNs results in low firing signal *in vivo* (Kreitzer & Malenka 2007).

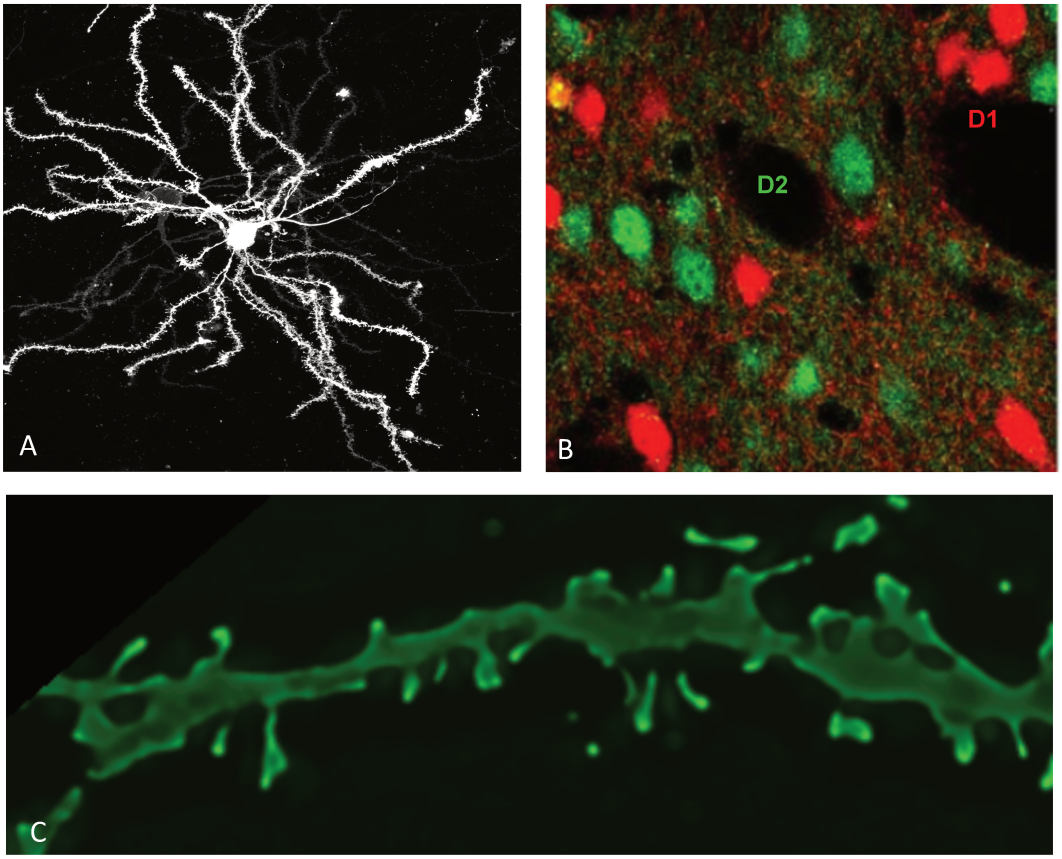

Figure 9: **Medium-sized spiny projection neurons (SPNs) A**. An MSN in striatal tissue from a C57BL/6 (Giralt A., unpublished data) **B**. Confocal section of striatum showing the segregation between D1R and D2R- expressing neurons. Obtained in the lab from Drd1-tomato-Drd2GFP double transgenic mice (this thesis) **C.** Golgi-stained dendrites of medium spiny neurons in the NAc (this thesis).

As already discussed, SPNs can be divided in two different sub-populations – so called striato-nigral or striato pallidal – on the basis of their target regions and on the expression of the D1 or D2 DA receptor. This segregation is fundamental to permit the correct functions of the basal ganglia.

Although SPNs in the striatum have long been thought to be similar, recent works suggest some differences between the two populations that could account for some of the dissimilarities in their physiology. Already in 1988, Gerfen and Young proposed that – depending on the connectivity with the GABAergic interneurons - SPNs could be divided in 2 sub-categories on the basis of the paired-pulse responses to the cortical stimulation(Gerfen & Young 1988). The recent development of the bacterial

artificial chromosome (BAC) transgenic mice expressing enhanced green fluorescent protein (eGFP) under the control of promoters for the D1 and D2 receptors allowed a clear distinction of the two populations (Day et al. 2006; Kreitzer & Malenka 2007; Ade et al. 2008; Cepeda et al. 2008).

Taking advantage of this technology, at least 2 different works showed that the dendritic tree of the D_2 SPNs is significantly smaller than D_1 SPNs (Gertler et al. 2008; Fujiyama et al. 2011). By making use of whole-cell patch-clamp recordings in D_1 and D_2 SPNs in brain slices from BAC transgenic mice, Tracy S. and collaborators were able to correlate this anatomical dichotomy with the differences in excitability observed in the 2 populations of SPNs. As already shown by Kreitzer and Malenka in 2007 – due to the smaller dendritic tree - D2 SPNs are more excitable than the D1 SPNs (Kreitzer & Malenka 2007).

As an additional level of complication, several studies pointed out the existence of some differences between the SPNs in the DS and in the NAc. The different projections of the SPNs that belong to the DS or the NAc, account for the different behaviours mediated by those two regions. Although SPNs in the DS and NAc look identical in phenotypes, they differ in their output connections (reviewed in (Yager et al. 2015)) and gene expression profile (Montalban E. et al., this thesis). It is widely accepted that in the DS, D1 SPNs mainly project to the SNr and to the medial part of the GP, whether the D2 project to the lateral part of the GP (Valjent et al. 2009; Bertran-Gonzalez et al. 2010), however, it is important to mention that, recently, Gangarossa and collaborators – taking advantage of the BAC technology – described a specific region in the caudal striatum, adjacent to the GPe, that is enriched D1R SPNs, cholinergic and GABAergic interneurons, while lacking markers for indirect pathway neurons (Gangarossa et al. 2013). This last study corroborated some of the results that have previously described the existence of D1 outputs to the lateral GP (Kawaguchi et al. 1990; Fujiyama et al. 2011). It is thought that the D1 outputs to the eGP may serve as a bridge between the direct and indirect pathways (Cazorla et al. 2014). Nevertheless it has been proposed that D2 neurons in DS control the D1 output to the GPe: an increase in the bridging collaterals is associated with enhanced inhibition of pallidal neurons in vivo, while the chronic inhibition of the D2 receptor with haloperidol decreases the amount of bridging collaterals (Cazorla et al 2014). Importantly, it has been recently suggested that, in contrast with the classical scheme of the basal ganglia circuit, both D1 and D2 are able to disinhibit the cortex by

inhibiting the acteyltransferase positive neurons in the eGP that send direct inhibitory projection to the frontal cortex (Saunders et al. 2015).

This "re-vision" of the connectivity of the basal ganglia circuit has been recently proposed by the group of Sabatini. Here, Saunders and collaborators described a direct projection from the eGP to the frontal cortex that comprises cholinergic and GABA-inhibitory cells. Importantly, D1 and D2 SPNs are both able to inhibit the neurons making up this projection. Thus, the direct connection globus pallidum-frontal cortex is under the direct control of striatum (Saunders et al; 2015).

The NAc is the only region of the striatum hosting the D3-SPNs. The D3 dopamine SPNs are enriched in the shell of the NAc in the region enriched in D1-SPN (Gangarossa 2013). The organization of the SPNs in the NAc, as for DS, challenges the classical view of the basal ganglia circuit. As mentioned above, two regions, the core and the shell, are distinguished in the NAc, based on histochemical differences, as well as differences in their afferents and efferents (Groenewegen & Berendse 1994; Voorn et al. 2004; Zahm 2000; Zahm & Brog 1992). Both core and shell project to the SNc and VTA, although the shell sends prominent reciprocal projections to the ventral pallidum (Zahm et al. 1996), but also to the lateral hypothalamus, the pedunculopontine tegmental nucleus and other several subcortical areas that are not part of the basal ganglia. (Winn et al. 1997; Zahm 2000; Zahm & Brog 1992). Because of the GABAergic nature of both NAc shell and ventral pallidum projection neurons it is possible to hypothesize that the shell of the NAc could act on their targets by mechanisms of disinhibition and inhibition similar to the one that are taking place in the direct and indirect pathway in the DS.

The NAc core as the shell projects to ventral pallidum but in different districts. As for the indirect pathway of the DS, the ventral pallidum reciprocally connects to the STN and projects to both the mediodorsal nucleus of the thalamus and to brainstem similarly to motor areas. On the other hand, the VP also projects to the STN, a characteristic shared by the indirect path dorsal striatal target (Groenewegen and Berendse 1994; Zahm and Brog 1992). Based on those connections it is possible to hypothesise that the ventral pallidum could control the mediodorsal nucleus of the thalamus by two different pathways: a "direct" path made up of D2 SPNs (Kupchik et al. 2015) consisting in a first connection of the NAc to

the VP that in turn projects to the thalamus, and a second "indirect" path composed by D1 SPNs (O'Connor et al. 2015) that include the reciprocal connection of the VP with STN ((Nicola 2007).

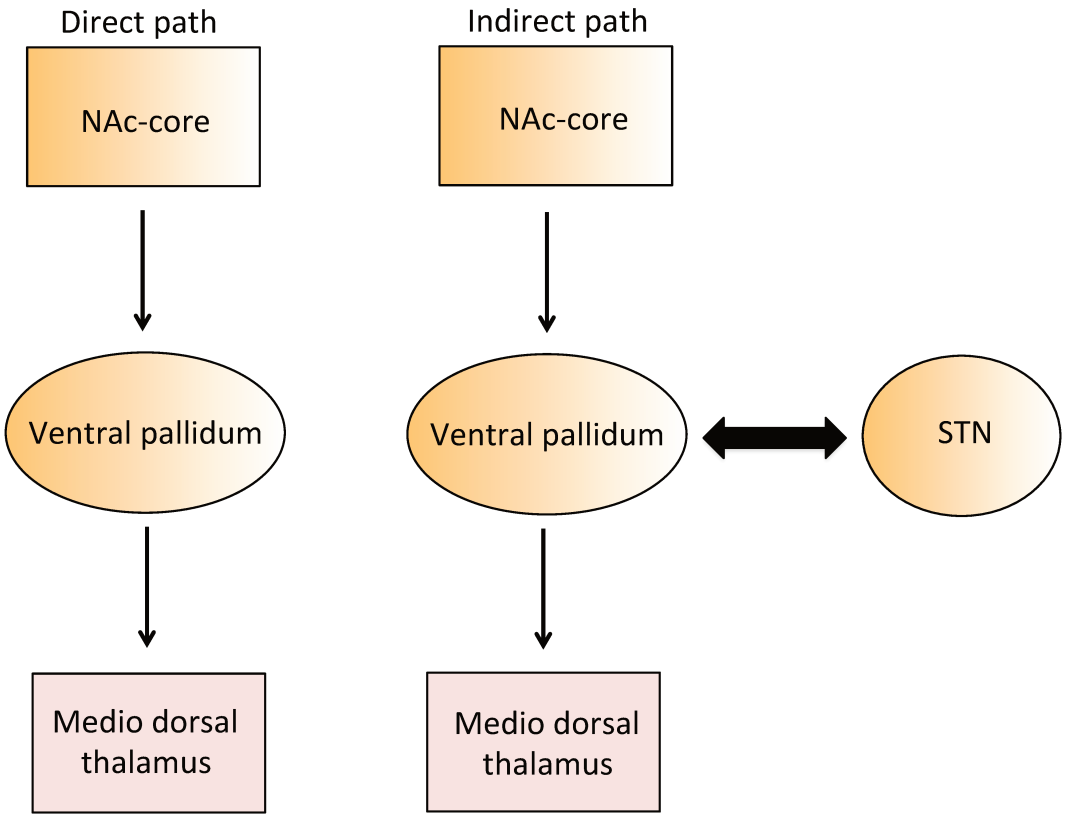

Lastly, only the core of the NAc projects directly to the entopeduncular nucleus (EP = GPi in primates) which projects to motor thalamic nuclei. This cascade of neuronal pathway connecting NAc, and EP, with the thalamic nucleus could have a direct disinhibitory effect on motor behaviour although a corresponding indirect pathway has not been identified yet

2.3 The globus pallidus

The globus pallidus (GP) is located caudomedial to the striatum. The GP is separated in two nuclei, named external globus pallidus (GPe) and internal globus pallidus (GPi in primates or entopeduncular nucleus in rodents), by small fibers of passage and pallidal border cells. These two divisions of the pallidal complex receive

striatal afferents originating from different population of striatal SPNs and project to different outputs. The GP is mainly composed by GABAergic neurons characterized by a large cell body of 20-50 μm, and a dense dendritic arborisation (Difiglia et al. 1982). SPNs in the striatum are the major input on the GP, however, the external globus pallidus also receives glutamatergic projections from the subthalamic nucleus (STN) and, although to lesser extent, from the cerebral cortex, GPi, raphe nucleus, pedunculopontine tegmentum and SN (Hazrati et al. 1990; Fink-Jensen & Mikkelsen 1991; Kita & Kitai 1994; Deschênes et al. 1996; Yasukawa et al. 2004; Kita 2007).

The GPe mainly projects to the STN but also to the GPi/SNr and the striatum. The GPi targets the motor thalamus and the ventral medial and parafascicular thalamic nuclei (Deniau & Chevalier 1984; Deniau et al. 2007).

2.4 The subthalamic nucleus

Although relatively small and with relatively few neurons, the STN is the second major port of entry of basal ganglia. Positioned on the medial side of the internal capsule and cerebral peduncle, the STN is the only excitatory structure of the BG that provide glutamatergic projections to the GPe (Bevan et al. 1994) GPi, and SNr (Nakanishi et al. 1987; Parent & Smith 1987). The STN receives three main inputs: a major GABAergic input (1) from GPe, and from the mesopontine tegmentum (Smith & Bolam 1989; Bevan & Bolam 1995), a glutamtergic input (2) from prefrontal cortex and the intralaminar thalamic nuclei (Kitai & Deniau 1981; Nambu et al. 1996; Bevan et al. 2007), and a third (3) input from the DA fibres arising by the SNc (Brown et al. 1979; Lavoie et al. 1989; Cragg et al. 2004). The cortico-subthalamic pathway bypasses the striatum and is often referred as the hyperdirect pathway, the fastest route by which cortical and thalamic information can influence activity in the output nuclei. Importantly, it has been proposed that this pathway could be involved in the inhibition of initiated movements, providing a STOP signal (Aron & Poldrack 2006).

2.5 The substantia nigra

The substantia nigra (SN) is a structure lying dorsally to the cerebral peduncle in the ventral midbrain. This structure can be sub-divided in two different compartments: the pars compacta (SNc) composed by a compact and a diffuse clusters of neurons, and the pars reticulata (SNr), which is characterized by lower density of cells which are interspaced within a dense neuropil of radiating dendrites originating from both SNr and SNc neurons. The SN, together with ventral tegmental area (VTA) and the retrorubral area, constitutes the major input of DA to the striatum and other forebrain structures. The SN receives connections both D1 and D2 SPNs, from GABAergic neurons in the GPe, and glutamatergic inputs from the striatum.

- Chapter 3 -

Long-lasting changes induced by cocaine

3.1 The brain reward system: neuroanatomical and general principles

In the study of behaviour, the term reward describes an event that produces a pleasant or positive affective experience. The rewarding effect of a stimuzlus can be measured by the willingness of the subject to work, in order to gain access to this goal. Along this idea the responses to stimuli that produce positive effects are likely to be repeated (Thorndike 1898). The idea that behavioural responses can be a direct measure of the rewarding properties of a certain object is the basis of the theory of reinforcement initially proposed by Skinner in 1938. In his pioneer work Skinner proposed that in an operant conditioning model - a behaviour paradigm that involves choice and reward measurement - the response strength can be determined by measuring the frequency and the intensity of behavioural responses. By measuring the motivation to work for a certain goal operant conditioning can offer an index of the rewarding properties of the object.

The operant training is the behavioural paradigm used when the reward circuit was first discovered by Olds and Milner in 1954. In this important study the authors showed that rats are willing to work in order to self-administer electrical stimulation in specific brain regions (OLDS & MILNER 1954). Later studies have shown that rats will perform the task particularly well if the electrical stimulation is elicited in the medial forebrain bundle (MFB) (BRIESE & OLDS 1964) and in the midbrain extension of this structure. More regions that seem to also be part of these reward circuits were later highlighted, and include the orbitofrontal cortex, the lateral hypothalamus, the NAc, the VTA and some brain stem structures (Corbett & Wise 1979). An amount of studies of self-stimulation helped to clarify which brain structures are mainly involved in the reward system and how they are connected with each other. The neural system that mediates the experience of reward consists of a complex network of several brain regions. The meso-corticolimbic pathway is a central component of this system. The meso-corticolimbic pathway arises from dopaminergic neurons located in the VTA, in the midbrain, that send projections to target areas in the limbic forebrain, particularly to the NAc, the DS, and the PFC. The

PFC provides descending projections to the NAc and the VTA. Experiments in mice have been confirmed by imaging studies in human in which the striatum is reported to be activated in response to food (DS) (Small et al. 2003), drugs (Breiter et al. 1997) money (Wilson et al. 2008) and romantic love (Acevedo et al. 2012), stimuli that all present reward-like properties in humans.

The nature of the major neurotransmitter produced by the VTA to modulate striatal function – DA – and the central role that the VTA plays in the reward network suggest that DA is involved in reward mechanisms. Elevated dopamine levels in the nucleus accumbens of rats were found following exposure to food (Hernandez & Hoebel 1988), sweets (Hajnal & Norgren 2001) sex (Pfaus et al. 1995) , and self-administered drugs (e.g., cocaine, morphine, and ethanol) (Di Chiara 1992). Of note, for sugar and drugs, the levels of DA are directly proportional to the increasing concentration of the stimulus. Dopamine's action in the striatum is neuromodulatory. It could reinforce synaptic strength in the area where it is secreted by VTA terminals. It is thus well positioned to modulate excitatory projections of cortical neurons onto striatal neurons.

3.2 Introduction to addiction

Drug addiction, also called substance use disorder, is an illness that can be described as loss of control over taking a legal or illegal drug or medication. Addiction is a complex phenomenon, which depends on both pharmacological and socio-cultural mechanisms. Genetic factors account for only half of the vulnerability to drugs; the other 50% of the risk for addiction is due to the interaction between environmental factors with the individual's genetic set. Although different types of environmental influences are considered to be fundamental to the development of the addiction, the necessary factor is exposure to a drug of abuse. Estimates from twins and adoption studies give ranges of 40% to 60% to heritability. Inherited contributions to addiction result from complex genetic differences; however, several studies in human addicts identified some of the genes that are clearly associated with cocaine addiction, those coding for: D2 receptor (Noble et al. 1993), dopamine

transporter DAT (Gelernter et al. 1994; Guindalini et al. 2006), CB1 cannabinoid receptor (Comings et al. 1997), prodynorphin (Chen et al. 2002), μ-opioid receptor (Zubieta et al. 1996), the serotonin transporter (Mash et al. 2000) and myelin-related genes (Albertson et al. 2006) In vulnerable individuals, the repeated exposure to addictive drugs can lead to stable maladaptive neural changes in specific regions of the brains over time that account for potentially life long abnormalities. Of note, in 2014, 5 % of the US population was composed of addicted people in the age of 12-17(Samsha 2014). Several different drugs seem to share the same mechanisms of action in the brain for both humans and mice. Lehrmann and collaborators showed that in human post-mortem brain samples, cocaine, cannabis, and phencyclidine all decrease transcription of calmodulin-related genes and increase transcription of genes connected to lipid/cholesterol and Golgi/endoplasmic reticulum function in the anterior PFC (Lehrmann et al. 2006). In mice, cocaine, nicotine, morphine, and THC (Valjent et al. 2004), cannabinoids (Tonini et al. 2006), alcohol, MDMA (Salzmann et al. 2003), phencyclidine (Kyosseva et al. 2001) and nicotine (Schroeder et al. 2008) can activate the ERK pathway. Thanks to studies that used both passive and active drug administration, we know today that drug addiction involves gene expression, neurochemical, neurophysiological, and structural changes in many different brain cell populations. The following section will focus on the neural changes induced by cocaine.

3.3 Cocaine

Cocaine is a strong and addictive stimulant, made from the leaves of coca plants, which acts as an indirect agonist of the monoaminergic system. Cocaine, can be inhaled, smoked or injected into the bloodstream. Its effects include euphoria (which might eventually turn into anxiety), hyperactivity, suppression of appetite, and – due to its capacity to block the voltage-dependent sodium channel - local anaesthesia (Reith et al. 1985). Intensity and duration of the effects depend on the route of administration. Once administered, cocaine can easily cross the blood-brain barrier, get into the central nervous system, and inhibit the dopamine- (DAT), norepinephrine- (NET), and serotonin- (SERT) re-uptake transporters, thereby

prolonging the availability of these monoamines in the extracellular space (Ritz et al. 1990). The effects of cocaine are not only restricted to the central nervous system. For example, by increasing the plasma catecholamine levels, cocaine acts also as a potent vasoconstrictor of blood vessels in the brain (Kaufman 1998). Not surprisingly cocaine administration can result in cardiac arrest and it has been associated with different cardiac problems such as myocardial infarction and heart failure (Schwartz et al. 2010).

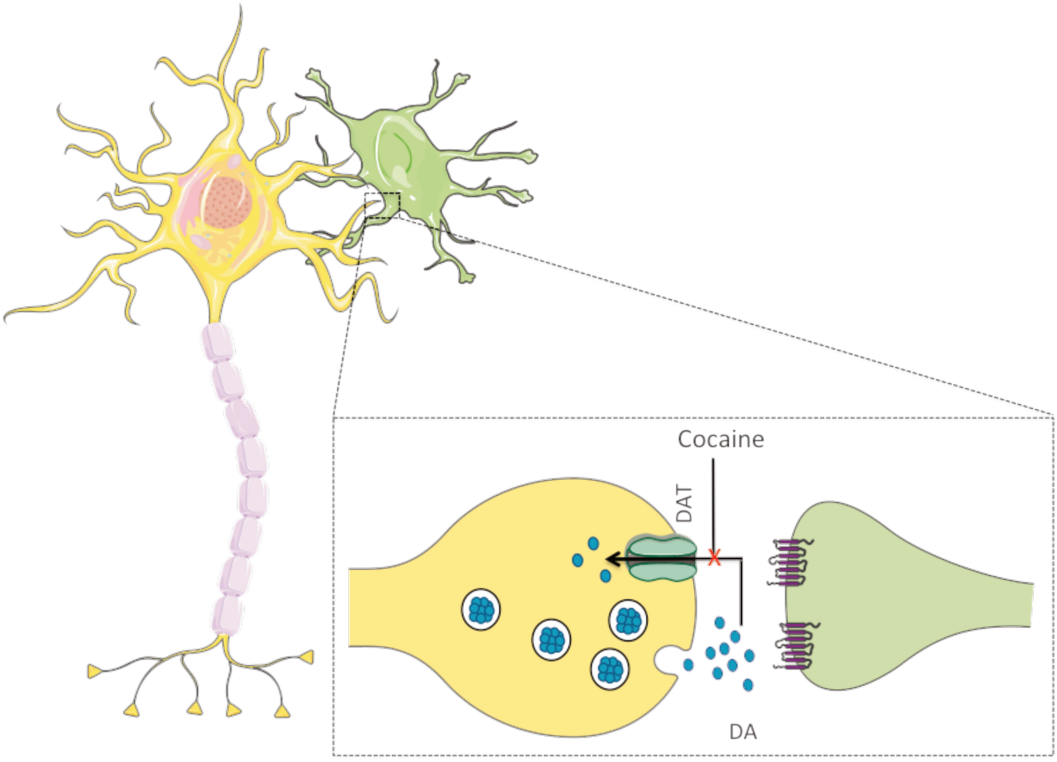

Figure 10: **Mechanism of action of cocaine on synaptic terminals of DA neurons.** Cocaine inhibits the dopamine transporter (DAT), decreasing DA clearance from the synaptic cleft and causing an increase in extracellular DA concentration

3.3.1 Neural circuits underlying cocaine addiction

Exposure to drugs of abuse results in long-lasting alterations throughout the brain reward circuitry. Early studies of intracranial self-administration showed that different drugs are self-administered in distinct parts of the brain. As an example,

while opioids and alcohol have been shown to be directly self-administered into the VTA, cocaine is preferentially self-administered into the frontal cortex (McBride et al. 1999). Importantly, even if the mechanisms of action is specific to each drug, most drugs of abuse increase dopaminergic release from VTA to other regions of the reward circuitry. It is commonly recognized that the DA innervation of the nucleus accumbens and the associated ventral parts of the striatum accounts for the primary reinforcing effect of the cocaine administration (Di Chiara et al. 2004; Wise 2004; Ikemoto et al. 2005; Wise 2008). Indeed, the acquisition of cocaine self-administration is impaired by DA depletion in the NAc or DA receptor blockade (Roberts & Koob 1982; Ito et al. 2004). It has been proposed that cocaine can hijack the normal reward circuit by increasing the dopaminergic transmission within corticostriatal systems that are normally involved in learning and memory processes in the context of natural rewards (Everitt & Robbins 2005; Belin et al. 2013). In vulnerable individuals, this leads to the habitual and compulsive drug use from the initial voluntary drug use. The transition from goal-directed behaviour to habits would reflect shifts from ventral to dorsal striatal control over behaviour, while the loss of control would be linked to the loss of the inhibitory control mediated by the afferents of the PFC to the DS (reviewed in Everitt & Robbins, 2005). Drug taking is often associated with environmental stimuli. Once associated to the drug, the presentation of an environmental stimulus alone can predict drug availability, evoke memories of the effect of the drug and ultimately elicit the drug taking (Garavan et al. 2000; Everitt et al. 2008). Those mechanisms are highly reproducible in animal models undergoing a classical pavlovian conditioning, in which the drug-associated stimulus is called conditioned stimulus (CS). It has been shown that in the presence of a CS, the instrumental learning for cocaine self-administration is selectively interrupted by disruption of the connection between NAc and basolateral amygdala (Whitelaw et al. 1996), or by selective lesions of both NAc core (Ito et al. 2004), and the connection between NAc core specifically and basolateral amygdala (Di Ciano & Everitt 2004). While the NAc seems to be more related to the instauration of goal-directed actions, two interesting studies of Yin and collaborators showed that lesions of the dorsolateral striatum, the striatal region mostly implicated in habits formation, preserved the outcome expectancy but disrupted habits formation in relation with cocaine conditioning (Yin et al. 2004; Yin et al. 2006). These hypotheses are strengthened by several other results that involve approaches different from neuronal

lesions. Evidences from in vivo microdialysis measurements of extracellular DA, showed a shift in the location of the DA release in rats trained over two months in a cocaine self-administration paradigm: self-administered cocaine increased extracellular DA levels in the NAc and DS However, while the presentation of the stimulus alone at the beginning of training increased DA only in the core of the NAc, the release of DA shifted to the DS when the stimulus was presented after a long training period (Ito et al. 2002; Ito et al. 2000). Indeed DA receptor antagonist α-flupenthixol, decreases cocaine self-administration under a second-order schedule of reinforcement when infused into the DS (Vanderschuren 2005). In the same period Porrino and collaborators used autoradiography of selected markers of the DA system to evaluate the neuronal adaptations of the striatum during chronic cocaine self-administration in monkeys. This instructive study showed that the response to cocaine self-administration within the striatum shifts dramatically over time (5 days, 3.3 months, and 15–22 months). The increase in the duration to the cocaine exposure correlates with both changes in functional activity and alterations in the dopamine system by involving larger and larger portions in the more dorsal part of striatum. In particular, a decrease of the D2 and D3 dopamine receptor density has been observed in the dorsal striatum following chronic, but not acute, cocaine self-administration (Porrino, Daunais 2004, Smith, & Nader, 2004). The same results have been reported in monkeys, after months but not weeks of cocaine self-administration. (Letchworth et al. 2001). More recent studies have proved that - contrary to the medial part of the dorsal striatum - the dorsolateral striatum in not involved in the instatement of the cocaine seeking behaviour: the administration of a DA antagonist in the dorsolateral striatum does not affect at all cocaine self-administration (Murray et al. 2012). The DS, with the PFC and the basolateral amygdala, is also involved in the mechanism of relapse: the specific inactivation of the dorsolateral striatum attenuates cocaine seeking after abstinence (Fuchs 2006). Also, in 2007 See and collaborators used a gamma-aminobutyric acid agonist in order to inhibit SN, VTA, DS, and NAc in rat that learned to self-administer cocaine: while the inactivation of the dorsal striatum and midbrain regions attenuated cocaine seeking, inactivation of the ventral striatum had no such effects. Interestingly, subsequent training sessions under extinction conditions revealed a rebound in cocaine seeking in animals that had undergone inactivation in all regions except the dorsolateral striatum (See et al. 2007).

The PFC is another region of the reward system highly involved in the drug addiction. Structural MRI pointed out that cocaine-addicted patients are – among other regions - affected by a significant decrease of the gray matter in the medial prefrontal cortex (Ersche et al. 2012) Importantly, the down-regulation of the D2 receptors in the striatum correlates with the hypometabolism of the orbitofrontal cortex, which is represented by the medial prefrontal cortex in its medial part (Ersche et al 2012). Different works have shown a direct reciprocal connection between VTA and PFC (Carr & Sesack 2000). The activity of the neurons of the VTA is regulated by the direct input from the PFC. Glutamate increases the activity of the dopaminergic neurons in the VTA (Taber & Fibiger 1995) and facilitates DA release from the presynaptic terminals in the NAc (Floresco et al. 1998). Thus, electrical or chemical stimulation of the PFC accounts for both dopamine release in the NAc and burst the firing of dopamine neurons (Murase et al. 1993; Taber & Fibiger 1995; Tong et al. 1996; You et al. 1998; Jackson et al. 2001). Cocaine stimulates glutamate release in the PFC and NAc (Reid & Berger 1996). The stimulation is potentiated by repeated cocaine exposure (Reid & Berger 1996). In the PFC cocaine binds also norepinephrine leading to increased levels of extracellular norepinephrine. In 2006, Han D. and Gu H. showed that cocaine can bind with an overall equal affinity to both the DA and the norepinephrine receptor (Han & Gu 2006). This would lead to activation of alpha1-noradrenergic receptors, and possibly influence the signal transmitted by the PFC to the VTA altering the action-potential dependent DA release. The PFC seems to be fundamental also in the inhibitory control of relapse. Lastly, it is now widely accepted that the connection between medial PFC (mPFC) and the posterior medial striatum accounts for the goal-directed system in both rats and humans (Shiflett et al. 2010). On the other hand, the habit system implicates the anterior dorsolateral striatum, and perhaps motor cortical areas (Balleine & O'Doherty 2010)

3.3.2 Effect of cocaine on neuroplasticity

General introduction.

Neuroplasticity is often referred as the capacity of the brain to functionally

remodel its neuronal circuits in response to experience and the environment. Although neuroplasticity can occur at a variety of levels, ranging from molecular changes in synapses to large scale changes involved in neurocircuitry remapping, it is possible to define two main different classes of neuroplasticity: (1) the activity-dependent alteration of connections among neurons, such as the creation of new synapses and the pruning of the existing ones, and (2) the changes in the intrinsic excitability of neurons (Malenka & Bear 2004; Lammel et al. 2011). It has been proposed that we could look at addiction as a disease of the goal-directed learning (Hyman 2005; Redish et al. 2008). According to this model, repeated exposure to drugs could promote learning of drug-related behaviours with such efficacy that they become compulsive. In other words, drugs would override the mechanisms that are taking place during normal reward learning (Redish 2004). All these considerations make the synaptic plasticity a good candidate for the persistence of addiction-related behaviour. Synaptic plasticity can be classified in two different forms: short-term and long-term synaptic plasticity. The short-term synaptic plasticity acts within milliseconds or minutes, and accounts only for transient and fast modification such as synaptic facilitations. Long-term synaptic plasticity acts within hours or day. Repeated stimulations, such as drug exposure, could turn the short-term synaptic plasticity into long-term synaptic plasticity. The best-characterized forms of synaptic plasticity are the activity dependent or N-methyl-D-aspartate receptor (NMDAR)-mediated long-term potentiation (LTP), and long-term depression (LTD) (Watt et al. 2004) LTP occurs when the presynaptic stimulation coincides with the postsynaptic depolarization (Hebb, D.O. (1949). *The Organization of Behavior*. New York: Wiley & Sons; (Nakamura et al. 1992)) while LTD occurs when presynaptic activation comes along with postsynaptic inactivity (Kullmann & Lamsa 2007).

Evidences of cocaine-dependent regulation of the synaptic plasticity in the VTA

A single non-contingent dose of cocaine is able to induce an augmentation of the AMPAR/NMDAR ratio, and so a considerable potentiation of the excitatory synaptic transmission, in the DA neurons of the VTA (Ungless et al., 2001). The potentiation can be measured 24 h after the cocaine injection, is lost one week later, and is

restricted to the DA neurons projecting to the Nac (Lammel et al. 2011). Mameli and collaborators in 2011, and Yuan and collaborators in 2013 showed that the increase in the ratio is due to an increase of the AMPAR-dependent currents, related to the insertion of Ca^{2+}-permeable Glu2A subunit containing AMPARs and to the reduction of the NMDAR-dependent currents, related to the insertion of the semi-Ca^{2+}-impermeable NMDARs containing GluN3A and GluN2B subunits (Yuan et al. 2013). mGluR5 and mGluR1 are two other receptors implicated in the mechanisms of synaptic plasticity in the context of cocaine action. Several studies have shown that the induction of mGluR1-dependent LTD is able to reverse the synaptic plasticity induced by cocaine (Bellone & Lüscher 2006; Mameli et al. 2007). In the VTA, mGluR1 binds to isoforms of the scaffolding protein Homer to induce LTD. When this interaction in the VTA is disrupted, the plasticity response to a single injection of cocaine in the NAc becomes comparable to the synaptic adaptations that are normally obtained by chronic cocaine injections. Interestingly, the opposite is true in the NAc, where mGluR1 is a positive modulator of synaptic plasticity (Knoflach et al. 2001; Mameli et al. 2009).

Evidences of the cocaine regulation of the synaptic plasticity in the NAc

Unlike in the VTA, multiple non-contingent doses of cocaine administration are required to elicit synaptic plasticity in excitatory synapses in the NAc (Thomas et al., 2001. Two different studies showed that in the NAc, 10 to 14 days of repeating cocaine administration cause a reduction in the AMPAR/NMDAR ratio (Thomas et al. 2001; Beurrier & Malenka 2002). Later, in 2008 Thomas and collaborators showed a repression of the AMPAR currents in brain slices from rats injected with cocaine for 8 days. Furthermore, the activation of D1Rs by DA leads to an enhanced reduction in the AMPAR-mediated synaptic transmission, but not NMDAR-mediated synaptic transmission in the NAc shell (Beurrier and Malenka, 2002). Interestingly, it has been recently shown that in the NAc, non-contingent exposure to cocaine leads to the generation of so-called silent synapses after one or two days of withdrawal (Huang et al. 2009). The number of synapses is increasing with the duration of cocaine injections and goes back to normal after a long period of

withdrawal. Two different studies in 2013 and 2014 respectively showed an increasing number of silent synapses in the 2 major glutamatergic inputs to the NAc: amygdala and PFC (Lee et al. 2013; Ma et al. 2014). In both conditions, extended withdrawal led to the recruitment to the AMPA receptors.

Cocaine-induced structural plasticity

Importantly, the regulation of synaptic plasticity described above correlates with a regulation of the structural plasticity. In 2007 Sarti and collaborators showed an increase in synaptic density in the VTA following a single injection of cocaine and in the same cells that exhibited the increase of the AMPAR/NMDAR ratio. Numerous studies reported that cocaine and other drugs of abuse produce persistent changes in the structure of dendrites and dendritic spines in D1 and D2 SPNs in the NAc (Lee et al. 2006; Li et al. 2012). Importantly, it appears that the new spines induced by cocaine in the NAc are more stable in D1 SPNs. Interestingly, cocaine induces ΔFosB preferentially in D1 neurons (Hope et al. 1994; Nestler 2008). Correlating with the persistent increase of spines in D1 neurons, ΔFosB accounts for the transcriptional regulation of several genes involved in the shaping of synapses: Cdk5 (Bibb et al. 2001), synaptogamin 6, and microtubule-associated protein 2 (McClung & Nestler 2003), activity-regulated cytoskeleton-associated protein (ARC) (Renthal et al. 2009). Moreover, chronic cocaine administration reduces the activity of Rac1, leading to the intensification of the polymerization rate of filamentous actin in the NAc

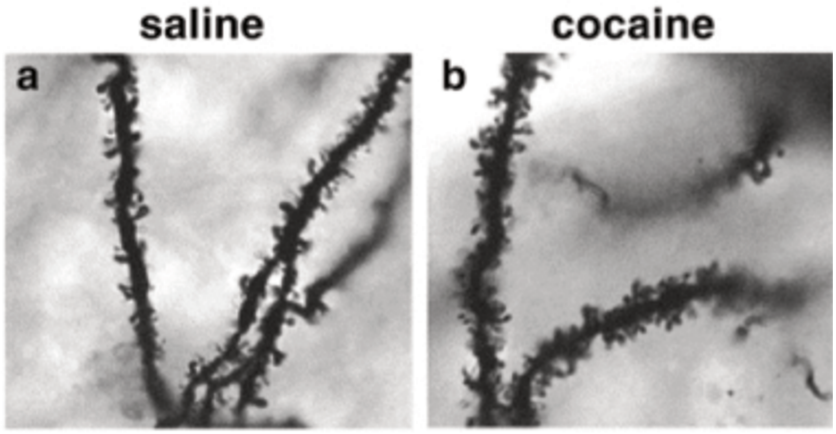

Figure 11: **Cocaine-induced structural plasticity**. Representative image of dendritic process from the NAc shell of rats daily administer with either cocaine (**B**) or saline (**A**) for 4 weeks. Repeated injection induce an increase in spines density as shown in b. Bar=10 micron (from Norrholm et al. 2003)

Cocaine-induced gene transcription.

Long-lasting modifications induced by exposure to drugs require *de novo* gene transcription and are likely to involve epigenetic modifications. Early works showed that drug administration regulates two different waves of gene expression. The first wave of genes that are transcribed are immediately early genes (IEGs). The transcription of those genes is mainly transient, does not require protein synthesis, and is activated within minutes after the drug administration. In the case of cocaine, the transcription level of the IEGs reaches a peak within 1 hour and returns to basal level by 2 hours after cocaine injection. Often the products of the IEGs are transcription factors that are in turn mediating the transcription of the second wave of genes. Several works focused on elucidating the regulation of the gene expression induced by cocaine administration in the striatum (e.g. Heiman et al. 2008). Interestingly those studies showed that the transcription factors such as ΔFosB, CREB, NFk B, and MEF2, and epigenetic histone acetylation are the main classes of genes induced by chronic cocaine administration. As an example of the importance of the transcriptional regulation dependent on cocaine treatment, two transcription factors regulated by cocaine and in feedback involved in the structural plasticity and the behavioural response induced by cocaine will be discussed: ΔFosB and CREB.

ΔFosB. Acute cocaine treatment increases the expression of the Fos family transcription factors in the NAc (Graybiel et al. 1990; Hope et al. 1992). All the Fos family members are able to form heterodimers with Jun family proteins (c-Jun, JunB, JunD). Once formed, the heterodimer can regulate the transcription of selected genes by binding to the activator protein-1 (AP-1) sites present within the promoters. The maximal induction of Fos proteins occurs within 1-2 h after drug administration and returns to normal levels within 8-12 h. All members of the Fos family proteins are induced by acute cocaine exposure; however, their expression is attenuated upon repeated drug treatment (tolerance). The truncated form of FosB, ΔFosB, accumulates for several weeks after repeated cocaine injections (Hope et al., 1994). This is due to its long half-life that is even further enhanced when it is phosphorylated on Ser27 (Ulery-Reynolds et al. 2009). In particular ΔFosB accumulation seems to occur preferentially in the D1 SPNs subtype. (Hope et al. 1994; Moratalla et al. 1996; Kelz et al. 1999; Nestler et al. 2001). ΔFosB stability provides a molecular mechanism by which drug-induced changes in gene expression can persist despite long periods of drug withdrawal (Nestler, 2001). As mentioned above, due to its capacity to induce the transcription of several genes related to the remodelling of the cytoskeleton, ΔFosB is necessary to the instauration of the structural synaptic plasticity induced by cocaine. However, this mechanism requires CaMKIIα, which expression is increased following chronic cocaine exposure as well; importantly those 2 proteins have been found to be up-regulated in the post-mortem NAc of patients addicted to cocaine (Robison et al. 2013). Although ΔFosB is only slightly induced after cocaine treatment, its overexpression is able to enhance the rewarding properties of cocaine, as assessed in the conditioned place preference (CPP) for cocaine, the cocaine self-administration, and the cocaine-induced locomotor activity. Of note, the overexpression of ΔFosB in D1 SPNs results in the decrease of the AMPAR/NMDAR ratio, the increase of silent synapses on these neurons in the NAc, and in a decrease of the immature spines (Grueter et al. 2013). Conversely, overexpression in D2 R-MSNs results in increased excitatory synaptic strength and in the decrease of silent synapses in the specifically in NAc shell only (Grueter et al., 2013).

CREB. CREB is a member of the leucine-zipper transcription factors family, that constitutively binds to a specific sequence of DNA called CRE (cAMP-response-element) in the promoter region of specific genes including *c-fos*, *dynorphin*, and *encephalin* (Shaywitz & Greenberg 1999). The phosphorylation of Ser133 by either PKA, CaMK II/IV, p90 ribosomal S6 kinases 1/2 (RSK1/2), mitogen- and stress-activated kinases 1/2 (MSK1/2), or PKC (Johannessen & Moens 2007) is necessary to activate CREB and to induce its interaction with its co-activators CREB binding protein (CBP) and p300 (Lundblad et al. 1995). Both co-activators have a histone acetyl-transferase activity. The acetylation of histones induced by the 2 co-activators, allows the relaxation of the chromatin and promotes the transcriptional activity of CREB together with the recruitment of RNA polymerase II that triggers mRNA synthesis (Bannister & Kouzarides n.d.; Kwok et al. 1994); Acute and chronic cocaine treatment is able to induce the CREB in different brain regions (Walters et al. 2003; Carlezon et al. 2005). The induction of CREB activity appears to become greater and more persistent with repeated drug exposures. CREB, unlike ΔFosB, reduces the sensitivity to the rewarding effects of cocaine (tolerance) and increases the self-administration and relapse via negative reinforcement. Virally- mediated overexpression of CREB in the NAc decreases tolerance to cocaine, whereas reduction in CREB activity - via overexpression of a negative-mutant form of CREB in the NAc - has the opposite effects (Carlezon et al. 1998; Barrot et al. 2002). The ability of CREB to decrease reward is mediated by the induction of the expression of dynorphin peptide (Cole et al. 1995). Dynorphin acts on κ opiod receptors in VTA neurons to decrease dopamine release in the NAc (Spanagel et al. 1992), thus impairing rewarding behaviours (Carlezon et al. 1998; Muschamp et al. 2011; Ehrich et al. 2014). Lastly, CREB is necessary for the induction of ΔFosB. The genetic deletion of CREB in the SPNs, increases the cocaine conditioned place preference (CPP) and the cocaine-induced locomotor sensitization (Carlezon et al. 1998; Walters et al. 2003; McClung & Nestler 2003).

Notably, the major limitation of those types of studies is the impossibility to distinguish the transcriptional changes occurring specifically in D1 and D2 SPNs.

Only one pioneer work in 2008 (Heiman et al. 2008), made use of the TRAP

technology to immune-precipitate cell specific mRNA from D1 or D2 neurons in the striatum. The mRNA was then used for microarrays analysis in order to elucidate the cocaine-induced transcriptional changes in the two populations of cells. For this study, adult mice were non-contingently treated with cocaine or saline in an acute or chronic paradigm and used for translational profiling of striatonigral (Drd1a) and striatopallidal (Drd2) SPNs Heiman et al. 2008. This work showed hundreds of genes being specifically regulated in the two types of neurons and confirmed some of the cocaine-induced genes already known, by adding additional information on the neurons in which those mRNA are regulated. Some examples of the genes already known as responsive to cocaine: Cartpt (Douglass et al. 1995) enriched after acute treatment in D1 neurons, Fosb (Hope et al. 1992) up-regulated in acute treatment in both striatonigral and striatopallidal, and only in D1 after chronic cocaine administration; Homer1 (Brakeman et al. 1997), up-regulated by both acute and chronic treatment, in both D1 and D2 neurons; Per2 (Yuferov et al. 2003) up-regulated in D2 after acute treatment and in both D1 and D2 after chronic treatment Vamp2 and Kcnd2 up-regulated by chronic cocaine treatment in D1 and already described in McClung and Nestler, 2003 and Zfp64 up-regulated striatopallidal neurons after acute cocaine treatment and down-regulated in striatopallidal following the chronic treatment (McClung & Nestler 2003)

Although really instructive, this work still presents two major limitations: first the mRNA study has been performed by microarray, that present as prior limitation the fact that only the genes on the chip can be investigated; second the study has been conducted in the full striatum. In the light of the different connections and responses in the NAc and the DS a profiling of D1 and D2 neurons taking into account the different location of the neurons in the striatum would give a more comprehensive view of the changes occurring in the striatum after the stimulation of the reward system.

- Chapter 4-

Homeostatic and hedonic mechanisms driving the feeding behaviour

4.1 The feeding behaviour

The regulation of an adequate energy intake in the body is the *sine qua non* condition for surviving. Indeed, the vertebrate's brain has evolved complex neural circuits in order to insure the high priority of the feeding process. The feeding behaviour represents a very complex mechanism involving homeostatic and motivation pathways. The homeostatic control of the food pathway involves the regulation of energy balance by increasing the motivation to eat following exhaustion of the energy store. The hedonic properties of food raise a valuable contribution to the feeding control. The hedonic based control of feeding exhibits a reward-based regulation. The exposure to highly palatable or highly fat food can disrupt the normal appetite regulation (Erlanson-Albertsson 2005) and induce the development of compulsive-like approach to the food leading to obesity (Johnson & Kenny 2010)

Thus, to understand the rewarding nature of food, it is necessary to comprehend the link between the homeostatic and hedonic brain circuit that is the basis of a correct intake of calories and feeding behaviour

4.2 Homeostatic aspects of food intake

The homeostatic control of food intake is mainly related to the regulation of the energy balance. To ensure the availability of a correct amount of food, the brain needs to tightly communicate with the periphery, control the levels of the different nutrients circulating in the blood system, and be informed about the availability of food in the external environment (Berthoud 2007).

The hypothalamus is one of the regions of the brain more implicated in collecting and integrating information from the peripheral organs. The hypothalamus can be divided in different nuclei based on anatomical boundaries (Bernardis & Bellinger 1993), gene expression (Broberger et al. 1998; Lein et al. 2007) and function (reviewed in Saper et al. 2002). The main nuclei of the hypothalamus include

the arcuate nucleus (ARC), the paraventricular nucleus (PVN), the ventromedial nucleus (VMN), the dorsomedial region (DMV), and the lateral hypothalamic area (LHA). The importance of these nuclei in energy homeostasis was first suggested by classic experiments of lesion performed in rodents (reviewed in Suzuki et al. 2012). According to those studies, ARC is the area that collects information on the body energy state from the blood brain barrier, DMV the area more related to the sense of satiety, and the LH the area involved in the activation of the feeding response (reviewed in Quarta & Smolders 2014). After the evaluation of the amount of nutrients in the body, two different mechanisms can be activated in the hypothalamus: the anabolic pathway or the catabolic pathway.

The catabolic pathway is activated by the peripheral production of anorectic signals and has as final effect the stimulation of the sense of satiety. Leptin is a well-known example of an anorectic hormone able to shift the system to the interruption of the feeding behaviour. Leptin is synthesized and released by adipose tissue and acts principally in the ARC nucleus of the hypothalamus where it stimulates the secretion of two potent anorexigenic neuropeptides: the melanocyte-stimulating hormone (MSH), and the cocaine and amphetamine-regulated transcript (CART) peptide. Simultaneously, leptin is also able to inhibit neurons expressing the Agouti-related protein (AgRP) and Neuropeptide Y (NPY)-producing neurons, which co-express the orexigenic neuropeptides AgRP and NPY, and antagonizes MSH.

Contrary to the catabolic pathway, the anabolic pathway is activated during low energetic states. It involves the production of orexigenic signals such as ghrelin, and has as final output the induction of feeding behaviour (Atalayer 2013). Interestingly, the receptors for ghrelin can also be found in the VTA while the leptin receptors are enriched in both VTA and SN, suggesting that these peptides can control even the reward regulation of the feeding (Morton & Schwartz 2011).

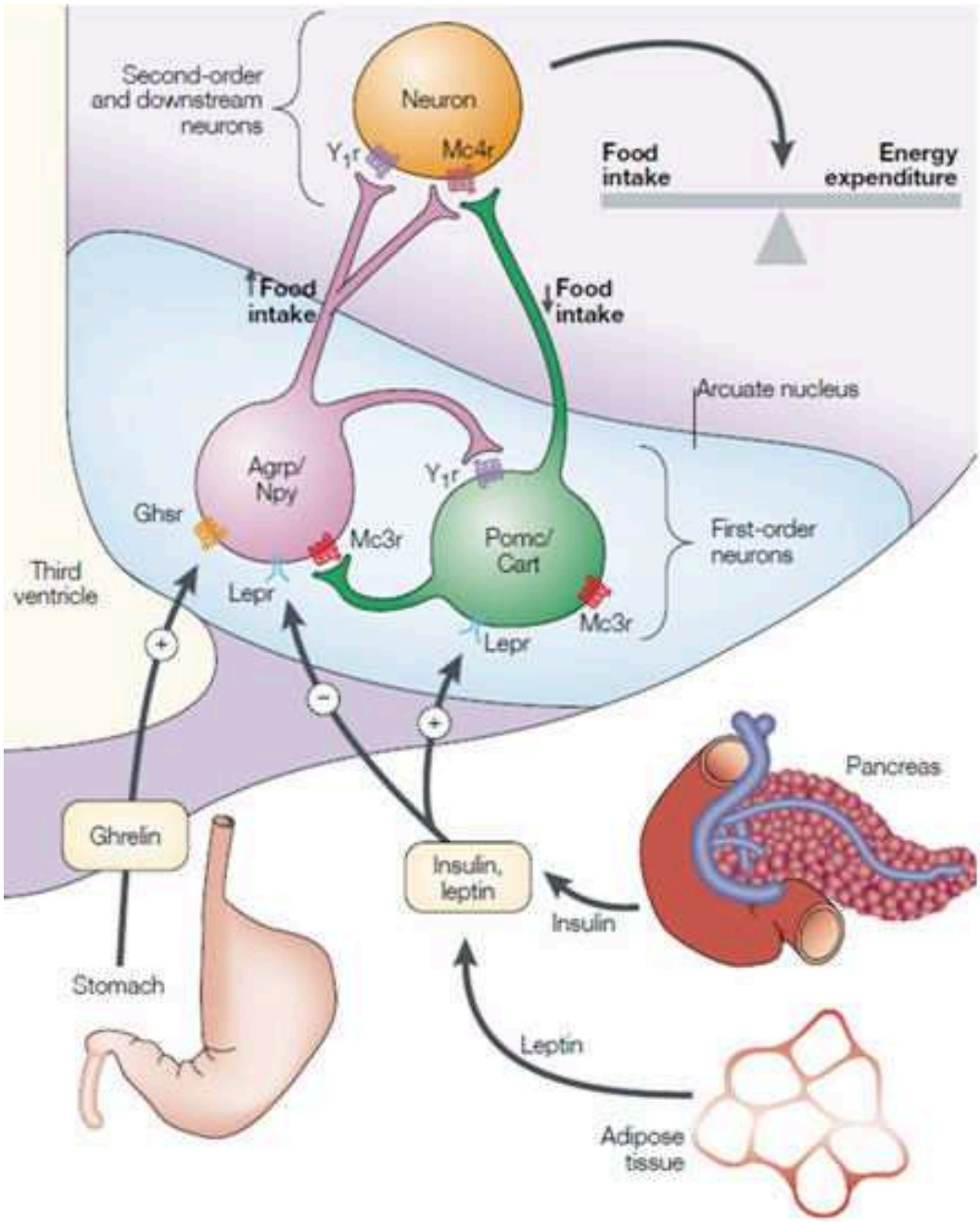

Figure 12: **Schematic representation of the homeostatic mechanisms of the regulation of food intake** In the arcuate nucleus, nneuropeptides AGRP and NPY stimulate food intake, whereas αMSH and CART inhibit food intake. Insulin and leptin are produced by the adipose stores. They inhibit AGRP/NPY neurons and stimulate adjacent POMC/CART neurons. The circulating peptide ghrelin is secreted from the stomach and can activate AGRP/NPY neurons and stimulate appetite.

4.2.1 The lateral hypothalamus, a centre of relay of homeostatic and hedonic control of food intake

Until 1990, the general mechanism accepted for regulation of food intake was based on a model that attributed to the lateral hypothalamus area (LHA) the drives to eat, and to the ventral hypothalamus the sense of satiety. While lesions of the LHA result in the suppression of both feeding (ANAND & BROBECK 1951) and drinking (MONTEMURRO & STEVENSON 1957), the lesion of the ventral hypothalamus promotes feeding and body weight gain (Hetherington & Ranson 1940).

Although this model is still useful in some aspects, different studies in the last 15 years proved the existence of a much more complex system, in terms of both molecules and circuits involved. The LHA is a heterogeneous structure located anterior to the VTA and through which pass the fibres of the medial forebrain (Nieuwenhuys et al. 1982). The LHA contains a plethora of different types of cells, including a mixture of excitatory and inhibitory neurons as confirmed by the enrichment in both vesicular glutamate transporter type 2 (Vglut2) mRNA (Collin et al. 2003; Rosin et al. 2003; Ziegler et al. 2002), and GABAergic markers (Karnani et al. 2013).

Orexin-producing neurons

Orexin is a neuropeptide that regulates arousal, wakefulness and appetite (Davis et al. 2011). The genetic ablation of the Orexin neurons results in narcolepsy, hypophagia and obesity (Harris et al. 2005). More recently it has been shown a major implication of the Orexin neurons in the regulation of arousal, as optogenetic stimulation of Orx neuron increases wakefulness (Adamantidis et al. 2007).

The name orexin comes from *orexis,* appetite in Greek. Consistently with its name, orexin is thought to be involved in feeding and in reward related behaviours. Injections of the peptide into the lateral ventricle increases food intake (Sakurai, T.

1999), while the treatment with Orx receptor antagonists or genetic removal of Orx results in a decrease of consumption (Haynes et al. 2002). Food restriction cause an increase of the orexin mRNA (Clegg et al. 2002; Sakurai 1999) and hypoglycaemia induces an increase of the Orx mRNA expression as well as an increase in Fos expression (Cai et al. 1999; Griffond et al. 1999; Moriguchi et al. 1999).

Melanin-concentrating hormone (MCH)-producing neurons

The melanin-concentrating hormone (MCH)-producing neurons constitute another important group of hypothalamic cells distinct from the Orx-producing neurons (Broberger et al. 1998). MCH-producing neurons are predominantly located in the LHA (Bittencourt et al. 1992) and project widely throughout the brain (Elias et al. 1998). MCH neurons are composed of subsets of inhibitory and excitatory cells as shown by co-expression of MCH with GAD67 or Vglut2 (Harthoorn et al. 2005). As the Orx producing neurons, MCH neurons have also been implicated in the regulation of feeding, and in the sleep-wakefulness balance. However, it has been hypothesized that MCH and orexin neurons have opposite roles in controlling arousal states (reviewed Brown et al. 2015). Indeed, contrary to orexin neurons, the activation of MCH neurons promotes REM sleep (Herrera et al. 2016).

MCH-producing neurons are thought to play a fundamental role in the regulation of feeding behaviour and body weight. Intracerebro-ventricular injections of the peptide increase feeding and body weight in rodents. MCH mRNA levels are increased by food deprivation, and leptin-deficient OB/OB mice express elevated levels of MCH (Qu et al. 1996). Furthermore, genetic studies have revealed that mice lacking MCH neurons (Alon & Friedman 2006) or the MCH gene (Shimada et al. 1998) are hypophagic and lean. On the other hand, the over-expression of MCH results in hyperphagia, resistance to insulin, and obesity (Ludwig et al. 2001). Interestingly, the NAc is a major input of the MCH producing neurons. This direct connection makes MCH neurons and their receptors suitable candidates to link the homeostatic aspects of feeding with the reward aspects of feeding.

Neurotensin-producing neurons

Neurotensin-producing neurons are a group of cells located in the pre-optic and anterior hypothalamic regions. Neurotensin neurons do not co-localize with MCH and Orx, however they present ~95% overlap with galanin-expressing neurons. Neurotensin producing neurons mediate the anorexigenic leptin action (Laque et al. 2013). The administration of Nts at both peripheral and central level suppresses feeding (Cooke et al. 2009). In agreement with these results, both the genetic ablation of a subset of Neurotensin neurons (Kim et al. 2008) and the knock out of the Neurotensin receptor (Leinninger et al. 2011) result in hyperphagia and obesity.

Input circuits of the LHA

The LHA collects excitatory and inhibitory inputs from both cortical and subcortical structures:

Glutamatergic inputs. The LHA receives two major glutamatergic inputs: the monosynaptic glutamatergic inputs from the hippocampus (NAUTA 1958), and the monosynaptic and polysynaptic inputs from the medial PFC (Kita & Oomura 1981)

GABAergic inputs. The GABAergic afferents represent the major input to the LHA. GABAergic inputs come from several structures of the basal forebrain and from other subcortical fibres via the septum (Anthony et al. 2014)

Input from the bed nucleus of the stria terminalis (BNST)/pre-optic area. The fibres of the ventral BNST and connected structures send monosynaptic inputs that predominately inhibit postsynaptic LHA glutamate neurons. This pathway seems to be tightly connected with the feeding control, such that the stimulation of this connection via optogenetics results in both the fast initiation and the increase of the feeding behaviour towards highly palatable or highly fat food. The amplitude of the response is proportional to the dose of stimulation. Mice learn quite fast to self-stimulate this circuit and interestingly, the self-stimulation is majorly regulated by satiety or food deprivation (Stamatakis et al.

2013).

Input from the nucleus accumbens shell. The majority of projections from the NAc are arising from the D1 SPNs, although some D2 projection can also be found. The very first work suggesting the communication between the NAc and hypothalamus dates back to 1995. In this work, Maldonado-Irizarry and collaborators investigated the role of excitatory amino acid inputs to the NAc (core and shell) in feeding behaviour of rats. In the first series of experiments, it was shown that blocking AMPA and glutamate receptors with DNQX in the medial shell, but not core, results in an increase of the feeding behaviour. This feeding response was blocked by the local injection of AMPA, while no effects were elicited by NMDA antagonist infusion. Interestingly, the prior administration of D1 or D2 antagonist receptors decrease by half the feeding induced by DNQX, suggesting a major implication of the DA in the feeding. Lastly, antagonizing directly in the lateral hypothalamus results in a complete inhibition of the ingestive behaviour, suggesting the existence of an important functional link between two major brain regions involved in the homeostatic and hedonic regulation of the food intake: the LHA and the NAc (Maldonado-Irizarry et al. 1995). Complementary works showed that local injections of GABA receptor agonists or glutamate receptor antagonists in the nucleus accumbens shell elicit an intense feeding response resembling to the one seen after stimulation of the lateral hypothalamus. Furthermore, injections of a GABA-A receptors agonist in the shell of the NAc increased the number of cells positive to Fos staining in the LH, as well as in the lateral septum, paraventricular hypothalamic nucleus, ventral tegmental area, substantia nigra pars compacta and nucleus of the solitary tract (Stratford & Kelley 1997). Several works during the last decade tried to better describe the function of the connection between NAc and LHA. A work recently published by the group of Lüscher showed that the D1-expressing SPNs in the NAc inhibit GABAergic neurons, but not orexin or MCH producing neurons, in the more ventro-laterlal part of the LHA. The optogenetic inhibition of D1R-MSNs prolongs feeding in satiated mice even in presence of distracting external stimuli, whereas the activation of D1R-MSN terminals in LH is sufficient to override immediate

metabolic need and rapidly stop food consumption despite hunger. Furthermore, optogenetic inhibition of postsynaptic LHA-GABA neurons, which are inhibited by D1R-MSNs, suppresses the licking for a palatable reward consumption of food (O'Connor et al. 2015).

Other inputs to the LHA. Other subcortical fibres innervate the LHA from the lateral septum (Anthony et al. 2014), ventral pallidum (Root et al. 2015) and substantia innominate (Grove 1988). Projections are also arising from the midbrain and brainstem, including the inputs from the serotoninergic neurons in the raphe (Moore et al. 1978), and from the norepinephrine neurons in the locus coeruleus. Of note, several works described different intra-hypothalamic connections. For example, LHA connects with the arcuate nucleus (Betley et al. 2013) and, importantly, the stimulation of this pathway can evoke the feeding behaviour. An increase of the feeding behaviour is also obtained by optogenetic stimulation of the GABAergic fibres connecting the LHA with the periventricular hypothalamus (Wu et al. 2015). A connection with the ventral medial hypothalamus has also been described (Thompson et al. 1996).

Output circuitry of the LHA

Classical anatomy studies have demonstrated the existence of multiple projections of the LHA to the VTA, periventricular thalamus, lateral habenula, and many other regions (Berk & Finkelstein 1982). Two recent studies confirmed the existence and the importance of a direct output from the LHA to the VTA. In the first work, Nieh and collaborators clarified that the output is arising from both glutamatergic and GABAergic LHA fibres, and functionally innervates both GABAergic and DA neurons of the VTA. The specific stimulation of the LH-GABA-VTA pathway leads to feeding behaviour (Nieh et al. 2015). The second work showed that hypothalamic neurotensin projections promote reward by enhancing glutamate transmission in the VTA (Kempadoo et al. 2013). Of note, a major target of the orexin- and MCH-producing neurons includes the brainstem motor systems that support behaviours like chewing, licking, and swallowing. Those innervations include trigeminal and reticular neurons engaged during ingestive behaviour (Yamamoto et al. 1989). MCH and orx neurons also innervate critical sites that regulate oesophageal and gastric

mobility, as well as insulin secretion: the sympathetic and parasympathetic preganglionic neurons in the spinal cord (Ahrén 2000).

Notably, other targets of MCH- and Orexin-producing neurons are serotoninergic cells in the dorsal and medial Raphe, noradrenergic cells in the locus coeruleus, the NAc and the entire cerebral cortex.

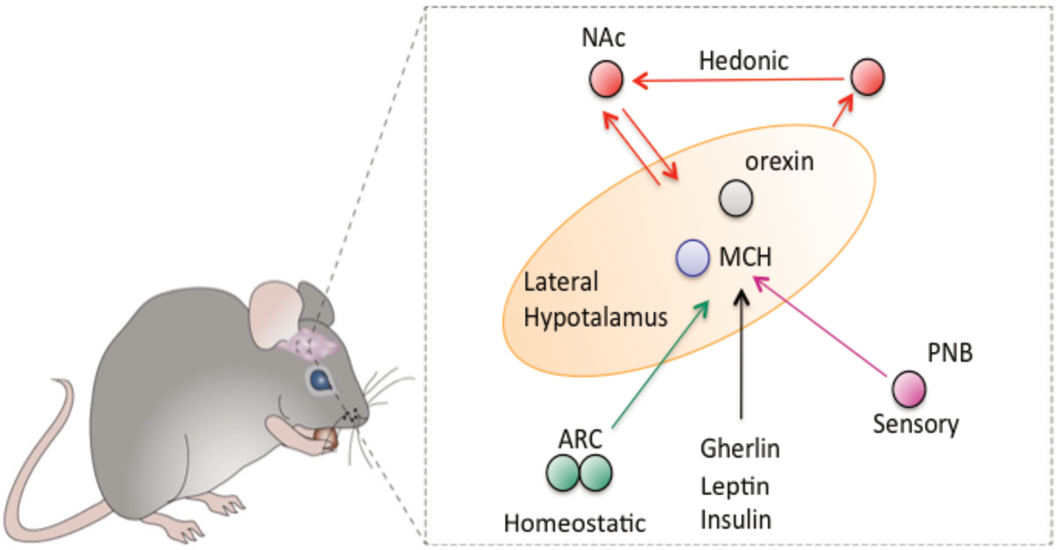

Figure 13: **Interaction between hedonic and homeostatic circuit regulating food intake.** The lateral hypothalamus connects to the homeostatic (ARC), hedonic (NAc, midbrain), and sensory (PBN) centres of regulation of the food intake. Abbreviations: ARC, arcuate nucleus; BNST, bed nucleus of the stria terminalis; LH, lateral hypothalamus; MCH, melanin-concentrating hormone; NAc, nucleus accumbens; PBN, parabrachial nucleus. (modified by Hess & Brüning 2014).

4.3 Hedonic aspects of food intake

It is now well recognized that appetite is not exclusively regulated by the homeostatic system within the hypothalamus. Certainly, the rewarding nature of food is one of the most potent drives for feeding. Avoiding the discomfort due to a hungry state may be itself a reward, and because of the rewarding properties of the food animals are willing to work. (Guegan et al. 2013). The liking and the wanting

properties of the food regulate the food intake (Berthoud 2007). While liking responses are mediated primarily by opioid and GABA mechanisms within the brainstem, wanting processes are predominantly mediated by enhanced dopamine transmission within the cortico-mesolimbic system (Alcaro et al. 2007; Berridge et al. 1996; Björklund & Dunnett 2007). Lesions impairing dopamine release within the cortico-mesolimbic structures substantially decrease rodents' food intake and body weight (Salamone et al. 1990; Salamone et al. 1993). Moreover, as discussed above, the mesolimbic DA system is sensitive to many important feeding peptides and chemicals, including ghrelin, leptin and other cannabinoids (Liu & Borgland 2015). The enhanced DA transmission within the reward system, induced by heightened VTA dopamine neuron activity, encourages motivational behaviours to obtain and consume food, especially palatable or rewarding foods (Lutter & Nestler 2009).

4.3.1 Signalling pathway underlying the hedonic control of the food

Signalling events downstream the dopamine receptors

Certain foods, such as highly palatable and highly caloric ones, can raise a reward effect even bigger than (that of) cocaine (Lenoir et al. 2007). From an evolutionary point of view, the rewarding properties of food are really advantageous: palatable food induces a major consumption and a major store of energy for the future needs. However, in modern societies, where food is widely available, this adaptation has become a liability: the major consumption can become overeating and lead to food disorders. Palatable food and environmental cues that predict their delivery, increase DA transmission within the striatum, thereby influencing striato-hypothalamic and striato-pallidal circuits that control the hedonic and incentive properties of food (Kenny 2011). Specifically, DA neurons in the VTA increase the firing rate and hence the DA release in the NAc in response to an unexpected food (Hajnal & Norgren 2001; Norgren et al. 2006). This DA response habituates with repeated exposure to the food reward, and is gradually transferred onto the stimuli associated with the reward (Epstein et al. 2009). The level of DA released in response to the

food reward is regulated by glutamatergic afferents from several other brain region related: a) to the sensory perception of the food (nucleus tractus solitarius and insula for taste, olfactory bulb and pyriform cortex for smell and visual cortices for the appearance of the food), b) to the homeostatic properties of the food (hypothalamus), c) to the reward (NAc), d) to the emotional (amygdala and hippocampus) and e) to the multimodal (OFC for salience attribution) properties of the food. In humans, ingestion of palatable food has been shown to release DA in the dorsal striatum in proportion to the self-reported level of pleasure derived from eating food (Small et al. 2003).

Signalling events downstream the opiod receptors

The endogenous opioid systems can regulate the hedonic value of food intake independently from the ongoing metabolic needs of the individual. β-endorphin and enkephalin positively contribute to the incentive-motivation to acquire food reinforcers. The lack of either enkephalin or β-endorphin peptides leads to a deficit in the ability of food reward to increase lever pressing behaviour, regardless of the palatability and nutrient content of the foods examined (Hayward et al. 2002). In both humans and mice, the exposure to sugar drives an analgesic response, suggesting an increase of the opiate signalling directly mediated by sugar (Lewkowski et al. 2003). Furthermore, it has been shown that it is possible to provoke an opiate withdrawal syndrome similar to that observed in animals chronically exposed to opioid drugs, in rodents previously exposed to a sugar-rich diet reviewed in Avena et al. 2008). The opiate signalling within the NAc and the VP mainly relates to food liking. The mu-opioid stimulates both the NAc shell, NAc core or VP and amplifies both the liking reactions to sweetness and appetitive wanting for food reward. NAc hotspots modulate the expression in the VP and *vice-versa*. The opioid signalling in the basolateral amygdala is implicated in conveying the affective properties of food, which contribute in food wanting as well as in modulating the incentive value of food and reward-seeking behaviour (Wassum et al. 2009).

Signalling events downstream the cannabinoid receptor

Several studies have highlighted the importance of endocannabinoids signalling in the regulation of feeding behaviour. In 2003, it has been shown that delta-9 tetrahydrocannabinol (THC), the active ingredient of cannabis, increases food intake. In this work, Higgs and collaborators examined the mode of action of cannabinoids on ingestion by studying the effect of CB1 receptor agonists and antagonists, on licking microstructure in rats ingesting a palatable sucrose solution. Contrary to the antagonist, the CB1 agonist decreased instrumental responding for food (Rasmussen & Huskinson 2008; Thornton-Jones et al. 2005). CB_1 receptor knockout mice display a reduced responding for sucrose or fat-enriched but not other types of food reward (Guegan 2012) as well as the absence of the structural plasticity induced by the training for highly sugar food (Guegan 2012).

The CB1 receptor is located on presynaptic terminals releasing GABA or glutamate in the cortex, hippocampus, amygdala, striatum, and hypothalamus. The retrograde activation of CB1 receptors regulates the release and the signalling of different neurotransmitters involved in feeding behaviour, such as DA, or orexin. Of note, when injected in the shell of NAc, the endogenous CB_1 receptor ligand anandamide enhances the liking of a sweet reward (Mahler et al. 2007). The endocannabinoid signalling elicited by the stimulation of the CB1 receptor takes part in several mechanisms of feeding: the homeostatic regulation (Lattemannand D., 2008) and the hedonic regulation of food intake, and the regulation of the energy expenditure (D. Richard, *et al.2009.* I. Matias, V. Di Marzo 2007).

Structural plasticity induced by highly palatable food

Surprisingly, although numerous studies have already reported that cocaine and other drugs of abuse produce persistent changes in the structure and number of dendritic spines on D1 and D2 SPNs, few groups investigated if the same changes are taking place following the stimulation of the reward system with natural rewards. In 2012, the group of Martinez gave a major contribution to the field. Guegan and co-workers showed that operant training for highly palatable food leads to an augmentation of the dendritic spines in the NAc-shell and in the medial PFC but not in the NAc-core. These structural changes seem to be specifically related to learning, as the yoked control groups (non-contingently receiving the same amount of food) did not display any structural rearrangement. In the same paper it was also shown that similar modifications were not induced in CB1R-KO mice, confirming a major implication of the CB1R in the regulation of the reward-related consumption of food (Guegan et al., 2012). In a similar work, Mancino S. and collaborators showed that changes in the density of specific dendritic spines could be found not only in the NAc shell and PFC, but also in the hippocampus (HP) of mice trained in an operant training to obtain chocolate-flavoured pellets. Moreover, the analysis of the spine morphology showed that the operant training increased stubby spines density in the HP and filopodia density in the PFC and NAc shell. Interestingly, the same paper has been also shown that knocking out the gene for the delta opioid receptor 1 (DOR1) results in the abolishment of the operant-induced spine formation. DOR1-KO mice showed also reduced levels of stubby spines in PFC and HP and a decreased filopodia spine density in the PFC and NAc shell. Consumption of high-energy diets may compromise health and may also impair cognition; these impairments have been linked to tasks that require hippocampal function. Conversely, food restriction has been shown to improve certain aspects of hippocampal function, including spatial memory and memory persistence. It has been recently proved that those observations correlate with changes of neuronal plasticity in hippocampus (Babits R., 2016).

All the studies discussed above focused on NAc, cortex and hippocampus. In a recent work, J. Ibias and co-workers examined whether schedule-induced polydipsia (SIP), an adjunctive behaviour in which rats exhibit excessive drinking as

a consequence of intermittent feeding, would induce modifications in SPNs in dorsolateral striatum (DLS) and in the basal dendrites of layer V pyramidal cells anterior prefrontal cortex (aPFC) neurons. The reported results showed that SIP caused an increase in dendritic spine density in DLS but not aPFC neurons. The authors hypothesized that SIP-induced structural plasticity in DLS neurons could be related to an inflexible response in compulsive behaviour and demonstrate the involvement of the dorsolateral striatum and anterior prefrontal cortex regions in compulsive disorders and in the control of the feeding behaviour (J. Ibias et al., 2016). Importantly, different studies suggest that this hypothesized inflexibility is due to a structural plasticity specific to the D2-SPNs (Bock R., 2013; Johnson PM., 2010).

In conclusion, in the last years considerable progress has been made in unveiling homeostatic and hedonic pathways that regulate signals for feeding. Today, the existence of a tight communication between the systems of neurotransmitters and peptides in midbrain and corticolimbic areas is unquestionable. The studies of the last 15 years consider the hypothalamus as the centre of the homeostatic control of the food, and the lateral area of the hypothalamus as the direct rely between the homeostatic and the rewarding control of the food intake. It is also clear that the meso-corticolimbic system with DA, 5HT, and opioid and cannabinoid systems, is likely to play prominent roles in the hedonic control of the feeding.

As discussed, the rewarding properties of highly palatable food can override the homeostatic control of food intake and lead to food disorders such as obesity. Indeed, it has been shown that - as for drugs of abuse –highly palatable food triggers the formation of new spines that could be the substrate of maladaptive neuronal modifications

- Chapter 5 -

Profiling discrete neuronal populations

The central nervous system is characterized by large cell heterogeneity as well as remarkable flexibility in gene expression that modulates the correct action in response to a wide variety of environmental cues. Multicellularity represents a serious limit to study the alterations in gene regulation within individual cell types.

The very first representation of the cell composition and diversity of the central nervous system dates from the end of the XIXth century, when Ramon y Cajal used Golgi staining to show that neurons are one main component of the mammalian central nervous system (CNS) and to illustrate their diverse appearance. Ever since Santiago Ramon y Cajal discovered the varied structure of neurons, scientists have attempted to classify them into discrete groups.

The problem of distinguishing different subpopulations of neurons is particularly evident in the striatum. D1 and D2 SPNs are mostly indistinguishable in shape, size and number but they are highly segregated in two inhibitory outputs, and form two main efferent pathways - the direct and indirect pathway - that respectively activate or inactivate their end targets. Considering this heterogeneity, it is crucial to distinguish the two different populations. Analysing lysates of pooled neuronal populations averages the responses, masks low signals and changes in opposite directions in the two populations can cancel each other.

In the following paragraphs we review different techniques currently utilized to elucidate the biological properties of discrete neurons populations

5.1 Trangenesis strategies

One of the most promising approaches to study a pure population of cells is still to use mouse genetics methods to identify specific cell populations.

The development of transgenic strategies has permitted the expression of specific genes in both spatially and temporally defined patterns. Early in the 1980's several research groups (Gordon and Ruddle 1981; Costantini and Lacy 1981; Harbers et al.,

1981; EF Wagner et al., 1981, TC Wagner et al., 1981) developed methods to introduce a specific gene into the mouse genome, which could be inherited in a Mendelian fashion. Coding DNA sequences are microinjected into one or both pronuclei of zygote-stage embryos. Microinjected embryos are subsequently transferred into recipient females allowing the embryonic development.

In 1996 Mayford and colleagues, by using the bacterial tetracycline operator system initially developed by Bujard, achieved for the first time an inducible expression of a mutant form of the activated calcium-independent form of calcium-calmodulin-dependent kinase II (CaMKII) that was forebrain-specific (Mayford et al., 1996). The TetOff tetracycline system involves the tetracycline transactivator (tTA) protein, which is created by fusing one protein, TetR (tetracycline repressor), found in Escherichia coli bacteria, with the activation domain of another protein, VP16, found in the Herpes simplex virus, and the TetO operator placed upstream of the gene of interest (Gossen and Bujard, 1992; Gossen et al., 1995). Usually several repeats of TetO sequences are placed upstream of a minimal promoter such as the CMV promoter, forming together a so-called tetracycline response element (TRE). In the presence of a tetracycline (usually doxycycline), binding of tTA to TetO is prevented, and the gene of interest is not transcribed until doxycycline regimen is interrupted. Later on, TetOn systems were developed in which rtTA (a modified form of tTA) binds to TetO only in the presence of doxycycline. In this case the transgene is induced by doxycycline administration. Mayford and collaborators used tTA (TetOff system) to control a portion of the αCaMKII promoter and thus obtained a mouse with region-specific inducible gene expression. In 1998 the same system was used to target a striatal neuronal population. Nestler's group generated two lines of bitransgenic mice that inducibly overexpressed ΔFosB selectively in striatal regions under the control of the tetracycline gene regulation system (Chen et al., 1998; Kelz et al., 1999; Werme et al., 2002). Those studies showed that the overexpression of ΔFosB selectively in D1 SPNs increases response to the rewarding and locomotor effects of cocaine (Kelz et al., 1999; Colby et al., 2003) as well as to the rewarding effects of morphine (Zachariou et al., 2006Voluntary). Consistently, mice overexpressing ΔFosB predominantly in striatopallidal neurons ran considerably less.

In 2008 first, and then in 2011 the Palmiter's group used the knock-in (KI) technology to gain an insight on the differential output obtained by the artificial modulation of gene expression in D1 or D2 SPNs. In a first paper published in 2008 the group obtained a mouse line expressing the Cre recombinase specifically in the D1 SPNs. These KI mice were then crossed with mice carrying a conditional allele of the Gad1 gene - which encodes GAD67, one of the two enzymes responsible for GABA biosynthesis - in order to achieve the selective reduction of the GABA synthesis in striatonigral neurons (Heusner et al., 2008). The mice showed mild motor deficits in tasks such as rotarod. The same KI mice have been used to obtain a mouse line in which the NR1 subunit of glutamate receptor NMDA was inactivated in D1 neurons. These KI mice failed to display locomotor sensitization to repeated cocaine administration and have a decreased ability to form a conditioned place preference to cocaine (Beutler et al. 2011). These results suggested that NMDA receptor signalling in the striatonigral pathway is required for the manifestation of behaviours associated with repeated drug exposure (Heusner and Palmiter, 2008; Beutler et al. 2011).

More recently Lambot and collaborators generated a conditional knock out mouse for the NMDA receptor in the indirect pathway to show a reduction of the corticostriatopallidal synapses both at the level of number and strength. The mice also displayed a reduced habituation, a delay in goal-directed learning, a lack of associative behaviour, and impairment in action selection or skill learning. (Lambot et al., 2016).

These results supported the importance of studying the two pathways independently and the opposite role of striatonigral and striatipallidal neurons in natural reward, drug reward and locomotion.

5.1.1 BAC strategies

The advent of bacterial artificial chromosome (BAC) transgenic mice, pioneered by Nat Heintz from the Rockefeller University (Yang et al., 1997; Heintz, 2001; Gong et al., 2003), allowed the development of high throughput genetic labelling of distinct neuronal populations using the GPCRs and neuropeptides promoters to drive the expression of reporters such as EGFP. BACs are fragments of 100-250 kb of genomic mouse DNA that contain almost all the regulatory sequences necessary for an accurate expression *in vivo*. The BAC-driven expression of tagged proteins allows an easy and reproducible identification of specific neuronal populations.

The most common transgenic lines used to target the two populations of striatal neurons are eGFP and the Cre recombinase (review in Valjent *et al*., 2009). *drd1a*-EGFP and *chrm4*-EGFP BAC mice express EGFP in striatonigral cells and their axonal projections to the internal globus pallidus and the sustantia nigra, whereas *drd2a*-EGFP BAC mostly label the striatopallidal neurons and their projections to the external globus pallidus (Gong et al., 2003; Lobo et al., 2006; Bertran-Gonzalez et al., 2008; Matamales et al., 2009). The use of the red fluorescent protein tdTomato (tandem dimer Tomato) in *drd1a*-tdTomato BAC, crossed with the *drd2a*-GFP lines (Gong *et al.*, 2003; Shuen *et al.*, 2008), allowed the visualization of the two populations in the same animals. These various reporter mice provide extremely important tools for deciphering the anatomical, electrophysiological and molecular differences of D1 and D2 SPNs.

5.3 Laser-capture microdissection (LCM)

The mRNAs of cells of distinct identity can be isolated by microdissection of tissue. The laser-capture microdissection (LCM) is a method to obtain subpopulations of cells by dissecting a tissue under direct microscopic visualization. The LCM couples a laser to a microscope and defines a trajectory on the tissue. This trajectory can be separated from the adjacent tissue. Harvesting the population of cells of interest or cutting away the unwanted cells will allow obtaining a pure cell

population, RNA seq, cDNA libraries generation, as well as genotyping are some examples of the possible downstream applications that could be performed after LCM (Emmert-Buck MR et al., 1996; Espina V. et al., 2006; Curran, S. et al., 2000). A few examples of the application of the LCM technologies in different cellular subpopulation of the striatum are summarized below.

In 2011 Sharp BM and collaborators, used the LCM technology to purify GABAergic neurons projecting from NAc to ventral pallidum, and compared by microarray the gene expression in GABAergic neurons projecting from NAc to ventral pallidum in inbred Lewis and Fisher 344 rats. This work allowed the identification of a group of genes (Mint-1, Cask, CamkII , Ncam1, Vsnl1, Hpcal1, and Car8) possibly involved in the higher susceptibility of the Lewis strand to self-administer cocaine.

The same technique, followed by RT-PCR, has been used in 2006 by Perez-Manso et al. in order to investigate the changes in gene expression of the vGLUT2 thalamostriatal pathway in unilaterally 6-OHDA lesioned rats. In 2003 it has been shown that LCM is accurate enough to perform proteomic studies on specifically defined cell groups. Immunostaining can be used to label specific cells and LCM can be used dissect single cells within a tissue (Moulédous L et al., 2003).

5.4 Flow cytometry and fluorescence-activated sorting

Flow cytometry, is a laser-based technology that measures and analyses the optical properties of single particles such as cells, nuclei, bacteria, passing in a single file through a focused laser beam. Physical properties, such as size (represented by forward angle light scatter) and internal complexity (represented by right angle scatter) can resolve certain cell populations. The laser can also excite fluorophores used to mark various molecules. The use of fluorophores with different fluorescence characteristics, multiple lasers and multiple photo-detectors allows flow cytometers to measure many characteristics of each particle simultaneously. An important feature of this technique is that with flow cytometer thousands of particles per

second are analysed. This allows a strong statistically significant picture of a specimen's physical and biochemical make-up.

FACS (fluorescence-activated sorting) allows the physical separation of particles of interest from a heterogeneous population in addition to collection of data. Particles are held into a stream of fluid, which breaks up into droplets, each of them containing one particle. Droplets are introduced into the laser beam for interrogation. As the droplets pass through the laser, a decision is made whether to sort that event. The sorting is typically based on fluorescent labelling. The positive droplet will be charged either positively or negatively by a charging electrode and travel toward positively or negatively charged platinum plates into the appropriate collection tube. Separated fractions can then be analysed independently and used for downstream applications.

One major issue of the flow cytometry is the involvement of the dissociation of the tissue. In the adult brain, the tissue dissociations lead to the loss of neurites and all the cytoplasmic proteins that could be characteristic of a particular cell population. Furthermore, the preparation of the tissue involves long incubation with proteases and chelators that could potentially lead to the alteration of important post-translational modification.

Nevertheless, FACS-based separation of different cell populations allowed several important studies of discrete population of neurons properties. In 2006, Lobo and collaborators use the GFP BAC mice to perform high throughput microarray gene expression analysis in the two SPNs subtypes developing the so called FACS-array approach. The FACS-array consists in isolating live EGFP-positive neurons using fluorescence-activated cell sorting (FACS) and purifying RNA from the sorted neurons for microarray profiling. For example, Ebf1, a D1-enriched lineage-specific transcription factor, was found essential for the maturation of D1 but not for D2 SPNs. The confirmation of the selective expression of Slc35d3, a gene encoding an uncharacterized nucleotide sugar transporter, in D1 SPNs, indicated that cell type–specific protein glycosylation may have a role in the function of the striatonigral neurons. The D2 SPNs enrichment of the G-protein coupled-receptor 6 (*Gpr6*) pointed out the importance of the cAMP signalling in these neurons for mediating in the context of instrumental learning (Lobo *et al.*, 2007).

Guez-Barber and co-workers have also used FACS-array in 2011 to purify adult striatal neurons based on their activation state, as defined by their *c-fos* promoter induction (Guez-Barber et al., 2011; Guez-Barber et al., 2012). Neurons activated by acute and repeated cocaine injection were isolated and used to compare their unique patterns of gene expression with those in the non-activated majority of neurons. This work confirmed the differential responses of striatal neurons following cocaine treatment. The authors found that the activated neurons showed higher expression of the D1 neuronal marker gene prodynorphin, as compared to the expression of the D2 neuronal marker genes (D2R and A2AR). A differential regulation of the IEGs expression was observed in the activated or inactivated neurons, with the IEGs being induced only in activated neurons, and unchanged or even decreased in the non-activated majority of neurons. Since many of these IEGs and neural activity markers are also transcription factors, it is likely that very different patterns of gene expression are subsequently induced within these activated neurons that may contribute to the physiological and behavioural effects of cocaine.

In 2009 Kriaucionis and collaborators (Kriaucionis et al., 200) pioneered a protocol to study discrete populations of nuclei. An advantage of this method is that the nuclei dissociation is faster than the cell dissociation and can be done at 4°C.

Recently our group used FACS based technique to evaluate the cocaine-induced epigenetic modifications specifically in striatonigral and striatopallidal neurons that account for the dramatic differences in gene expression between the two cell-types. In this work, E. Jordi and co-workers showed that a single injection of cocaine triggers the acetylation of K_5H4 the tri-methylation of K_9H3 and that this increase persists 24 h after a single injection of cocaine in D1 (Jordi et al., 2013). Of note, those results were opposite in the D2 SPNs.

Although flow cytometry is really useful for studying DNA modifications, or the enrichment of nucleolar proteins, one major limitation of the flow cytometry in nuclei is the main loss of the nuclear protein due to the preparation of the samples. To overcome this problem, we have recently developed a method for isolating and analyzing cell type-specific nuclei from fixed adult brain (fluorescence-activated sorting of fixed nuclei; FAST-FIN) (see paper as Annex 1). The method is based on

the same protocol as developed in Jordi et al., 2013, except for a prior fixation of the brain with paraformaldehyde. The fixation of tissue covalently binds to the nuclei the proteins that normally would be lost during homogenization and maintains the more labile posttranslational modifications. Although it decreases the yield of nuclei preparation as compared to unfixed tissue, it has the advantage to be usable in transgenic mice expressing GFP or tdTomato, or after immunolabeling of nuclei.

5.5 Genetic profiling of discrete populations of neurons

One important consequence of the possibility to distinguish discrete populations of neurons is the possibility to combine those techniques with neuronal population-specific genetic profiling.

5.5.1 Single cell RNA-sequencing

The single-cell RNA sequencing is a method that aims to provide new perspectives to our understanding of genetics by bringing the study of genome expression to the cellular level. The single-cell approach provides high-resolution of a sample's genomic content by reducing the complexity of the genomic signal through the physical separation of cells. Clustering analyses allow the identification of rare cell types within a cell population. The possibility of obtaining an indication of the transcriptional profile of cells content allows the analysis of RNA with low copy number, which may exert important functions in the cells and that is mainly undetected when the sequencing is performed on an averaged cell population. The single cell RNA-seq is a relatively new method that is not yet standardized. Single cells can be obtained following FACS, serial samples-dilution or LCM, combined with microfluidics. Although single cell sequencing is a really promising technique, it introduces several bias compared to other RNA-sequencing methods. For example, FACS preparation, as other methods, requires the separation of cells from their natural milieu. This could possibly cause perturbation in the transcriptional profiles of RNA expression analysis; the serial dilution is susceptible to misidentification of the cells under the microscope and is really difficult to limit the contamination from neighbouring cells in the LCM.

5.6 BAC-TRAP

The BAC-TRAP (translating ribosome affinity purification) technology consists of a rapid affinity purification strategy for the isolation of translated mRNA from genetically targeted cell types. In BAC transgenic mice, a fluorescent EGFP is fused to the N terminus of the large subunit ribosomal protein L10a and inserted under the control of the promoter of either Drd1a or Drd2 (or other promoters) (Doyle et al., 2008; Heiman et al., 2008). EGFP-tagged polysomes can be immunoprecipitated with anti-GFP-coated beads and purified mRNA analysed by microarray or RNA sequencing.

The major advantage of the BAC-TRAP is that it allows to study changes within an identified cell population in response to a challenge. .

In 2008, Heiman and collaborators combined the BAC-TRAP technology to microarray analysis and identified more than 300 genes differentially expressed between the D1 and D2 SPNs. Some of them were common to the work of Lobo and colleagues but this approach revealed many more differences between the two neuronal populations than those observed with the FACS-array. Furthermore, they evaluated the expression changes in the two populations after acute and chronic cocaine treatments, confirming some of the genes already known as regulated by cocaine and showing a major activation of the D1 SPNs to the cocaine.

5.7 Conclusion

In this literature review I introduced all the topics linked to the main objectives of my thesis work. In chapter one and two I focused on the DA signalling and in the basal ganglia. I intensively described the striatum and the different sub-populations of SPNs, pointing out the importance of considering the differences between the anatomical sub-territories (NAc, DS, patch/matrix) as well as its different populations of neurons to fully understand the functions that this region mediates. In Chapter 3 I reviewed the mechanisms and the substrates of action of the drug of abuse cocaine. I introduced some of the modifications induced by cocaine focusing on the striatum and the PFC. In particular, in the last part I described the transcriptional modifications induced by cocaine. I pointed out that the transcriptional modifications are likely responsible for the long-lasting modifications that are induced by cocaine intake. Although a lot of work has been already done on this topic, only few researches tried to distinguish the cocaine effect in pure populations of dopamine receptor expressing neurons. Although there is information on the cocaine induced transcriptional modifications on the different populations of SPNs, knowledge about their position in the striatum (NAc or DS) is still incomplete. In the first part of chapter 4 I summarized the mechanisms of the homeostatic control of food intake. In the second part I focused on the reward-related control of the food intake and on the structural plasticity induced by highly palatable food. Compared to cocaine, the transcriptional regulation induced by the natural reward food, is much less described. Comprehensive information of the transcriptional effects induced by the palatability of the food in pure populations of neurons is still missing. Lastly, I introduced the different techniques available to distinguish discrete populations.

- Aims of the thesis -

Dopamine (DA) controls movement execution, action selection, and incentive learning by regulating the efficacy and plasticity of cortico/thalamo-striatal transmission. Long-term modifications require changes in gene transcription. Both natural rewards and drugs of abuse are able to induce structural changes in prefrontal cortex (PFC), nucleus accumbens (NAc) and dorsal striatum (DS) in the striatum (reviewed in Russo et al., 2010; Geugan T., 2012). The aim of the present work was to study the transcription profiles of selected population of neurons in PFC, NAc and DS in basal condition, following operant learning, or after mimicking the stimulation of the reward system with cocaine.

The striatum is composed of several cell types that exhibit different responses to drugs and mediate different features of "rewarding" stimuli. The largest neuronal population of the striatum is comprised of medium-sized spiny projection neurons (SPNs), which can be further differentiated in two population, based on the subtype of dopamine (DA) receptor they express, namely D1 or D2 receptors with few expressing both. Both D1 and D2 SPNs express their own subsets of markers and share many morphological characteristics and functional properties. They participate in distinct pathways that exert opposite effects on their target regions. Various functional studies showed that the NAc and the DS mediate distinct aspect of the striatal function. SPNs in those two striatal regions look similar in phenotype but they differ in their input/output connections and functions. Until today, this diversity was still not well understood and it is crucial to distinguish the response in the two populations of SNPs in the two different regions. So, in order do better characterize these cells, we used transgenic mice that express a tagged ribosomal protein (L10a-EGFP) under control of the D1 or D2 receptor promoter to isolate currently translated mRNA and nuclei from each population of SPNs, as well as from D1 pyramidal neurons of the PFC.

With this strategy we were able to tackle different questions and to facilitate their comprehension, the thesis work is subdivided in three parts with three main objectives.

Aim 1:

Characterization of the basal gene expression in the different neuronal populations expressing either D1 or D2 receptors in the NAc, and DS, or, for D1 in PFC. The first part of this study allowed for the first time profiling the translated (polysome-

associated) mRNAs of D1 and D2 SPNs belonging to the ventral or dorsal striatum as well as a comparison between those cells and the D1 receptor-expressing neurons in the PFC. In the second part of this work we provided an *in vivo* validation of our analysis. Starting with an upstream analysis of the genes specifically expressed in the DS, we were able to modulate its normal function by using drugs known to have an effect on the expression of the genes enriched in this region.

Aim 2:

Analysis of the transcriptional changes following the active recruitment of the reward system (operant learning for food). In this part of the work we characterized for the first time the transcriptional changes induced by a natural reward – regular or highly palatable food – across the cortico-striatal system. This work provided an insight on different issues: 1) we profiled the genes regulated by the learning process and 2) we identified the regions, the neurons and the genes more responsive to the highly palatable food, 3) we compared the regulation of gene expression by a drug of abuse, cocaine, with that exerted by natural reward (highly palatable food). The *in vivo* manipulation of one of the genes differentially regulated by one of the treatment allowed the validation of part of the findings of our study.

Aim 3:

Characterization of the long-lasting modifications induced in each of these 5 neuronal populations by seven days of exposure to cocaine. In this part we provide a comprehensive study of the effects of cocaine administration on the two populations of neurons depending on their localization. Furthermore, we identify networks of co-regulated genes associated that could be associated with features of drug addiction

All these data allowed us a better comprehension of the neuronal type-specific gene expression in the main striatal regions and PFC, and its responsiveness to the stimulation of the reward system with a drug of abuse, cocaine, or natural reward.

- Materials & Methods -

6.1 Animals

For our experiments we used BAC (bacterial artificial chromosome) transgenic mice expressing the enhanced green fluorescent protein fused to the N-terminus of the large subunit ribosomal protein L10a under the control of dopamine D1a or D2 receptor promoter (Drd1a::EGFP-L10a or Drd2::EGFP-L10). These mice lines were generated by Heiman et al., 2008 and maintained as heterozygotes on a C57Bl/6J background. Male and female mice were maintained on a 12 h light/dark cycle (light off 19:00 hours) and had, before the beginning the experiment, free access to water and food. Animal protocols were performed in accordance with the National institutes of Health Guide for the Care and Use of Laboratory Animals, and approved by Rockefeller University's Institutional Animal Care and Use Committee; or in accordance with the guidelines of the French Agriculture and Forestry Ministry for handling animals (decree 87-848) under the approval of the "Direction Départementale de la Protection des Populations de Paris" (Authorization number C-75-828, license B75-05-22)

6.2 Operant conditioning experiments

Drd1a::BACTRAP, or Drd2::BACTRAP, $Ncdn^{FLOX/FLOX;iCRe}$ (Ncdn-KO), $Ncdn^{FLOX/FLOX}$ and WT mice were trained in an operant conditioning paradigm. Seven days before the beginning of the experiment all the animals were individually housed and maintained in an environment with controlled temperature and humidity with a 12:12-h reversed light dark cycle. All the experiments were carried out during the dark phase of the dark/light cycle. All the animals were randomly assigned to one of the following 4 groups: master highly palatable (mHP), master standard (mST), yoked highly palatable (yHP), yoked standard (yST). Five days before the starting conditioning all the mice were mildly food-deprived to maintain their weight to their original weight. The food restriction was maintained until the 9^{th} operant training session in order to facilitate the acquisition of the task. Mice then received *ad libitum* food from the 10^{th} session until the end of training. During the operant conditioning

sessions animals were presented with either 20 mg dustless precision standard pellets (TestDiet 5UTM #1811143) or highly palatable isocaloric pellets (TestDiet 5UTL #1811223). The standard diet was similar to the standard diet used to maintain the mice (TestDiet Purina 5053) in composition and taste (3.30 kcal/g, 24.1 % protein, 10.4 % fat, 65.5 % carbohydrates). The highly palatable diet was similar in calories content to the standard diet (3.48 kcal/g) but contained a higher level of sucrose among the carbohydrates (49%) and was modified by the addition of chocolate flavour. The training session started with a fixed ratio (FR)-1 reinforcing schedule. During this period master animals had to poke once in the active hole to receive a pellet. Each poke in the active hole was followed by a 10-second time-out period, independently of the reinforcing schedule. The FR1 was followed by five days of FR5, during which mice were fasted at 90% of their original weight. The last phase consisted of 6 days of FR5 in which mice had *ad libitum* access to food between operant sessions. Only mice maintaining at least 75% responding on the active hole, a minimum of 10 reinforces per session and less than 20% deviation from the mean of the total number of reinforces earned in three consecutive days were allowed to continue the experiment, all the mice reach the criterion. Twenty four hours after the last training session the Ncnd-ko mice and their control were presented to a progressive ratio (PR) schedule in order to evaluate the relative reinforcement efficacy of the reward. During the PR the response requirements increased systematically within the session, after each reinforce. The PR schedule lasted for 1 h and respected the following series 1, 2, 3, 4, 5, 6, 7, 8, 10, 12, 14, 16, 18, 20, 22, 24, 28, 32, 36, 40, 44, 48, 52, 56, 64, 72, 80, 88, 96, 104, 112, 120, 128, 136, 144, 152, 160, 168, 176, 184, 192, 200, 208, 216, 224, 232, 240, 248, 256, 264, 272, 280, 288, 296, 304, 312, 320, 328, 336, 344, 352, 360, 368, 376, 384, 392, 400, 408, 416, 424, 432, 440, 448, 456, 464.

The operant conditioning experiments were carried out in mouse Med Associate operant chamber (model ENV-307A-CT). Each chamber was composed by a grid floor (model EVV-414), 2 nose-poke holes, one randomly selected as active and the other as inactive, one house light, a food dispenser and a food magazine between the 2 nose-poke holes. The operant chambers were located in an isolation box equipped with fan. The beginning of the session was concomitant with the fan activation and the turning on of the house light for 3 seconds, and a pellet delivery. The session ended either after 60 minutes or after 100 pellets had been

delivered. Poking in the active hole resulted in the delivery of one pellet concomitant with a 2-second poke-light. The pellet delivery was followed by 10 s of time out. During this period, the pokes were inactive. Mice were sacrificed by decapitation 24 h after the last session, the brain was removed and prefrontal cortex, nucleus accumbens and dorsal striatum were rapidly dissected on ice. The tissues were homogenised and subjected to nuclear fractionation and RNA immunoprecipitation.

6.3 Pharmacological treatments

Mice received a single intraperitoneal injection (i.p.) of either 20 mg/kg cocaine·HCl (Sigma) or its saline vehicle for 7 consecutive days and were killed 24 h after the last injection.

6.4 mRNA extraction

Cell specific translated-mRNA purification, was performed as described in Heiman et al., 2008 with some modifications. Each sample consisted of a pool of 2-3 mice. BAC TRAP transgenic mice were sacrificed by decapitation. The brain was rapidly dissect out on ice and placed in a brain mouse brain matrix with 0.5 mm coronal section interval (Alto Stainless Steel Coronal 0.5 mm Brain Matrix). In the matrix, three blades were used do obtain two thick slices containing the PFC and the striatum. The first blade was used divide the olfactory bulb from the cortex, the second was placed at 2 mm from the first and defined the region containing the s PFC cortex, the third was placed at 3 mm from the second to define a slice containing the entire striatum. The prefrontal cortex was quickly dissected out and the nucleus accumbens and the dorsal striatum removed with small metal punches on ice. Each tissue were homogenised in 1 ml of cold lysis buffer (20 mM HEPES KOH [pH 7.4], 5 mM $MgCl_2$, 150 mM KCl, 0.5mM DTT, 100 µg/ml CHX protease and the RNAse inhibitors Superasin (final concentration 200 U/mL, Life Technologies) and Rnasin (final concentration 400 U/mL, Promega) with loose and tight glass-glass 2 ml Dounce homogenizers. Each homogenate was centrifuged at 2000 x g, at 4°C,

for 10 minutes. The supernatant was separated from cell debris, and supplemented with NP-40 (EDM Bioscences) (final concentration of 1% vol/vol) and DHPC (Avanti Polar lipids) to a final concentration of 30 mM. After mixing and 5-minute incubation on ice the lysate was centrifuged for 10 minutes at 20,000 x g to separate the supernatant from the insolubilized material (Heiman et al., 2008; Heiman et al.,2014). Magnetic beads coated with anti-GFP antibody were prepared as follows: 300 µL of Streptavidin MyOne T1 Dynabeads (Invitrogen) per sample were washed in PBS, incubated 35 min at room temperature with 120 µg of biotinylated protein L in PBS, washed 5 times with PBS Bovine Serum Albumine 3% (wt/vol), incubated 1h at room temperature with 100 µg of monoclonal anti-GFP antibodies (50 µg of clone 19F7 + 50 µg of clone 19C8, Memorial Sloan-Kettering Monoclonal Antibody Facility, New York) in the homogenization buffer containing 1% (vol/vol) NP-40, washed 3 times and finally ressuspended in 200 µL of homogenization buffer complemented with 1% (vol/vol) NP-40. The mixture of magnetic beads coated with anti-GFP antibody was added to the homogenates. After addition of Superasin (final concentration 200 U/mL, Life Technologies) and Rnasin (final concentration 400 U/mL, Promega), the samples underwent 18 h incubation at 4°C under gentle end-over-end rotation. After 4 washes with homogenization buffer complemented with 1% (vol/vol) NP-40 and 200 mM KCl (total concentration KCl 350mM), the RNA was eluted with RLT Plus buffer from the RNeasy micro plus kit (Qiagen) and 10

µL/mL β-mercaptoethanol (10 min incubation at room temperature and vortex). Then the RNA was purified according to the manufacturer's instructions, with an on-column DNAse-I digestion step. The quantity of RNA was determined by fluorimetry using the Quant-iT Ribogreen, and the quality was determined checked using the Bio-Analyzer Pico RNA kit before library preparation.

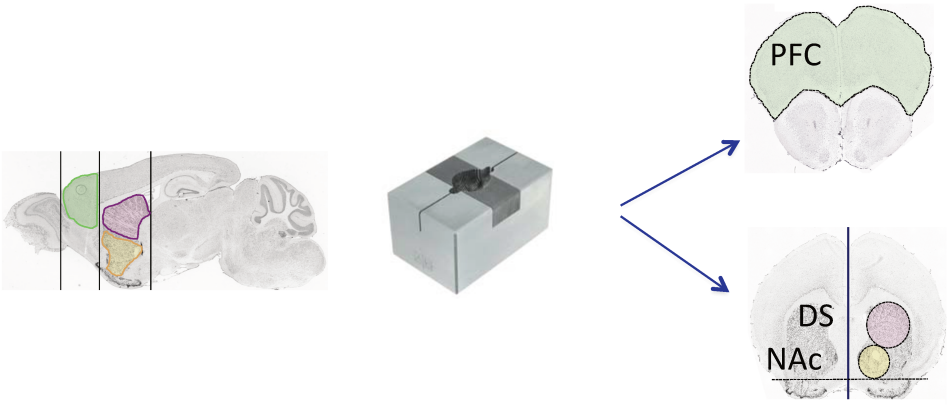

Figure 14: Schematic representation of the tissue selection.

6.5 Libraries and sequencing

Five ng of RNA were used for reverse-transcription, performed with the Nugen Ovation RNA-Seq System V2. cDNA was ultra-sonicated using a Covaris S2 sonicator with the following parameters: duty cycle 10%, intensity 5, 100 cycles/burst, 5 minutes. Two hundred nanograms of sonicated cDNA were then used for library construction using the Illumina TruSeq RNA sample prep kit, starting at the End-Repair step, and following the manufacturer's instructions. The libraries were quantified with the Bio-Analyzer High-sensitivity DNA kit, multiplexed and sequenced on an Illumina HiSeq 2500 instrument. At least 20 million 50-bp paired-end reads were collected for each sample. Reads were then aligned to the Genome Reference Consortium Mouse Build 38 GRCm38 / UCSC mm10 mouse genome assembly. The DEseq algorithm was used to test for differential expression of each gene in each pair-wise comparison

6.6 Bioinformatics analysis

The quality of the raw data were assessed using FastQC [Andrews] from the Babraham Institute for common issues including low quality of base calling, presence of adaptators among the sequenced reads or any other overrepresented sequences, and abnormal per base nucleotide percentage. The different libraries were

then mapped to the genome of Mus musculus (UCSC mm10) using TopHat2 2.0.9 [Kim et al. 2013], a splice junction mapper, with a set of matching gene annotation (genes.gtf downloaded from UCSC on December 8th 2015). Conservative options have been used to keep only reliable levels of expression for each gene such as the obligation to map only to one possible location for each read and by taking only into account the paired reads mapped in proper pairs. The gene counting step was then made with HTSeq-counts v0.6.0 (Anders et al. 2014). The exons were chosen as the mapping features and the reads of the same pair had to be mapped to the opposite strands of the gene. Before statistical analysis each library was checked using principal component analysis and also correlation matrix. Differentially expressed genes were identified with R using the Bioconductor package DESeq2 v1.10.1 (Love et al. 2014) taking advantage of its capacity to perform multi-factor analysis. Genes with adjusted p-value less than 5 % (with false discovery rate method from Benjamini and Hochberg) were declared differentially expressed. Gene ontology (GO) analysis was performed on a list of significantly differentially expressed genes (adj $p<0.05$) identified with DESeq2. The cluster Profiler v3.0.4 (Yu et al. 2012) package from Bioconductor was used. Overrepresented GO were identified using GSEA method. Conservative options were used to filter results (Bonferroni p value adjustment and 0.01 p-value threshold). We tested 3 sets of genes of interest for each comparison, the differentially expressed and the overexpressed for each condition. Each set of genes was compared with all known genes present in the annotation. The GO categories were found in org.Mm.eg.db[Carlson] Bioconductor package based on official gene symbol

6.7 Total RNA purification and cDNA preparation

Each sample consisted of the tissue deriving from one mouse brain. Mice were sacrificed by cervical dislocation, the prefrontal cortex was quickly dissected out and mircodisks punched out from the nucleus accumbens and the dorsal striatum with a stainless steel cannula and placed on ice (slice thickness 3 mm). Each tissue sample was homogenized in TRIzol with loose and tight glass-glass 2 ml Dounce homogenizers. Total RNA was extracted with TRIzol Reagent (Life Technologies) according to manufacturer's instructions. The RNA was quantified by using the

NanDrop 1000 spectrophotometer and its integrity checked with the Bionalyzer (agilent 2100 Bioanalyzer, Agilent RNA 6000 nano kit). Five hundred ng of mRNA from each sample were used for retro-transcription, performed with the Reverse Transcriptase II (Life Technologies) following the manufacturer's instructions.

6.8 Real-Time PCR

Quantitative real time PCR, was performed using SYBR Green PCR kit in 96-well plates according to the manufacturer's instructions. Results are presented as normalised to the house-keeping gene and the delta-CT method was used to obtain a FC.

6.9 Western blots

The NAc, DS, and PFC were rapidly dissected on an ice-cooled dish and stored at -80°C. Each sample was sonicated in 150 uL of RIPA buffer. Protein content was estimated using BCA protein assay (Thermo scientific, prod #23235) following manufacturer's instructions and an equal amount of lysate was mixed with denaturing 3X STOP buffer. Fifteen µg of protein for each sample were separated in 4-20% SDS-polyacrylamide gel (BIO-RAD mini-protean-TGX) before electrophoretic transfer onto a nitrocellulose blotting membrane (Amersham, Lot No G9990998). Membranes were blocked 45 minutes in 30 g/L bovine serum albumin and 10 g/L non-fat dry milk in 0.1 M phosphate buffer saline (PBS). Membranes were then incubated overnight with the primary antibody Norbin (RU1002). The bound primary antibody was detected with a secondary luminescent antibody to mouse (IRDye 800 CW-conjugated, antimouse IgG, Rockland Immunochemical, dilution 1:5000) and visualized with Odyssey–LI-COR infrared fluorescence

detection system (LI-COR). The optical density after acquisition was assessed using the GELpro32 software. Results were normalized to the detection of β-tubulin in the same sample and plotted as percentage of the control treatment.

6.10 Golgi-cox staining and analysis of spine density and morphology

The Golgi staining was performed as in Marco S. et al., 2013. Briefly, 24 h after the last training session or the last cocaine injection mice were sacrificed by cervical dislocation and their brain was quickly dissected out. One mouse brain hemisphere was subsequently dipped in the Golgi dye filtered solution (1% potassium dichromate, 1% mercury chloride and 0.8% potassium chromate. After 21 days incubation in dark, each hemisphere was washed 3 x 2 min in distilled water, and EtOH 90 % (v/v) for 30 minutes. The brains were next cut with a vibratome (Leica) in a 200 microns slices in a solution of 70 % (v/v) EtOH. Slice, were next washed for 5 minutes in distilled water. The slices were then reduced in 16 % (v/v) ammonia for 60 minutes, washed 2 minutes in distillate water for 2 minutes, and mounted on coverlips (ThermoFisher). As next dehydration of the slices was performed by placing the coverslips for 3 min in 50% (v/v), then 70, 80 and 100% (v/v) EtOH. Incubation for 2 × 5 min in a 2:1 (v/vo) isopropanol:EtOH mixture was followed by 1 × 5 min in pure isopropanol and 2 × 5 min in xylol. Finally, samples were mounted in mounting medium (Eukitt) and left for 24 h to settle.

Secondary dendrites from SPNs from the NAc and DS, and from pyramidal neurons of the layer 5 of the PFC were photographed using Z-stacks from 0.2-µm optical sections in bright field at × 100 resolution on a DM6000-2 microscope (Leica). A maximum of three dendrites per neuron and from at least 5 slices per animal were photographed. Files were analysed with the ImageJ software as follows: first, Z-stacks were summed using the plugin Bio-format importer, the scale was adjusted according to the pixel size of the images. The total number of spines was obtained using the cell counter tool. At least 40 dendrites per group, with at least eight mice per group were counted. For spines morphology, at least 3 dendrites per mouse were analysed. At least 20 spines on the dendrites that were clearly observed in the X–Y plane were analysed. An average of 480 spines per group were analysed for major head diameter as well as neck length. Two investigators performed acquisition and analysis. Results were subsequently pooled and showed minor differences in the counts from the two investigators.

- Experimental Results -

7.1 Aim 1: Characterization of the basal gene expression in the different neuronal populations expressing either D1 or D2 receptors in the NAc, and DS, or, for D1 in PFC.

In the following section we present in the form of a preliminary manuscript the study of the transcriptional profiles characterizing the neurons expressing the DA receptors in the NAc, the DS and the PFC. This study includes the results from the animals that served as control in the operant training for food, the yoked-standard group, as they didn't go through any operant training neither were influenced by the palatability of the food

Regional specificity of gene expression in dopaminoceptive neurons

Enrica Montalban[1,2,3], Jean-Pierre Roussarie[4], Lieng Taing[1,2,3], Albert Giralt[1,2,3], Yuki Nakamura[1,2,3], Benoit de Pins[1,2,3], Assunta Pelosi[1,2,3], Jack Zhang[4], Paul Greengard[4], Jean-Antoine Girault[1,2,3,*]

((this is an early draft of the manuscript and additional authors may be included and the authors order is not definitive))

1- Inserm UMR-S 839, Paris, 75005, France;

2- Sorbonne Universités, UPMC, Université Paris 06, Paris, 75005, France;

3- Institut du Fer à Moulin, 17 rue du Fer à Moulin, Paris, 75005, France;

4- Laboratory of Molecular and Cellular Neuroscience, the Rockefeller University, 1230 York Avenue, New York, NY 10065, USA

* To whom correspondence should be sent:

Dr Jean-Antoine Girault

Inserm UPMC UMR-S 839

Institut du Fer à Moulin

17, rue du Fer à Moulin

75005 Paris, France.

Contact: jean-antoine.girault@inserm.fr

Running Title: Gene expression in dopaminoceptive neurons

ABSTRACT

Each cell type is defined by its pattern of gene expression. Forebrain dopaminoceptive neurons play a key role in movement, action selection, and motivation and are dysregulated in addiction, Parkinson's disease and many other conditions. To investigate similarities and differences between the main types of neurons sensitive to dopamine we compared the full complement of translated mRNAs in neurons expressing D1 or D2 dopamine receptors in the dorsal striatum and nucleus accumbens and in prefrontal cortex D1 receptor-expressing neurons. As large difference was observed between D1-positive prefrontal and striatal neurons and the differences in mRNA profiles between D1 and D2 striatal projection neurons were further characterized disclosing similarities and differences between the dorsal and ventral striatum. Intrastriatal comparisons revealed the important differences between these two regions, some being common to D1 and D2 neurons others being specifically found in one cell population. Further analysis allowed the identification of potential upstream regulators, with prostaglandin E2 being a potential regulator in the two neuronal populations of the dorsal striatum. Chronic stimulation with a prostaglandin agonist improved performance of mice in dorsal striatum-dependent behaviors, supporting the functional significance of this pathway. This study provides a powerful resource for the molecular studies of the striatum and new clues about its regional organization.

INTRODUCTION

In multicellular organisms, differentiation depends on the acquisition by each cell type of different patterns of gene expression. Although these transcriptional profiles are stable, work on induced pluripotent stem cells demonstrated that it is largely reversible (Yamanaka and Blau, 2010). Identifying the characteristic complement of genes expressed in a cell population allows to better understand its functional properties as well as its vulnerability to pathological conditions. The nervous system represents a major challenge in terms of cells diversity and the definition and number of different cell types is still an open question (Sharpee, 2014). Neuromodulators such as dopamine exert their effects on large brain regions containing many cell types. Major targets of dopamine (DA) are the striatum and the prefrontal cortex. The importance of this innervation in physiology and in a wide variety of pathological conditions has been abundantly documented. Tonic DA is necessary for the correct function of its target regions due to the existence of high affinity receptors, while phasic increase is triggered by errors in reward prediction and related salient stimuli, and is critical for incentive learning (Schultz, 2007). The absence of DA results in Parkinson's disease and its repeated increase by drugs of abuse is a key element leading to addiction. DA is also involved in many other conditions ranging from attention deficit disorder to schizophrenia. Although there are 5 types of dopamine receptors expressed at various levels in many cell types, the D1 and D2 dopamine receptors (DRD1 and DRD2) are the most abundant in the striatum and are also expressed at a much lesser level in the cerebral cortex (Beaulieu and Gainetdinov, 2011). In the striatum, the expression of these two receptors is largely segregated with few neurons expressing both (Valjent et al., 2009). These neuronal populations have different functional properties although they function in an integrated manner to shape behavior (Tecuapetla et al., 2016). In the dorsal striatum (DS), DRD1 is expressed by striatal projection neurons (SPNs) forming to the direct pathway which monosynaptically innervates the substantia nigra pars compacta and internal medial) globus pallidus, whereas DRD2 is expressed in SPNs which form the first step of the indirect pathway (Gerfen et al., 1990). DRD2 is also expressed, albeit at a lower level, in cholinergic interneurons (Bertran-Gonzalez et al., 2008a). In the ventral striatum corresponding to the nucleus accumbens (NAc), the correspondence between the type of expressed DA receptor and the projection pattern of SPNs is more complex (Kupchik et al., 2015).

D1R- and D2R-expressing SPNs have been known for many years to specifically express other genes, such as those coding for substance P and enkephalin for example (Gerfen et al., 1990). Recent studies have shown that a large number of genes are also differentially expressed between the two cell types (Heiman et al., 2008; Doll et al., 2011). However there are several additional levels of anatomical and functional heterogeneity within the striatum which are less well characterized. This

heterogeneity includes the distinction between dorsal and ventral regions, the NAc being itself a highly heterogenous structure, as well as the distinction between the patches/striosomes and the matrix (Voorn et al., 2004). There is therefore a need for further characterize the subpopulations within the SPNs.

A number of approaches have been used to address the challenge of identifying the transcriptional profile of specific cell types including single cell PCR and, more recently, single cell RNAs sequencing (Gokce et al., 2016), as well as various methods for cell labeling and microdissection or sorting (Lobo et al., 2006; Ena et al., 2013). A particularly powerful approach to investigate the patterns of genes expressed in a specific cell population is the BAC-TRAP (bacterial artificial chromosome-translated RNA affinity purification) strategy (Doyle et al., 2008; Heiman et al., 2008). In this method transgenic mice express an eGFP fused L10a ribosomal protein under the control of cell-type specific promoter. GFP-immunoprecipitation allows the isolation of cell type specific polysomes and thus access to currently translated mRNAs or "translatome". This method coupled to microarrays has been applied to D1 and D2 SPNs and showed the different profiles between the two cell types. Here, we use BAC-TRAP to study the translatome in D1R- and D2R-expressing cells of the DS and the NAc and the D1R-cells in the prefrontal cortex. We show the existence of major differences in the mRNA profile in DS and NAc, some being common to the D1 and D2 populations, others being specific. Analysis of the differences allowed the identification of potential common upstream regulators and we demonstrate the functional role of one of them suggested to be active on both D1 and D2 neurons of the DS.

METHODS

Animals

BAC (bacterial artificial chromosome) transgenic mice expressing the enhanced green fluorescent protein fused to the N-terminus of the large subunit ribosomal protein L10a under the control of dopamine D1a or D2 receptor promoter (*Drd1a*::EGFP-L10a or *Drd2*::EGFP-L10) were previously described (Heiman et al., 2008). These mice lines were maintained as heterozygotes on a C57Bl/6J background. They express eGFP-L10a in the striatum and in striatofugal fibers (**Figure 1A and B**) with a pattern consistent with the previously described expression in D1 and D2 SPNs (Bertran-Gonzalez et al., 2008b; Heiman et al., 2008). In the PFC eGFP-L10a expression in *Drd1a*::eGFP-L10a mice was sufficient for further analysis whereas it was not the case for *Drd2*::eGFP-L10 mice (**Figure 1A and B**). Male C57Bl/6 mice were purchased from Janvier (France) and used at 10-12 weeks. Mice were maintained on a 12 h light/dark cycle (light off 7:00 pm) and had, before the beginning the

experiment, free access to water and food. Animal protocols were performed in accordance with the National institutes of Health Guide for the Care and Use of Laboratory Animals, and approved by Rockefeller University's Institutional Animal Care and Use Committee or in accordance with the guidelines of the French Agriculture and Forestry Ministry for handling animals (decree 87-848) under the approval of the "*Direction Départementale de la Protection des Populations de Paris*" (Authorization number C-75-828, license B75-05-22).

mRNA extraction

Cell specific translated-mRNA purification, was performed as described (Heiman et al., 2008) with some modifications. Each sample consisted of a pool of 2-3 mice. BAC-TRAP transgenic mice were sacrificed by decapitation. The brain was quickly dissected out placed in cold buffer and then in an ice-cold brain form to cut thick slices from which the PFC was obtained and the NAc and the DS punched out using ice-cold stainless steel cannulas (**Figure 1C**). Each tissue piece was homogenized in 1 ml of lysis buffer (20 mM HEPES KOH [pH 7.4], 5 mM $MgCl_2$, 150 mM KCl, 0.5mM dithiothreitol, 100 µg/ml CHX protease and RNAse inhibitors) with successively loose and tight glass-glass 2 ml Dounce homogenizers. Each homogenate was centrifuged at 2000 x g, at 4°C, for 10 min. The supernatant was separated from cell debris, and supplemented with NP-40 (EDM Biosciences) to a final concentration of 1% (vol/vol? 10 ml/l??) and DHPC (Avanti Polar lipids) to a final concentration of 30 mM. After mixing and a 5-minute incubation on ice, the lysate was centrifuged for 10 minutes at 20,000 x g to separate the supernatant from the insolubilized material. A mixture of streptavidin-coated magnetic beads were incubated biotinylated protein L and then with GFP antibody was added to the supernatant and incubated ON at 4°C with gentle end-over rotation. After incubation, beads were collected with a magnetic rack and washed 5 times with high-salt washing buffer (20 mM HEPES-KOH [pH 7.4], 5 mM $MgCl_2$, 150 µl 1M, 350 mM KCl, 1% NP-40) and immediately placed in "RTL plus" buffer (Qiagen). The mRNA was purified using the RNase micro KIT (Qiagen).

Libraries and sequencing

Five ng of RNA were used for reverse-transcription, performed with the Ovation RNA-Seq System V2 (Nugen). cDNA was quantified by fluorimetry, using the Quant-iT Picogreen reagent and ultra-sonicated using a Covaris S2 sonicator with the following parameters: duty cycle 10%, intensity 5, 100 cycles/burst, 5 minutes. Two hundred ng of sonicated cDNA were then used for library construction using the Illumina TruSeq RNA sample prep kit, starting at the End-Repair step, and following the manufacturer's instructions. The libraries were quantified with the Bio-Analyzer high-sensitivity DNA

kit, multiplexed and sequenced on an Illumina HiSeq 2500 instrument. At least 20 million 50-bp paired-end reads were collected for each sample. Reads were then aligned to the Genome Reference Consortium Mouse Build 38 GRCm38 / UCSC mm10 mouse genome assembly. The DEseq algorithm was used to test for differential expression of each gene in each pair-wise comparison.

Bioinformatic analysis

The quality of the raw data were assessed using FastQC [Andrews] from the Babraham Institute for common issues including low quality of base calling, presence of adaptors among the sequenced reads or any other overrepresented sequences, and abnormal per base nucleotide percentage. The different libraries were then mapped to the *Mus musculus* genome (UCSC mm10) using TopHat2 2.0.9 [Kim et al. 2013], a splice junction mapper, with a set of matching gene annotation (genes.gtf downloaded from UCSC on December 8th 2015). Conservative options were used to keep only reliable levels of expression for each gene including the obligation to map only to one possible location for each read and taking only into account the paired reads mapped in proper pairs. The gene counting step was then done with HTSeq-counts v0.6.0 (Anders et al., 2015). The exons were chosen as the mapping features and the reads of the same pair had to be mapped to the opposite strands of the gene. Before statistical analysis each library was checked using principal component analysis and correlation matrix. Differentially expressed genes were identified with R using the Bioconductor package DESeq2 v1.10.1 (Love et al., 2014) taking advantage of its capacity to perform multi-factor analysis. Genes with adjusted p-value less than 5 %, with false discovery rate (Benjamini and Hochberg, 1995) were declared differentially expressed. Gene ontology (GO) analysis was performed on a list of significantly differentially expressed genes (adj $p<0.05$) identified with DESeq2. The cluster Profiler v3.0.4 (Yu et al., 2012)package from Bioconductor was used. Overrepresented GO were identified using GSEA method. Conservative options were used to filter results (Bonferroni p value adjustment and 0.01 p-value threshold). We tested 3 sets of genes of interest for each comparison, the differentially expressed and the overexpressed for each condition. Each set of genes was compared with all known genes present in the annotation. The GO categories were found in org.Mm.eg.db [Carlson] Bioconductor package base on the gene reporter, official gene symbol.

Total RNA purification and cDNA preparation

Each sample consisted of the tissue deriving from one mouse brain prepared as described above. Mice were sacrificed by cervical dislocation, the PFC was quickly dissected out and microdisks punched out from the NAc and the DS with a stainless steel cannula and placed on ice. Each tissue

sample was homogenized in TRIzol with loose and tight glass-glass 2 ml Dounce homogenizers. Total RNA was extracted with TRIzol Reagent (Life Technologies) according to manufacturer's instructions. The RNA was quantified by using the NanDrop 1000 spectrophotometer and its integrity checked with the Bionalyzer (agilent 2100 Bioanalyzer, Agilent RNA 6000 nano kit). Five hundred ng of mRNA from each sample were used for retro-transcription, performed with the Reverse Transcriptase II (Life Technologies) following the manufacturer's instructions.

Real-Time PCR

Quantitative real time PCR, was performed using SYBR Green PCR kit in 96-well plates according to the manufacturer's instructions. Results are presented as normalized to the indicated house-keeping genes and the delta-CT method was used to obtain a FC.

RESULTS

Comparison of polysomes-associated mRNA in D1 neurons of the prefrontal cortex and the striatum

The overall experimental approach is summarized in **Figure 1C** and **D**. Translated mRNA profiles were obtained from D1R-expressing neurons in the NAc, DS, and PFC, and from D2R-expressing neurons in the NAc and DS. Note that all the data were analyzed together and different comparisons are presented separately for clarity. We first compared the genes differentially expressed between D1 neurons of the PFC and those in the DS (**Figure 2A**) and in the NAc (**Figure 2B**, the full results are provided as **Supplementary Table 1**). Overall 2 942 genes were significantly more expressed in the PFC than in the DS and 2 872 in the DS than in the PFC (**Figure 2C**). For the NAc these numbers were 2 819 and 2 863 respectively (**Figure 2D**). Among all the genes more expressed in the DS or NAc than in the PFC, 1 787 were common (49%). Similarly, among those more expressed in the PFC than in the DS or NAc 2 182 were common (54%). This high degree of overlap between DS and NAc in the comparison is not surprising since both are GABAergic projection neurons whereas PFC D1R-expressing neurons are for a large part, albeit not only, glutamatergic pyramidal neurons (Smiley et al., 1994). However the differences suggested the existence of pronounced differences between the complement of genes expressed in the dorsal and ventral striatum (see below). The genes included in part or totality in the Drd1 BAC (Drd1, Sfxn1, and Hrh2) and in the Drd2 BAC (Drd2, GM4894, Ankk 1, and Ttc12) used for transgenesis were excluded from further analysis, since their expression levels did not reflect that of the endogenous gene. To obtain a first glimpse about the biological

significance of these differences we selected the differentially expressed genes which match the IUPHAR list of genes (http://www.guidetopharmacology.org/download.jsp) including receptors, enzymes, channels, and transporters that are directly relevant for neuronal physiology or pharmacology (**Tables 1** and **2**). Only genes with the strongest expression differences, i.e. four-fold or higher, are shown in these tables (the full list can be found in **Supplementary Table 2**). As expected mRNAs known to be enriched in SPNs as compared to glutamatergic neurons were identified (e.g., glutamic acid decarboxylase 2, GAD2, adenylyl-cyclase 5, Adcy5, adenosine receptor A2A, Adora2a, m4 muscarinic acetylcholine receptor, Chrm4). Examples of genes highly enriched in D1 neurons of the DS and/or NAc as compared to those of the PFC included several phosphodiesterases (Pde1b, Pde1c, Pde7b, Pdb10a), adenosine receptors (Adora2a and 2b), Drd3 dopamine receptor, several orphan receptors (Gpr6, 55, 83, 88, 139, and 149), retinoic acid receptors (Rarb, Rxrg), and the regulators of G protein signaling Rgs4 and 9. Interestingly some genes not usually associated with brain function and with relatively low expression were highly enriched in the striatum including interleukin receptors for IL-10 and IL-17 (about 20-fold enrichment) and the tyrosine kinase MuSK (>100-fold enrichment). Conversely, genes associated with glutamate transmission (e.g., vGluT1, slc17a7) were enriched in cortical neurons, as expected. Other highly cortically-enriched genes included those for GDNF and EGF receptors (Gfra2 and Egfr), adenosine receptors 1 (Adora1a and Adora1b), dopamine receptor 5 (Drd5), metabotropic glutamate receptor 2 (Grm2), nicotinic acetylcholine receptor α5 (Chrna5), as examples of potential pharmacologically relevant targets. The most significant over-represented gene ontologies (GO) included many related to synaptic and membrane regulation or function in the striatum and to neural development and axon extension in the PFC (**Table 3**, the full list of significantly over-represented GO are in **Supplementary Table 3**).

Comparison of polysomes-associated mRNA in D1 and D2 striatal neurons

Several publications have previously achieved global comparisons between genes expressed in striatal D1 and D2 neurons (Lobo et al., 2006; Heiman et al., 2008; Ena et al., 2013; Heiman et al., 2014). Here we could examined the differences between D1 and D2 neurons separately in the DS and in the NAc (**Figure 3A** and **B**). In the DS 443 genes were significantly more expressed in D1 neurons and 308 in D2 neurons (**Figure 3C**, complete list for DS in **Supplementary Table 4**). The most significantly differently expressed genes in the DS are shown in **Table 4** (higher in D1) and **Table 5** (higher in D2). The differences were not as pronounced as between striatum and PFC both in terms of number of significant genes and fold-change. The significant differences in relation with IUPHAR identified genes are shown in **Tables 6** and **7** (complete list in **Supplementary Table 5)**. Pronounced enrichments in D1 neurons were found for abundantly expressed genes such as Chrm4, and Tac1, as

expected. Interestingly less expressed genes highly enriched in D1 neurons included homeobox protein Arx (10-fold enrichment in D1) and integrin-α8 (7-fold) which may have potential significance for their differentiation. The genes most enriched in D2 neurons in the DS included known markers of these neurons, such as Adora2a, 5'-ectonucleotidase (Nt5e), preproenkephalin (Penk). Other genes included a number with potential pharmacological interest such as purinergic receptor P2ry1, opiate receptor Oprd1, several orphan receptors (Gpr6 and Gpr52), and the receptor tyrosine phosphatase RPTPμ (Ptprm).

In the NAc 456 genes were significantly more expressed in D1 neurons and 640 in D2 neurons (**Figure 3D**, complete list for DS in **Supplementary Table 6**). The top significant enrichments in D1 and D2 neurons are indicated in **Tables 8** and **9** respectively. The most significantly highly expressed genes in D1 SPNs of the NAc included known markers of these neurons such as Pdyn, Drd1, Chrm4, and Tac1, as well as the phosphatase Eya1, the G protein subunit β4 (Gnb4). Other genes with lower mRNA levels but with predominant expression in D1 neurons of the NAc and potential pharmacological interest included GDNF receptor Gfra1, Drd3, the somatostatin receptor Ssrtr4, and the muscarinic acetylcholine receptor Chrm5. In D2 neurons of the NAc, a high enrichment of Drd2, P2ry1, Penk, Gpr52, Nt5e, Adora2a, Oprd1, and Ptprm was observed as in the DS. When comparing the D1 and D2 neurons, more genes appeared to display a high fold-increase in D2 than in D1 neurons, possibly reflecting a more homogenous phenotype among the D2 SPNs in the NAc. Overall comparison between DS and NAc indicated the existence of common differences between D1 and D2 neurons in the two regions but also pointed to many specificities, with 20-45% common genes identified (**Figure 3E** and **F**). These values are only indicative since the number of differences which reach the significance threshold depends on the size of the samples. Nevertheless they underline the differences that exist betwee the two man regions of the striatum. In this context it is noticeable that neither in the DS nor in the NAc did we find a pronounced enrichment of messengers coding for acetylcholine metabolism. Choline acetyl-transferase and choline transporter Slc5a7 were enriched 7- to 15-fold in D2 neurons but found at low levels (<150 reads and <270 reads, respectively). This indicated that with the BAC transgenic mice expressing L10a-eGFP directly under the control of the Drd2 receptor, the activity of the promoter is relatively low in cholinergic interneurons and together with the low abundance of these neurons as compared to SPNs, their contribution to the extracted mRNAs is negligible.

Comparison of polysomes-associated mRNAs in the dorsal and ventral striatum

The comparisons between PFC and DS and NAc, as well as the D1/D2 comparisons in the DS and NAc showed many similarities but also numerous differences, strongly indicating that the complement of genes expressed and translated in these two regions of the striatum are different, as anticipated from the abundant literature emphasizing the differences between dorsal and ventral striatum. We first carried out a global analysis using a multifactorial approach, taking onto consideration all striatal neurons analyzed to evaluate the transcriptional differences between the dorsal and ventral striatum (**Tables 12** and **13**, **Supplementary Table 8**). This comparison indicated that 1838 mRNAs were found at significantly different levels between DS and NAc. Among these, 924 were higher in the DS and 914 in the NAc. We then conducted a separate analysis in D1 and D2 neurons (**Figures 4A** and **B**). A higher proportion of differentially expressed genes was found in the D1 neurons, possibly reflecting the lower size of the D2 sample (**Figure 4C** and **D**). In D1 neurons the cannabinoid receptor 1 (Cnr1) was among the most significantly highly expressed in the DS (**Tables 14**-**17**, **Supplementary Table 9**). Other genes with a high degree of enrichment and fair expression level included in the DS neurogranin (Nrgn), sphingosine-1-P phosphatase (Sgpp2), an activin receptor (Acvr1c), and Gpr155 (**Table 14** and **16**), and in the NAc Peg10, Stard5 Dlk1, and cGMP-dependent protein kinase 1 (Prkg1) (**Table 15** and **18**). Integrin $\alpha 8$, which was found to be enriched in D1 (see above) was also more abundant in the DS as compared to the NAc (**Table 16**). In the D2 neurons, many genes were also differently expressed, including Acvr1c and Cnr1 (**Tables 18-21**). The genes relatively enriched in DS included Cnr1, Acvr1c, synaptopodin 2 (Synpo2), and reelin (Reln), while in the NAc the enriched genes included CART (Cartpt), diacylglycerol kappa (dgkk), and Kv channel interacting protein 1 (Kcnip1). Comparison between D1 and D2 neurons indicated that many of the differences between dorsal and ventral striatum were common in the two types of neurons (**Figure 4E** and **F**).

Validation of the observed regional differences and comparison with other approaches

To assess the validity of the differences observed with BAC-TRAP and RNA sequencing we selected a few genes and carried out reverse transcription followed by real time Q-PCR. Focusing first on genes enriched in the PFC as compared to the striatum we confirmed that Tbr1 which was highly enriched in the PFC with RNAseq (5.2-fold apparent enrichment as compared to DS) was indeed clearly more expressed in the PFC using RT-PCR (about 20-fold, **Figure 5A**). We similarly verified a few other differences with smaller fold-change differences, Ppp2r2b (1.4-fold according to RNAseq), Shank2 (1.7), or lower apparent expression, Tac2 (13.5-fold). All these were confirmed by RT-PCR (**Figure 5A**). It should eb emphasized that the amplitude of the differences could differ between RNAseq from BAC-TRAP and RT-PCR for multiple reasons including the selection of cell specific mRNA and the focus on translated mRNAs in BAC-TRAP but not in our verification experiments. We then examined the

corresponding in situ hybridization patterns available at the Allen Brain Institute (http://mouse.brain-map.org/). For the strong quantitative differences that we observed the hybridization differences were striking (e.g. Tbr1, **Figure 5B**), whereas for the less pronounced ones the RNAseq and RT-PCR were clearly more informative (**Figure 5A** and **B**).

We then investigated some typical genes that were different between the DS and NAc according to the BAC-TRAP experiments. We looked at some genes for which BAC-TRAP/RNAseq indicated a high degree of enrichment in the NAc as compared to the DS: Dlk1 (12.5-fold enrichment in NAc vs DS), Drd3 (4-fold), and Arhgap36 (3.8-fold). The differences observed with RT-PCR were consistently much larger (8- to 23-fold higher in NAc, **Figure 5C**). For genes with smaller apparent differences in RNAseq, Wfs1 (2.5-fold), Ahi1 (2.4-fold) or Gda (2.4-fold), RT-PCR also confirmed the enrichment with enrichment ranging from 2- to 4-fold (**Figure 5C**). Comparison with Allen Brain Atlas in situ hybridization showed that differences were visually detectable in all cases.

In the DS we investigated Hpca (hippocalcin, 2-fold enriched in DS), ATP2b1 (plasma membrane ATP-dependent Ca^{2+} transporter 1, 2.5-fold), Slc24a2 (plasma membrane $Na^{+}/K^{+}/Ca^{2+}$ exchanger 2, 2.7-fold), and phosphodiesterase 10a (Pde10a, 1.9-fold). RT-PCR confirmed the mRNA enrichment in DS as compared to NAc (**Figure 5E**). The differences were also on in situ hybridization for Slc24a2 but not for the others, underlining the interest of the sequencing approaches.

Putative upstream regulators of dorso-ventral striatal gene expression

We next used the Ingenuity Pathway analysis (IPA) to identify putative upstream transcriptional regulators that could explain the observed differences in mRNAs between NAc and DS. We carried out this analysis in the comparison of the DS-NAc within both the D1 and D2 SPNs (**Figure 6A** and **B**). This approach identifies pharmacological or toxic agents as well as endogenous compounds. For example the analysis suggested the possible role of transcription factors such as PR Domain 8 (PRMD8) in D2-SPNs and Forkhead box protein O1 (FOXO1) in D1-SPNs in DS (**Figure 6 A** and **B**). To provide a testable hypothesis for the gene regulatory networks possibly commonly involved in the two types of SPNs, we looked for common regulators between these two populations. Prostaglandin 2 (PGE2) appeared as a suitable candidate among the different regulators since it appeared to regulate a set of genes in both D1- and D2-SPNs in the DS (**Figure 6C**). Although few studies have investigated the role of prostaglandins in the striatum outside their involvement in inflammatory conditions, it was reported that PGE2 acting through prostaglandin 1 receptor (EP1) could amplify both D1 and D2 signaling (Kitaoka et al., 2007). We therefore decided to investigate further the role of this pathway.

Evaluation of the possible role of prostaglandins as a regulator of dorsal striatum function

To evaluate the possible effects of PGE2 as an upstream regulator we tested the behavioral effect of the chronic treatment with a non-selective agonist of PGE2 receptors that can be used parenterally misoprostol. Twelve week-old wild type mice were intra-peritoneally implanted with an osmotic mini-pump system to chronically administrate either misoprostol (50 µg/kg/day) or vehicle (**Figure 7A**). The mice were then subjected to several behavioral tests and were killed after 4 weeks for mRNA analysis. ((The mRNA studies are in progress at the time of the writing of this draft)). Behavioral tests explored dorsal striatal functions.

In the open field mice showed a decreased locomotor activity after 6 days of misopristol treatment but no difference in the time spent in the center of the field (**Figure 7B** and **C**). Then, we tested motor coordination and learning using the rotarod task. Using successive trials of accelerating rotarod task there was no apparent differences in the ability of the two groups of mice to improve their performance (**Figure 7 D**). In contrast the use of two challenging fixed speeds once the task was acquired, 16 and 24 rpm, revealed differences between misopristol- and vehicle-treated mice. At 16 rpm the misoprostol group fell approximately twice less than the vehicle-treated mice but this difference did not reach the significance threshold. At 24 rpm the difference between the two groups was significant at 24 rpm indicating a better motor coordination in the misoprostol-treated group. Finally, the two groups were subjected to a behavioral paradigm that evaluates striatum-dependent memory. The two groups of mice were first mildly food-deprived to 90 % of their weight and their ability to find the food-reinforced arm was evaluated in a Y maze during 10 consecutive sessions. In each group half of the mice were assigned to the right arm and the other half to the left arm. A score of 1 was assigned when the mice entered the reinforced arm and of 0 when they entered the non-reinforced arm. Results are plotted as averages of blocks of 10 trials. The mice reached about 80% of correct choices after 3 days of training, with no significant difference detected between the two groups (**Figure 7G**). Twenty-four hours after the training session, the mice were challenged in a reversal learning test. The habitual reinforced arm was systematically exchanged with the non-reinforced arm. The mice chronically treated with misoprostol were significantly faster in reversing the established memory and learning the new reward position (**Figure 7G**). These results indicated an improvement of misopristol-treated mice as compared to vehicle-treated controls in several tests that depend on dorsal striatum function.

DISCUSSION

This manuscript reports the first comprehensive study of the genome-wide study of translated mRNAs expressed in the main forebrain cellular populations expressing either D1 or D2 dopamine receptors, including a differentiation between the DS and the NAc. As expected the most striking differences were identified between PFC D1 receptor-expressing neurons and D1 SPNs. We provide a region-specific comparison of genes differentially expressed in D1 and D2 neurons, showing that there exist important variances between the DS and the NAc for the D1 D2 differences. We further characterize the important differences between these two striatal regions showing that they are comparable in amplitude to the differences between the D1 and D2 populations. We show that our data about the regional differences are supported by replication by RT-PCR experiments on total mRNA from wild type mice. Finally we identify PGE2 as a putative upstream regulator of genes expressed in the dorsal striatum, and we provide experimental functional evidence in support of this hypothesis.

The differences in gene expression between D1 and D2 SPNs have already been explored by BAC-TRAP and microarrays (Heiman et al., 2008; Heiman et al., 2014). Our current study extends these findings in two ways. First the use of RNA-sequencing instead of microarrays increased the sensitivity of the approach, as indicated by the fact that it led to the identification of 2-6 times more significant differences depending on the region and population differences. Second it allowed to approach the comparison between the two types of SPNs on a regional basis, underlining the marked differences between the DS and the NAc. In a very recent paper (Gokce et al., 2016) the authors used single-cell RNA sequencing to study the whole striatal cell diversity. This paper confirmed most of the data already reported in literature, and showed that the D1 and the D2 neurons could be divided in 2 additional subpopulations that express a gradient of transcriptional states that could be related to the patch matrix organization of the striatum. Interestingly, the genes that the authors have chosen as defining the opposite gradient of expression in the two SPNs populations correspond to some of the genes that we identified as highly enriched in the NAc (Wfs1-Crym) or the DS (Cnr1). Further analysis will clearly be needed to determine whether the gradient observed in this paper correlates with the patch-matrix organization or the dorso-ventral gradient.

In relation with the anatomical organization of the inputs converging to the striatum and on the basis of multiple functional studies, the NAc has been associated to the motivation-related processes, while the DS is implicated in motor behavior, associative learning, and habits formation(Corbit and Balleine, 2016). To evaluate whether the gene expression differences identified in the present study had some functional significance, we looked for potential upstream regulators common to several genes. Of course it is extremely unlikely that a single pathway could account for

all the observed regional differences. Nevertheless we were intrigued by the potential role of PGE2, which was the only compound predicted to be a possible positive regulator of the genes expressed in both D1 and D2 neurons in the DS. Therefore, we chose it as possible target to study the effects of its manipulation on striatal function. Prostaglandins (PGs) are a family of lipid mediators involved in a plethora of processes including vascular homeostasis, inflammation, and reproduction (Narumiya et al., 1999). Although little is known about the role of PGs in general and of PGE2 in the striatum, it has been previously shown that PGE2 amplifies both the D1 and D2 signaling pathways (Kitaoka et al., 2007). Here we tested the effects of a chronic infusion of a non-selective agonist of PGE2 receptors that could be administered by osmopump. The treated mice displayed an improved performance in several behavioral tasks that are related with the dorsal striatum, including the time on rotarod and in reversal learning. This result supports the hypothesis that PGs, and possibly PGE2, are regulators of dorsal striatal function. Work in progress addresses the effects of misopristol on transcription of putative target genes and the pharmacological specificity of the effects.

In conclusion this work provides an extensive characterization of the translated mRNAs in the two main populations of striatal projection neurons, comparing them to D1-positive cortical neurons and unraveling the differences between the dorsal and ventral striatum. Our data should provide a useful resource for any further analyses of genes expressed in the striatum and should help the interpretation of results from other approaches, including single cell sequencing. In addition our results allowed the identification of PGE2 as an important regulator of dorsal striatum function.

References

Anders S, Pyl PT, Huber W (2015) HTSeq--a Python framework to work with high-throughput sequencing data. Bioinformatics 31:166-169.

Beaulieu JM, Gainetdinov RR (2011) The physiology, signaling, and pharmacology of dopamine receptors. Pharmacol Rev 63:182-217.

Benjamini Y, Hochberg Y (1995) Controlling the false discovery rate: a practical and powerful approach to multiple testing. J Roy Statist Soc Ser B 57:289-300.

Bertran-Gonzalez J, Bosch C, Maroteaux M, Matamales M, Herve D, Valjent E, Girault JA (2008a) Opposing patterns of signaling activation in dopamine D1 and D2 receptor-expressing striatal neurons in response to cocaine and haloperidol. J Neurosci 28:5671-5685.

Bertran-Gonzalez J, Bosch C, Maroteaux M, Matamales M, Herve D, Valjent E, Girault JA (2008b) Opposing patterns of signaling activation in dopamine D1 and D2 receptor-expressing striatal neurons in response to cocaine and haloperidol. J Neurosci 28:5671-5685.

Corbit LH, Balleine BW (2016) Learning and Motivational Processes Contributing to Pavlovian-Instrumental Transfer and Their Neural Bases: Dopamine and Beyond. Curr Top Behav Neurosci 27:259-289.

Doll BB, Hutchison KE, Frank MJ (2011) Dopaminergic genes predict individual differences in susceptibility to confirmation bias. J Neurosci 31:6188-6198.

Doyle JP, Dougherty JD, Heiman M, Schmidt EF, Stevens TR, Ma G, Bupp S, Shrestha P, Shah RD, Doughty ML, Gong S, Greengard P, Heintz N (2008) Application of a translational profiling approach for the comparative analysis of CNS cell types. Cell 135:749-762.

Ena SL, De Backer JF, Schiffmann SN, de Kerchove d'Exaerde A (2013) FACS array profiling identifies Ecto-5' nucleotidase as a striatopallidal neuron-specific gene involved in striatal-dependent learning. J Neurosci 33:8794-8809.

Gerfen CR, Engber TM, Mahan LC, Susel Z, Chase TN, Monsma FJ, Jr., Sibley DR (1990) D_1 and D_2 dopamine receptor-regulated gene expression of striatonigral and striatopallidal neurons. Science 250:1429-1432.

Gokce O, Stanley GM, Treutlein B, Neff NF, Camp JG, Malenka RC, Rothwell PE, Fuccillo MV, Sudhof TC, Quake SR (2016) Cellular Taxonomy of the Mouse Striatum as Revealed by Single-Cell RNA-Seq. Cell Rep 16:1126-1137.

Heiman M, Heilbut A, Francardo V, Kulicke R, Fenster RJ, Kolaczyk ED, Mesirov JP, Surmeier DJ, Cenci MA, Greengard P (2014) Molecular adaptations of striatal spiny projection neurons during levodopa-induced dyskinesia. Proc Natl Acad Sci USA 111:4578-4583.

Heiman M, Schaefer A, Gong S, Peterson JD, Day M, Ramsey KE, Suarez-Farinas M, Schwarz C, Stephan DA, Surmeier DJ, Greengard P, Heintz N (2008) A translational profiling approach for the molecular characterization of CNS cell types. Cell 135:738-748.

Kitaoka S, Furuyashiki T, Nishi A, Shuto T, Koyasu S, Matsuoka T, Miyasaka M, Greengard P, Narumiya S (2007) Prostaglandin E2 acts on EP1 receptor and amplifies both dopamine D1 and D2 receptor signaling in the striatum. J Neurosci 27:12900-12907.

Kupchik YM, Brown RM, Heinsbroek JA, Lobo MK, Schwartz DJ, Kalivas PW (2015) Coding the direct/indirect pathways by D1 and D2 receptors is not valid for accumbens projections. Nat Neurosci 18:1230-1232.

Lobo MK, Karsten SL, Gray M, Geschwind DH, Yang XW (2006) FACS-array profiling of striatal projection neuron subtypes in juvenile and adult mouse brains. Nat Neurosci 9:443-452.

Love MI, Huber W, Anders S (2014) Moderated estimation of fold change and dispersion for RNA-seq data with DESeq2. Genome Biol 15:550.

Narumiya S, Sugimoto Y, Ushikubi F (1999) Prostanoid receptors: structures, properties, and functions. Physiol Rev 79:1193-1226.

Schultz W (2007) Multiple dopamine functions at different time courses. Annu Rev Neurosci 30:259-288.

Sharpee TO (2014) Toward functional classification of neuronal types. Neuron 83:1329-1334.

Smiley JF, Levey AI, Ciliax BJ, Goldman-Rakic PS (1994) D1 dopamine receptor immunoreactivity in human and monkey cerebral cortex: predominant and extrasynaptic localization in dendritic spines. Proc Natl Acad Sci USA 91:5720-5724.

Tecuapetla F, Jin X, Lima SQ, Costa RM (2016) Complementary Contributions of Striatal Projection Pathways to Action Initiation and Execution. Cell 166:703-715.

Valjent E, Bertran-Gonzalez J, Herve D, Fisone G, Girault JA (2009) Looking BAC at striatal signaling: cell-specific analysis in new transgenic mice. Trends Neurosci 32:538-547.

Voorn P, Vanderschuren LJ, Groenewegen HJ, Robbins TW, Pennartz CM (2004) Putting a spin on the dorsal-ventral divide of the striatum. Trends Neurosci 27:468-474.

Yamanaka S, Blau HM (2010) Nuclear reprogramming to a pluripotent state by three approaches. Nature 465:704-712.

Yu G, Wang LG, Han Y, He QY (2012) clusterProfiler: an R package for comparing biological themes among gene clusters. OMICS 16:284-287.

Figure Legends

Figure 1: D1 and D2 BAC-TRAP mice and experimental design.

A-B. Brain sections from Drd1a::EGFP-L10a (A) and Drd2::EGFP-L10a (B) mice showing the location of the cells expressing EGFP-L10a (direct EGFP fluorescence). A, left panel sagittal section of a Drd1a::EGFP-L10a mouse, middle panel higher magnification of the area indicated on the left panel, right panel higher magnification of the striatum and blow up of a single neuron to illustrate the cytoplasmic and nucleolar labeling. B, left panel sagittal section of a Drd2::EGFP-L10a mouse, middle and right panels coronal sections through the prefrontal cortex and striatum, respectively. Images are stitched confocal sections, scale bar 1.5 mm. **C.** Isolation of the brain samples. The brain was rapidly dissected and placed in a stainless steel matrix with 0.5 mm coronal section interval, and two thick slices containing the PFC (green, 2 mm-thick) and the striatum (3 mm-thick). The olfactory bulb was removed from the cortex. The dorsal striatum (pink) and the nucleus accumbens (yellow) were punched out with a metal cannula on ice.

Figure 2: Differential gene expression in the PFC and striatum of D1 BAC-TRAP mice.

A-B. mRNAs were purified by BAC-TRAP from Drd1a::EGFP-L10a. In each mouse the PFC, DS and NAc were dissected out as indicated in Fig. 1. Tissues from 3 mice were pooled, polysomes immunopurified, and mRNAs quantified by RNAseq. Scatter plots of the expression levels, as $\log_{10}$(reads), of all identified genes expressed in the PFC and DS (A) and NAc (B) from Drd1::BAC-TRAP mice. n = 4 pools of 3 mice each. Genes significantly more expressed in PFC are in blue, in DS in red, and in NAc in green. **C-D.** Venn diagrams showing the number of genes differentially expressed in the PFC vs DS (C) and the PFC vs NAc (D). The number at the intersection corresponds to the number of genes that were not different between regions.

Figure 3: Differential gene expression in D1 and D2 BAC-TRAP mice.

A-B. mRNAs were purified by BAC-TRAP from Drd1a::EGFP-L10a and Drd2::EGFP-L10A mice and analyzed by RNAseq. The differences in expression patterns between D1 and D2 were compared in the DS (A) and in the NAc (B). Scatter plots of the expression levels, as $\log_{10}$(reads), of all identified genes expressed in D1 (x axis) and D2 (y axis) samples. n = 4 pools of 3 mice each. Genes significantly more expressed in D1 are in magenta, in D2 in dark grey. **C-D.** Venn diagrams showing the number of genes differentially expressed in the D1 vs D2 in the dorsal striatum (C) and NAc (D). The number at

the intersection corresponds to the number of genes that were not different between D1 and D2. **E-F.** Venn diagrams comparing the number of genes differentially expressed at a higher level in D1 (E) or in D2 (F) for the DS (left circle, red) or the NAc (right circle, green).

Figure 4: Differential gene expression between the DS and the NAc.

A-B. mRNAs were purified by BAC-TRAP from Drd1a::EGFP-L10a and Drd2::EGFP-L10A mice. In each mouse the DS and NAc were dissected out as indicated in Fig. 1. mRNAs were purified by BAC-TRAP and analyzed by RNAseq.). Scatter plots of the expression levels, as $\log_{10}$(reads), of all identified genes in DS (x axis) and NAc (y axis) samples of Drd1a::EGFP-L10a (A) and Drd2::EGFP-L10A mice (B). n = 4 pools of 3 mice each. Genes significantly more expressed in DS are in red, in NAc in green. **C-D.** Venn diagrams comparing the number of genes differentially expressed at a higher level in NAc (left, green) or in DS (right, red) for the D1 samples (C) or the D2 sample (D). The number at the intersection corresponds to the number of genes that were not different between regions. **E.** Venn diagram comparing the numbers of mRNAs more abundant in the DS when D1 samples were analyzed separately (magenta circle), D2 samples separately (grey circle), or when all the samples were analyzed simultaneously (D1 and D2, black circle). **F.** Same as in E, except that numbers are shown for the mRNAs more abundant in the NAc.

Figure 5: Expression analysis of selected mRNAs enriched in DS, NAc or PFC.

A number of genes were selected from the regional BAC-TRAP analysis for verification with independent methods. mRNA levels were studied by qRT-PCR in wild type mice. **A.** mRNAs analysis by qTR-PCR of gene products expressed at higher levels in the PFC than in the DS. The expression levels were calculated by the comparative DDCt method and expressed relative to the DS; β-actin was used as internal control. Data are means + SEM from 6 independent experiments. Statistical analysis with two-tailed unpaired t-test. **B.** Representative Allen Brain Atlas in situ hybridization images corresponding to the genes studied in A. **C-D.** Same as in A and B except that the selected mRNAs were more expressed in the NAc than in the DS. **E-F.** Same as in C and D except that the selected mRNAs were more expressed in the DS than in the NAc. *p<0.05; **, p<0.01, ***p<0.01; ****p<0.0001

Figure 6: Ingenuity pathway analysis of upstream regulators of genes differentially expressed in the DS and NAc.

A-B. Ranks of the putative up-stream regulators of the mRNAs enriched in the DS of D1-SPN (A, magenta) and D2 SPNs (B, orange). Up-streams regulators are ranked as function of the Z-score, only the up-streams regulators with a z-score >2 are considered as significant and shown. **B.** Circular network showing the upstream regulator prostaglandinE2 in the center (PGE2) with its targets colored according to their higher expression in the DS in D1 mice (magenta), D2 mice (orange), or both (yellow).

Figure 7: Behavioral effects of a prostaglandin agonist on dorsal striatum function.

A. Outline of the experiment. Wild type mice were implanted on day 1 (surgery) with an i.p. osmopump containing either vehicle (Veh) of misopristol (Miso). They were tested for locomotor activity in the open field at day 6 (OF), rotarod at days 9-15, and in a Y maze at days 20-25. **B.** Distance traveled in the open field in xx min. Two-way ANOVA interaction $F_{(14,345)} = 0.19$, $p = 0.99$, time effect, $F_{(14, 345)} = 3.12$, $p = 0.0001$, treatment effect, $F_{(1,345)} = 42.35$, $p<0.0001$, n = 12-13 mice/group. **C.** Analysis of time in center. Student's t test $t_{23} = 0.85$, $p = 0.41$. **D.** Accelerating rotarod, latency to fall during the learning phase. Two-way ANOVA interaction $F_{(15,367)} = 0.76$, $p = 0.72$, time effect, $F_{(15, 367)} = 23.36$, $p<0.0001$, treatment effect, $F_{(1,367)} = 1.23$, $p = 0.27$, n = 12-13. **E.** Fixed speed rotarod in trained mice (16 r.p.m.). Student's t test $t_{24} = 1.99$, $p = 0.058$. **F.** Fixed speed rotarod (24 r.p.m.). Student's t test $t_{21} = 2.24$, $p = 0.036$. **F.** Acquisition and reversal of the food-rewarded arm choice in a Y maze. Two-way ANOVA acquisition: interaction $F_{(5,132)} = 0.41$, $p = 0.84$, trial effect, $F_{(5,132)} = 2.98$, $p = 0.014$, treatment effect, $F_{(1,132)} = 0.14$, $p = 0.71$; reversal, interaction $F_{(3,88)} = 0.94$, $p = 0.42$, trial effect, $F_{(3,88)} = 14.72$, $p<0.0001$, treatment effect, $F_{(1,88)} = 8.18$, $p = 0.0053$. n =11-13 mice/group.

Figure 1

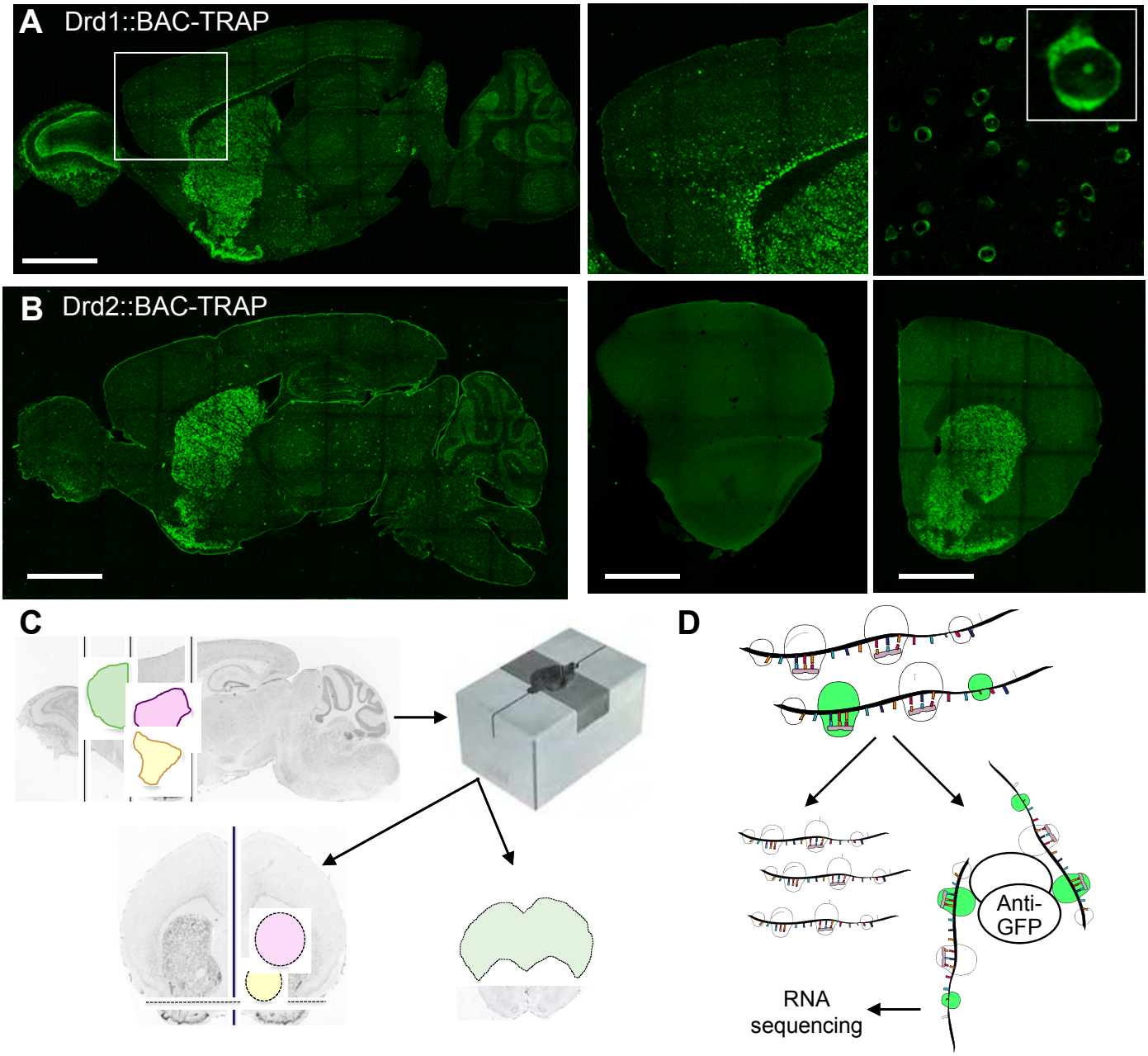

Figure 2

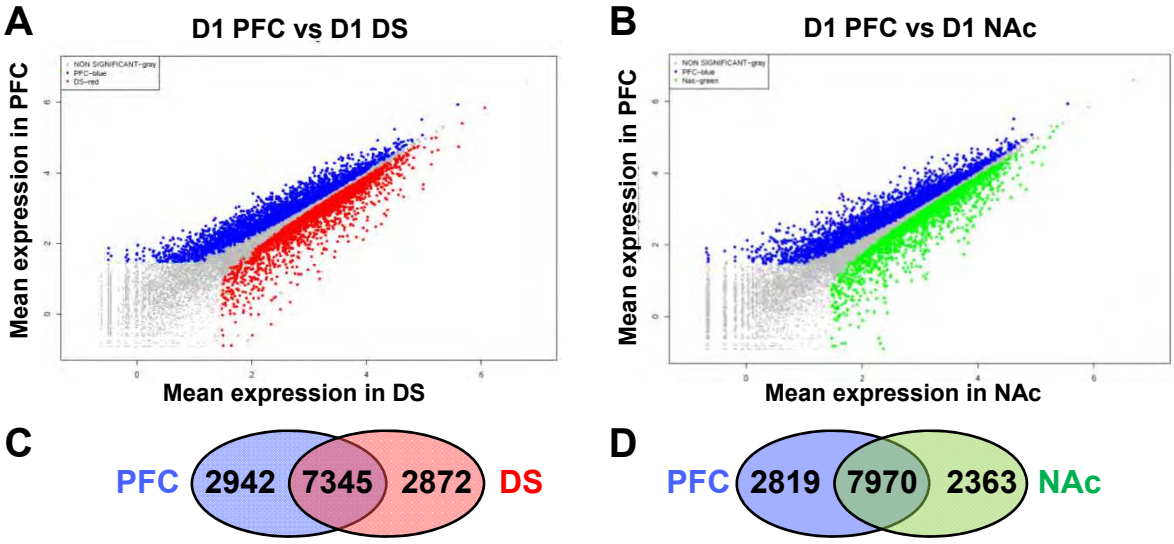
A
D1 PFC vs D1 DS
Mean expression in PFC
Mean expression in DS
B
D1 PFC vs D1 NAc
Mean expression in PFC
Mean expression in NAc
C
PFC
2942
7345
2872
DS
D
PFC
2819
7970
2363
NAc

Figure 3

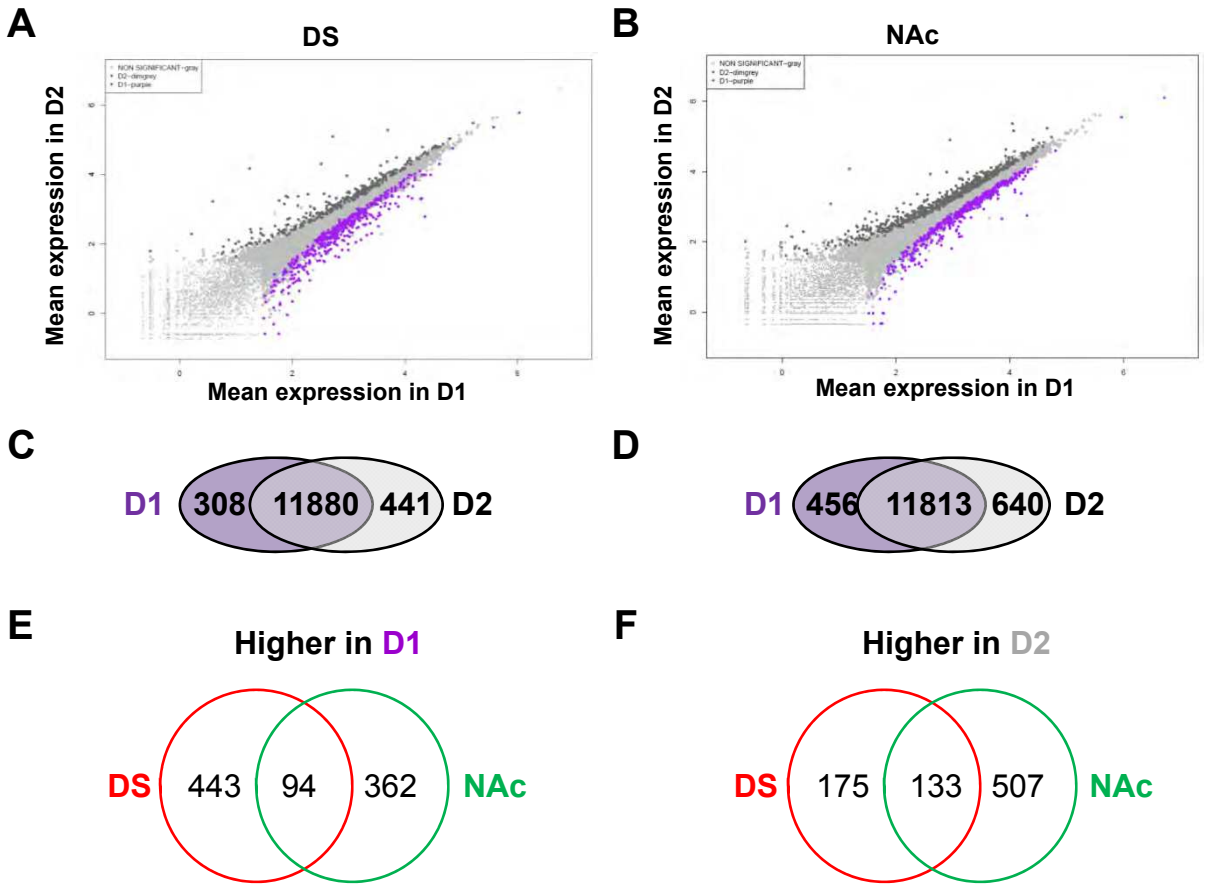
A
DS
Mean expression in D2
Mean expression in D1
B
NAc
Mean expression in D2
Mean expression in D1
C
D1
308
11880
441
D2
D
D1
456
11813
640
D2
E
Higher in D1
DS
443
94
362
NAc
F
Higher in D2
DS
175
133
507
NAc

Figure 4

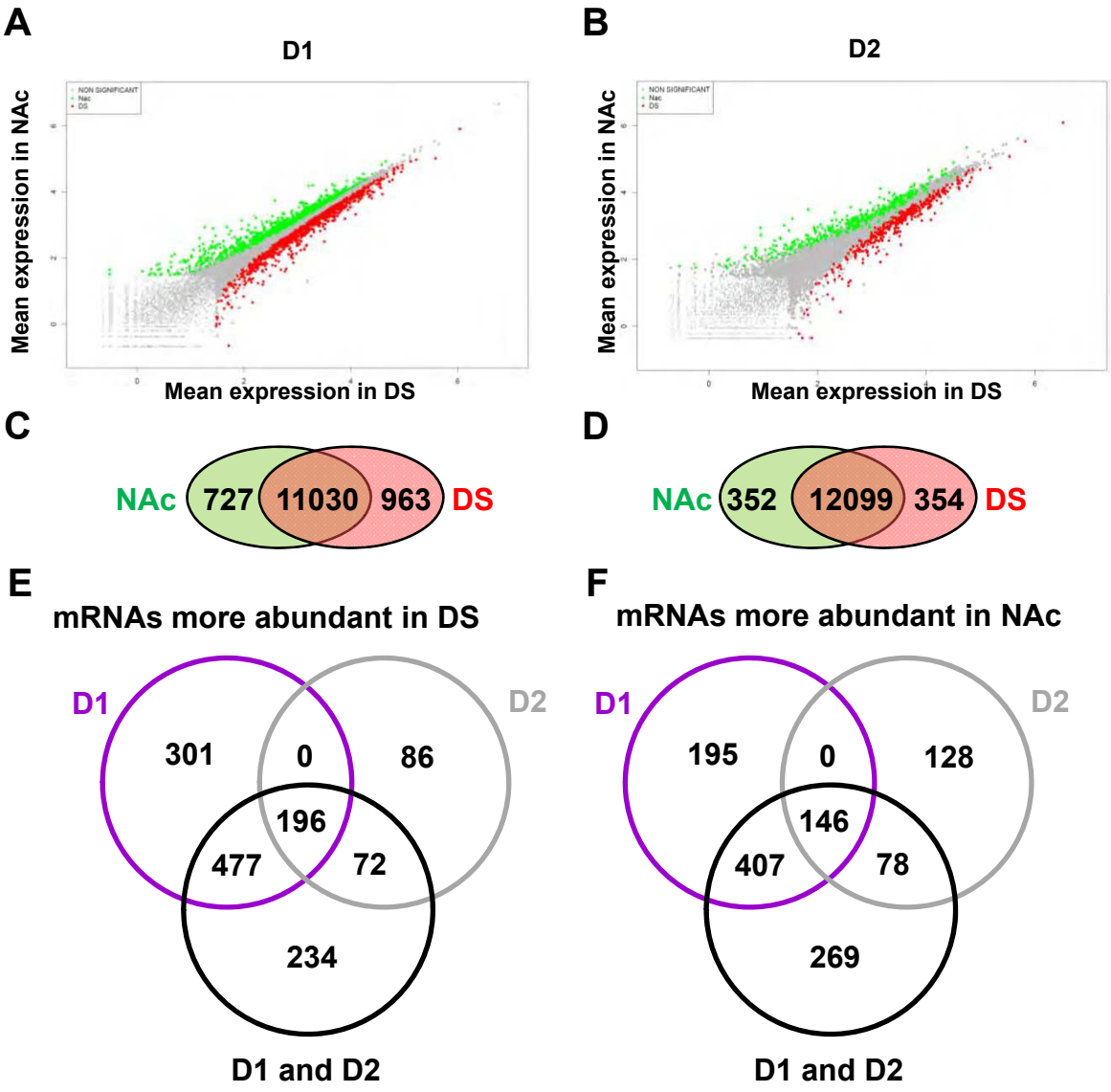
A
D1
Mean expression in NAc
Mean expression in DS
B
D2
Mean expression in NAc
Mean expression in DS
C
NAc
727
11030
963
DS
D
NAc
352
12099
354
DS
E
mRNAs more abundant in DS
D1
D2
301
0
86
196
477
72
234
D1 and D2
F
mRNAs more abundant in NAc
D1
D2
195
0
128
146
407
78
269
D1 and D2

Figure 5

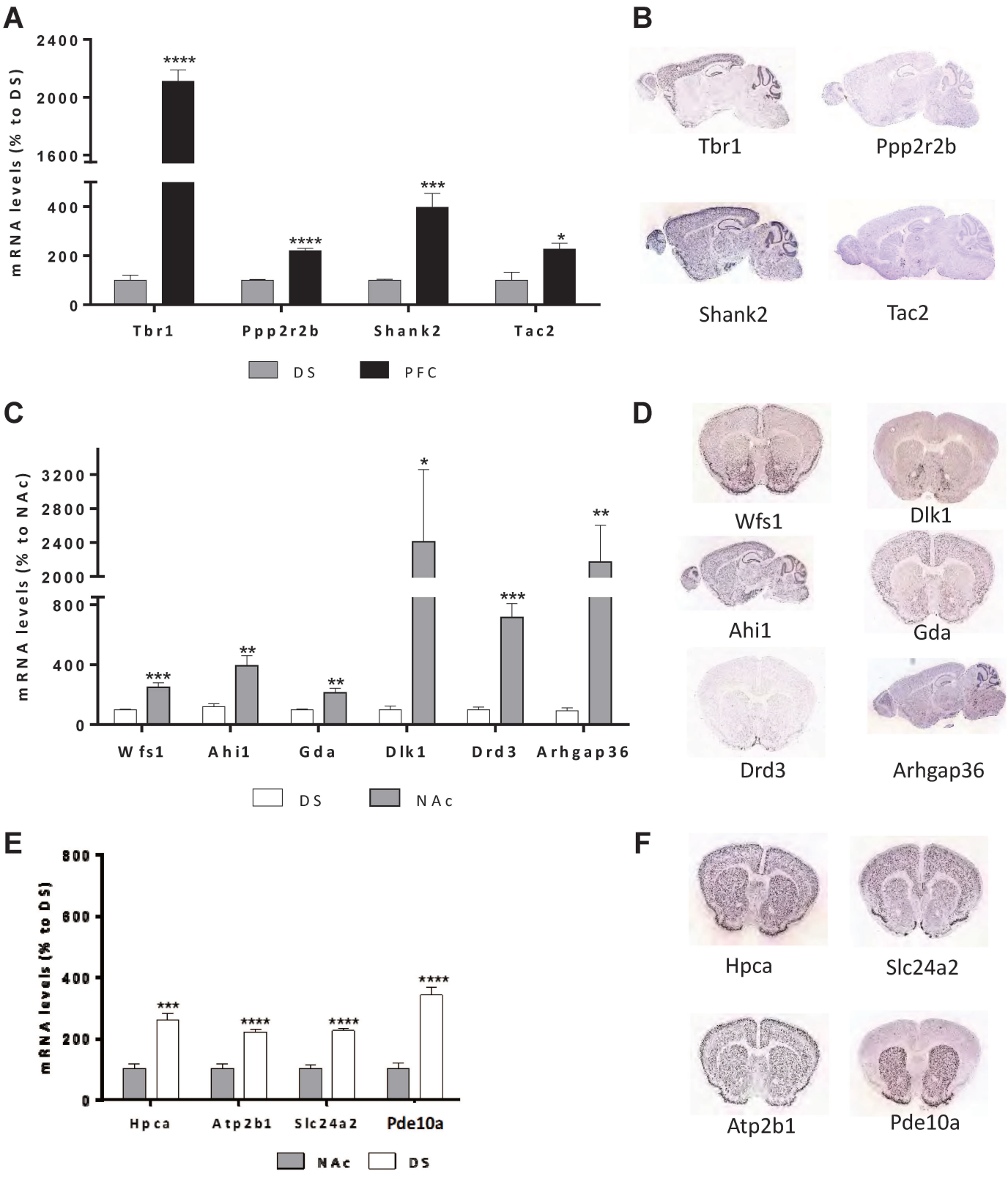
A
mRNA levels (% to DS)
2400
2000
1600
400
200
0
****
****
***
*
Tbr1
Ppp2r2b
Shank2
Tac2
DS
PFC
B
Tbr1
Ppp2r2b
Shank2
Tac2
C
mRNA levels (% to NAc)
3200
2800
2400
2000
800
400
0
***
**
**
*
***
**
Wfs1
Ahi1
Gda
Dlk1
Drd3
Arhgap36
DS
NAc
D
Wfs1
Dlk1
Ahi1
Gda
Drd3
Arhgap36
E
mRNA levels (% to DS)
800
600
400
200
0
***
****
****
****
Hpca
Atp2b1
Slc24a2
Pde10a
NAc
DS
F
Hpca
Slc24a2
Atp2b1
Pde10a

Figure 6

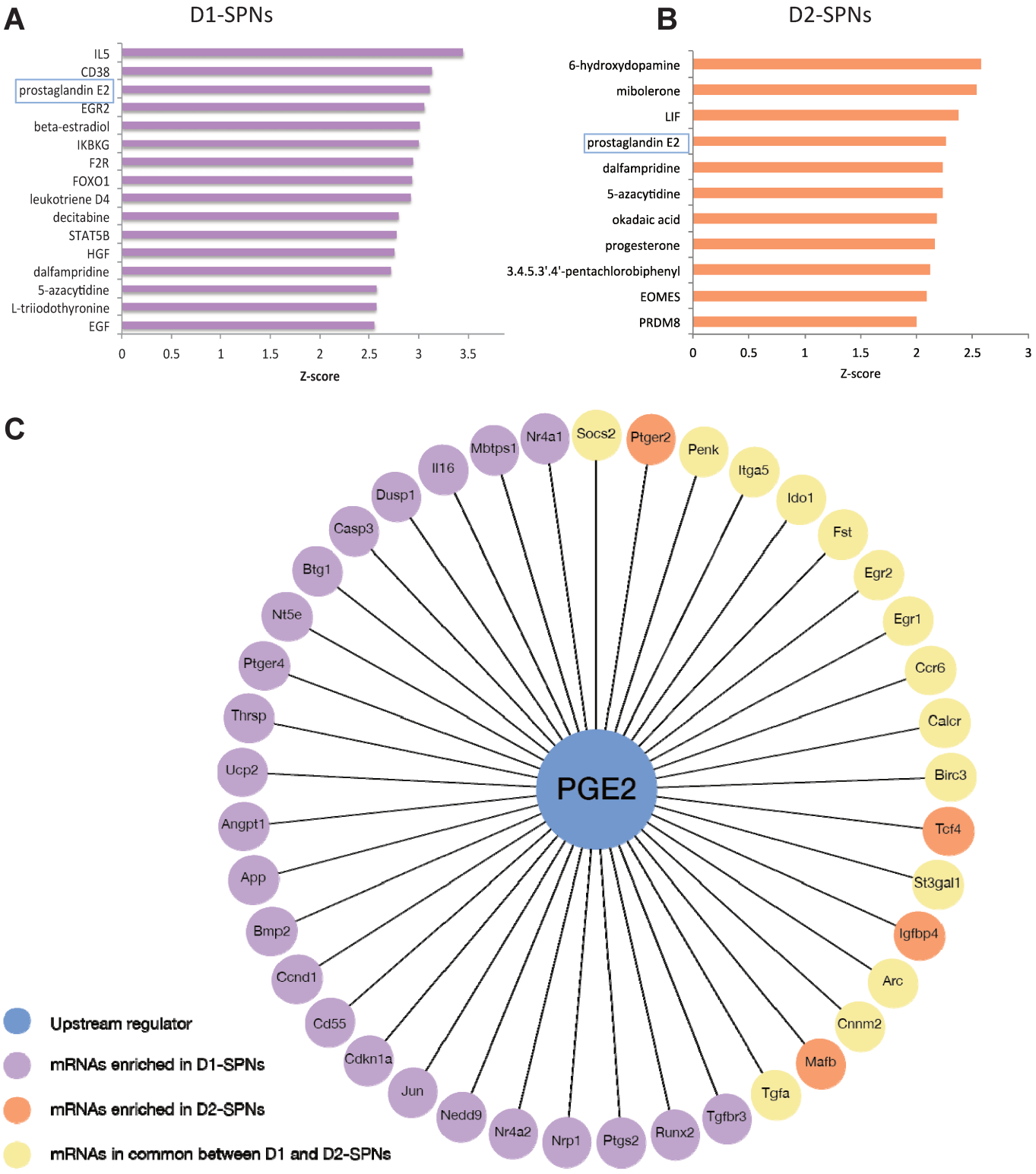
A
D1-SPNs
IL5
CD38
prostaglandin E2
EGR2
beta-estradiol
IKBKG
F2R
FOXO1
leukotriene D4
decitabine
STAT5B
HGF
dalfampridine
5-azacytidine
L-triiodothyronine
EGF
0
0.5
1
1.5
2
2.5
3
3.5
Z-score
B
D2-SPNs
6-hydroxydopamine
mibolerone
LIF
prostaglandin E2
dalfampridine
5-azacytidine
okadaic acid
progesterone
3.4.5.3'.4'-pentachlorobiphenyl
EOMES
PRDM8
0
0.5
1
1.5
2
2.5
3
Z-score
C
PGE2
Socs2
Ptger2
Penk
Itga5
Ido1
Fst
Egr2
Egr1
Ccr6
Calcr
Birc3
Tcf4
St3gal1
Igfbp4
Arc
Cnnm2
Mafb
Tgfa
Tgfbr3
Runx2
Ptgs2
Nrp1
Nr4a2
Nedd9
Jun
Cdkn1a
Cd55
Ccnd1
Bmp2
App
Angpt1
Ucp2
Thrsp
Ptger4
Nt5e
Btg1
Casp3
Dusp1
Il16
Mbtps1
Nr4a1
Upstream regulator
mRNAs enriched in D1-SPNs
mRNAs enriched in D2-SPNs
mRNAs in common between D1 and D2-SPNs

Figure 7

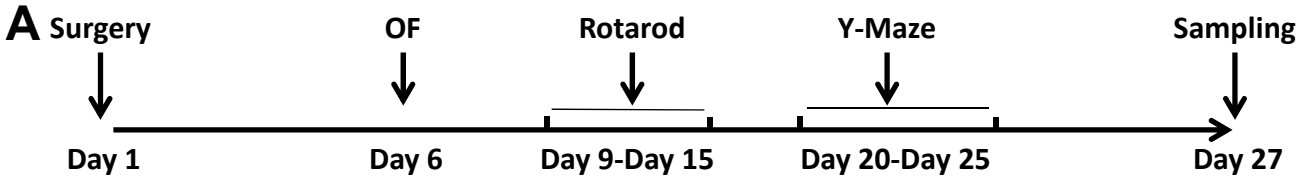
A
Surgery
OF
Rotarod
Y-Maze
Sampling
Day 1
Day 6
Day 9-Day 15
Day 20-Day 25
Day 27

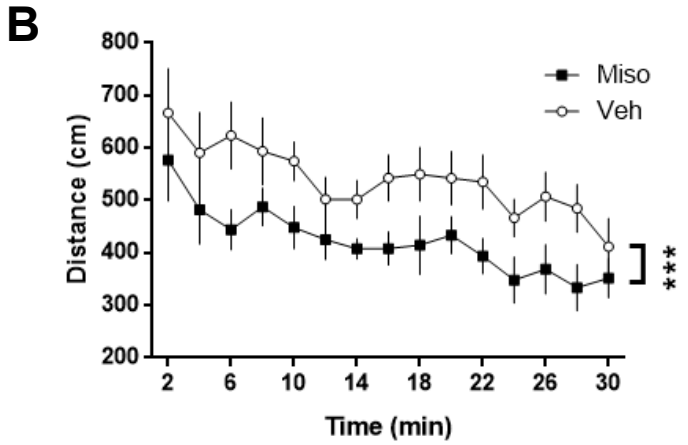
B
Distance (cm)
Time (min)
Miso
Veh
***

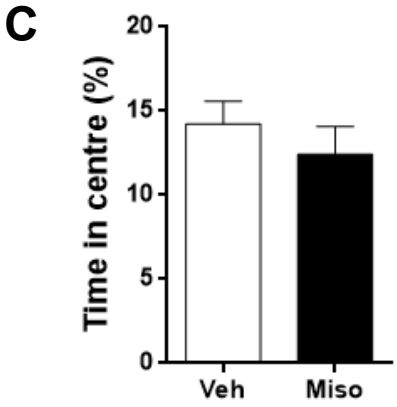
C
Time in centre (%)
Veh
Miso

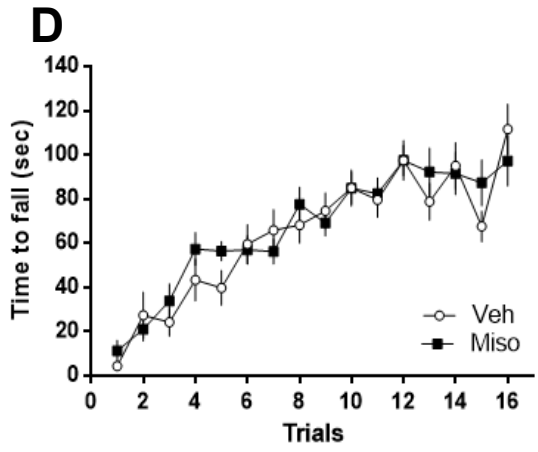
D
Time to fall (sec)
Trials
Veh
Miso

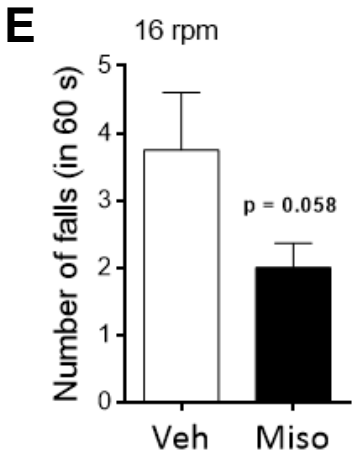
E
16 rpm
Number of falls (in 60 s)
p = 0.058
Veh
Miso

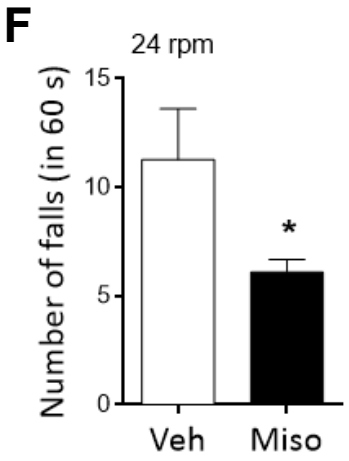
F
24 rpm
Number of falls (in 60 s)
*
Veh
Miso

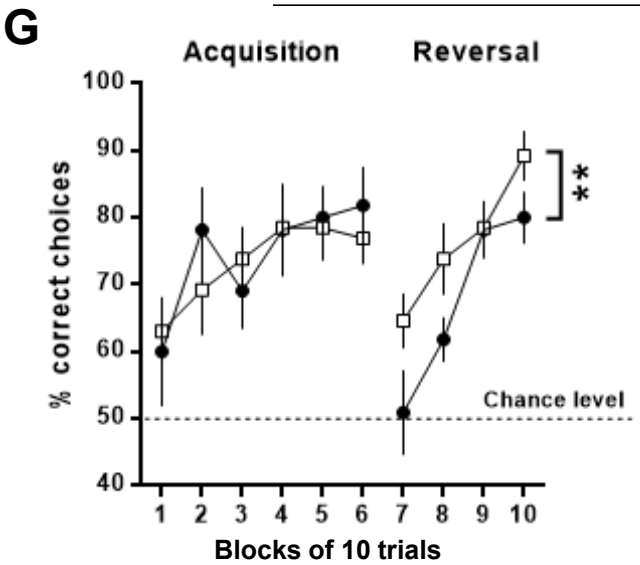
G
Acquisition
Reversal
% correct choices
Chance level
**
Blocks of 10 trials

Table 3: Examples of highly significantly overrepresented GOs in DS or NAc as compared to PFC

ID	Description	p.adjust
	Overrepresented in DS	
GO:0034765	regulation of ion transmembrane transport	1.9035E-12
GO:0050804	modulation of synaptic transmission	6.9118E-12
GO:0050803	regulation of synapse structure or activity	1.0207E-11
GO:0034762	regulation of transmembrane transport	1.3053E-11
GO:0007611	learning or memory	2.4767E-10
GO:0048167	regulation of synaptic plasticity	8.2147E-09
GO:0007626	locomotor behavior	4.5827E-08
GO:0007212	dopamine receptor signaling pathway	3.2926E-06
	Overrepresented in NAc	
GO:0007264	small GTPase mediated signal transduction	4.3007E-09
GO:0007611	learning or memory	8.74E-09
GO:0007212	dopamine receptor signaling pathway	3.5703E-08
GO:0007626	locomotor behavior	8.852E-08
GO:0050803	regulation of synapse structure or activity	4.4129E-07
GO:0050806	positive regulation of synaptic transmission	1.0238E-06
GO:0048813	dendrite morphogenesis	1.4236E-06
GO:0008277	regulation of G-protein coupled receptor protein signaling pathway	2.0011E-06
	Overrepresented in PFC vs DS	
GO:0061564	axon development	7.8506E-14
GO:0007409	axonogenesis	1.9686E-13
GO:0060560	developmental growth involved in morphogenesis	9.3731E-13
GO:0050804	modulation of synaptic transmission	1.2269E-11
GO:0010975	regulation of neuron projection development	1.5734E-11
GO:0030900	forebrain development	1.5463E-10
GO:0042391	regulation of membrane potential	1.589E-10
GO:0007264	small GTPase mediated signal transduction	3.4792E-10
GO:1990138	neuron projection extension	4.1222E-10
GO:0090066	regulation of anatomical structure size	1.3917E-09
GO:0007265	Ras protein signal transduction	2.1259E-09
GO:0021537	telencephalon development	6.4059E-09

Table 4: Top 30 most significant genes with mRNA enriched in D1 as compared to D2 neurons of the DS

Gene	Gene Description	log2 FC	padj	D1 mean	D2 mean
Arx	aristaless related homeobox	-3.215	2.70E-27	675	41
Chrm4	cholinergic receptor, muscarinic 4	-2.957	2.70E-27	2 110	177
Fxyd7	FXYD domain-containing ion transport regulator 7	-2.147	2.43E-17	1 036	157
Tac1	tachykinin 1	-2.560	3.48E-17	19 058	1 983
Hpcal1	hippocalcin-like 1	-2.202	4.50E-16	833	122
Cntnap3	contactin associated protein-like 3	-2.619	6.30E-15	583	44
Gnb4	guanine nucleotide binding protein (G protein), beta 4	-2.035	1.61E-13	2 038	371
Dgkz	diacylglycerol kinase zeta	-1.739	5.89E-13	5 524	1 426
Stmn2	stathmin-like 2	-1.805	7.62E-13	6 869	1 468
Tns1	tensin 1	-1.648	6.40E-12	2 059	620
Nrxn1	neurexin I	-1.318	1.62E-11	9 549	4 098
Rasgrf2	RAS -specific guanine nucleotide-releasing factor 2	-2.078	1.67E-11	2 405	388
Itga8	integrin alpha 8	-2.604	2.19E-11	101	2
Myh3	myosin, heavy polypeptide 3, skeletal muscle, embryonic	-2.565	2.24E-11	206	9
Isl1	ISL1 transcription factor, LIM/homeodomain	-2.448	2.44E-11	1 347	109
Cpeb1	cytoplasmic polyadenylation element binding protein 1	-1.520	3.14E-10	1 160	336
Hs3st2	heparan sulfate (glucosamine) 3-O-sulfotransferase 2	-1.944	6.81E-10	563	103
Cplx3	complexin 3	-2.240	7.38E-10	991	67
Gng2	guanine nucleotide binding protein (G protein), gamma 2	-1.885	7.51E-10	7 636	1 200
Tmem178	transmembrane protein 178	-1.962	2.80E-09	620	92
Ube2ql1	ubiquitin-conjugating enzyme E2Q family-like 1	-1.778	3.01E-09	2 757	582
Otof	otoferlin	-1.665	4.13E-09	604	136
Dlk1	delta-like 1 homolog (Drosophila)	-2.227	4.26E-09	373	31
Scn1b	sodium channel, voltage-gated, type I, beta	-1.413	5.47E-09	3 740	1 154
Pitpnm3	PITPNM family member 3	-1.691	6.43E-09	2 562	666
Rassf3	Ras association (RalGDS/AF-6) domain family member 3	-1.595	8.62E-09	1 590	460
Ikzf1	IKAROS family zinc finger 1	-1.993	1.16E-08	378	61
Cpne9	copine family member IX	-1.486	1.28E-08	934	286
Lingo2	leucine rich repeat and Ig domain containing 2	-2.174	1.29E-08	980	99
Lrpap1	LDL receptor-related protein associated protein 1	-0.988	1.67E-08	4 596	2 090

Table 5: Top 30 most significant genes with mRNA enriched in D2 as compared to D1 neurons of the DS

Gene	Gene Description	log2 FC	padj	D1 mean	D2 mean
Adora2a	adenosine A2a receptor	4.865	2.20E-69	327	19 945
Gpr52	G protein-coupled receptor 52	3.396	1.04E-61	191	2 671
Nt5e	5' nucleotidase, ecto	3.692	2.63E-57	72	1 427
Penk	preproenkephalin	4.176	1.26E-51	4 970	189 913
P2ry1	purinergic receptor P2Y, G-protein coupled 1	3.721	9.78E-48	84	2 177
Oprd1	opioid receptor, delta 1	3.962	3.73E-43	77	2 376
Sp9	trans-acting transcription factor 9	3.539	5.98E-41	127	2 325
Fig4	FIG4 phosphoinositide 5-phosphatase	2.292	1.62E-39	460	2 308
Gpr6	G protein-coupled receptor 6	3.711	6.78E-31	58	1 778
Upb1	ureidopropionase, beta	3.332	1.48E-19	2	192
Gucy1a3	guanylate cyclase 1, soluble, alpha 3	1.671	1.59E-16	7 095	30 497
Necab1	N-terminal EF-hand calcium binding protein 1	1.912	3.04E-16	3 705	18 024
Grik3	glutamate receptor, ionotropic, kainate 3	2.577	3.15E-16	936	9 130
Sema3e	semaphorin) 3E	1.446	3.66E-14	1 014	3 135
Prkd1	protein kinase D1	1.694	7.99E-12	250	1 020
Ptprm	protein tyrosine phosphatase, receptor type, M	2.181	4.69E-11	367	2 736
Gpr88	G-protein coupled receptor 88	1.180	1.16E-10	20 501	60 797
Gprin3	GPRIN family member 3	0.976	2.93E-10	2 588	5 482
Fnip2	folliculin interacting protein 2	1.519	2.02E-09	445	1 550
Nell1	NEL-like 1	1.857	2.89E-09	177	757
Kctd12	K+ channel tetramerisation domain containing 12	1.024	6.67E-09	2 648	6 466
Adk	adenosine kinase	1.759	1.29E-08	244	1 053
Wnt7a	wingless-type MMTV integration site family, 7A	1.800	2.29E-08	85	359
Mro	maestro	1.844	2.89E-08	209	1 203
Thpo	thrombopoietin	2.091	3.06E-08	28	269
Sox11	SRY (sex determining region Y)-box 11	1.380	3.68E-08	608	2 083
Trim62	tripartite motif-containing 62	1.493	4.01E-08	605	2 002
Galnt13	UDP-N-ac-αD-galactosamine:polypept. transferase 13	1.057	5.43E-08	3 019	7 758
Tacr1	tachykinin receptor 1	1.500	6.41E-08	128	496
Kcnk2	potassium channel, subfamily K, member 2	1.067	6.86E-08	3 940	9 694

Table 6: IUPHAR data base-selected genes with mRNA enriched in D1 as compared to D2 neurons in the DS*

Type	Family name	MGI symbol	Mean	log2 FC	padj
Catalytic receptors	GDNF receptor family	Gfra1	238	-1.69	2.82E-05
		Gfra2	428	-0.98	9.90E-03
	IL-17 receptor family	Il17rc	83	-1.16	5.68E-03
	Integrins	Itga8	52	-2.60	2.19E-11
	Receptor tyrosine phosphatases (RTP)	Ptprt	2 190	-0.99	1.26E-03
		Ptprf	653	-0.80	1.02E-02
		Ptprn	7 117	-0.55	4.09E-02
	Type I RTKs: ErbB (EGF) receptor family	Erbb4	253	-1.64	4.13E-07
Enzymes	1.-.-.- Oxidoreductases	Impdh1	895	-0.64	8.61E-03
	2.1.1.43 Histone methyltransferases (HMTs)	Smyd2	690	-0.82	1.23E-02
	4.2.1.1 Carbonate dehydratases	Car12	1 365	-1.17	5.07E-05
	ABC1-B subfamily	Adck4	231	-0.90	2.73E-02
	Adenosine turnover	Nt5c	625	-0.85	4.15E-02
	Alpha subfamily	Prkcg	15 544	-1.13	2.31E-05
	Amino acid hydroxylases	Th	64	-1.05	3.22E-02
	BARK/GRK2 subfamily	Adrbk1	1 321	-0.82	1.59E-02
	C12: Ubiquitin C-terminal hydrolase	Uchl1	16 479	-0.83	1.17E-02
	CAMK1 family	Camk1	142	-1.65	1.13E-05
		Camk1g	1 263	-0.82	1.26E-02
	CAMK2 family	Camk2d	855	-1.24	3.47E-05
	Catecholamine turnover	Th	64	-1.05	3.22E-02
	Cyclin-dependent kinase-like (CDKL) family	Cdkl4	600	-0.98	1.75E-04
	Delta subfamily	Prkca	5 569	-0.73	5.51E-04
	Endocannabinoid turnover	Faah	200	-0.96	4.26E-02
	Eta subfamily	Prkch	3 354	-0.92	3.68E-04
	FRAY subfamily	Stk39	2 693	-0.69	1.87E-03
	Hydrolases	Faah	200	-0.96	4.26E-02
		Lta4h	657	-0.66	2.49E-02
	Inositol polyphosphate phosphatases	Inpp4b	128	-1.19	2.30E-03
	KHS subfamily	Map4k1	65	-1.40	1.98E-03
	Leukotriene and lipoxin metabolism	Lta4h	657	-0.66	2.49E-02
	M1: Aminopeptidase N	2010111I01Rik	554	-0.72	7.37E-03
		Lta4h	657	-0.66	2.49E-02
	M2: Angiotensin-converting (ACE and ACE2)	Ace	577	-1.11	6.69E-04
	Meta subfamily	Camkk1	2 225	-0.89	5.56E-06
	Nucleoside synthesis and metabolism	Impdh1	895	-0.64	8.61E-03
	Phosphodiesterases, 3',5'-cyclic nucleotide	Pde1a	2 826	-1.41	3.99E-06
		Pde9a	340	-1.34	1.26E-04
	Protein kinase A	Prkar1b	10 951	-0.94	2.18E-05
	S8: Subtilisin	Pcsk9	82	-1.57	1.85E-04
	S9: Prolyl oligopeptidase	Fap	31	-0.98	3.18E-02
	STE11 family	Map3k5	1 008	-0.74	1.08E-03
	Trio family	Obscn	119	-1.09	2.43E-02
	Wnk family	Wnk4	253	-0.88	3.76E-02
GPCR	Acetylcholine receptors (muscarinic)	Chrm4	1 143	-2.96	2.70E-27
	Adhesion Class GPCRs	Adgra1	694	-1.01	9.93E-03
	Adrenoceptors	Adra2a	70	-1.29	5.61E-03
		Adra2c	993	-1.29	2.01E-05
	Class A Orphans	Gpr139	344	-1.54	1.87E-04
		Gpr26	413	-1.31	4.57E-04

		Mas1	152	-1.25	1.45E-03
	Neuropeptide Y receptors	Npy2r	69	-1.07	3.25E-02
		Npy1r	430	-0.90	6.30E-03
	Opioid receptors	Oprl1	435	-0.92	1.80E-02
	Somatostatin receptors	Sstr2	172	-1.60	2.24E-04
	Vasopressin and oxytocin receptors	Oxtr	66	-1.16	2.02E-02
LGIC	GABA-A receptors	Gabra5	1 259	-0.60	3.08E-02
	Glycine receptors	Glra2	201	-1.11	1.28E-03
	Ionotropic glutamate receptors	Grin2d	57	-1.04	3.57E-02
		Grik4	76	-0.99	3.73E-02
NHR	4A. Nerve growth factor IB-like receptors	Nr4a2	1 866	-1.52	6.32E-04
		Nr4a3	1 010	-0.84	2.57E-02
Other proteins	Fatty acid-binding proteins	Crabp1	301	-1.09	2.13E-02
		Rbp4	402	-1.05	1.57E-02
	R12 family	Rgs12	759	-0.92	4.85E-04
	Tubulins	Tuba4a	12 668	-0.42	2.09E-02
Transporters	ABCC subfamily	Abcc8	163	-1.07	1.40E-02
	Mitochondrial amino acid transporter subfamily	Slc25a22	2 540	-0.63	1.43E-02
	Organic cation transporters (OCT)	Slc22a3	392	-0.96	1.24E-03
	SLC30 zinc transporter family	Slc30a3	114	-1.52	7.03E-04
	SLC35 nucleotide sugar transporters	Slc35d3	896	-1.15	1.53E-02
	SLC45 family of putative sugar transporters	Slc45a1	750	-0.66	3.70E-02
	System A-like transporters	Slc38a4	56	-1.23	1.02E-02
	Vesicular glutamate transporters (VGLUTs)	Slc17a7	1 803	-1.68	4.08E-06
VGIC	Ryanodine receptor	Ryr1	263	-0.96	1.79E-02
	Two-P potassium channels	Kcnk3	127	-1.45	2.82E-05
		Kcnk13	71	-1.14	2.26E-02
	Voltage-gated potassium channels	Kcns1	126	-1.45	2.16E-04
		Kcna6	1 433	-1.12	1.60E-03

* Translated mRNAs were isolated from the dorsal striatum of *Drd1*::BAC-TRAP and *Drd2*::BAC-TRAP mice. Only identified in the IUPHAR nomenclature, with adjusted p value <0.05 and expression levels > 30 reads are included. Fold change D2/D1.

Abbrev.: FC, fold-change, GPCR, G protein-coupled receptor, IC, ion channel, IUPHAR, International Union of Basic and Clinical Pharmacology, LGIC, ligand-gated ion channel, MGI, mouse genome informatics database symbol, NHR, nuclear hormone receptor, padj, adjusted p value, VGIC, voltage-gated ion channel.

http://www.guidetopharmacology.org/download.jsp

Table 7: Selected IUAPHAR genes whose mRNA is enriched in D2 as compared to D1 neurons in the DS*

Type	Family name	MGI symbol	Mean	log2 FC	padj
Catalytic receptors	Receptor tyrosine phosphatases (RTP)	Ptpro	923	1.09	1.79E-05
		Ptprm	1 551	2.18	4.69E-11
	Type II receptor serine/threonine kinases	Acvr2a	1 371	0.80	1.14E-02
		Tgfbr2	117	1.87	2.64E-06
	Type II RTKs: Insulin receptor family	Igf1r	2 302	0.68	2.13E-02
	Type IV RTKs: VEGF receptor family	Flt4	113	1.50	2.89E-04
	Type XIX RTKs: LTK receptor family	Alk	60	1.46	1.09E-03
Enzymes	1.14.11.- Histone demethylases	Kdm6b	1 002	1.02	2.01E-03
	2.1.1.43 Histone methyltransferases (HMTs)	Setd8	4 379	0.56	2.16E-02
		Kmt2e	23 688	0.62	1.54E-02
	2.3.1.48 Histone acetyltransferases (HATs)	Kat6a	6 051	0.48	1.00E-02
		Ncoa2	10 410	0.58	2.44E-02
		Kat2b	749	0.67	3.60E-02
	2.4.2.30 poly(ADP-ribose)polymerases	Parp3	143	1.38	3.70E-04
	Acetylcholine turnover	Chat	84	1.69	6.85E-05
	Adenosine turnover	Adk	648	1.76	1.29E-08
		Nt5e	750	3.69	2.63E-57
	Arginine:glycine amidinotransferase	Gatm	723	0.77	3.32E-02
	CAMK1 family	Camk4	47 467	0.46	2.86E-02
	CLK family	Clk1	948	0.75	3.32E-04
	Lipid phosphate phosphatases	Pten	18 622	0.72	4.83E-05
	M13: Neprilysin	Mme	7 941	0.93	2.75E-04
	MLK subfamily	Zak	821	1.29	9.51E-07
	Phosphatidylinositol kinases	Pik3c2a	1 196	0.73	3.73E-03
		Pik3r5	173	0.98	2.96E-02
	Phosphatidylinositol-4-phosphate 3-kinase	Pik3c2a	1 196	0.73	3.73E-03
	Phosphodiesterases, 3',5'-cyclic nucleotide	Pde4b	17 424	0.73	1.11E-04
		Pde3a	32	1.20	1.25E-02
	Protein kinase D (PKD) family	Prkd3	221	0.80	3.78E-02
		Prkd1	635	1.69	7.99E-12
	RCK family	Ick	889	0.78	1.14E-02
	Soluble guanylyl cyclase	Gucy1b3	8 751	0.66	1.84E-03
		Gucy1a3	18 796	1.67	1.59E-16
	Trbl family	Trib2	2 297	0.73	5.52E-04
	YANK family	Stk32a	2 354	0.53	1.22E-02
GPCR	5-Hydroxytryptamine receptors	Htr2c	1 450	1.20	1.37E-04
	Acetylcholine receptors (muscarinic)	Chrm3	302	1.02	3.64E-02
	Adenosine receptors	Adora2a	10 136	4.86	2.20E-69
	Calcitonin receptors	Calcrl	53	1.11	3.07E-02
	Class A Orphans	Gpr88	40 649	1.18	1.16E-10
		Gpr149	436	1.38	9.35E-07
		Gpr52	1 431	3.40	1.04E-61
		Gpr6	918	3.71	6.78E-31
	Histamine receptors	Hrh3	9 026	0.94	3.47E-05
	Opioid receptors	Oprm1	540	0.82	1.79E-02
	Opioid receptors	Oprd1	1 226	3.96	3.73E-43
	P2Y receptors	P2ry1	1 130	3.72	9.78E-48
	Prostanoid receptors	Ptger2	44	1.73	5.92E-05
	Tachykinin receptors	Tacr1	312	1.50	6.41E-08
LGIC	GABA-A receptors	Gabra2	1 051	0.87	2.72E-03
		Gabrg3	1 962	1.21	7.75E-06
	Ionotropic glutamate receptors	Grik3	5 033	2.58	3.15E-16
	Nicotinic acetylcholine receptors	Chrna4	1 214	0.93	3.98E-02

NHR	1A. Thyroid hormone receptors	Thrb	5 411	1.01	1.67E-04
	3C. 3-Ketosteroid receptors	Nr3c1	3 601	0.59	2.36E-03
Other proteins	Non-enzymatic BRD containing proteins	Brwd3	1 595	0.55	2.59E-02
		Phip	2 944	0.59	1.65E-02
	R4 family	Rgs8	21 976	0.61	1.52E-02
Transporters	ABCG subfamily	Abcg1	2 313	0.54	2.86E-02
	Choline transporter	Slc5a7	139	1.48	1.03E-03
	GABA transporter subfamily	Slc6a1	3 981	0.64	3.07E-02
	Neutral amino acid transporter subfamily	Slc6a15	820	0.61	3.65E-02
	SLC35 family of nucleotide sugar transporters	Slc35f1	7 096	1.07	5.93E-05
	SLC41 family of divalent cation transporters	Slc41a1	4 840	0.73	4.47E-02
VGIC	Ryanodine receptor	Ryr3	2 848	0.67	6.02E-03
	Transient Receptor Potential channels	Trpc4	211	1.38	1.98E-03
	Two-P potassium channels	Kcnk2	6 817	1.07	6.86E-08

* Translated mRNAs were isolated from the dorsal striatum of *Drd1*::BAC-TRAP and *Drd2*::BAC-TRAP mice. Only identified in the IUPHAR nomenclature, with adjusted p value <0.05 and expression levels > 30 reads are included. Fold change D2/D1.

Abbrev.: FC, fold-change, GPCR, G protein-coupled receptor, IC, ion channel, IUPHAR, International Union of Basic and Clinical Pharmacology, LGIC, ligand-gated ion channel, MGI, mouse genome informatics database symbol, NHR, nuclear hormone receptor, padj, adjusted p value, VGIC, voltage-gated ion channel.

http://www.guidetopharmacology.org/download.jsp

Table 8: Top 30 most significant genes with mRNA enriched in D1 as compared to D2 neurons of the NAc

Gene	Gene Description	log2 FC	padj	D1 mean	D2 mean
Pdyn	prodynorphin	-3.57	9.23E-42	7 308	458
Eya1	EYA 1	-4.14	2.85E-36	19 975	551
Isl1	ISL1 transcription factor, LIM/homeodomain	-2.93	3.16E-24	1 427	145
Arhgap36	Rho GTPase activating protein 36	-3.18	2.80E-22	960	65
Chrm4	cholinergic receptor, muscarinic 4	-2.28	3.50E-20	1 170	218
Ebf1	early B cell factor 1	-2.29	2.93E-15	1 280	173
Gnb4	G protein, beta 4	-1.83	9.71E-15	3 508	839
Gfra1	GDNF family receptor alpha 1	-2.25	1.04E-13	1 149	201
Ngb	neuroglobin	-2.83	4.68E-13	282	20
Asic4	proton-gated ion channel family member 4	-2.06	3.68E-12	1 258	269
Dlk1	delta-like 1 homolog (Drosophila)	-1.62	7.81E-12	6 218	1 676
Irak3	interleukin-1 receptor-associated kinase 3	-2.55	3.46E-11	337	29
Cntnap3	contactin associated protein-like 3	-2.13	1.00E-10	573	109
Gpr101	G protein-coupled receptor 101	-1.64	1.20E-10	1 392	365
Cyb5r3	cytochrome b5 reductase 3	-1.41	1.23E-09	6 271	2 149
Tac1	tachykinin 1	-1.81	1.57E-08	12 231	3 035
Chrm5	cholinergic receptor, muscarinic 5	-2.60	4.25E-08	97	4
Agbl2	ATP/GTP binding protein-like 2	-1.88	9.80E-08	668	146
Arl4a	ADP-ribosylation factor-like 4A	-1.09	3.77E-07	6 173	2 724
Ano7	anoctamin 7	-2.22	1.97E-06	252	23
Pde1a	phosphodiesterase 1A, calmodulin-dependent	-1.17	2.98E-06	18 873	7 409
Calb2	calbindin 2	-1.70	1.06E-05	585	157
Peg10	paternally expressed 10	-1.24	1.32E-05	17 193	5 955
Rapgef1	Rap guanine nucleotide exch. factor (GEF) 1	-0.96	1.35E-05	4 387	2 186
Tns1	tensin 1	-1.48	1.39E-05	1 313	388
Tspyl2	TSPY-like 2	-0.96	1.44E-05	9 126	4 118
Sstr4	somatostatin receptor 4	-2.06	2.33E-05	218	22
Camk1g	CaMK1 gamma	-1.15	2.35E-05	2 101	865
Mapk8ip3	MAP kinase 8 interacting protein 3	-0.94	2.46E-05	9 315	4 654

Table 9: Top 30 most significant genes with mRNA enriched in D2 as compared to D1 neurons of the NAc

Gene	Gene Description	log2 FC	padj	D1 mean	D2 mean
P2ry1	purinergic receptor P2Y, G-protein coupled 1	3.76	1.83E-36	402	8 318
Penk	preproenkephalin	3.18	2.39E-26	11 608	145 837
Gpr52	G protein-coupled receptor 52	2.75	2.83E-16	236	2 238
Fst	follistatin	3.01	2.68E-14	45	634
Nt5e	5' nucleotidase, ecto	2.34	2.70E-14	181	1 137
Sp9	trans-acting transcription factor 9	1.91	1.30E-12	362	1 610
Adk	adenosine kinase	1.91	1.36E-12	313	1 473
Upb1	ureidopropionase, beta	2.96	2.21E-11	35	710
Adora2a	adenosine A2a receptor	2.71	2.51E-11	783	9 430
Gucy1a3	guanylate cyclase 1, soluble, alpha 3	1.60	4.55E-11	12 146	38 014
Mro	maestro	2.21	1.03E-10	110	718
Malat1	Metastasis-assoc. lung adenocarc. transcript 1	1.94	1.23E-09	8 524	42 128
Oprd1	opioid receptor, delta 1	2.45	2.33E-09	137	1 232
Gpr88	G-protein coupled receptor 88	1.44	1.38E-08	9 662	25 825
Stc1	stanniocalcin 1	2.13	3.11E-08	364	2 158
Skap2	src family associated phosphoprotein 2	1.78	6.99E-08	312	1 337
Marcks	myristoylated alanine rich PKC substrate	1.18	9.80E-08	5 411	10 640
Htr2a	5-hydroxytryptamine (serotonin) receptor 2A	1.43	1.40E-07	652	1 889
Fgfr2	fibroblast growth factor receptor 2	1.92	2.93E-07	104	517
2900097C17Rik	RIKEN cDNA 2900097C17 gene	1.41	4.56E-07	25 855	80 167
Gse1	genetic suppressor element 1	1.40	1.17E-06	3 096	9 555
Klf3	Kruppel-like factor 3 (basic)	1.32	1.28E-06	607	1 554
Plp1	proteolipid protein (myelin) 1	1.49	1.31E-06	943	2 991
Yeats2	YEATS domain containing 2	1.72	1.74E-06	1 434	6 151
4930465K10Rik	RIKEN cDNA 4930465K10 gene	2.38	2.00E-06	2	189
Fam101b	family with sequence similarity 101, member B	1.36	2.01E-06	586	1 573
Bcor	BCL6 interacting corepressor	1.89	3.51E-06	1 804	9 584
Uqcrb	ubiquinol-cyt c reductase binding protein	1.40	3.86E-06	2 357	7 458
C330007P06Rik	RIKEN cDNA C330007P06 gene	1,13	5,12E-06	3 795	7 738
Cldn11	claudin 11	2.16	5.18E-06	28	232
Qk	quaking	1.30	5.40E-06	2 532	6 487

Table 10: IUPHAR data base-selected genes with mRNA enriched in D1 as compared to D2 neurons in the NAc*

Type	Family name	MGI symbol	Mean	log2 FC	padj
Catalytic Receptors	GDNF receptor family	Gfra1	833	-2.25	1.04E-13
	IL-10 receptor family	Il20ra	67	-1.90	4.48E-04
	NOD-like receptor family	Nlrp10	121	-1.16	4.15E-02
	Prolactin receptor family	Epor	294	-1.10	9.04E-03
	Receptor tyrosine phosphatases (RTP)	Ptprn	6 411	-0.57	4.02E-02
	Type I RTKs: ErbB (EGF) receptor family	Erbb4	541	-1.35	1.77E-03
Enzymes	1.14.11.- Histone demethylases	Kdm8	61	-1.17	4.55E-02
	1-phosphatidylinositol 4-kinase family	Pi4kb	1 142	-0.81	4.15E-02
	2.1.1.- Protein arginine N-methyltransferases	Fbxo10	1 103	-0.97	2.92E-02
	2.1.2.- OHMet-, formyl- and related transferases	Gart	597	-0.71	4.33E-02
	2.3.-.- Acyltransferases	Fasn	4 629	-0.79	3.56E-03
	3.1.1.- Carboxylic Ester Hydrolases	Ppme1	3 467	-0.82	4.66E-02
	3.5.1.- Histone deacetylases (HDACs)	Hdac11	7 044	-0.56	3.36E-02
		Sirt2	3 709	-0.57	4.35E-02
	6.3.3.- Cyclo-ligases	Gart	597	-0.71	4.33E-02
	Alpha subfamily	Prkcg	20 313	-0.87	3.84E-04
	BARK/GRK2 subfamily	Adrbk2	586	-0.77	4.09E-02
	C12: Ubiquitin C-terminal hydrolase	Bap1	3 477	-0.53	4.33E-02
		Uchl1	16 503	-0.69	2.29E-02
	C19: Ubiquitin-specific protease	Usp5	2 775	-0.96	4.41E-04
	CAMK1 family	Camk1g	1 689	-1.15	2.35E-05
	Catecholamine turnover	Comt	3 446	-0.55	4.09E-02
	Csk family	Csk	485	-0.92	4.44E-02
		Matk	2 487	-0.94	2.98E-02
	Delta subfamily	Prkca	8 811	-0.68	3.67E-03
		Prkcq	168	-1.48	2.30E-03
	GABA turnover	Aldh9a1	346	-1.04	3.80E-02
	GEK subfamily	Cdc42bpb	4 297	-0.63	3.92E-02
	Inositol polyphosphate phosphatases	Inpp4b	326	-1.04	2.59E-02
	Interleukin-1 receptor-associated kinase (IRAK)	Irak3	234	-2.55	3.46E-11
	Lanosterol biosynthesis pathway	Pmvk	1 183	-0.90	7.64E-03
	Lipoxygenases	Aloxe3	220	-1.30	4.92E-03
	MARK subfamily	Mark4	1 155	-0.91	3.68E-02
	Nucleoside synthesis and metabolism	Gart	597	-0.71	4.33E-02
	Numb-associated kinase (NAK) family	Gak	3 425	-0.58	4.44E-02
	Other DMPK family kinases	Cit	5 166	-0.59	4.16E-02
	PAKB subfamily	Pak6	2 348	-1.30	1.65E-03
	Phosphatidylinositol kinases	Pi4kb	1 142	-0.81	4.15E-02
	Phosphodiesterases, 3',5'-cyclic nucleotide	Pde1a	15 052	-1.17	2.98E-06
	Phosphoinositide-specific phospholipase C	Plcd3	98	-1.38	1.36E-02
		Plce1	930	-0.94	5.98E-03
	Protein kinase A	Prkar1b	15 991	-0.61	1.47E-02
	S33: Prolyl aminopeptidase	Ppme1	3 467	-0.82	4.66E-02
	STE11 family	Map3k5	1 658	-1.06	1.05E-04
	STE20 family	Map3k19	120	-1.94	1.23E-04
	STE7 family	Map2k7	4 138	-0.98	3.59E-02
	STE-unique family	Map3k14	133	-1.20	4.94E-02
	TESK subfamily	Tesk1	2 580	-0.90	2.38E-02
GPCR	Acetylcholine receptors (muscarinic)	Chrm4	853	-2.28	3.50E-20
	Acetylcholine receptors (muscarinic)	Chrm5	66	-2.60	4.25E-08

	Class A Orphans	Gpr101	1 050	-1.64	1.20E-10
	Class A Orphans	Gpr26	323	-1.36	1.23E-02
	Dopamine receptors	Drd3	169	-1.29	2.41E-02
	Neuropeptide S receptor	Npsr1	137	-1.29	2.89E-02
	Other 7TM proteins	Gpr107	374	-1.16	8.73E-03
	Somatostatin receptors	Sstr4	153	-2.06	2.33E-05
	Thyrotropin-releasing hormone receptors	Trhr2	57	-1.43	1.36E-02
LGIC	GABA-A receptors	Gabrb1	579	-0.76	2.98E-02
		Gabrd	1 833	-0.89	2.30E-03
	Ionotropic glutamate receptors	Grin3a	422	-1.20	5.92E-04
Other IC	Connexins and Pannexins	Gja5	66	-1.69	1.32E-03
Other proteins	Fatty acid-binding proteins	Rbp1	1 119	-1.08	3.81E-02
		Rbp4	205	-1.03	3.40E-02
	R7 family	Rgs6	257	-1.26	3.18E-02
	Ribosomal factors	Eef2	13 135	-0.54	3.79E-02
	Tubulins	Tuba4a	11 002	-0.55	3.51E-02
		Tubb3	6 840	-0.93	3.90E-03
	WD repeat-containing proteins	Wdr5	592	-0.90	2.15E-02
Transporters	Ca2+-ATPases	Atp2b4	4 724	-1.10	1.26E-03
	MFS of transporters	Sv2a	3 778	-1.10	2.14E-02
	Na+-ATPases	Atp1a1	7 690	-0.86	1.87E-02
	Neutral amino acid transporter subfamily	Slc6a17	8 290	-0.79	2.89E-02
	SLC12 cation-coupled chloride transporters	Slc12a9	141	-1.60	1.79E-03
	SLC24 sodium/potassium/calcium exchangers	Slc24a3	1 174	-0.93	1.89E-02
	SLC35 family of nucleotide sugar transporters	Slc35d3	914	-1.82	5.15E-04
	SLC9 family of sodium/hydrogen exchangers	Slc9a5	376	-1.03	8.01E-03
	System A-like transporters	Slc38a4	53	-1.30	3.02E-02
	V-type ATPase	Atp6v1c2	146	-1.37	1.44E-02
VGIC	Ryanodine receptor	Ryr1	160	-1.26	2.03E-02
	Voltage-gated calcium channels	Cacna1e	11 431	-0.65	2.55E-02
		Cacna1h	769	-0.91	6.86E-03
	Voltage-gated potassium channels	Kcnb2	411	-0.98	9.34E-03

* Translated mRNAs were isolated from the dorsal striatum of *Drd1*::BAC-TRAP and *Drd2*::BAC-TRAP mice. Only identified in the IUPHAR nomenclature, with adjusted p value <0.05 and expression levels > 30 reads are included. Fold change D2/D1.

Abbrev.: FC, fold-change, GPCR, G protein-coupled receptor, IC, ion channel, IUPHAR, International Union of Basic and Clinical Pharmacology, LGIC, ligand-gated ion channel, MGI, mouse genome informatics database symbol, NHR, nuclear hormone receptor, padj, adjusted p value, VGIC, voltage-gated ion channel.

http://www.guidetopharmacology.org/download.jsp

Table 11: IUPHAR data base-selected genes with mRNA enriched in D2 as compared to D1 neurons in the NAc*

Type	Family name	MGI symbol	Mean	log2 FC	padj
Catalytic receptors	Integrins	Itgb1	487	1.15	6.75E-03
	Receptor tyrosine phosphatases (RTP)	Ptprm	1 100	0.91	5.92E-03
	TNF receptor family	Tnfrsf11a	111	1.02	5.00E-02
	Type I receptor serine/threonine kinases	Bmpr1a	1 725	0.84	1.12E-02
	Type II receptor serine/threonine kinases	Acvr2a	2 032	0.74	2.68E-02
		Tgfbr2	93	2.01	1.31E-04
	Type V RTKs: FGF receptor family	Fgfr2	241	1.92	2.93E-07
	Type XIII RTKs: Ephrin receptor family	Epha7	3 635	1.00	4.15E-02
Enzymes	1.14.11.- Histone demethylases	Kdm6a	2 777	0.78	2.40E-02
	1.14.11.- Histone demethylases	Kdm6b	1 981	1.26	8.83E-06
	1.17.4.1 Ribonucleoside-diphosphate reductases	Rrm2	101	1.70	2.20E-03
	2.1.1.43 Histone methyltransferases (HMTs)	Ezh2	285	1.13	2.91E-02
	2.3.1.48 Histone acetyltransferases (HATs)	Hat1	1 120	0.83	4.33E-02
		Jmjd1c	7 360	0.93	8.40E-03
		Ncoa2	10 210	0.56	4.35E-02
	2.4.2.30 poly(ADP-ribose)polymerases	Parp3	111	1.60	2.41E-03
	3.6.1.3 ATPases	Atad2	381	1.03	8.38E-03
	Adenosine turnover	Adk	700	1.91	1.36E-12
		Nt5e	500	2.34	2.70E-14
	Adenylyl cyclases	Adcy1	2 359	0.70	3.10E-02
	Arginine:glycine amidinotransferase	Gatm	638	1.22	5.97E-04
	ERK subfamily	Mapk1	43 432	0.56	3.82E-02
	Inositol monophosphatase	Impa1	2 603	0.55	4.37E-02
	Interleukin-1 receptor-associated kinase (IRAK)	Irak1	1 705	0.72	3.18E-02
	Lanosterol biosynthesis pathway	Idi1	1 056	0.85	2.77E-03
	Lipid phosphate phosphatases	Pten	20 199	0.71	7.94E-03
	Lipoxygenases	Alox12b	98	1.33	2.77E-02
	M12: Astacin/Adamalysin	Bmp1	40	1.34	2.32E-02
	M13: Neprilysin	Mme	2 744	1.14	5.95E-06
	M14: Carboxypeptidase A	Cpm	127	1.18	4.02E-02
	Neutral ceramidases	Asah2	405	0.92	4.21E-02
	NKF1 family	Sbk1	1 631	0.70	3.62E-02
	nmo subfamily	Nlk	12 736	0.83	2.59E-02
	Nucleoside synthesis and metabolism	Rrm2	101	1.70	2.20E-03
	Phosphatidylinositol kinases	Pik3c2a	1 432	0.62	3.02E-02
	Phosphatidylinositol-4-phosphate 3-kinase family	Pik3c2a	1 432	0.62	3.02E-02
	Phosphodiesterases, 3',5'-cyclic nucleotide	Pde3b	242	1.60	5.23E-04
		Pde4b	21 626	0.83	2.61E-02
		Pde8a	60	1.43	1.15E-02
	Protein kinase D (PKD) family	Prkd1	336	1.35	8.63E-05
		Prkd3	194	1.52	1.03E-04
	RAS subfamily	Kras	4 802	0.69	3.18E-03
		Nras	6 264	0.64	3.07E-02
	RCK family	Ick	882	1.02	5.05E-04
	Rho kinase	Rock1	844	1.00	3.49E-02
	S1: Chymotrypsin	Klk6	31	1.19	4.33E-02
	S8: Subtilisin	Pcsk2	6 324	0.56	4.01E-02
	SGK family	Sgk3	1 543	0.80	3.02E-02
	Soluble guanylyl cyclase	Gucy1a3	20 769	1.60	4.55E-11
		Gucy1b3	9 866	1.11	8.38E-06
	Sphingolipid Delta4-desaturase	Degs1	2 186	0.84	8.33E-03

	Sphingomyelin phosphodiesterase	Smpdl3a	131	1.06	4.38E-02
	TAIRE subfamily	Cdk17	26 189	0.58	3.04E-02
	Trbl family	Trib2	1 693	1.07	5.97E-03
	Trio family	Kalrn	87 139	1.50	5.30E-04
GPCR	5-Hydroxytryptamine receptors	Htr2a	1 064	1.43	1.40E-07
		Htr2c	2 818	0.74	1.85E-02
		Htr7	99	1.61	3.35E-03
	Adenosine receptors	Adora2a	3 665	2.71	2.51E-11
	Adhesion Class GPCRs	Adgra2	83	1.42	1.31E-02
		Adgrl2	2 234	0.56	3.63E-02
	Class A Orphans	Gpr149	594	0.82	4.15E-02
		Gpr52	903	2.75	2.83E-16
		Gpr6	509	1.60	1.60E-05
		Gpr88	15 049	1.44	1.38E-08
	Class Frizzled GPCRs	Fzd5	247	1.12	1.07E-02
	Histamine receptors	Hrh3	5 465	0.79	6.58E-03
	Lysophospholipid (LPA) receptors	Lpar1	56	1.39	1.56E-02
	Metabotropic glutamate receptors	Grm4	2 743	1.03	5.98E-03
	Opioid receptors	Oprd1	502	2.45	2.33E-09
	P2Y receptors	P2ry1	3 041	3.76	1.83E-36
	Prostanoid receptors	Ptgdr	35	1.19	3.01E-02
	Tachykinin receptors	Tacr3	57	1.28	3.25E-02
LGIC	GABA-A receptors	Gabra2	930	1.09	1.34E-03
		Gabrg3	2 051	1.54	1.64E-04
	Ionotropic glutamate receptors	Grik3	2 912	1.53	4.60E-04
NHR	6A. Germ cell nuclear factor receptors	Nr6a1	414	0.91	2.32E-02
Other IC	Connexins and Pannexins	Gjc3	286	1.56	2.86E-05
Other proteins	B-cell lymphoma 2 (Bcl-2) protein family	Mcl1	3 103	0.59	4.55E-02
	Notch receptors	Notch2	201	1.58	6.67E-04
	Reticulons and associated proteins	Rtn4	16 127	0.61	8.73E-03
	RZ family	Rgs17	11 729	0.79	5.80E-04
Transporters	ABCB subfamily	Abcb6	192	1.00	3.10E-02
	Choline transporter	Slc5a7	122	1.74	7.82E-04
	F-type ATPase	Atp5j	8 950	0.56	4.55E-02
	GABA transporter subfamily	Slc6a1	4 235	0.55	4.29E-02
	Phospholipid-transporting ATPases	Atp11b	853	0.89	7.66E-03
	Selective sulphate transporters	Slc26a2	129	1.29	1.88E-02
	SLC10 family of sodium-bile acid co-transporters	Slc10a4	57	1.43	1.27E-02
	SLC16 family of monocarboxylate transporters	Slc16a10	42	1.29	3.30E-02
	SLC29 family	Slc29a3	215	1.49	2.14E-03
	SLC35 family of nucleotide sugar transporters	Slc35f1	6 452	0.95	6.72E-03
	SLC44 choline transporter-like family	Slc44a1	439	1.08	5.52E-03
	SLC7 family	Slc7a2	100	1.22	3.82E-02
	System A-like transporters	Slc38a2	1 682	0.84	2.55E-03
	V-type ATPase	Atp6v0e	231	1.21	1.32E-03
VGIC	Cyclic nucleotide-regulated channels	Hcn4	52	1.40	1.84E-02
	Inwardly rectifying potassium channels	Kcnj10	204	1.05	2.55E-02
	Two-P potassium channels	Kcnk2	2 870	0.61	2.50E-02
	Voltage-gated potassium channels	Kcna2	6 759	0.76	3.49E-02
		Kcng2	97	1.49	2.62E-03

* Translated mRNAs were isolated from the dorsal striatum of *Drd1*::BAC-TRAP and *Drd2*::BAC-TRAP mice. Only identified in the IUPHAR nomenclature, with adjusted p value <0.05 and expression levels > 30 reads are included. Fold change D2/D1.

Abbrev.: FC, fold-change, GPCR, G protein-coupled receptor, IC, ion channel, IUPHAR, International Union of Basic and Clinical Pharmacology, LGIC, ligand-gated ion channel, MGI, mouse genome informatics database symbol, NHR, nuclear hormone receptor, padj, adjusted p value, VGIC, voltage-gated ion channel.

http://www.guidetopharmacology.org/download.jsp

Table 12: Top 30 most significant genes with mRNA enriched in DS as compared to NAc (D1 and D2 combined)

Gene	GeneDescription	log2 FC	padj	Nac mean	DS mean
Entpd1	ectonucleoside triphos. diphosphohydrolase 1	-2.65	6.74E-41	108	827
Sgpp2	sphingosine-1-phosphate phosphotase 2	-2.62	1.50E-38	174	1 269
Synpo2	synaptopodin 2	-2.77	3.99E-36	163	1 493
Coch	cochlin	-2.91	5.53E-33	303	3 280
Reln	reelin	-1.95	3.13E-32	1 094	4 026
Ace	ACE (peptidyl-dipeptidase A) 1	-3.10	8.31E-32	56	613
C030013G03Rik	RIKEN cDNA C030013G03 gene	-3.01	8.64E-31	34	329
Acvr1c	activin A receptor, type IC	-1.67	8.64E-31	923	3 068
Dab2ip	disabled 2 interacting protein	-1.25	4.76E-27	2 046	5 137
Sema7a	semaphorin 7A	-1.97	1.82E-26	671	2 821
Cnr1	cannabinoid receptor 1	-2.39	5.87E-25	1 935	12 211
Cyp2s1	cytP450, family 2, subfamily s, polypeptide 1	-2.25	8.59E-25	163	1 019
Itga9	integrin alpha 9	-1.89	1.29E-24	278	1 250
Pld5	phospholipase D family, member 5	-1.76	5.06E-24	531	2 515
Clspn	claspin	-2.56	4.10E-23	189	1 439
Gpr155	G protein-coupled receptor 155	-1.95	9.04E-23	1 821	10 871
Atp2b1	ATPase, Ca^{++} transporting, plasma memb. 1	-1.29	3.22E-22	20 880	57 549
Lpcat4	lysophosphatidylcholine acyltransferase 4	-1.74	1.40E-21	2 426	8 500
Gcnt2	Glucosaminyl transfer. 2, I-branching enzyme	-1.53	6.88E-21	1 849	6 181
Vmp1	vacuole membrane protein 1	-1.31	1.73E-20	1 045	2 964
Scn4b	sodium channel, type IV, beta	-1.39	2.46E-20	8 286	23 257
AI593442	expressed sequence AI593442	-1.30	1.62E-19	13 929	45 872
Nrgn	neurogranin	-1.70	4.64E-19	11 747	40 087
Ctsb	cathepsin B	-1.11	6.20E-19	5 737	12 317
Tpm2	tropomyosin 2, beta	-1.94	3.49E-18	414	1 769
Prima1	proline rich membrane anchor 1	-1.95	1.54E-17	120	564
Fam84b	family with sequence similarity 84, member B	-1.43	1.54E-17	312	1 054
Slitrk2	SLIT and NTRK-like family, member 2	-1.27	1.64E-17	780	2 303
Slc24a2	solute carrier family 24 (Na/K/Ca exchanger) 2	-1.43	2.13E-17	9 454	31 342
Kcnt1	potassium channel, subfamily T, member 1	-1.00	2.73E-17	1 301	2 876

Table 13: Top 30 most significant genes with mRNA enriched in NAc as compared to DS (D1 and D2 combined)

Gene	GeneDescription	log2 FC	padj	Nac mean	DS mean
Fam196b	family with sequence similarity 196, member B	2.50	6.23E-43	702	107
Dgkk	diacylglycerol kinase kappa	2.96	6.23E-43	1 126	150
Crym	crystallin, mu	1.98	6.23E-43	4 766	1 023
Dlk1	delta-like 1 homolog (Drosophila)	3.64	5.27E-37	4 307	214
Peg10	paternally expressed 10	2.43	7.60E-29	12 310	1 799
AW551984	expressed sequence AW551984	3.55	3.12E-28	771	29
Zcchc12	zinc finger, CCHC domain containing 12	1.50	3.03E-27	3 567	1 178
Cpne2	copine II	1.57	5.24E-26	3 808	1 093
Stard5	START domain containing 5	2.75	8.83E-25	1 907	334
Hap1	huntingtin-associated protein 1	1.76	9.75E-24	4 311	1 037
Gda	guanine deaminase	1.28	1.92E-23	11 691	4 899
Tcerg1l	transcription elongation regulator 1-like	2.71	3.05E-23	1 456	142
Ntn1	netrin 1	2.56	1.79E-22	682	79
Lin7a	lin-7 homolog A (C. elegans)	1.17	6.84E-22	8 413	4 137
Kcnip1	Kv channel-interacting protein 1	2.45	3.36E-21	2 047	277
Prkg1	protein kinase, cGMP-dependent, type I	2.01	1.07E-20	2 162	450
Enah	enabled homolog (Drosophila)	1.09	5.00E-19	11 165	5 466
Fat1	FAT atypical cadherin 1	1.58	4.40E-18	1 224	420
Nnat	neuronatin	2.50	4.40E-18	15 066	1 675
Dcx	doublecortin	1.25	6.54E-18	1 485	681
Trhr	thyrotropin releasing hormone receptor	2.95	1.94E-17	553	29
Soga1	suppressor of glucose, autophagy associated 1	1.57	4.74E-17	2 715	902
Pea15a	phosphoprotein enriched in astrocytes 15A	1.40	2.37E-16	9 931	3 181
Pde1a	phosphodiesterase 1A, calmodulin-dependent	1.87	2.40E-16	13 780	3 005
Gm5607	predicted gene 5607	1.96	2.66E-15	1 730	352
Tunar	Tcl1 upstream neural differentiation assoc. RNA	1.68	4.38E-15	2 170	601
Sox1	SRY (sex determining region Y)-box 1	2.04	1.31E-14	4 256	853
Zbtb7c	zinc finger and BTB domain containing 7C	2.84	1.98E-14	875	25
Fam126a	family with sequence similarity 126, member A	1.64	2.11E-14	1 065	335
Gabrg1	GABA-A receptor, subunit gamma 1	2.18	2.30E-14	411	68

Table 14: Top 30 most significant genes with mRNA enriched in DS as compared to NAc in D1 neurons

Gene	Gene Description	log2 FC	padj	Nac mean	DS mean
Cpne9	copine family member IX	-2.67	1.99E-47	136	958
Nrgn	neurogranin	-2.12	4.96E-44	8 481	39 234
Sgpp2	sphingosine-1-phosphate phosphatase 2	-2.65	2.64E-34	182	1 355
Gcnt2	glucosaminyl transferase 2, I-branching enzyme	-1.76	3.62E-33	1 420	5 031
Lpcat4	lysophosphatidylcholine acyltransferase 4	-1.58	9.87E-33	2 848	8 822
Tpm2	tropomyosin 2, beta	-2.42	2.35E-32	245	1 504
Pld5	phospholipase D family, member 5	-1.87	6.24E-32	463	1 814
Synpo2	synaptopodin 2	-2.55	9.87E-30	171	1 161
Gpr155	G protein-coupled receptor 155	-2.12	6.39E-28	1 554	7 829
Gpx6	glutathione peroxidase 6	-2.32	2.90E-27	79	448
Gpm6b	glycoprotein m6b	-1.32	5.61E-27	5 775	14 833
Grm1	glutamate receptor, metabotropic 1	-1.58	3.37E-26	1 064	3 367
Dach1	dachshund 1 (Drosophila)	-1.69	2.22E-24	893	3 032
Zbtb18	zinc finger and BTB domain containing 18	-1.19	8.37E-24	1 919	4 469
Ace	ACE (peptidyl-dipeptidase A) 1	-2.99	1.05E-22	71	843
Acvr1c	activin A receptor, type IC	-1.58	7.68E-22	1 056	3 314
Cd59a	CD59a antigen	-2.52	1.48E-21	106	767
Entpd1	Ectonucleos. triphosphate diphosphohydrolase 1	-2.64	2.26E-21	97	816
B3gnt2	UDP-GlcNAc:betaGal beta-1,3-N-ac. gluc.am.transf. 2	-1.62	2.39E-21	1 351	4 522
Shb	SH2 domain-containing transforming protein B	-1.60	2.02E-20	345	1 112
Pvalb	parvalbumin	-2.33	6.55E-20	122	777
Scn4b	sodium channel, type IV, beta	-1.56	9.55E-20	7 121	22 116
Ano3	anoctamin 3	-1.30	1.80E-19	9 865	25 648
Ctsb	cathepsin B	-1.16	3.08E-19	5 315	12 069
C030013G03Rik	RIKEN cDNA C030013G03 gene	-2.82	5.95E-19	45	496
Kcnh4	K+ voltage-gated chan., subfam H, eag-related, 4	-1.40	1.10E-18	361	985
AI593442	expressed sequence AI593442	-1.42	1.85E-18	13 119	36 881
Coch	cochlin	-2.74	3.06E-18	313	3 208
Cnr1	cannabinoid receptor 1	-2.27	3.42E-18	2 099	12 407
Cyp2s1	cyt P450, family 2, subfamily s, polypeptide 1	-2.34	3.47E-18	132	816

Table 15: Top 30 most significant genes with mRNA enriched in NAc as compared to DS in D1 neurons

Gene	Gene Description	log2 FC	padj	Nac mean	DS mean
AW551984	expressed sequence AW551984	3.86	7.30E-78	872	48
Peg10	paternally expressed 10	3.04	2.71E-63	15 150	1 627
Dgkk	diacylglycerol kinase kappa	2.77	3.73E-46	978	122
Crym	crystallin, mu	2.00	1.71E-35	4 644	1 125
Nnat	neuronatin	2.84	9.87E-33	15 712	1 936
Stard5	START domain containing 5	3.32	3.13E-30	1 375	91
Ahi1	Abelson helper integration site 1	1.51	1.01E-27	14 971	5 090
Dlk1	delta-like 1 homolog (Drosophila)	3.21	1.72E-27	5 479	383
Tmem255a	transmembrane protein 255A	2.10	5.95E-27	1 272	269
Fam196b	family with sequence similarity 196, member B	2.33	2.21E-26	708	123
Prkg1	protein kinase, cGMP-dependent, type I	1.87	4.50E-25	2 226	554
Zbtb7c	zinc finger and BTB domain containing 7C	3.52	3.28E-22	797	26
Pde1c	phosphodiesterase 1C	1.46	8.76E-22	4 374	1 522
Pea15a	phosphoprotein enriched in astrocytes 15A	1.60	3.23E-20	11 053	3 476
Baiap3	BAI1-associated protein 3	2.88	2.63E-19	649	57
Gabrg1	GABA-A receptor, subunit gamma 1	2.35	3.90E-19	422	67
Ngb	neuroglobin	2.53	1.61E-18	248	32
Cpne2	copine II	1.58	1.76E-18	4 460	1 403
Zcchc12	zinc finger, CCHC domain containing 12	1.43	2.17E-18	3 695	1 310
Hap1	huntingtin-associated protein 1	1.87	2.23E-18	4 908	1 238
Tcerg1l	transcription elongation regulator 1-like	2.70	3.06E-18	1 608	168
Scml4	sex comb on midleg-like 4 (Drosophila)	2.81	4.90E-18	169	15
Ntn1	netrin 1	2.57	1.73E-17	761	91
Zic3	zinc finger protein of the cerebellum 3	3.15	1.94E-17	130	5
Plxnc1	plexin C1	1.53	3.36E-17	1 571	511
Wnt7a	wingless-type MMTV integration site family, 7A	2.06	2.35E-16	418	87
Carhsp1	calcium regulated heat stable protein 1	1.08	2.95E-16	7 923	3 681
Gpr101	G protein-coupled receptor 101	1.99	1.16E-14	1 226	264
Kctd12b	K+ channel tetramerisation domain containing 12b	2.97	2.05E-14	112	4
Stra6	stimulated by retinoic acid gene 6	3.02	2.17E-14	395	15

Table 16: IUPHAR data base-selected genes with mRNA enriched in DS as compared NAc in D1 neurons*

Type	Family name	MGI symbol	Mean	log2 FC	padj
Catalytic receptors	IL-17 receptor family	Il17rc	84	-1,39	1,66E-04
	Integrins	Itga5	327	-1,38	5,03E-05
		Itga8	59	-1,60	5,31E-04
		Itga9	610	-1,85	1,59E-13
		Epor	411	-0,61	4,82E-03
	Type I receptor serine/threonine kinases	Acvr1c	2 185	-1,58	7,68E-22
		Acvrl1	335	-2,60	1,73E-11
	Type IX RTKs: MuSK	Musk	147	-1,20	3,38E-05
	Type V RTKs: FGF receptor family	Fgfr2	145	-0,96	2,65E-03
	Type VII RTKs: Neurotrophin receptor/Trk family	Ntrk2	5 626	-0,57	2,86E-03
	Type VII RTKs: Neurotrophin receptor/Trk family	Ntrk3	2 165	-0,57	3,88E-03
	Type XIII RTKs: Ephrin receptor family	Epha3	77	-1,47	1,09E-04
		Epha4	4 704	-0,77	2,98E-07
		Ephb1	1 623	-0,88	8,72E-05
		Ephb6	499	-1,20	2,72E-08
	Type XVIII RTKs: LMR family	Lmtk2	4 122	-0,71	3,79E-03
Enzymes	1.13.11.- Dioxygenases	Ido1	1 919	-1,19	1,35E-07
	1.14.11.- Histone demethylases	Kdm4b	1 000	-0,60	3,44E-04
	A22: Presenilin	Psen1	1 318	-0,81	2,51E-07
	Adenylyl cyclases	Adcy5	10 799	-0,65	1,20E-04
	C1: Papain	Ctsb	8 692	-1,16	3,08E-19
		Ctsz	261	-1,04	4,71E-03
	C2: Calpain	Capn1	948	-0,80	1,13E-04
	CDK8 subfamily	Cdk19	6 669	-0,62	3,61E-04
	CYP2 family	Cyp2s1	474	-2,34	3,47E-18
	CYP39, CYP46 and CYP51 families	Cyp46a1	3 575	-1,17	2,05E-14
	Delta subfamily	Prkcd	202	-1,60	2,06E-04
	Endocannabinoid turnover	Dagla	2 313	-1,05	2,55E-05
	Haem oxygenase	Hmox1	104	-1,07	5,76E-04
	HIPK subfamily	Hipk4	1 063	-1,15	2,28E-04
	Hydrolases	Dagla	2 313	-1,05	2,55E-05
	Inositol polyphosphate phosphatases	Inpp5a	1 386	-0,47	2,01E-03
	Iota subfamily	Prkci	4 527	-0,53	2,37E-03
	Leucine-rich repeat kinase (LRRK) family	Lrrk2	2 893	-0,47	3,69E-03
	M1: Aminopeptidase N	2010111I01Rik	529	-0,95	2,17E-05
	M12: Astacin/Adamalysin	Adam23	6 586	-0,78	7,91E-04
	M13: Neprilysin	Mme	3 373	-1,35	8,64E-11
	M14: Carboxypeptidase A	Cpd	1 457	-0,50	3,36E-03
	M2: Angiotensin-converting (ACE and ACE2)	Ace	457	-2,99	1,05E-22
	Meta subfamily	Camkk2	5 300	-1,07	2,40E-07
	Phosphatidylinositol kinases	Pik3r4	2 381	-1,24	1,90E-10
	Phosphodiesterases, 3',5'-cyclic nucleotide	Pde10a	72 816	-0,76	1,04E-03
		Pde1b	31 661	-0,53	1,10E-03
	Phosphoinositide-specific phospholipase C	Plcb1	23 601	-0,79	5,40E-10
	S8: Subtilisin	Pcsk2	6 826	-0,88	6,76E-09
	Sphingomyelin phosphodiesterase	Smpd3	3 574	-0,90	7,19E-05
	Sphingosine 1-phosphate phosphatase	Sgpp2	769	-2,65	2,64E-34
	Trbl family	Trib2	1 363	-0,67	2,75E-03
	Trio family	Kalrn	64 022	-0,93	4,99E-03
	Vaccina related kinase (VRK) family	Vrk1	2 027	-0,69	1,26E-03
	VPS15 family	Pik3r4	2 381	-1,24	1,90E-10
	Wnk family	Wnk4	235	-1,43	1,69E-07
	YANK family	Stk32a	1 554	-0,68	4,22E-05
		Stk32c	1 761	-0,94	3,25E-09
GPCR	Acetylcholine receptors (muscarinic)	Chrm4	1 597	-1,01	1,86E-06

	Adhesion Class GPCRs	Adgrl2	2 358	-0,75	5,21E-07
	Cannabinoid receptors	Cnr1	7 253	-2,27	3,42E-18
	Class A Orphans	Gpr139	313	-2,99	6,02E-18
		Gpr88	14 799	-1,20	5,22E-13
	Class C Orphans	Gpr158	11 778	-1,02	4,92E-09
	GABA-B receptors	Gabbr1	13 180	-0.57	4.48E-03
	Histamine receptors	Hrh3	5 013	-0.65	2.83E-03
	Metabotropic glutamate receptors	Grm1	2 215	-1.58	3.37E-26
		Grm4	2 258	-0.56	3.84E-03
		Grm5	7 587	-0.48	4.86E-03
		Grm8	169	-1.65	6.05E-06
	Prostanoid receptors	Ptger4	41	-1.53	1.34E-03
LGIC	Acid-sensing (proton-gated) ion channels (ASICs)	Asic1	2 132	-0.57	6.18E-04
	GABA-A receptors	Gabra1	3 561	-0.75	3.48E-05
		Gabra4	4 285	-0.67	6.47E-06
		Gabrd	2 522	-0.66	2.41E-03
	Ionotropic glutamate receptors	Gria4	1 335	-0.69	8.96E-04
		Grin1	5 197	-0.78	1.73E-04
	IP3 receptor	Itpr1	31 358	-0.64	4.87E-04
NHR	1F. Retinoic acid-related orphans	Rora	3 191	-0.85	9.30E-07
	2B. Retinoid X receptors	Rxrg	2 987	-0.69	4.13E-05
	4A. Nerve growth factor IB-like receptors	Nr4a1	1 926	-0.85	6.83E-04
Other proteins	R4 family	Rgs4	42 104	-1.25	7.92E-08
	R7 family	Rgs9	8 208	-0.65	3.12E-05
	Tubulins	Tuba4a	13 092	-0.53	5.12E-05
Transporters	ABCB subfamily	Abcb9	462	-1.15	2.39E-11
	ABCC subfamily	Abcc12	61	-1.49	9.09E-04
	ABCD subfamily of peroxisomal ABC transporters	Abcd2	852	-1.13	1.60E-08
	Ca2+-ATPases	Atp2a2	24 002	-0.84	5.61E-06
		Atp2b1	36 752	-1.29	6.27E-17
		Atp2b2	25 521	-0.85	9.99E-05
	Glutamate transporter subfamily	Slc1a1	2 341	-0.85	2.21E-06
	Organic cation transporters (OCT)	Slc22a3	367	-1.37	1.36E-08
	Other SLC26 anion exchangers	Slc26a10	88	-1.39	9.13E-04
	SLC16 family of monocarboxylate transporters	Slc16a7	433	-0.72	1.16E-03
	SLC24 sodium/potassium/calcium exchangers	Slc24a2	15 741	-1.44	5.11E-10
	SLC29 family	Slc29a1	256	-1.24	8.54E-05
	SLC30 zinc transporter family	Slc30a4	1 146	-0.86	1.55E-04
	SLC35 family of nucleotide sugar transporters	Slc35e2	893	-0.71	1.20E-04
	SLC37 phosphosugar/phosphate exchangers	Slc37a4	162	-1.44	1.64E-04
	SLC39 family of metal ion transporters	Slc39a10	4 717	-0.55	3.12E-03
	SLC41 family of divalent cation transporters	Slc41a1	2 468	-1.04	3.45E-04
	SLC43 large neutral amino acid transporters	Slc43a2	1 167	-0.82	3.74E-03
	SLC44 choline transporter-like family	Slc44a1	423	-0.97	4.40E-04
	SLC8 family of sodium/calcium exchangers	Slc8a2	2 999	-0.91	2.14E-04
	SLC9 family of sodium/hydrogen exchangers	Slc9a1	2 593	-0.67	5.83E-05
		Slc9a2	115	-1.23	2.31E-05
		Slc9a5	586	-0.86	1.65E-05
	Sodium-dependent HCO3- transporters	Slc4a4	7 075	-1.01	1.09E-07
	V-type ATPase	Atp6v0b	2 119	-0.76	2.96E-03
VGIC	Calcium-activated potassium channels	Kcnt1	1 919	-1.01	7.61E-10
	Inwardly rectifying potassium channels	Kcnj10	204	-1.18	1.17E-05
		Kcnj4	1 416	-0.79	1.53E-06
	Ryanodine receptor	Ryr2	3 095	-0.73	2.10E-07
	Two-P potassium channels	Kcnk1	2 068	-1.37	1.14E-09
		Kcnk2	3 121	-0.79	1.56E-05
	Voltage-gated calcium channels	Cacna1c	3 734	-0.70	8.20E-04
	Voltage-gated potassium channels	Kcna2	6 453	-0.69	3.71E-03

		Kcnb1	9 215	-0.68	1.22E-03
		Kcnc3	917	-0.92	6.94E-05
		Kcnd1	289	-0.72	1.54E-03
		Kcnd2	5 468	-0.86	2.01E-07
		Kcnh3	1 232	-0.64	6.15E-04
		Kcnh4	673	-1.40	1.10E-18
		Kcns1	143	-1.25	2.78E-05
	Voltage-gated sodium channels	Scn1a	2 664	-1.03	1.14E-06
		Scn2a1	9 836	-0.45	3.35E-03
		Scn8a	8 843	-0.76	2.52E-05

* Translated mRNAs were isolated from the dorsal striatum of *Drd1*::BAC-TRAP and *Drd2*::BAC-TRAP mice. Only identified in the IUPHAR nomenclature, with adjusted p value <0.05 and expression levels > 30 reads are included. Fold-change NAc/DS.

Abbrev.: FC, fold-change, GPCR, G protein-coupled receptor, IC, ion channel, IUPHAR, International Union of Basic and Clinical Pharmacology, LGIC, ligand-gated ion channel, MGI, mouse genome informatics database symbol, NHR, nuclear hormone receptor, padj, adjusted p value, VGIC, voltage-gated ion channel.

http://www.guidetopharmacology.org/download.jsp

Table 17: IUPHAR data base-selected genes with mRNA enriched in NAc as compared DS in D1 neurons*

Type	Family name	MGI symbol	Mean	log2 FC	padj
Catalytic receptors	GDNF receptor family	Gfra1	719	1.15	5.58E-04
	NOD-like receptor family	Nlrp10	84	1.38	4.16E-03
	Receptor tyrosine phosphatases (RTP)	Ptprg	1 230	0.91	3.20E-03
	Type XIX RTKs: Leukocyte tyrosine kinase (LTK)	Alk	57	1.59	1.97E-04
Enzymes	1.1.1.42 Isocitrate dehydrogenases	Idh1	530	0.67	1.36E-03
	3.5.1.- Histone deacetylases (HDACs)	Hdac1	591	0.77	1.33E-03
	BARK/GRK2 subfamily	Adrbk2	441	1.00	2.19E-04
	Bromodomain kinase (BRDK) family	Brd3	2 870	0.65	1.87E-06
	CAMK1 family	Pnck	2 547	1.15	9.05E-11
	CAMK2 family	Camk2d	1 827	0.82	2.47E-05
	Catecholamine turnover	Ddc	130	2.21	4.38E-08
	Csk family	Csk	388	0.89	7.40E-05
	Cyclin-dependent kinase-like (CDKL) family	Cdkl1	223	0.96	1.75E-03
	Decarboxylases	Ddc	130	2.21	4.38E-08
	Decarboxylases	Gad2	64 415	0.88	2.99E-09
	ERK subfamily	Mapk3	6 775	0.56	1.20E-04
	Exchange protein activated by cyclic AMP (Epac)	Rapgef3	104	1.48	1.18E-04
	GABA turnover	Gad2	64 415	0.88	2.99E-09
	Interleukin-1 receptor-associated kinase (IRAK)	Irak3	185	1.53	5.58E-05
	Lipid phosphate phosphatases	Lpin2	2 788	0.58	2.74E-03
	M12: Astacin/Adamalysin	Adam12	195	1.59	3.78E-05
	NIMA- related kinase (NEK) family	Nek4	1 165	0.55	2.75E-03
	PAKA subfamily	Pak3	5 729	0.83	1.07E-10
	PAKB subfamily	Pak6	2 050	0.82	7.46E-05
	Phosphatidylinositol kinases	Pik3r5	181	1.27	1.42E-05
	Phosphodiesterases, 3',5'-cyclic nucleotide	Pde11a	47	1.48	2.17E-03
	Phosphodiesterases, 3',5'-cyclic nucleotide	Pde1a	10 578	1.66	2.06E-09
	Phosphodiesterases, 3',5'-cyclic nucleotide	Pde1c	2 948	1.46	8.76E-22
	Phosphodiesterases, 3',5'-cyclic nucleotide	Pde4b	13 517	0.44	3.32E-03
	Phosphoinositide-specific phospholipase C	Plce1	660	1.44	6.45E-06
	Protein kinase A	Prkar2a	2 315	1.08	2.44E-04
	Protein kinase G (PKG)	Prkg1	1 390	1.87	4.50E-25
	RAF family	Ksr1	929	0.72	2.67E-03
	RSK subfamily	Rps6ka2	2 693	0.50	3.05E-04
	RSK subfamily	Rps6ka6	350	1.40	4.16E-14
GPCR	5-Hydroxytryptamine receptors	Htr2c	1 416	1.22	6.26E-06
	Acetylcholine receptors (muscarinic)	Chrm5	53	1.37	2.35E-03
	Adrenoceptors	Adra1a	177	1.09	2.44E-04
	Class A Orphans	Gpr101	745	1.99	1.16E-14
	Class A Orphans	Gpr6	147	1.41	1.19E-03
	Dopamine receptors	Drd3	113	1.81	4.94E-05
	Opioid receptors	Oprm1	549	0.93	5.52E-04
	P2Y receptors	P2ry1	220	1.75	1.68E-08
	Thyrotropin-releasing hormone receptors	Trhr	248	2.83	4.89E-14
	VIP and PACAP receptors	Adcyap1r1	1 597	0.93	1.64E-06
LGIC	GABA_A receptors	Gabrg1	245	2.35	3.90E-19
	GABA_A receptors	Gabrq	62	1.77	1.12E-04
NHR	3A. Estrogen receptors	Esr1	41	1.93	1.16E-05
Other proteins	Fatty acid-binding proteins	Rbp1	726	2.03	3.06E-08
	RZ family	Rgs17	6 664	0.78	2.75E-05

Transporters	Sodium myo-inositol cotransporter transporters	Slc5a3	1 108	0.99	1.05E-04
	V-type ATPase	Atp6v1c2	111	1.45	1.80E-04
VGIC	Transient Receptor Potential channels	Trpc7	310	1.33	7.69E-07

* Translated mRNAs were isolated from the dorsal striatum of *Drd1*::BAC-TRAP and *Drd2*::BAC-TRAP mice. Only identified in the IUPHAR nomenclature, with adjusted p value <0.05 and expression levels > 30 reads are included. Fold-change NAc/DS.

Abbrev.: FC, fold-change, GPCR, G protein-coupled receptor, IC, ion channel, IUPHAR, International Union of Basic and Clinical Pharmacology, LGIC, ligand-gated ion channel, MGI, mouse genome informatics database symbol, NHR, nuclear hormone receptor, padj, adjusted p value, VGIC, voltage-gated ion channel.

http://www.guidetopharmacology.org/download.jsp

Table 18: Top 30 most significant genes with mRNA enriched in DS as compared to NAc in D2 neurons

Gene	Gene Description	log2 FC	padj	NAc mean	DS mean
Clspn	claspin	-3.30	2.30E-20	82	1 442
Synpo2	synaptopodin 2	-3.21	8.59E-20	141	1 888
Reln	reelin	-2.29	1.78E-19	494	3 228
Wnt8b	wingless-type MMTV integration site family, member 8B	-3.74	6.40E-16	3	265
Coch	cochlin	-2.76	4.97E-15	271	3 426
Lrrc10b	leucine rich repeat containing 10B	-2.25	3.03E-14	4 682	18 980
Entpd1	ectonucleoside triphosphate diphosphohydrolase 1	-2.32	6.47E-13	129	855
Cd72	CD72 antigen	-3.44	1.83E-12	0	184
Hipk4	homeodomain interacting protein kinase 4	-2.24	2.18E-12	365	2 053
Gabrd	GABA-A receptor, subunit delta	-1.87	6.86E-12	1 093	2 950
Cldn1	claudin 1	-2.86	1.96E-11	16	370
Arhgdib	Rho, GDP dissociation inhibitor (GDI) beta	-1.75	6.32E-11	1 141	4 478
Ace	angiotensin I converting enzyme 1	-2.96	6.55E-11	20	375
Prima1	proline rich membrane anchor 1	-2.35	1.49E-09	99	688
Cnr1	cannabinoid receptor 1 (brain)	-2.43	1.63E-09	1 514	12 257
Rasd2	RASD family, member 2	-1.41	2.46E-09	14 474	39 805
Lpcat4	lysophosphatidylcholine acyltransferase 4	-2.11	3.59E-09	1 430	8 331
Sgpp2	sphingosine-1-phosphate phosphotase 2	-2.36	1.40E-08	152	1 202
Mmp17	matrix metallopeptidase 17	-1.48	1.55E-08	2 650	6 426
Hs6st3	heparan sulfate 6-O-sulfotransferase 3	-2.50	4.50E-08	77	687
Hpca	hippocalcin	-1.53	6.58E-08	118 750	341 365
Meis1	Meis homeobox 1	-2.24	8.79E-08	176	1 334
Actn2	actinin alpha 2	-1.76	3.17E-07	388	1 510
Acvr1c	activin A receptor, type IC	-1.73	3.20E-07	605	2 861
Sema7a	sema7A	-1.92	3.38E-07	681	3 023
Cacna1h	Ca2+ chan., voltage-dependent, T type, alpha 1H subunit	-1.63	6.89E-07	430	1 469
Deptor	DEP domain containing MTOR-interacting protein	-1.43	6.89E-07	1 535	5 417
Slc41a1	solute carrier family 41, member 1	-1.59	8.11E-07	1 901	7 138
Ldlrad4	LDL receptor class A domain containing 4	-1.86	1.25E-06	364	1 342
Etl4	enhancer trap locus 4	-1.33	1.26E-06	3 315	10 902

Table 19: Top 30 most significant genes with mRNA enriched in NAc as compared to DS in D2 neurons

Gene	Gene Description	log2 FC	padj	NAc mean	DS mean
Cartpt	CART prepropeptide	4.26	1.04E-31	3 110	67
Fgf10	fibroblast growth factor 10	4.64	2.25E-29	870	9
Dlk1	delta-like 1 homolog (Drosophila)	4.02	6.85E-21	1 616	35
Dgkk	diacylglycerol kinase kappa	3.31	8.03E-20	1 421	184
Stard5	StAR-related lipid transfer (START) domain containing 5	2.50	6.44E-14	3 020	606
AW551984	expressed sequence AW551984	3.40	2.18E-12	528	9
Kcnip1	Kv channel-interacting protein 1	2.78	1.96E-11	2 472	210
Pcdh19	protocadherin 19	1.93	8.18E-11	1 607	514
Plcxd3	phosphatidylinositol-specific PLC, X domain containing 3	2.19	1.13E-10	911	273
Sox1	SRY (sex determining region Y)-box 1	2.50	1.97E-10	3 611	413
Inadl	InaD-like (Drosophila)	2.16	6.97E-10	1 246	259
Marcks	myristoylated alanine rich protein kinase C substrate	1.88	6.76E-09	10 253	5 628
Fam196b	family with sequence similarity 196, member B	2.33	3.66E-08	669	92
Adam12	a disintegrin and metallopeptidase domain 12	2.38	4.50E-08	604	92
Crym	crystallin, mu	1.83	9.44E-08	4 907	932
Phyh	phytanoyl-CoA hydroxylase	1.79	2.08E-07	1 906	536
Phactr2	phosphatase and actin regulator 2	2.02	5.20E-07	806	382
Dpp10	dipeptidylpeptidase 10	1.37	5.36E-07	3 611	1 623
Ralyl	RALY RNA binding protein-like	1.92	7.17E-07	9 947	2 094
Peg10	paternally expressed 10	1.50	9.13E-07	5 734	2 025
Trhr	thyrotropin releasing hormone receptor	2.57	9.54E-07	728	30
Enah	enabled homolog (Drosophila)	1.20	1.37E-06	10 830	5 712
Rgs17	regulator of G-protein signaling 17	1.23	1.72E-06	15 453	8 386
P2ry1	purinergic receptor P2Y, G-protein coupled 1	1.93	1.87E-06	8 025	2 448
Tcerg1l	transcription elongation regulator 1-like	2.17	1.89E-06	1 084	115
Slc8a1	solute carrier family 8 (Na+/Ca2+ exchanger), member 1	1.59	2.34E-06	4 062	1 316
Fhl1	four and a half LIM domains 1	1.41	2.49E-06	3 285	1 334
Prkg1	protein kinase, cGMP-dependent, type I	1.85	2.54E-06	1 960	346
Gda	guanine deaminase	1.33	6.37E-06	11 248	5 067
Npas3	neuronal PAS domain protein 3	2.26	7.29E-06	523	61

Table 20: IUPHAR data base-selected genes with mRNA enriched in NAc as compared DS in D2neurons*

Type	Family name	MGI symbol	Mean	log2 FC	padj
Catalytic receptors	IL-17 receptor family	Il17ra	181	-1.44	2.60E-02
	Integrins	Itga9	1 164	-1.65	1.74E-06
	Receptor tyrosine phosphatases (RTP)	Ptprm	2 594	-0.76	1.92E-02
	Type I receptor serine/threonine kinases	Acvr1c	2 109	-1.73	3.20E-07
	Type I receptor serine/threonine kinases	Acvrl1	369	-1.39	3.15E-02
	Type VII RTKs: Neurotrophin receptor/Trk family	Ntrk3	2 450	-0.73	3.85E-02
	Type XIII RTKs: Ephrin receptor family	Epha4	7 781	-0.86	8.43E-03
		Epha6	1 133	-1.11	1.61E-02
		Ephb6	517	-1.53	5.86E-03
	Type XVIII RTKs: LMR family	Lmtk2	4 154	-0.91	1.65E-03
Enzymes	1.13.11.- Dioxygenases	Ido1	2 785	-0.76	2.98E-02
	Adenylyl cyclases	Adcy3	521	-1.16	3.57E-02
		Adcy5	13 466	-0.83	3.07E-02
	Akt (Protein kinase B)	Akt2	3 937	-1.01	1.60E-03
	C1: Papain	Ctsb	10 735	-1.01	4.81E-03
	C12: Ubiquitin C-terminal hydrolase	Bap1	3 004	-0.68	3.96E-02
	CAMK-unique family	Camkv	21 635	-0.70	3.03E-02
	Carboxylases	Pcx	338	-1.02	4.43E-02
	Catecholamine turnover	Comt	3 347	-0.73	4.06E-02
	CDK8 subfamily	Cdk19	9 953	-0.95	1.59E-03
	CYP2 family	Cyp2s1	919	-1.89	5.51E-06
	CYP39, CYP46 and CYP51 families	Cyp46a1	4 515	-1.32	1.03E-04
	Endocannabinoid turnover	Dagla	2 291	-1.04	8.59E-03
	HIPK subfamily	Hipk4	1 490	-2.24	2.18E-12
	Hydrolases	Dagla	2 291	-1.04	8.59E-03
		Pld2	198	-1.28	4.94E-02
	Leucine-rich repeat kinase (LRRK) family	Lrrk2	3 852	-0.90	1.13E-02
	M10: Matrix metallopeptidase	Mmp17	5 167	-1.48	1.55E-08
	M12: Astacin/Adamalysin	Adam22	9 407	-1.01	7.90E-04
		Adam23	7 281	-0.72	1.76E-02
	M13: Neprilysin	Ece1	2 796	-1.02	1.69E-02
		Mme	9 635	-1.12	1.47E-03
	M2: Angiotensin-converting (ACE and ACE2)	Ace	257	-2.96	6.55E-11
	MAST family	Mast3	21 636	-0.74	7.66E-03
	MSK subfamily	Rps6ka5	1 584	-1.04	4.92E-02
	MSN subfamily	Mink1	10 097	-1.14	9.37E-03
	Other DMPK family kinases	Cit	6 953	-1.13	4.00E-04
	PEK subfamily	Eif2ak3	260	-1.20	4.82E-02
	Phosphatidylcholine-specific phospholipase D	Pld2	198	-1.28	4.94E-02
	Phosphatidylinositol kinases	Pik3r4	2 739	-1.02	2.66E-03
	Phosphodiesterases, 3',5'-cyclic nucleotide	Pde10a	118 406	-1.20	1.06E-04
		Pde1b	33 086	-0.89	1.30E-03
	RAS subfamily	Hras	6 772	-1.03	2.26E-03
	Sphingomyelin phosphodiesterase	Smpd3	5 111	-0.84	1.68E-02
	Sphingosine 1-phosphate phosphatase	Sgpp2	852	-2.36	1.40E-08
	STE7 family	Map2k7	3 520	-1.06	4.99E-02
	TESK subfamily	Tesk1	2 423	-0.98	3.86E-02
	Trbl family	Trib1	567	-1.09	2.33E-02
	Vaccina related kinase (VRK) family	Vrk1	2 866	-0.95	1.27E-02
	VPS15 family	Pik3r4	2 739	-1.02	2.66E-03

	YANK family	Stk32a	2 625	-0.93	5.62E-03
GPCR	5-Hydroxytryptamine receptors	Htr1b	931	-1.24	2.96E-02
	Acetylcholine receptors (muscarinic)	Chrm1	4 508	-0.79	3.47E-02
		Chrm3	382	-1.28	2.69E-02
	Adenosine receptors	Adora2a	18 005	-1.26	1.70E-02
	Adhesion Class GPCRs	Adgrl1	14 581	-1.00	3.38E-03
	Cannabinoid receptors	Cnr1	8 676	-2.43	1.63E-09
	Class A Orphans	Gpr6	1 655	-1.31	4.50E-04
	Class C Orphans	Gpr158	19 006	-0.75	4.33E-02
	Histamine receptors	Hrh3	11 492	-0.92	2.55E-03
	Metabotropic glutamate receptors	Grm1	3 005	-0.96	3.67E-02
		Grm8	197	-1.46	2.33E-02
	Opioid receptors	Oprd1	2 179	-1.06	1.87E-02
LGIC	GABA-A receptors	Gabrd	2 331	-1.87	6.86E-12
	Ionotropic glutamate receptors	Grik3	8 696	-0.79	1.13E-02
		Grin1	5 380	-1.17	9.07E-03
		Grin2a	2 938	-0.86	2.07E-02
		Grin2b	7 815	-0.81	1.64E-02
	IP3 receptor	Itpr1	38 566	-0.85	1.91E-02
NHR	2B. Retinoid X receptors	Rxrg	3 980	-1.00	1.17E-03
	3B. Estrogen-related receptors	Esrra	442	-1.14	2.52E-02
other_protein	R7 family	Rgs9	7 819	-1.07	8.78E-05
	Tubulins	Tuba4a	10 478	-0.66	2.90E-02
Transporters	Ca2+-ATPases	Atp2b1	49 573	-1.23	3.35E-04
	MFS superfamily of transporters	Sv2a	3 277	-1.20	2.14E-02
	Na+/K+-ATPases	Atp1a3	46 679	-0.66	4.81E-02
	SLC12 cation-coupled chloride transporters	Slc12a9	103	-1.34	4.26E-02
	SLC24 family of sodium/potassium/calcium exchangers	Slc24a2	31 183	-1.22	2.95E-05
		Slc24a3	1 252	-1.33	4.10E-05
	SLC41 family of divalent cation transporters	Slc41a1	5 392	-1.59	8.11E-07
	SLC8 family of sodium/calcium exchangers	Slc8a3	2 021	-1.49	3.62E-06
	SLC9 family of sodium/hydrogen exchangers	Slc9a1	2 411	-0.89	3.19E-02
		Slc9a5	457	-1.40	2.64E-03
	Sodium-dependent HCO3- transporters	Slc4a4	11 384	-0.78	3.57E-02
VGIC	Calcium-activated potassium channels	Kcnt1	2 626	-0.92	7.81E-03
	Ryanodine receptor	Ryr2	3 725	-0.81	1.49E-02
		Ryr3	3 238	-1.11	6.49E-04
	Two-P potassium channels	Kcnk2	8 439	-1.20	9.65E-05
	Voltage-gated calcium channels	Cacna1a	2 020	-0.76	2.76E-02
		Cacna1c	6 155	-0.88	9.28E-03
		Cacna1e	14 803	-0.99	2.26E-03
		Cacna1h	1 122	-1.63	6.89E-07
		Cacna1i	2 243	-1.27	1.00E-04
	Voltage-gated potassium channels	Kcnh3	1 144	-0.99	4.40E-02
		Kcnh4	600	-1.57	5.25E-03
		Kcnh7	737	-1.00	3.22E-02
		Kcnq3	2 958	-1.04	4.49E-03
	Voltage-gated sodium channels	Scn1a	3 364	-0.93	1.51E-02

* Translated mRNAs were isolated from the dorsal striatum of *Drd1*::BAC-TRAP and *Drd2*::BAC-TRAP mice. Only identified in the IUPHAR nomenclature, with adjusted p value <0.05 and expression levels > 30 reads are included. Fold-change NAc/DS.

Abbrev.: FC, fold-change, GPCR, G protein-coupled receptor, IC, ion channel, IUPHAR, International Union of Basic and Clinical Pharmacology, LGIC, ligand-gated ion channel, MGI, mouse genome informatics database symbol, NHR, nuclear hormone receptor, padj, adjusted p value, VGIC, voltage-gated ion channel.
http://www.guidetopharmacology.org/download.jsp

Table 21: IUPHAR data base-selected genes with mRNA enriched in NAc as compared DS in D2neurons*

Type	Family name	MGI symbol	Mean	log2 FC	padj
Catalytic Receptor	Interferon receptor family	Ifngr2	1 002	1.02	4.41E-02
	TNF receptor family	Tnfrsf21	2 269	1.05	3.48E-04
	Type XIII RTKs: Ephrin receptor family	Epha5	664	1.04	8.43E-03
Enzyme	1.1.1.42 Isocitrate dehydrogenases	Idh1	570	1.12	2.33E-02
	1.17.4.1 Ribonucleoside-diphos. reduct.	Rrm2	96	1.37	2.78E-02
	Adenylyl cyclases	Adcy7	25	1.26	4.09E-02
	Alkaline ceramidases	Acer2	1 558	0.94	4.51E-02
	Amino acid hydroxylases	Th	95	1.44	2.45E-02
	C14: Caspase	Casp3	49	2.00	4.47E-04
	CAMK2 family	Camk2d	912	1.37	1.02E-02
	Catecholamine turnover	Th	95	1.44	2.45E-02
	Eta subfamily	Prkch	3 382	0.75	3.15E-02
	Interleukin-1 receptor-assoc. kinase (IRAK)	Irak1	1 611	0.88	1.89E-02
	Lanosterol biosynthesis pathway	Hmgcs1	3 196	1.16	1.33E-03
		Idi1	922	1.05	1.26E-02
	M12: Astacin/Adamalysin	Adam12	263	2.38	4.50E-08
	Nucleoside synthesis and metabolism	Rrm2	96	1.37	2.78E-02
	PAKA subfamily	Pak3	7 256	0.71	3.93E-02
	Phosphatidylinositol kinases	Pik3r1	7 118	0.78	9.32E-03
	Phosphodiesterases, 3',5'-cyclic nucleotide	Pde1a	3 307	1.75	8.62E-06
		Pde3b	253	1.45	7.78E-03
	Protein kinase G (PKG)	Prkg1	884	1.85	2.54E-06
	S9: Prolyl oligopeptidase	Dpp4	24	1.15	4.23E-02
	Soluble guanylyl cyclase	Gucy1a3	35 071	0.67	4.94E-02
GPCR	5-Hydroxytryptamine receptors	Htr1a	101	1.44	2.50E-02
	Calcitonin receptors	Calcr	19	1.24	2.39E-02
	Chemokine receptors	Ackr3	68	1.52	1.53E-02
	Class Frizzled GPCRs	Fzd5	157	1.97	8.82E-05
	P2Y receptors	P2ry1	4 307	1.93	1.87E-06
	Prostanoid receptors	Ptgdr	32	1.31	1.98E-02
	Thyrotropin-releasing hormone receptors	Trhr	262	2.57	9.54E-07
	Vasopressin and oxytocin receptors	Oxtr	85	1.70	3.88E-03
LGIC	GABA-A receptors	Gabra5	1 480	0.97	3.47E-02
		Gabrg1	172	1.61	7.36E-03
		Gabrq	44	1.79	1.83E-03
	Glycine receptors	Glra2	270	1.62	3.27E-03
NHR	3A. Estrogen receptors	Esr1	25	1.56	6.55E-03
Other proteins	Fatty acid-binding proteins	Fabp5	3 477	0.70	4.92E-02
	Fatty acid-binding proteins	Rbp1	222	1.38	3.57E-02
	RZ family	Rgs17	10 742	1.23	1.72E-06
Transporters	Mitochondrial nucleotide transporter	Slc25a24	35	1.85	9.14E-04
	SLC16 monocarboxylate transporters	Slc16a2	675	1.01	1.42E-02
	SLC18 vesicular amine transporters	Slc18b1	617	1.00	3.90E-02
	SLC30 zinc transporter family	Slc30a3	91	1.58	1.12E-02
	SLC44 choline transporter-like family	Slc44a5	109	1.44	1.73E-02
	SLC8 family of sodium/calcium exchangers	Slc8a1	2 231	1.59	2.34E-06
VGIC	Cyclic nucleotide-regulated channels	Hcn4	50	1.44	2.69E-02

* Translated mRNAs were isolated from the dorsal striatum of *Drd1*::BAC-TRAP and *Drd2*::BAC-TRAP mice. Only identified in the IUPHAR nomenclature, with adjusted p value <0.05 and expression levels > 30 reads are included. Fold-change NAc/DS.

Abbrev.: FC, fold-change, GPCR, G protein-coupled receptor, IC, ion channel, IUPHAR, International Union of Basic and Clinical Pharmacology, LGIC, ligand-gated ion channel, MGI, mouse genome informatics database symbol, NHR, nuclear hormone receptor, padj, adjusted p value, VGIC, voltage-gated ion channel.

http://www.guidetopharmacology.org/download.jsp

In conclusion, in the first part of my thesis we provide an overall characterization of the genes expressed, or more correctly the polysomes-associated mRNAs, in the D1 neurons of the prefrontal cortex and of the striatum. We then showed the differences between D1 and D2 SPNs separately in the dorsal striatum and the nucleus accumbens. Finally we characterized the important differences between the neurons of the dorsal and ventral striatum, in both the D1 and the D2 populations. These results provide a thorough characterization of the "translatome" in D1 and D2 striatal neurons with the first investigation of their regional differences. They should provide a strong background for future studies and set the stage for the functional investigations in the next part of the thesis

7.2 Aim 2: Long-lasting transcriptional modification induced by operant training for food in D1 and D2 SPNs of NAc and DS and in D1 neurons in the PFC

7.2.1 Highly palatable food increases the behavioural responses in mice trained in an instrumental learning

The palatability of the food is a potent drive to eat even in the absence of an actual caloric need. Here we evaluated the index of the rewarding properties of the food by using an operant paradigm. The protocol includes different batches of mice, mildly food-deprived to be at 90% of their original body weight, learning to nose poke in an active hole to obtain either standard food (ST) or highly palatable food (HP). The conditioning lasts 15 days and is then extended for a period of time in which the mice are fed ad libitum. Controls are provided by groups of yoked mice exposed to the same environmental conditions and food diet as the master mice, except that their pokes are inactive and they receive food non-contingently when the paired master mouse obtains it (**Figure 15**).

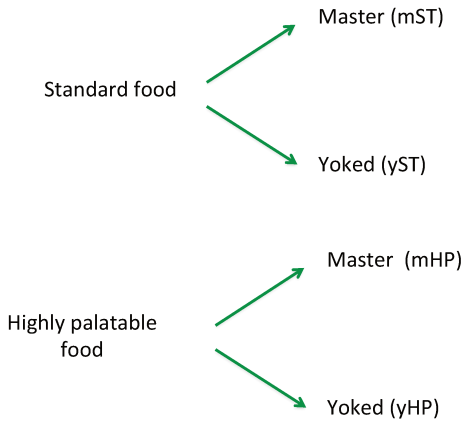

Figure 15 **Figure 1: Experimental design**. Outline of the different groups involved in the operant training

The two foods are similar in shape and calories (ST=3.30 kcal/g, HP=3.48 kcal/g); however the highly palatable food is contains chocolate flavour and 50% of the carbohydrates are substituted by sucrose. During the 15 days of conditioning the mice pass trough two different phases: a learning phase, in which animals are kept under caloric restriction (9 days), and an *ad libitum* phase tin which the mice are fed ad libitum in their home cage (**Figure 16-A**). During this last phase we considered that mice had learned the task and we expected that only the mice motivated by the food palatability kept working in spite of the cessation of calories need. The behavioural results showed that mice working for the highly palatable food performed an increased number of positive pokes, obtained rewards, and consumed pellets already during the restriction phase. In these mice, the nose pokes in the active hole were maintained in the *ad libitum* phase and higher than the standard food group (**Figure 16 B-D**). As expected yoked mice did not show any learning, however, the amount of consumed pellets was comparable to the master group.

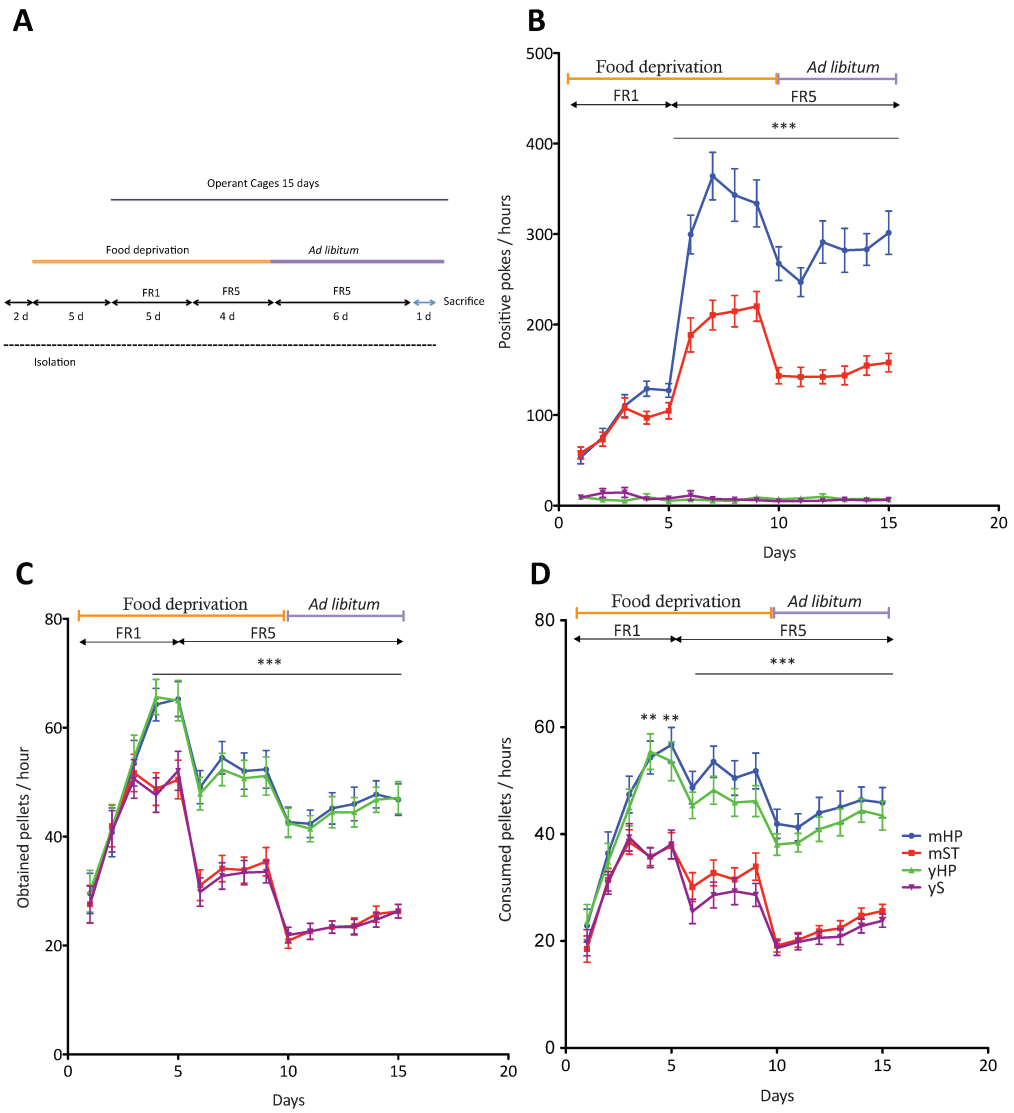

		F	Dfn	Dfd	p-value
Positive pokes Two-way ANOVA	Interaction	26.66	42	1904	<0.0001
	Time	56.95	14	1904	<0.0001
	Food	241.26	3	1904	<0.0001
Obtained pellets Two-way ANOVA	Interaction	3.59	42	1946	<0.0001
	Time	58.58	14	1946	<0.0001
	Food	23.81	3	1946	<0.0001
Consumed Two-way ANOVA	Interaction	3.39	42	1988	<0.0001
	Time	43.87	14	1988	<0.0001
	Food	36.8	3	1988	<0.0001

Figure 16: **Highly palatable food increases the operant training and leads to obesity**. **A**. Outline of the operant training schedule. Mice had to nose poke to obtain food pellets with the indicated fixed ratios (FR). **B**. Daily number of positive pokes in mice working for highly palatable (master, mHP, blue) and standard (master, mST, red) food, and in their respective yoked controls (yHP in green, yST in purple). **C.** Daily number of obtained pellets in the same mice as in B (same color code). **D.** Daily number of consumed pellets in the same mice as in B. in B-D, data are expressed as means +/- SEM, n = 36-38. Two-way ANOVA, followed by Bonferroni Post-hoc test mS vs mHP *** $p<0.00$

7.2.2 Highly palatable food strongly promotes the loss of control over food consumption

Obesity is due to the accumulation of excess body fat occurring when energy intake exceeds that expended. This is a normal adaptive mechanism to variable food availability that allows storage in periods of abundance. Repeated exposure to palatable food can disrupt appetite regulation and it has been shown that the daily consumption of highly palatable and caloric food can become a habit that leads to develop obesity (Jarosz P.A., 2007). Due to the differences observed in operant training, we examined how mice exposed to the two types of food gained weight even though highly palatable food was almost isocaloric with the standard food. Two cohorts of wild type (WT) mice were randomly assigned to two groups. One group had access only to standard food while the other one had free access to both highly palatable and standard food. Mice weight was measured every 3 days over 30 days. The mice having free access to highly palatable food ate more and gained a significantly more weight compared to the mice exposed to the standard food (**Figure 17**). This result suggests that the operant paradigm can provide information about the possible instauration of obesity with highly palatable, almost isocaloric food.

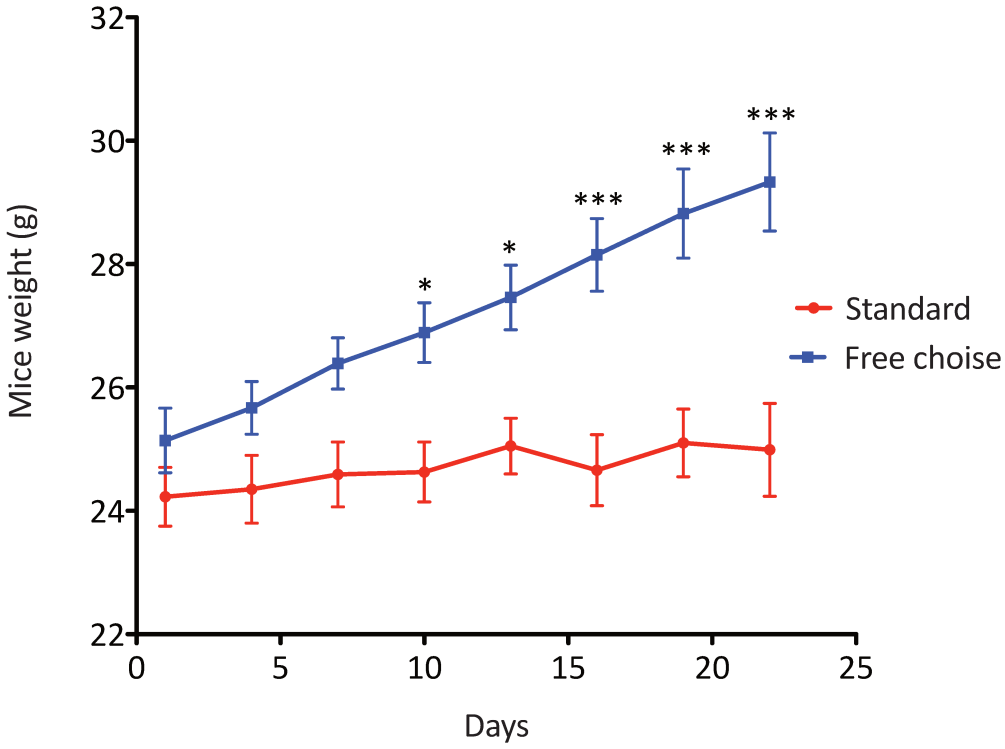

Two-way ANOVA	F	Dfn	Dfd	p-value
Interaction	14.1.	8	144	<0.0001
Time	26.3	8	144	<0.0001
Food	10.09	1	144	0.0052

Figure 17: **Highly palatable food leads to obesity.**

Free access to the HP food used in B-D figure 15 can lead to a strong body weight gain. Wild type mice were exposed to ST food (red curve) or had free choice between ST and HP food (blue curve). Two-way ANOVA followed by Bonferroni post-hoc test. *** $p<0.001$ $n=10$

7.2.3 Highly palatable food increases spines gain in PFC, NAc and DS

The instauration and the maintenance of a learned behaviour are likely to modify the structural plasticity in the brain regions that serve as substrate of this behaviour. Indeed, it has been already shown that a long period of access to both cocaine (Lee et al., 2006) and highly palatable food (Guegan T et al., 2012) has an effect on the structural plasticity of selected regions of the reward circuit. We measured the structural plasticity induced in the PFC and striatum by operant conditioning or non-contingent exposure to the two types of foods. WT mice were trained in the operant conditioning paradigm for 15 days and killed 24 h after the last training session. The brains were quickly dissected and stained with a Golgi-Cox solution. Spine density was measured in the layer five of PFC, NAc and DS in master and yoked mice trained with the two types of food. The analysis of spine density in both master and yoked group allowed separating the effect of conditioning from the effect of the simple exposure to the food (**Figure 18**). Our results show that the highly palatable food itself or the learning for the highly palatable food - but not regular or learning for regular food - had an effect on structural plasticity. Spine number was not changed in mice conditioned for standard food as compared to the yoked mice receiving the same food. In contrast, operant conditioning for highly palatable food increased the spine number in all the three regions analysed, whereas in yoked mice receiving highly palatable food this number was only increased in NAc. These results show that operant conditioning for highly palatable food specifically increases spine density in the PFC and DS, whereas the mere availability of highly palatable food is sufficient to increase the spine number in the NAc, independently of active conditioning.

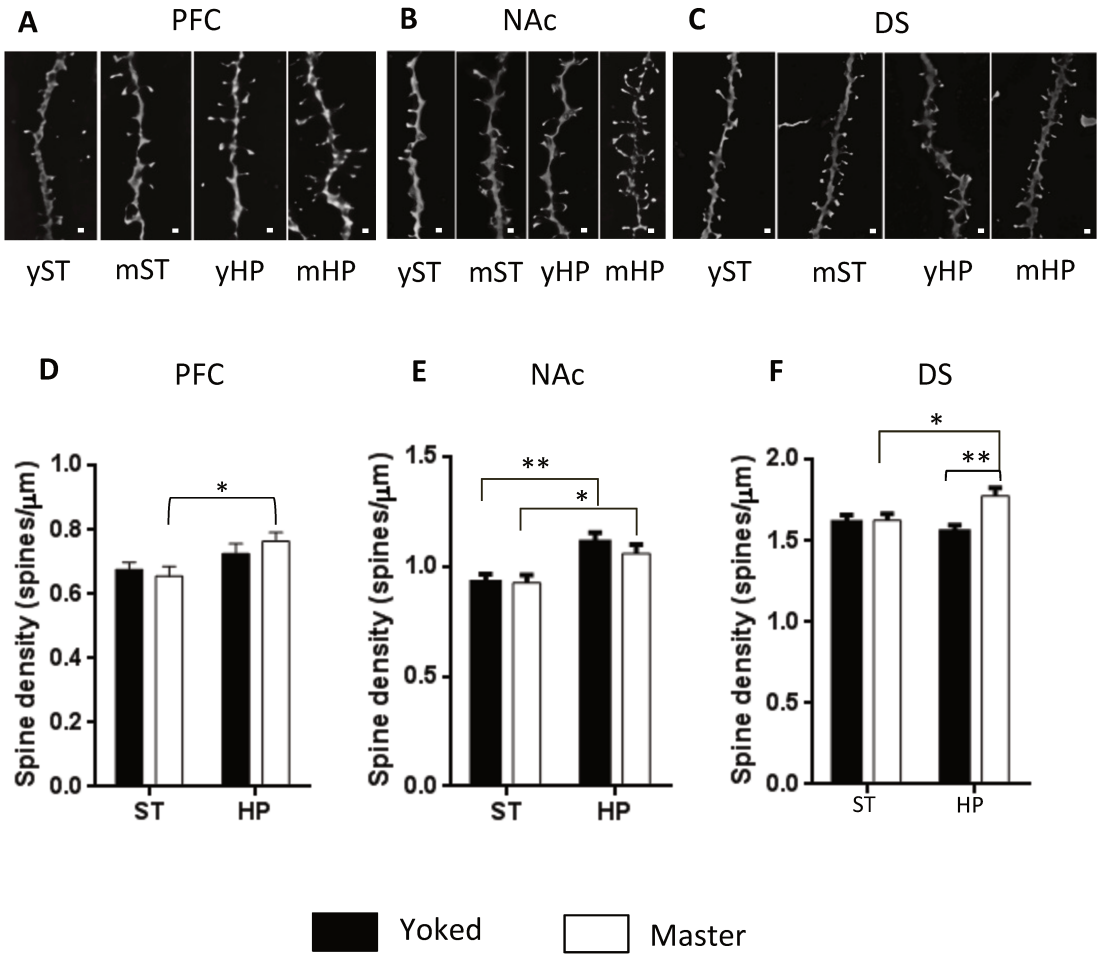

	Nac		DS		PFC	
Interaction	F (1, 171) = 0,4040	P = 0,5259	F (1, 165) = 5,936	P = 0,0159	F (1, 166) = 1,125	P = 0,2904
Learning	F (1, 171) = 0,4748	P = 0,4917	F (1, 165) = 7,307	P = 0,0076	F (1, 166) = 0,1037	P = 0,7479
Food	F (1, 171) = 15,90	P < 0,0001	F (1, 165) = 1,215	P = 0,2720	F (1, 166) = 7,977	P = 0,0053
Bonferroni's post-hoc						
mHP vs yHP	*		**		ns	
yHP vs yST	**		ns		ns	
mST vs yST	ns		ns		ns	
mHP vs mST	ns		*		*	

Figure 18: **Effect of operant conditioning and food type on dendritic spines**. Wild type mice were subjected to operant training for standard (ST) or highly palatable (HP) food as described in Fig. 2A. Controls were yoked mice for each type of food. Their brain was processed for Golgi Cox staining. A-C-F. Representative bright field images of dendrites in the PFC (A), NAc (B) and DS (C) of the different groups of mice. Scale bar = 10 µm D-F. Dendritic spines density was measured in neurons as in A-C from PFC (D), NAc (E), and DS (F). Data are expressed as means +/- SEM (8 mice/group, 4-5 dendrites/mouse). Two-way ANOVA followed by Bonferroni's post hoc.

7.2.4 Profiling the transcriptional modifications induced by operant training in D1 and D2 neurons of NAc, DS, and PFC

Different studies have shown that palatable food and associated cues lead to an increase in DA release in the NAc (Hernandez L., 1988, Hajnal A., 2001) and DS (Small DM, 2003). Continuous consumption of high caloric food produces neuroadaptive changes in the brain reward systems that may drive the development of compulsive eating (P. M. Johnson., 2010). Although much work has been done on natural rewards, a clear description of the corresponding transcriptional profiles is still missing. Thus we aimed to identify the transcriptional profiles in D1 and D2 SPNs in the NAc, DS and D1 pyramidal neurons of the PFC in mice working in an operant training paradigm to obtain either standard or HP food and in yoked control mice that received the same foods passively. To do so we used transgenic mice that express a tagged ribosomal protein (L10a-EGFP) under the control of the D1 or D2 receptor promoter to isolate currently translated mRNA (Heiman et al. 2008) from each population of SPNs , as well as from D1 pyramidal neurons of the PFC. mRNAs were studied 24 h after the last training session. For each region and each population of neurons we performed three different types of comparisons: 1) the master groups versus their respective control (mHP vs yHP and mST vs yST), 2) the mice working for highly palatable food versus the mice working for standard food (mHP vs mST), and 3) the mice non-contingently receiving highly palatable or standard food (yHP vs yST). Those comparisons were done to gain insight on two different aspects of the regulation of the gene expression: the regulation induced by the learning for each food (master vs yoked and master vs master) and the regulation induced by the simple exposure to the food yoked vs yoked. The largest changes were driven by the learning for the highly palatable food in the D2 SPNs (101 up regulated genes, 135 down regulated) of both NAc and DS (622 up regulated genes, 417 down regulated genes) (adj pv <0.05 FC>1.3 FC<0.7 reads number>30). Furthermore, the comparison of the transcriptional profile in the yoked mice showed that in the D2 neurons of the DS, a large number of genes is regulated by the consumption of the HP food. Together these results suggest that the D2 neurons undergo a more stable modification of the gene expression following the stimulation of the reward system by HP food (**Figure 19**) To further characterize the observed

changes in gene expression we observed the population- region- treatment- gene ontologies (GOs). In the D2 SPNs of the DS we found an enrichment in genes involved in the GABA transmission (GABA receptor adj pvalue= 0.01, GABA-A receptor adj pvalue=0.008) In the D2 SPNs we found enrichment in genes involved in the regulation of the chromatin (e.g. nucleosome DNA binding adj p-value=0.00008, chromatin binding, adj p-value=0.0002, transcription activity adj p-value=0.001).

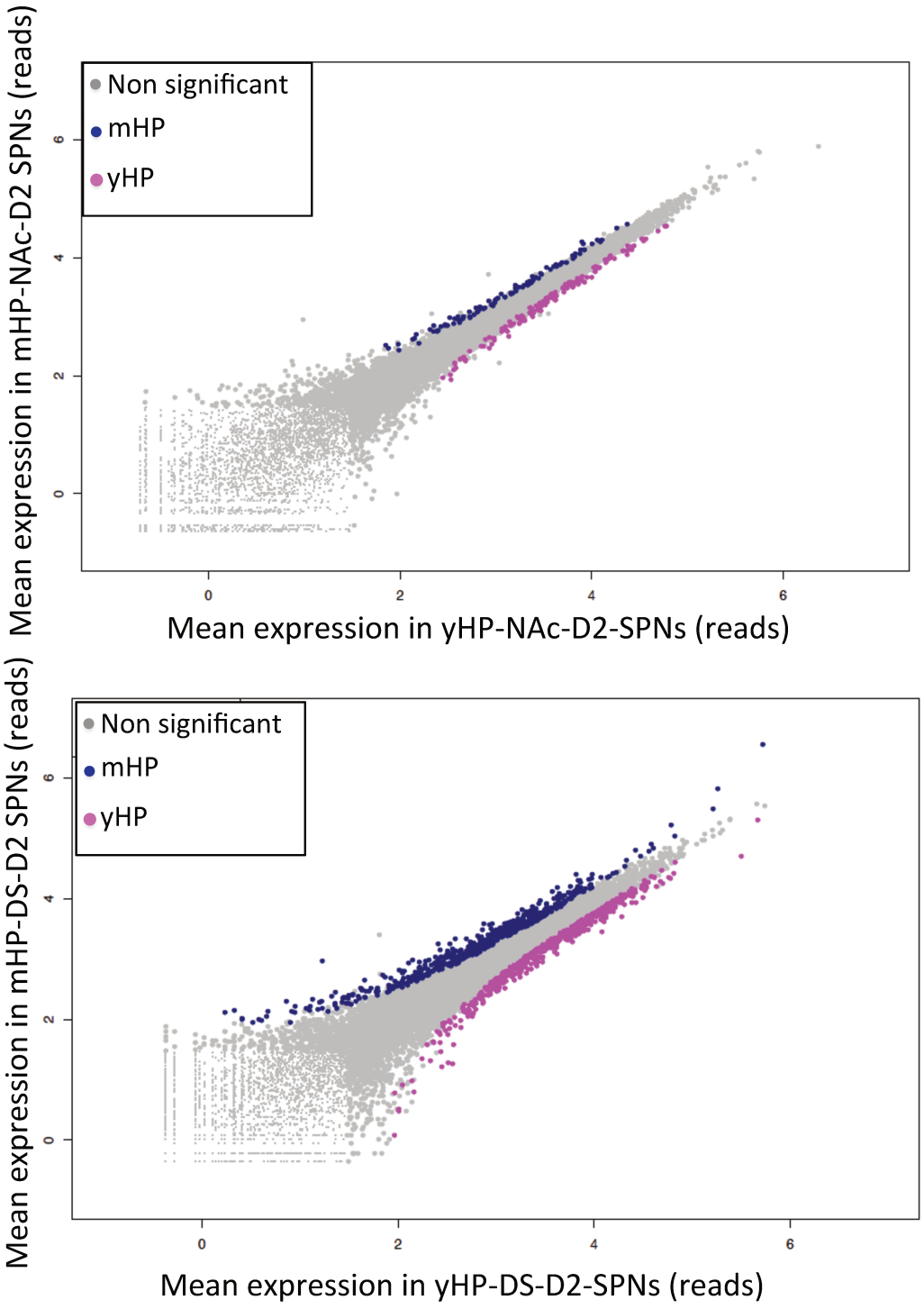

Figure 19: **Overview the differential gene expression induced by the learning for HP food in D2 SPNs of the NAc and the DS. A)** Scatter plot showing the expression of all genes expressed in mHP vs yHP in NAc-D2 SPNs. n = 4, pool of 3 mice/condition. Genes significantly differentially expressed are represented in blue for up-regulated in mHP and in magenta for down-regulated in mHP. **B)** Scatter plot showing the expression of all genes expressed in mHP vs yHP in DS c-D2 SPNs. n =2, pool of 3 mice/condition. Genes significantly differentially expressed are represented in blue for up-regulated in mHP and in magenta for down-regulated in mHP.

7.2.5 Effect of a specific treatment across different regions

We took advantage of the different groups, regions, and neuronal populations to analyse the effect of a specific treatment in regulating the transcription of the same set of genes in different regions. Concerning the learning for HP food, we found that a large set of genes is regulated in the D2 neurons of both the NAc and DS (420 genes, nominal p-value <0.05, FC>1.3 or <0.7, >30 reads at least in one condition). Interestingly, among the 420 genes, only 29 genes are regulated in the same direction in the 2 regions, all the rest being regulated in a different fashion. To gain insight into the function of this opposite regulation, we performed a GO analysis of the different groups of genes. Among the oppositely regulated genes we found an overrepresentation of mRNAs linked to neuronal spines (Adj p=0.008), postsynapse (Adj p=2.88^10-6), postsynaptic membrane (Adj p=0.00073), synaptic membranes (Adj p=0.0010) axon (Adj p=0.001), and GABA-A receptor complex (Adj p=0.009). Of note, we observed the completely opposite result when comparing the effects of learning for the ST food in the D2 neurons in the NAc and DS. Only 15 regulated genes were common between the 2 regions and all were regulated in the same direction. Interestingly, the gene ontology on this group of genes showed an over-representation of mRNAs potentially implicated in the "transcriptional activator activity" (Adj p=0.007). In the D1 neurons, we found only two genes commonly regulated by the HP food conditioning in the DS and NAc: the actin nucleator Pkib, and G protein-coupled receptor 107, both up-regulated by learning (i.e. they were not changed in yoked mice). According to our cut-off, conditioning for standard food regulated only 1 gene in the D1 neurons of the DS and NAc: the Ext 2 exostosin glycosyltransferase. This gene encodes one of two glycosyltransferases involved in the chain elongation step of heparan sulfate biosynthesis. Interestingly, we found 3 mRNAs commonly up-regulated by conditioning for ST food in the D1 neurons of the NAc, DS and PFC: the intellectual disability-associated hivep2 (human immunodeficiency virus type I enhancer binding protein 2), Kcnv1 (potassium channel, subfamily V, member 1), and the brain specific protein Ank2 (ankyrin 2). In some of the regions, the increase in mRNA expression was only around 20% (FC=1.20). Two of these genes are already known to be regulated in relation with the reward system: Hivep2 has been already shown to be regulated by cocaine self-administration (Reynolds et al. 2006) and there is evidence supporting the

involvement of Ank2 in cocaine-induced locomotion (Scotland P., 1998). Finally two genes regulated by conditioning for HP food were common between the 3 regions: Pkib, up-regulated in the 3 regions and Syndigin1L (synapse differentiation inducing-1-like), down-regulated in DS and NAc and up-regulated in PFC.

This preliminary analysis of our results shows that the conditioning for HP food and for ST food exerts different effects on transcription depending on the neuronal type and the regional location of the neurons. In D2 neurons, the HP food-related learning induces a major opposite regulation of the transcriptional profiles of the NAc and DS. In D1 neurons, in agreement with the lower amount of changes induced by the operant training, we found much less common genes in the different region. When in common the genes were always regulated in the same fashion in the NAc and DS. Importantly, we also identified 3 genes commonly regulated by learning for the ST food in the NAc, DS and PFC, while only 2 genes were found in common in the 3 regions after learning for the HP food.

7.2.6 Effect of a specific treatment across different regions

We reasoned that by comparing the effect of conditioning for ST and HP food in the same region, we could gain insight on the genes that may be generally regulated by operant conditioning in the specific region and type of neurons. This analysis is not fully completed yet. However, we already have some information. In the D2 NAc, conditioning for HP and ST food had an effect on the transcription of 80 common genes. Among those, only 19 were regulated in the same direction, while the majority were regulated in different fashion by the 2 types of food. 34 mRNAs were up-regulated by conditioning for ST food and down-regulated by conditioning for HP food, 29 are down-regulated by conditioning for ST food and up-regulated by the learning for the HP food. The opposite tendency can be observed in the DS, where among the 10 genes in common between the 2 types of conditioning, only 3 were regulated in opposite fashion. Interestingly, among those 3 genes Fos was down-regulated in the D2 neurons of the DS of mice working for HP food. The D1 neurons share much less common genes. Only one gene was common to HP and ST conditioning in both the NAc and DS, which is the nuclear factor of kappa light

polypeptide gene enhancer in B cells inhibitor, epsilon (Nfkbie). The same types of comparisons are in progress for the neurons in PFC, DS and NAc.

7.2.7 Probing a candidate gene in operant learning for highly palatable food: the possible role of norbin

To validate our analysis of the effects of the operant training on the regulation of gene expression, we tested the consequence of the genetic manipulation of one of the genes differentially regulated by conditioning for HP food. We focused on Ncdn, a gene coding for the protein norbin (also known as neurochondrin) as our analysis showed that conditioning for HP food exerted an opposite regulation on Ncdn transcription in the D2-SPNs of the NAc and the DS (**Figure 20 A & B**). We hypothesized that if this regulation is functionally relevant, the deletion of Ncdn in neurons should have a specific effect on the behavioural consequences of training for HP food. We first used two different techniques, in two independent experiments, to confirm the positive regulation on the Ncdn gene expression exerted by the operant training for highly palatable food. RT-PCR on D2-mRNA, purified by immunoprecipitation with anti-GFP antibodies from *drd2*::L10a-GFP transgenic mice, confirmed the up-regulation of the Ncdn mRNA in the DS of mice trained with HP food compared to the yoked control group (**Figure 20C**). In addition, we measured norbin protein levels in the DS of WT mice trained to obtain highly palatable food. The levels of norbin were increased in the DS of mice conditioned for HP food when compared to the yoked group (**Figure 20D**). These results confirmed the results of RNA-seq in the DS and showed that mRNA alterations had consequences on protein levels.

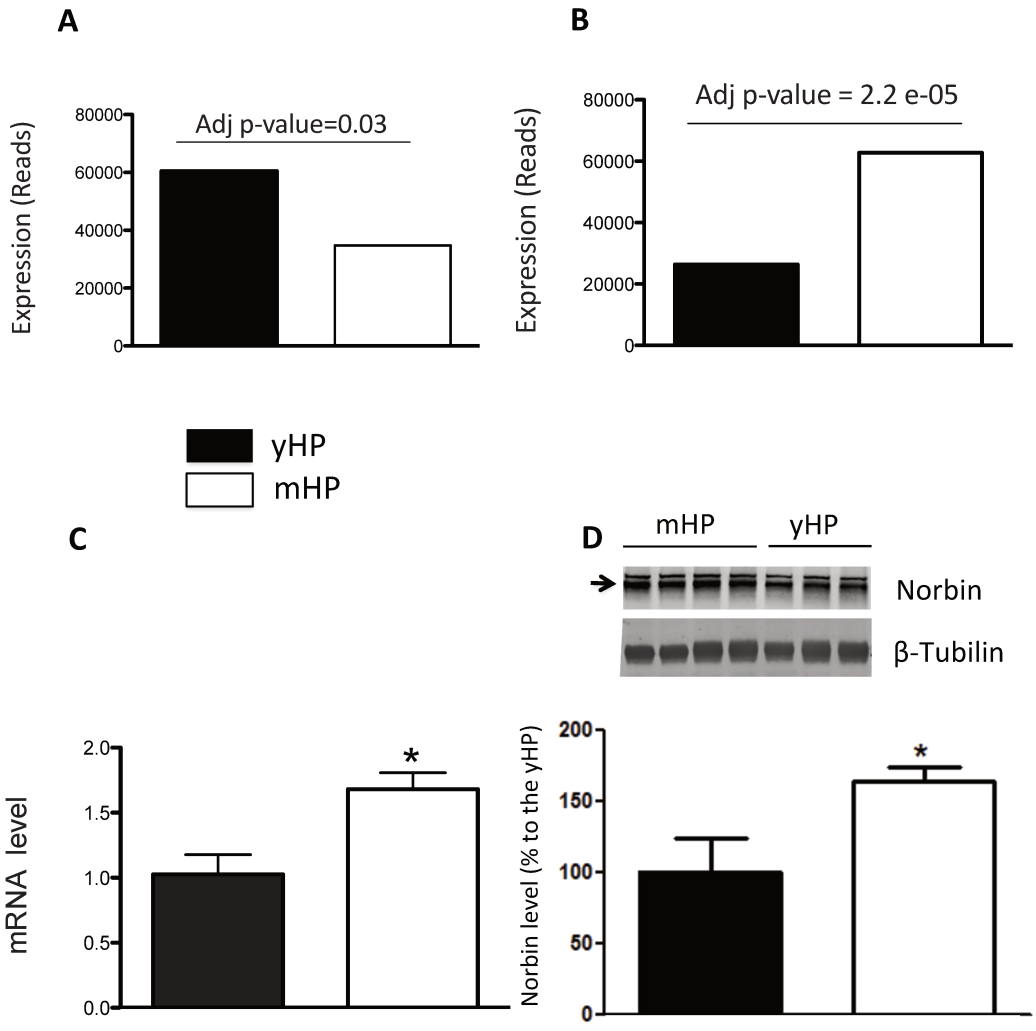

Figure 20: **Regulation of norbin (*Ncdn*) expression after training for HP food**. **A.** Norbin expression in D2 neurons in the NAc of yoked (yHP) and master (mHP) mice conditioned for HP food, plotted as number of reads calculated from RNA-seq (n = 4 pools of 3 mice). **B**. Norbin expression in D2 neurons in the DS as in A (n = 2 pools of 3 mice). C. Expression levels of norbin mRNA measured by RT-PCR in the DS of mice trained for HP food (mHP) or yoked (yHP), n = 3, two-tailed unpaired t test, $t_4 = 3.306$, p = 0.0298. **D**. Expression level of norbin protein determined by immunoblot in the DS of mice trained for HP food (black bar mHP) and their ontrol (white bar, yHP). N= 7 yHP, 8 mHP. Two tailed unpaired t test, $t_{13} = 2.65$, p = 0.021.

We then used norbin conditional KO mice ($Ncdn^{Flox/Flox}$), crossed with CamK2::Cre or wt mice (Fig. 7A). Norbin was absent in the post-natal forebrain of the first group whereas it was not altered in the control group ($Ncdn^{Flox/Flox}$). These mice were conditioned for 15 days for ST or HP food and subsequently subjected to

a progressive ratio schedule to obtain food. Our results showed that the deletion of the Ncdn exert differential regulation of learning depending on the different phases of the paradigm (Fig. 7B). During the food restricted learning phase, the mice lacking Ncdn learned faster to obtain HP food as compared to their Cre-negative controls, as demonstrated by the increase in positive pokes and consumed pellets (Fig. 7B). Interestingly, this difference was inverted when the mice were switched to the *ad libitum* phase. During this last phase the norbin mutant mice showed a more pronounced decrease in the positive pokes and consumed pellets as compared to their WT control (**Fig. 21B and C**).

We then examined the behavioural consequences of the mutation after the conditioning period using a progressive ratio schedule (**Fig. 21C**). The norbin mutant mice were willing to work significantly less to obtain HP pellets, as compared to their WT littermates. These results indicate that in the absence of norbin, the persistently increased apparent motivation to obtain HP food was not acquired.

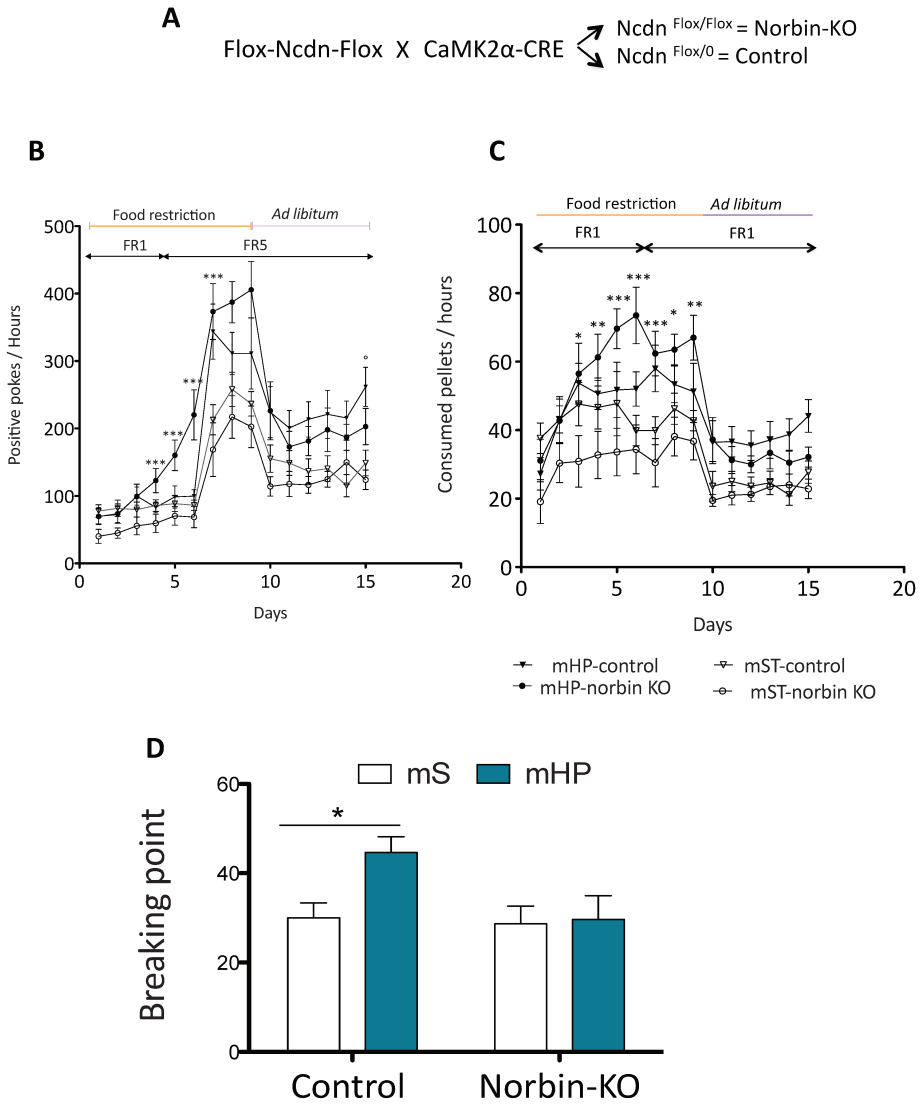

Figure 21: **The conditional deletion of Ncdn in forebrain neurons differentially alters the two phases of operant learning.**

A. Description of the different groups of mice used in the training behavior**.** Norbin floxed mice have been crossed with CamKIIα-cre mice. In the mice CRE positive Ncdn is selected KO in all the neurons expressing CamKIIα. The littermates CRE negative are used WT control. **B.** Daily posirive pokes in Norbin-KO mice and control trained to work for either ST or HP food. Data are expressed as mean +/- sem. * mST vs mHP, n=6-3. Two-way ANOVA (interaction $p<0.0001$, time $p<0.0001$, genotype $p<0.0001$), followed by Bonferroni post-hoc test. *** $p<0.001$=mHP-KO vs mST-KO. ° $p<0.05$ mST vs mSHP **C.** Daily consumed pellets in Norbin-KO mice and control trained to work for either ST or HP food. Data are expressed as mean +/- sem. * mS vs mHP, n=6-8. Two-way ANOVA (interaction $p=0.0172$, time $p<0.0001$, genotype $p<0.0001$), followed by Bonferroni post-hoc test. * $p<0.05$ *** $p<0.001$=mHP-KO vs mST-KO **D**. Breaking point reached by norbin-ko mice and littermates control in a progressive ratio schedule to obtain HP (blue bars) or standard food (white bars). One way ANOVA($p=0.03$), followed by Bonforerroni post-hoc test * $p<0.05$.

In conclusion, in the second part of this work we used a combination of behavioural and genome-wide approach to study the effects of the operant learning for standard and highly palatable food in D1 and D2 SPNs of the NAc and DS and in D1 pyramidal neurons of the PFC. The preliminary analysis of our results allowed to define the regions (NAc and DS), the neurons (D2 SPNs) and the genes more responsive to the highly palatable food. The in vivo manipulation of one of the genes (Ncdn) differentially regulated by the training for the highly palatable food allowed a first validation of part of the findings of our study. However, a lot should still be done with the results we obtained. A validation by independent techniques of some target genes that we have found as regulated in the different conditions is in progress. In parallel, a systems biology approach to explore the transcriptional synchrony induced by food conditioning would give a reasonable indication of the overall mechanisms that are taking place during conditioning for highly palatable food, as well as of the targets that could be fundamental to the loss of the eating control. The clusterization of the genes would allow measuring if the connectivity of certain clusters is affected by a certain treatment compared to the control, as well as to find the hub of cluster, and modify its expression.

7.3 Aim 3: Long-lasting transcriptional modification induced by cocaine in D1 and D2 SPNs of NAc and DS and in D1 neurons in the PFC

7.3.1 Cocaine induced structural plasticity in NAc, DS, and PFC

Early investigations established that a robust form of neuronal plasticity associated with repeated psychostimulant administration is a long-lasting restructuring of dendritic spines in components of the brain reward circuits (Robinson and Kolb, 1997). We checked whether our protocol of chronic cocaine treatment was able to induce structural plasticity by Golgi staining in NAc, DS, and PFC of mice i.p. with cocaine or vehicle for 7 days, and sacrificed 24 h after the last injection. This chronic cocaine regimen induced different types of morphological alterations in three different regions. In the NAc, chronic cocaine increased spine density and spine head area, without altering neck length. (**Fig. 22A-D**). In the DS chronic cocaine increased spine neck length, without altering spine density or head area (**Fig. 23A-D**). In the PFC, repeated cocaine did not significantly change the spine density or spine head surface (**Fig. 24A-C**). It tended to increase spine neck length, without reaching the statistical significance (**Fig. 24D**).

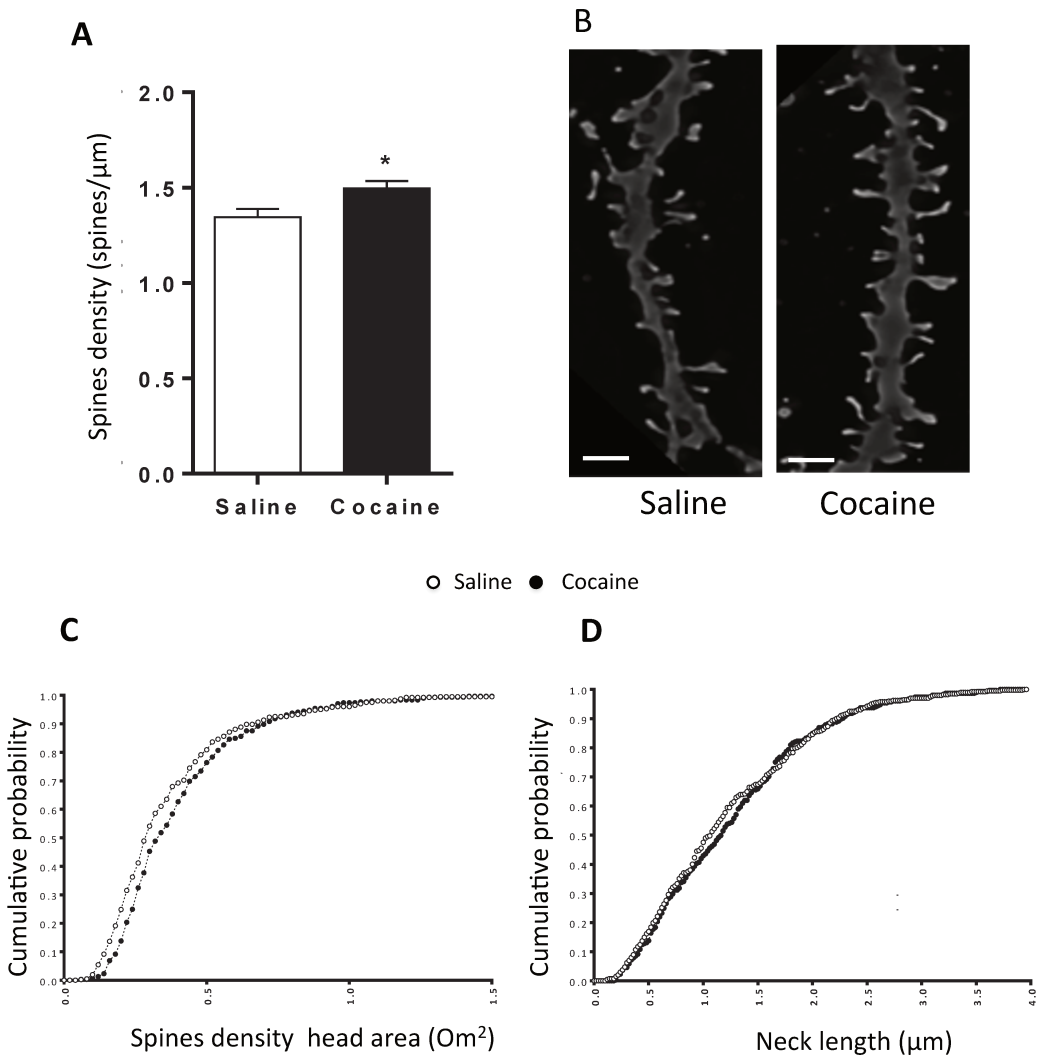

Figure 22**: Effect chronic cocaine on spines in the NAc**

A. Total dendritic spines density in neurons from PFC in saline (controls, white bars) or cocaine-treated (white bars) mice. Data are expressed as mean + SEM. Unpaired 2-tailed t-test (8 mice/group, 4-5 dendrites/mouse, n =32-408. **B**. Representative bright field pictures of dendritic processes. Scale bar = 10 µm. **C an D** Quantitative analysis of the effect of the cocaine treatment on head area (C) and neck length (D). Y axis: cumulative probability X axis: head area (um) or neck length (um). Comparison of distributions using the Kolmogorov-Smirnov test ~500 spines from ~60-80 dendrites from 4 animals per condition). Head area p-value=0.0051, neck length ns.

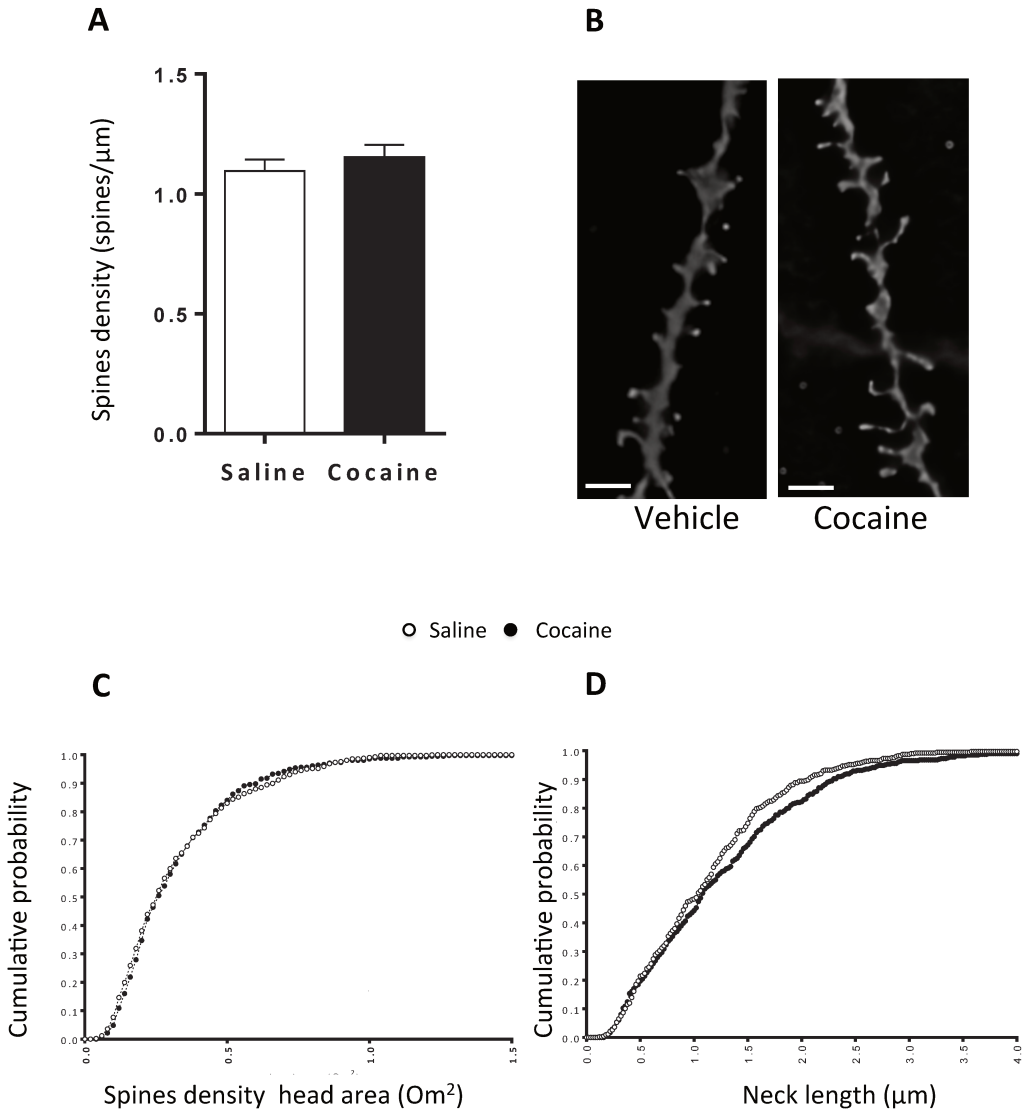

Figure 23: **Effect chronic cocaine on spines in the DS**

A. Total dendritic spines density in neurons from DS in saline (controls, white bars) or cocaine-treated (white bars) mice. Data are expressed as mean + SEM. Unpaired 2-tailed t-test (8 mice/group, 4-5 dendrites/mouse, n =32-40. **B**. Representative bright field pictures of dendritic processes. Scale bar = 10 µm. **C an D** Quantitative analysis of the effect of the cocaine treatment on head area (C) and neck length (D). Y axis: cumulative probability X axis: head area (um) or neck length (um). Comparison of distributions using the Kolmogorov-Smirnov test ~500 spines from ~60-80 dendrites from 4 animals per condition). Head area ns, neck length p-value=0.03.

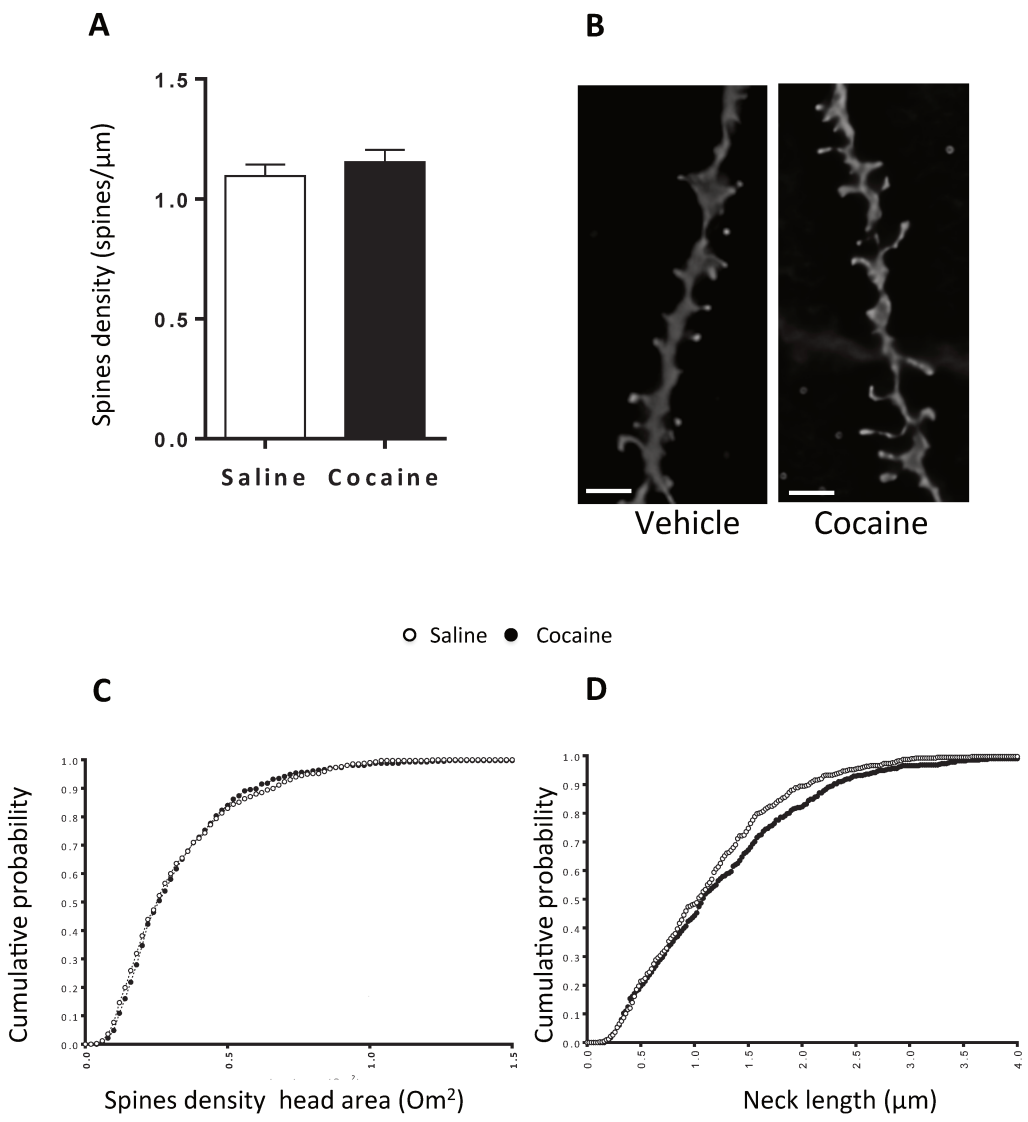

Figure 24: **Effect chronic cocaine on spines in the DS**

A. Total dendritic spines density in neurons from DS in saline (controls, white bars) or cocaine-treated (white bars) mice. Data are expressed as mean + SEM. Unpaired 2-tailed t-test (8 mice/group, 4-5 dendrites/mouse, n =32-40. **B**. Representative bright field pictures of dendritic processes. Scale bar = 10 µm. **C an D** Quantitative analysis of the effect of the cocaine treatment on head area (C) and neck length (D). Y axis: cumulative probability X axis: head area (um) or neck length (um). Comparison of distributions using the Kolmogorov-Smirnov test ~500 spines from ~60-80 dendrites from 4 animals per condition). Head area ns, neck length ns.

7.3.2 Differential gene expression in identified neuronal populations of the NAc, DS and PFC following chronic cocaine treatment

To generate circuit-wide transcriptional profiles, we used RNA-seq to analyse D1 and D2 neurons in the NAc, DS, and PFC, from controls, and mice treated with cocaine for seven days. Mice were sacrificed 24 h after the last injection to analyse only the long-lasting modifications (**Fig. 25**)

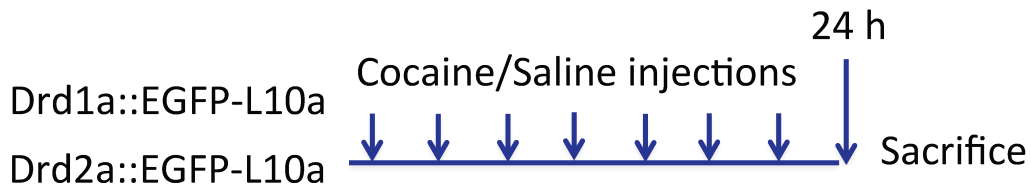

Figure 25: **Experimental design**. Transgenic BAC-TRAP mice were daily i.p.-injected with saline vehicle or cocaine (20 mg/kg) for 7 days and sacrificed 24 h after the last injection.

7.3.3 Differential gene expression induced by cocaine in D1 and D2 neurons of the NAc and DS

In D1-SPNs of the NAc 136 genes differentially regulated in cocaine-treated as compared to saline-treated mice (**Fig. 26A**). Fifty-seven genes were positively regulated and 79 down-regulated. Among the up-regulated mRNAs we found some genes related to "plasticity" – such as BDNF – or more specifically to the plasticity induced by cocaine such as Homer2, (Knoflach et al., 2001; Mameli et al., 2009; Brakeman et al., 1997), Nfib (Feng et al.; 2014) or Grin3a (Mameli et al., 2007).

To further characterize the observed cocaine-induced patterns, we carried out a gene ontology analysis (GO, **Fig. 26B**). Interestingly, among the genes positively regulated by cocaine, we found an enrichment in mRNAs coding for proteins involved in "pathways such as axon development", and "central nervous system development", indicating an major involvement of the genes regulated by to

developmental processes, possibly linked withcocaine in the plasticity. The GO on the totality of the genes altered by cocaine (i.e. positively or negatively) showed an enrichment in genes linked to “axon”, “neuron projection”, “dendrite-membrane”, and “ actin skeleton” indicating an involvement of genes possibly linked with plasticity (**Fig. 26B**).

In NAc D2 SPNs, the number of genes changing in response to cocaine -72- was smaller than the D1 SPNs. However, the regulation exerted by the cocaine administration was apparently stronger when comparing the fold of expression. As for the D1 neurons we found genes already reported as associated to cocaine. Among others, we found the kinase domain-containing 1, Ankk1, a gene closely linked to the Drd2 gene, that has been already connected to the susceptibility to addiction (Bao Zhu-Yang et al., 2008) and to the subjective modulation of the acute effects of cocaine in humans (C.J. Soellicy; 2004). Interestingly, we found two genes co-regulated regulated by cocaine in D1 and D2 NAc: Ret (ret proto-oncogene), down regulated in both neuronal populations, and Lpl (lipoprotein lipase) up in D2 and down in D1 (**Fig. 26D**).

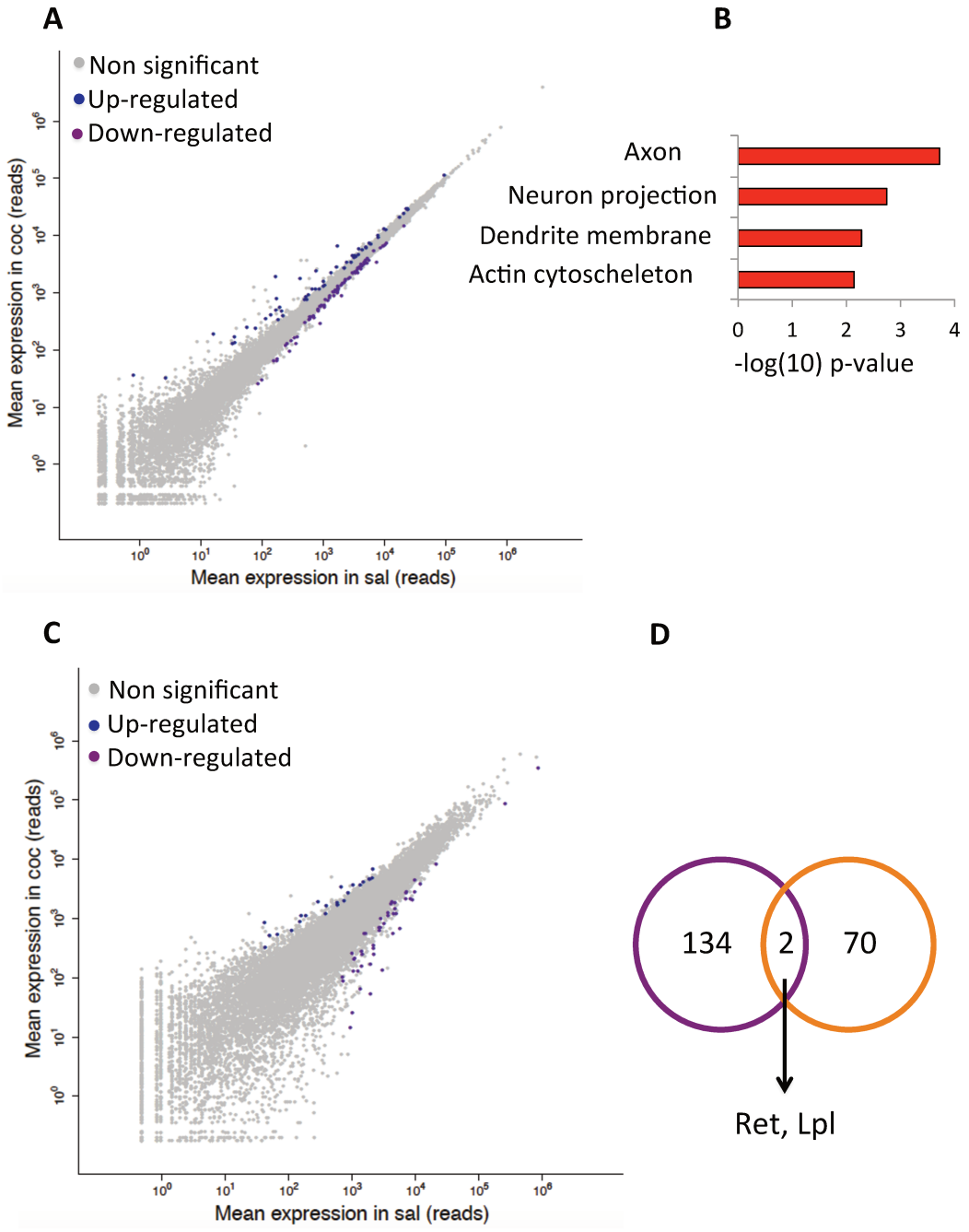

Figure 26: **Overview of the differential gene expression induced by cocaine in D1 and D2 SPNs of the NAc**

A) Scatter plot showing the expression of all genes expressed in cocaine vs saline in NAC-D1 SPNs. n = 4 single mice per drug condition. B) Summary of GO enrichment for differentially expressed genes in A). Data are plotted as –log10 (p value). C) Scatter plot showing the expression of all genes expressed in cocaine vs saline in NAC-D2 SPNs. n = 4 single mice per drug condition. D) Venn diagram showing the genes commonly regulated in D1 and D2 SPNs in the NAc

Interestingly, with our p-value cut-off (adj p-value <0.05), we did not find any cocaine-induced changes in the DS. By moving the cut-off to a less stringent p-value criteria (nominal p-value<0.05) (**Figure 27**) we observed that cocaine tended to increase the expression of 422 genes and to decrease the expression 531 in D1 SPNs with two genes inversely regulated in the Nac and the DS (upregulated in the NAc and own regulated in the DS): Bdnf and Lypd6b (LY6/PLAUR Domain Containing 6B). In D2 SPNs cocaine increases increase 177 genes, and decrease 246 genes in D2 SPNs (Fig. 6A and B), with only one gene in common with the D2-NAc: MAM domain containing glycosylphosphatidylinositol anchor 1 (Madga1) up regulated in the DS-D2 and down regulated in the D2-NAc.

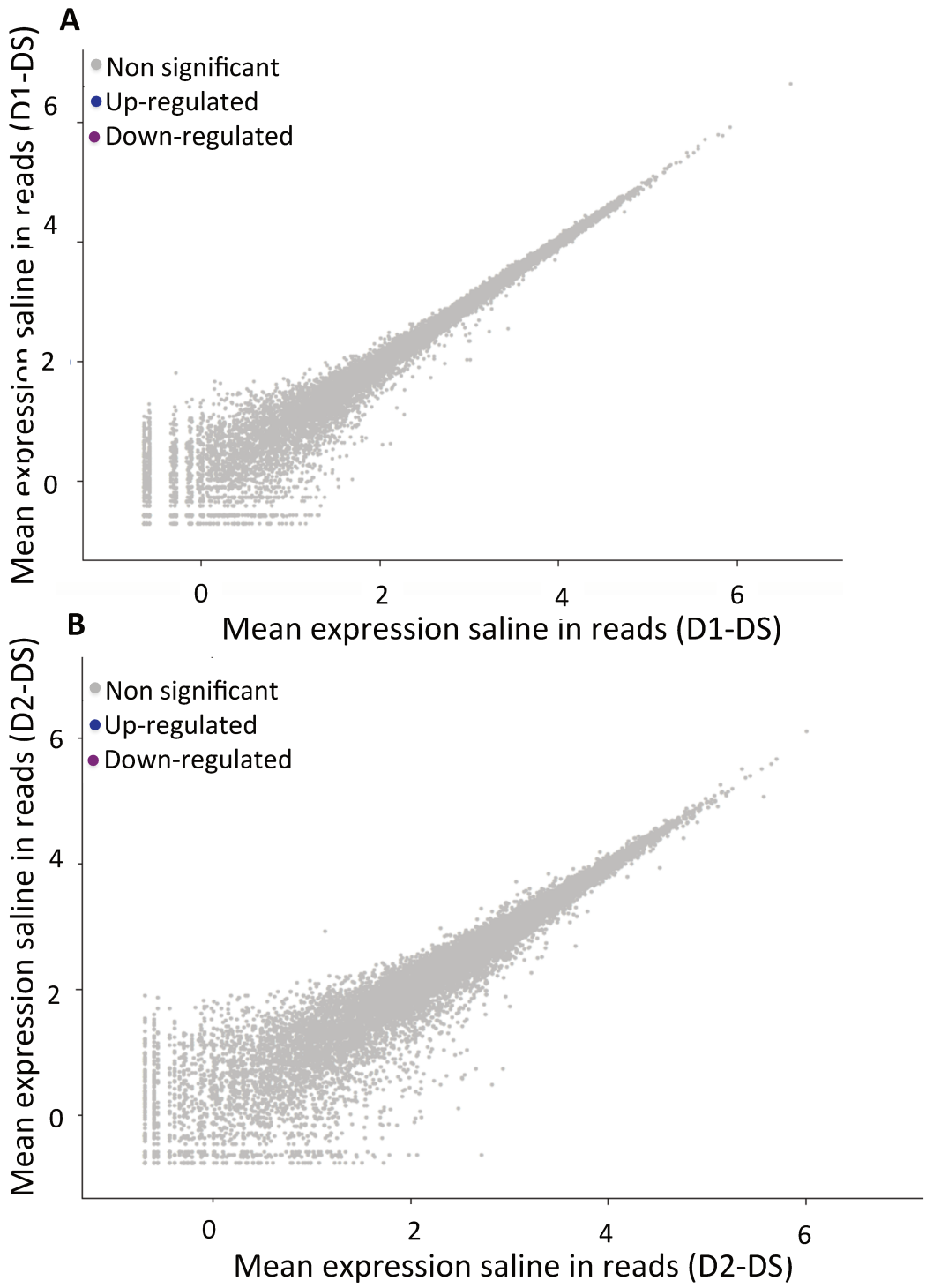

Figure 27: **Differential gene expression induced by cocaine in D1 neurons of the PFC.**

A-B Scatter plot showing the means of expression in reads of all genes expressed in cocaine vs saline in DS D1R (A) and D2R(B)-expressing isolated with BAC-TRAP. Genes significantly differentially expressed are represented in blue for up-regulated genes and in purple for down regulated genes.

7.3.4 Cocaine-induced gene expression changes in D1 pyramidal neurons of the PFC

Several lines of studies have already shown that the PFC plays a key role in the development of addiction to cocaine. Human studies of post mortem dorsolateral PFC of cocaine abusers showed that cocaine triggers the activation of several genes in this region (Lehrmann E., 2003). However a clear information about the genes regulated in the DA-expressing receptors neurons in the PFC is still missing. Using BAC-TRAP to identify translated mRNA from D1R-expressing neurons in the PFC, we identified 48 genes differentially regulated by cocaine (**Fig. 28A**). There were 46 up-regulatd genes and 29 down-regulated ones. The GO analysis on the genes differentially regulated by cocaine showed enrichment in genes involved in "postsynapse", "postsynaptic density" and "postsynaptic specialization" (**Fig. 28B**). By crossing this data set with the data obtained in NAc D1 and D2 SPNs, we found only one gene commonly regulated by cocaine between PFC and NAc D1, *Stx1a* (coding for Syntaxin 1A, **Fig. 28C**), and 2 genes commonly regulated by cocaine in NAc-D2 and PFC (Pcid2, PCI domain containing 2, and Ntng1, netrin G1, **Fig. 28D**).

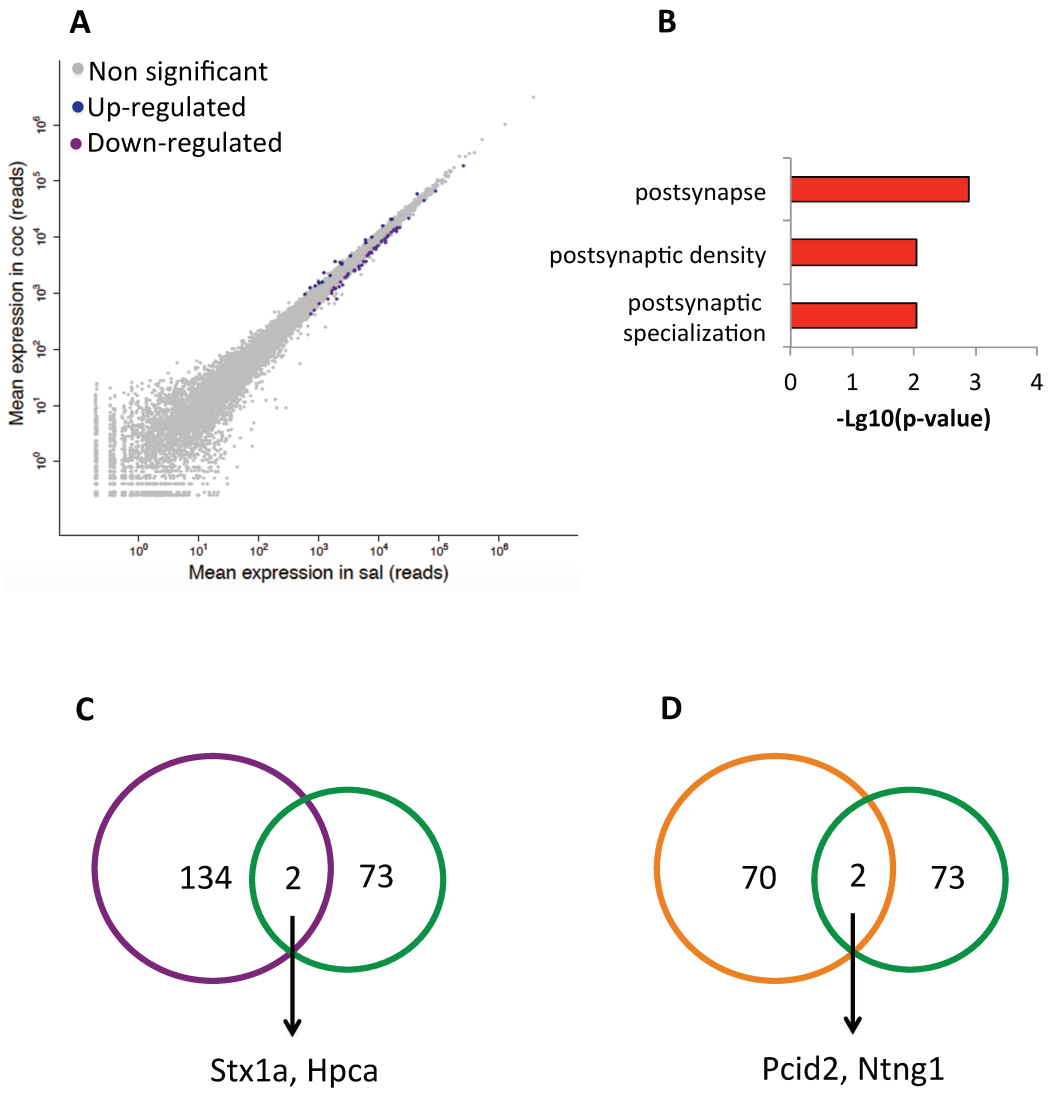

Figure 28: **Differential gene expression induced by cocaine in D1 neurons of the PFC.**

A. Scatter plot showing the means of expression in reads of all genes expressed in cocaine vs saline in PFC D1R-expressing isolated with BAC-TRAP. Genes significantly differentially expressed are represented in blue for up-regulated genes and in purple for down regulated genes. **B)** GO enrichment of the genes significantly regulated by cocaine in A) data are plotted as –lg10(p value). **C-D** Venn diagrams indicating the genes commonly regulated in D1R-expressing cells of the PFC and in D1 (C) and D2 SPNs (D2) in the NAc.

7.3.5 Coexpression analysis identifies modules of genes clustering in response to the cocaine treatment

Several studies suggest that gene coexpression analysis is useful for identifying transcriptional alterations in disorders whose phenotype is characterized by the orchestrated alteration of numerous small changes rather than from isolated single gene effects (Ghazalpour et al., 2006; Gaiteri et al., 2014). Having identified the broad patterns of transcriptome-wide changes in D1 and D2 neurons across several brain regions, we then thought to identify specific gene coexpression networks that could be critical in determining the exact response of D1 and D2 SPNs and D1 cortical neurons to the cocaine administration. We used a weighted gene co-expression network analysis (WCGNA) approach to construct a gene coexpression network integrating expression data across brain regions and specific neurons – D1 pyramidal neurons in PFC and D1 SPNs in NAc - and treatment – cocaine and saline – to identify module of co-expressed genes that could underlie the response to chronic cocaine treatment. WCGNA Is a systems biology method for describing the correlation patterns among genes across microarray and RNA-seq samples. It can be used for finding cmodules of highly correlated genes, for summarizing such clusters using the module eigengene or an intramodular hub gene, for relating modules to one another and to external sample traits (using eigengene network methodology), and for calculating module membership measures. For both D1 neurons in NAc and PFC we found four different modules in which the genes differentially regulated by cocaine are highly intra-correlated (**Fig. 29A and 30A**). The two networks are completely independent and while the modules names and the arbitrary (blue, yellow, brown, turquoise) colours on the figures are the same, there is no common gene implicated in the two neuronal populations, as showed by the fact that cocaine induced a common regulation of only 2 genes in NAc and PFC. For each module we calculated its overall correlation with cocaine treatment and we performed a GO analysis to get an insight about the biological relevance of the identified coexpression modules. In NAc D1 SPNs, the GO of the cocaine-associated genes clusters, indicated an enrichment in genes implicated in the synaptic and structural plasticity, axogenesis, modulation of synaptic transmission, regulation of synaptic plasticity, dendrites development, and synaptic vesicles localization among the most

represented pathways among the GO terms (**Fig. 31A**). Interestingly, the same analysis performed on the D1 pyramidal neurons showed a major enrichment in genes involved in the epigenetic modifications such as histone methylation (**Fig. 31b**). To gain insight into the biology of the cocaine related modules, we identified the most interesting modules for further study. In particular we used STRING (*Search Tool for the Retrieval of Interacting Genes/Proteins*), a database predicting the protein-protein interaction , to reconstruct the network structure of genes within each of the modules mostly related to presence or the absence of cocaine for each type of D1 neurons and identified so-called key-drivers or hub genes. A key-driver gene is a gene that has the highest probability to connect with the highest number of genes. Our analysis showed a network-type organization in the module D1-SPNs-NAc that mainly clusters in response to the presence of cocaine (blue module) (**Fig. 32**) in which we observed several potential hub-genes, such as Tuba4a (Tubulin Alpha 4a), Phlpp1 (PH Domain And Leucine Rich Repeat Protein or phosphatase 1) or Prkaca (Protein Kinase CAMP-Activated Catalytic Subunit Alpha) The other module in which we could resolve a network organization was in the D1 pyramidal neurons of the PFC, specifically in the module that mostly anti-correlates with the cocaine stimulation (**Fig. 33**). The network analysis of this module clearly revealed 4 hubs or key drivers genes Acly, Srsf1, Adrkb1, Crebbp.

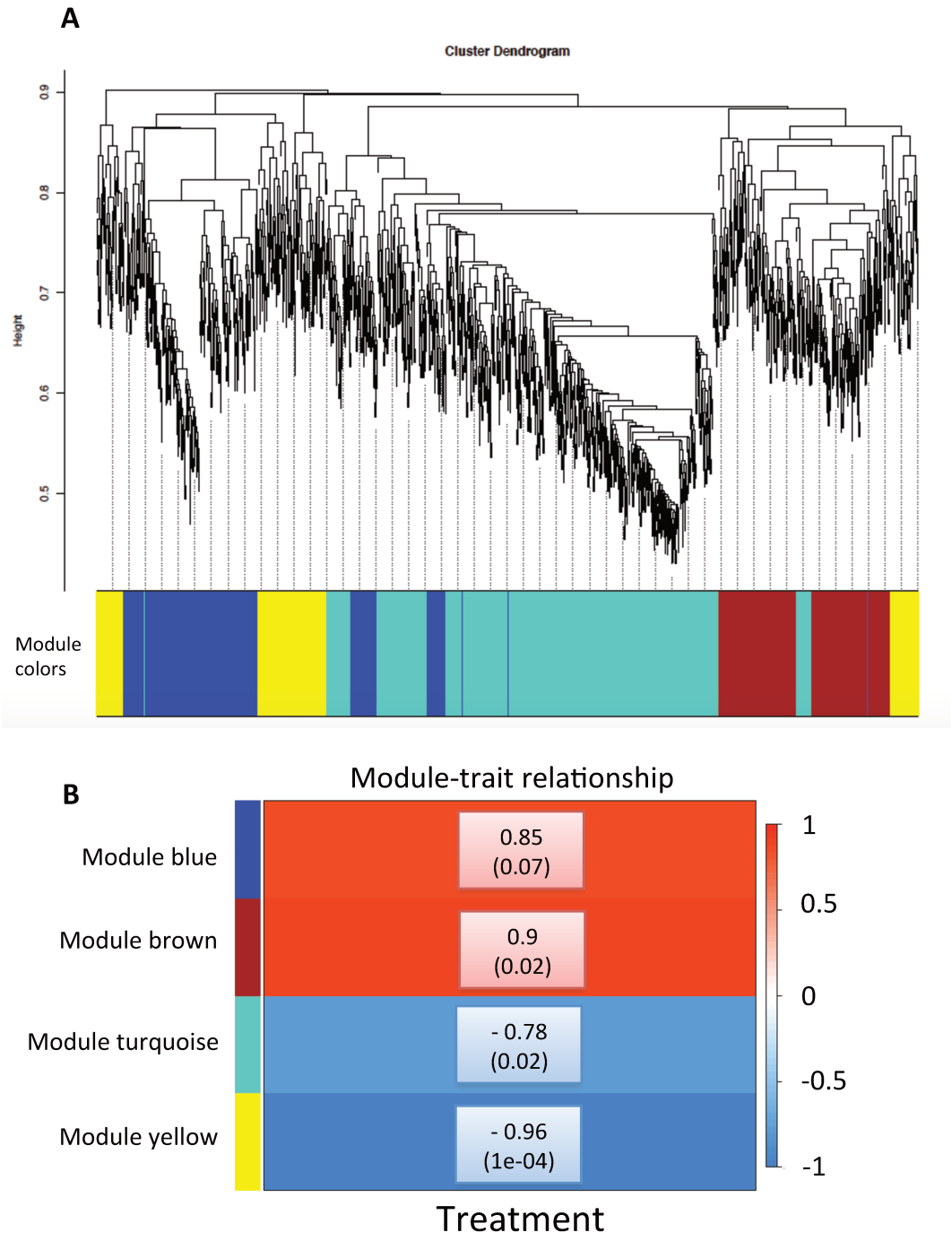

Figure 29: **Module analysis on D1-NAc-SPNs reveals clusters of genes that co-cluster in response to cocaine treatment A**) Hierarchical clustering of D1-NAc-SPNs genes and visualization of gene module partitioning. The colored bars (below) directly correspond to the module (color) designation for the clusters of genes. One can visualize where in the whole clustering dendrogram the gene modules were defined. **B**) Module trait matrix showing the correlation between the levels of genes clusterization and cocaine presence (+1) or absence (-1).

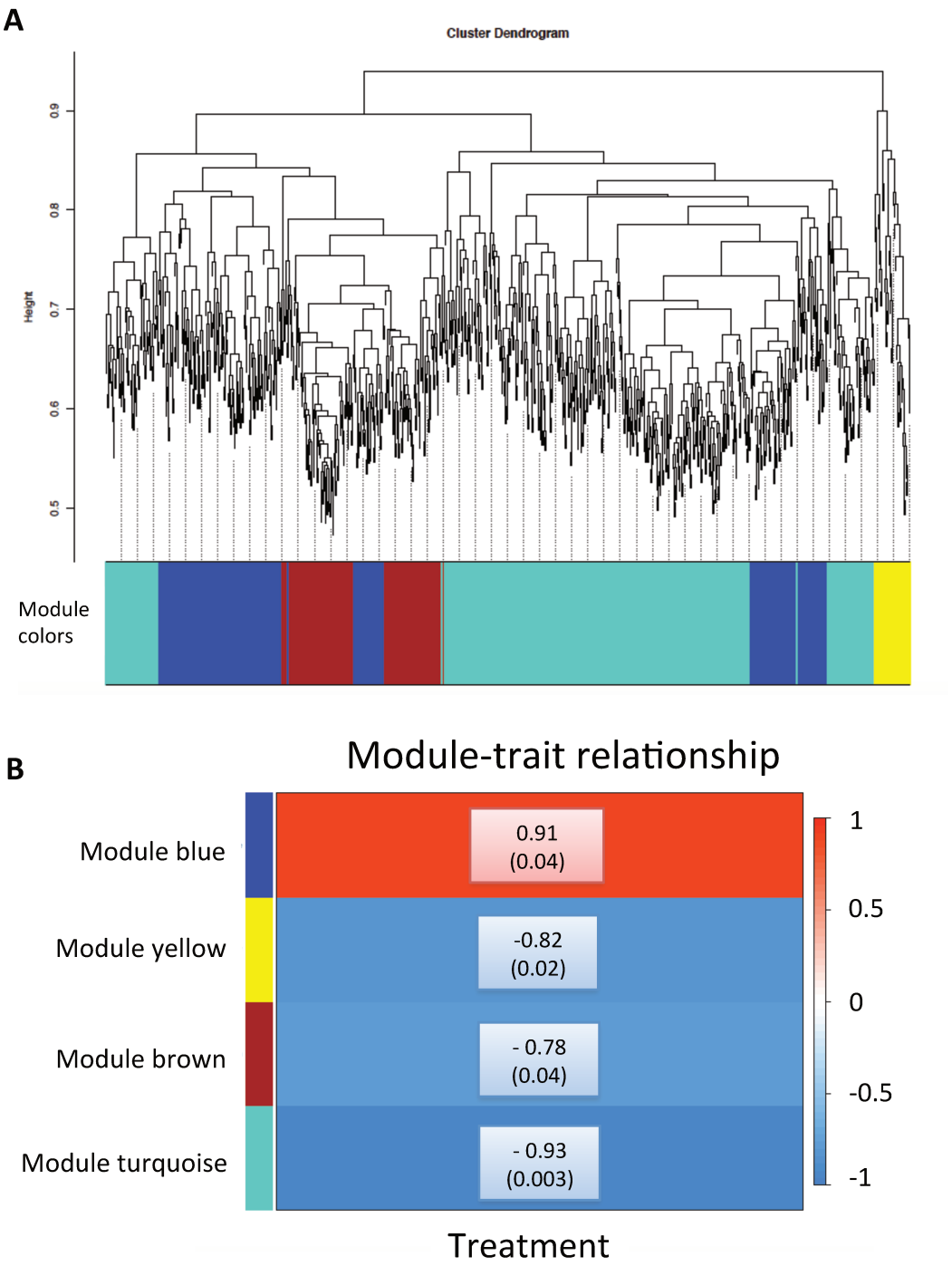

Figure 30: **Module analysis on D1-PFC-SPNs reveals clusters of genes that co-cluster in response to cocaine treatment A**) Hierarchical clustering of D1-NAc-SPNs genes and visualization of gene module partitioning. The colored bars (below) directly correspond to the module (color) designation for the clusters of genes. One can visualize where in the whole clustering dendrogram the gene modules were defined. **B**) Module trait matrix showing the correlation between the levels of genes clusterization and cocaine presence (+1) or absence (-1).

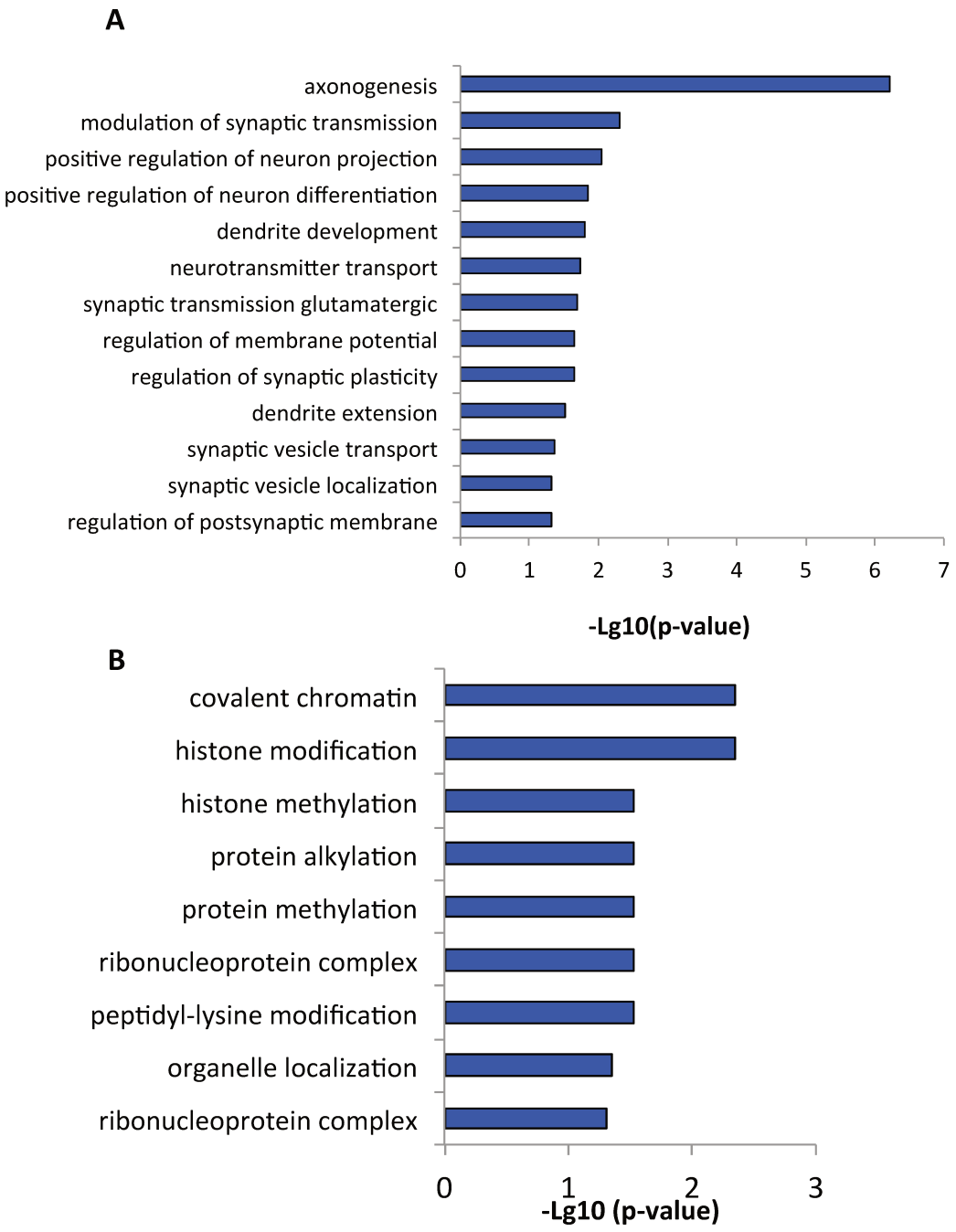

Figure 31: **GOs analysis on the module more associated to the cocaine presence or absence.**

A. GOs analysis on the module more associated to the cocaine presence in D1-NAc-SPNs. **B.** GOs analysis on the module more associated to the cocaine absence in D1-PFC-neurons.

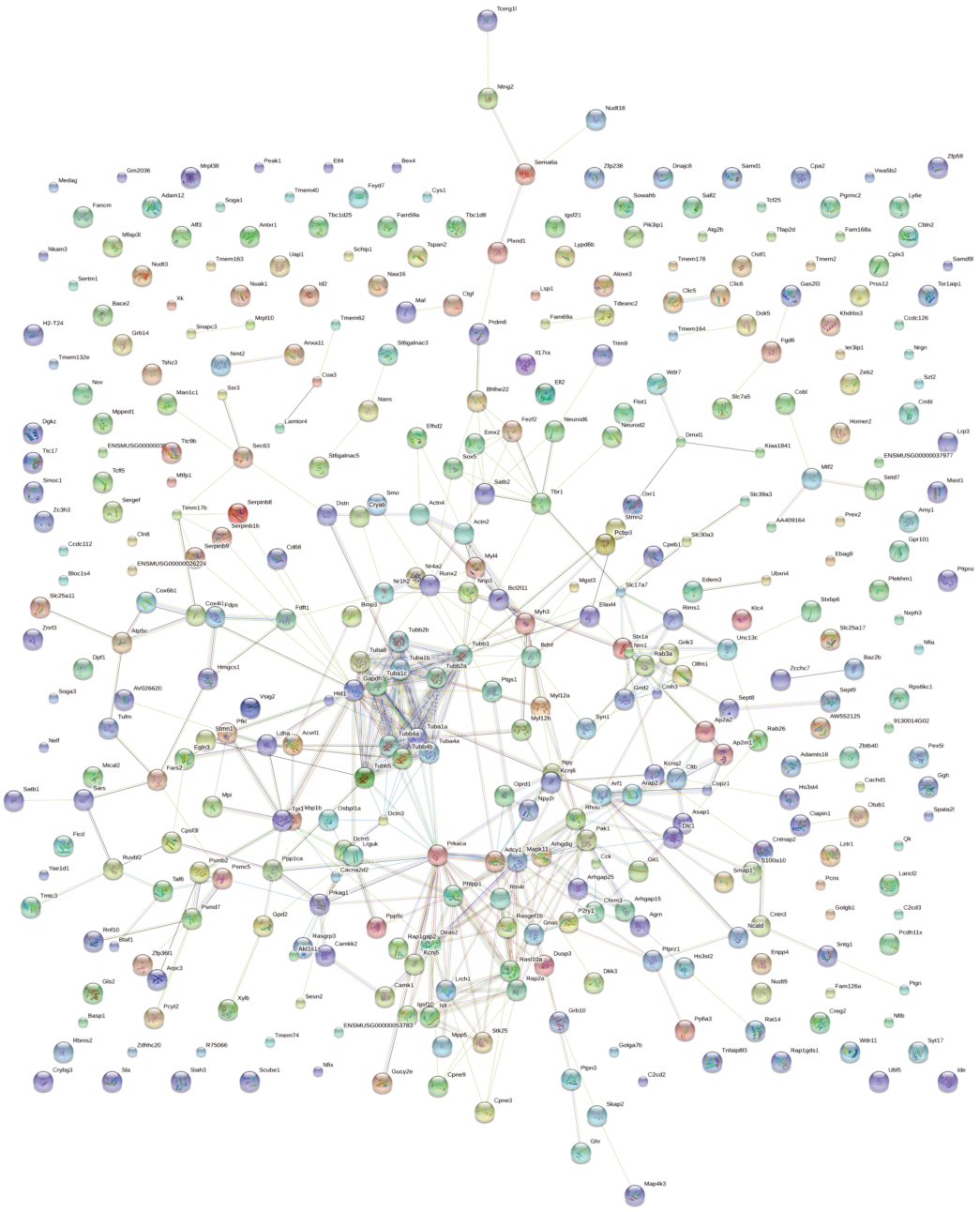

Figure 32: **Genes coexpression networks of blue module in NAc-D1-SPNs**

Network plot of genes identified within blue module. Small nodes: protein of unknown structure large nodes: some structure is known or predicted. Colored nodes: query proteins and first shell interaction, white nodes: second shell of interaction. Node size is proportional to node's network centrality. Edges: turquoise from curated database, magenta experimentally determined, green gene neighborhood, red gene fusion, blue gene co-occurrence, black co-expression, light blue protein homology

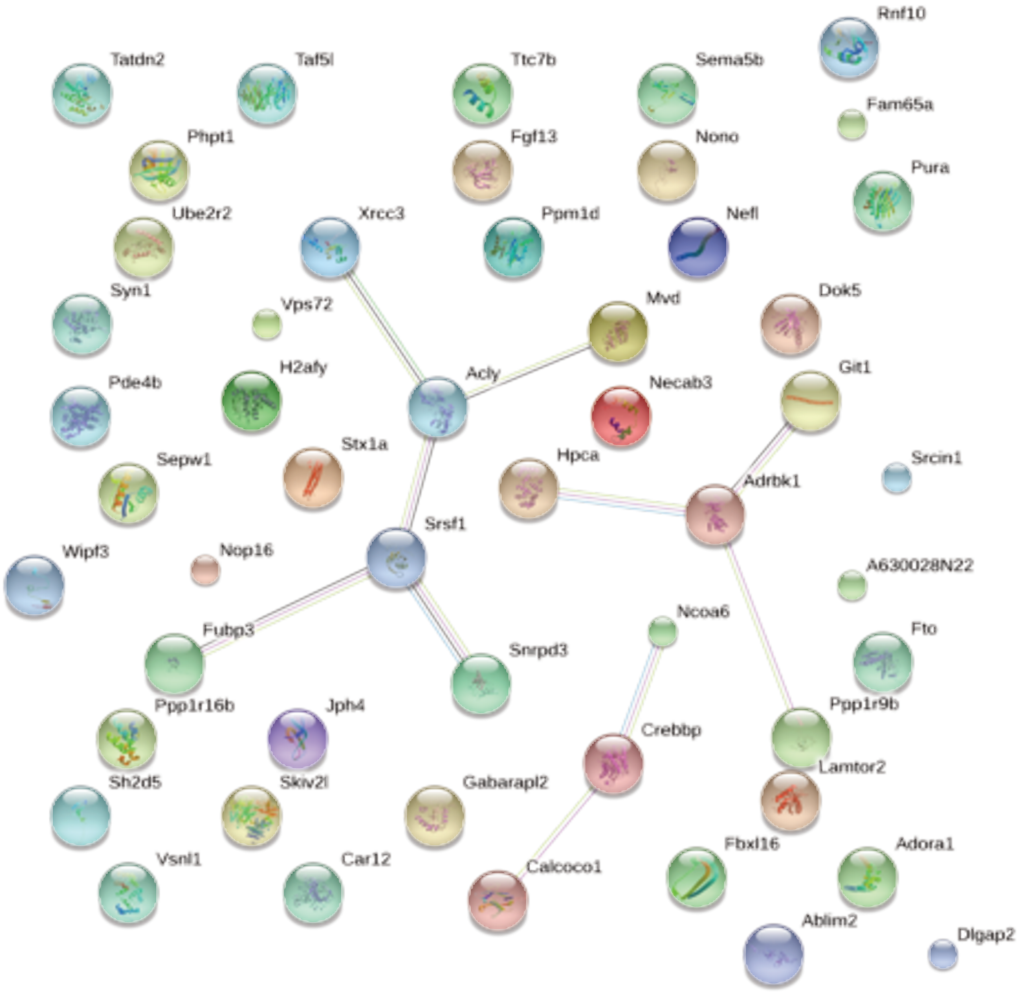

Figure 33: **Genes coexpression networks of blue module in PFC-D1-SPNs**

Network plot of genes identified within blue module. Small nodes: protein of unknown structure large nodes: some structure is known or predicted. Colored nodes: query proteins and first shell interaction, white nodes: second shell of interaction. Node size is proportional to node's network centrality. Edges: turquoise from curated database, magenta experimentally determined, green gene neighborhood, red gene fusion, blue gene co-occurrence, black co-expression, light blue protein homology

In conclusion in this part of work we showed which are the regions, and subtype of neurons more responsive to the chronic cocaine regimen. Importantly it should be underlined that this work is still in progress. A full modules analysis on the D2 neurons is ongoing. The data presented in this section have been obtained recently and an independent validation of the genes differentially regulated will be important to carry out.

7.4 Comparison between food and cocaine

7.4.1 Comparison of the effects on dendritic spines induced by highly palatable food and chronic cocaine injections

First, we compared the structural plasticity induced in the NAc, the DS and PFC in the various treated groups as compared to their respective controls (See experimental results aim 2 and 3). On the one hand we identified the changes induced by 1) active stimulation of the reward system by operant conditioning for highly palatable food (HP) (mHP) 2) active stimulation of the reward system induced by operant conditioning for standard food (ST) (mST) 3) passive stimulation of the reward system by non-contingent presentation of HP food, (yHP), as compared to yoked controls which received non contingently ST food, (yST). On the other hand we identified changes induced by chronic cocaine injections (cCoc) as compared to saline-treated controls (saline) (**Figure 2**). Then we compared qualitatively the changes observed in the two types of conditions. Since the batches of animals were different and the experiments were not done at the same time, we did not compare the two control groups to each other.

In the NAc we didn't observe any changes in spines number in mice conditioned for ST food as compared to yST. In contrast both operant conditioning for highly palatable food and the non-contingent presentation of HP increased the number of spines (**Figure 34 this section and figure 18, results section 2**). The NAc was also the only region in which we found an increase in spines density in the cCoc group.

In the DS (**Figure 34 this section and figure 19, results section 2**), only the operant training for highly palatable food increased spines density. This suggests that the operant conditioning for HP food by itself played a critical role in the morphological change in this brain region.

Lastly, the comparison between the effect of food and cocaine on the PFC showed that spines density was increased only by conditioning for the highly

palatable food compared to the mST, while no difference was observed in the groups that receive either food or cocaine reward non contingently (**Figure 34 this section and figure 20, results section 2**) or which were conditioned for standard food. This result is not surprising considering the fact that the PFC is implicated mainly implicated in higher function such as learning, habits formation or relapse, all functions that involve specifically the connection between PFC and DS.

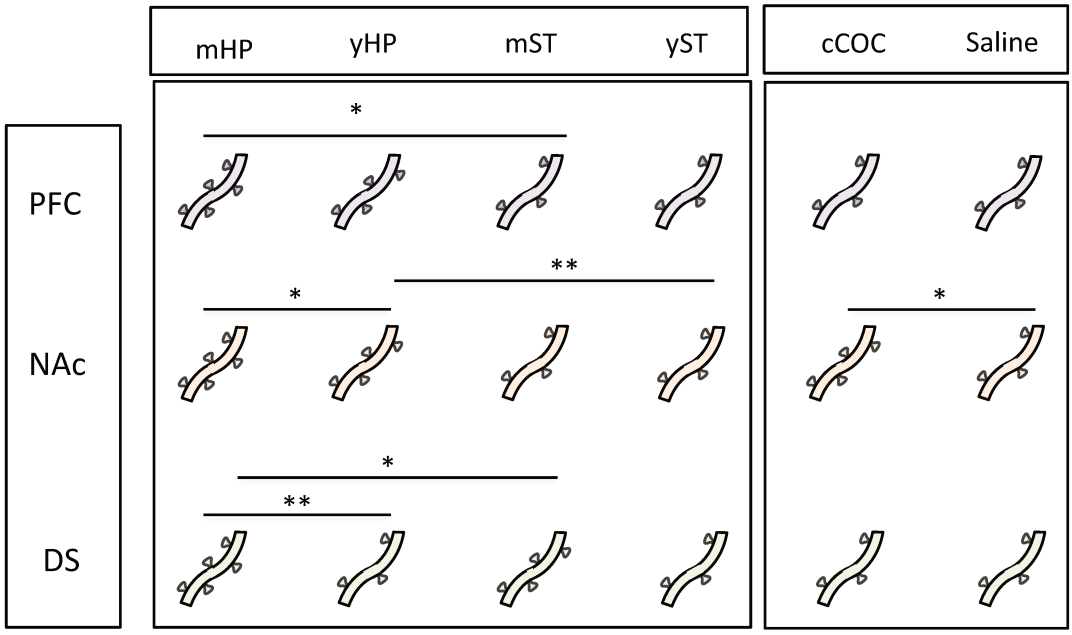

Figure 34 **Summary of the effects of operant conditioning for food and chronic cocaine treatment on dendritic spines.** Different groups of WT mice were subjected to operant training for standard (ST) or highly palatable (HP) food or to chronic cocaine treatment. Controls were yoked mice for each type of food and mice injected with vehicle for the cocaine group, respectively. Dendritic spines density was measured using Golgi-Cox staining, 24 h after the last conditioning session or the last injection. PFC: *=mHP vs y. NAc: *=mHP vs yHP, **=yHP vs yST, * = cCoc vs saline, DS: ** =mHP vs yHP, *= mHP vs mST,

7.4.2 Comparison of the transcriptional alterations induced by operant conditioning for food and chronic cocaine injections

We compared the effects of the six different treatments (mHP, mST, yHP, yST, cocaine, saline) on the transcriptional profiles in PFC, NAc, and DS, taking into account the specific types of neuron (i.e. D1 or D2). Importantly, all the analyses that we reported until now were performed exclusively on the genes that showed an Adj p-value <0.05; here - in order to have the possibility to make all the comparisons - we did perform our first analysis taking into consideration all the genes that showed a nominal p-value <0.05.

Common genes were found in all comparison (see table below). For each population of neurons in each regions we compared the effect of the cocaine with: the effect of the non contingent presentation of the food (yHP-cCOC), the effect of the training for the ST food (mST-cCOC), and the effect of the training for the HP food (mHP-cCOC). In D1 NAc–SPNs, the yHP-cCOC comparison resulted in 85 common genes, 50 regulated in opposite fashion, 35 regulated in the same direction; the mHP-cCOC revealed 85 common genes. Interestingly only 15 are regulated in the same fashion. Lastly, the comparison mST-cCOC revealed 77 common genes, 37 regulated in the same direction and 41 in opposite direction. Contrary to the other comparisons of the PFC, when comparing the cocaine exposure with the operant training for the ST food we find a striking anti-correlation of the common genes: among the 96 genes commonly regulated only 4 are regulated in the same direction. Conversely, in the comparison mHP-cCOC we can observe mainly a co-regulation of the gene expression, among the 87 common genes only 26 are regulated in opposite fashion.

In the D1-SPNs of the DS we found 25 genes in common in comparison yHP-cCOC, only 3 inversely regulated. In the mHP-cCOC 52 genes are in common, among them only 9 are regulated in the same direction. Lastly, for the comparison to mST-cCOC, 79 genes were common, with only 4 genes regulated in the same fashion. Lastly, in comparison with the PFC, we found 73 genes in common in yHP-cCOC, 23 co-regulated and 20 oppositely regulated.

Concerning the D2-DS-SPNs, we found 109 common genes in yHP-cCOC, 59 regulate in the opposite direction, 50 commonly regulated, 73 common genes in mHP-cCOC 36 co-regulated 37 anti-regulated, and only 5 genes common in comparison to mST-cCOC, 2 commonly regulated, 3 regulated in opposite fashion.

The comparison that revealed the most striking results was that between the effects of HP food and those of cocaine in the D2 neurons of the NAc. The analysis

of our data set showed that cocaine and highly palatable food, when administered non-contingently, regulated in an opposite fashion a common set of genes (among the 41 common genes only 5 are co-regulated). Interestingly, the same was not true when we considered the conditioning effect, since the mHP group and the cCoc group showed a set of commonly co-regulated genes. In this comparison, we found 336 common genes and 318 regulated in the same fashion. We also identified a number of genes that were regulated in the same direction (81 over 93) in mST and cCoc groups, as compared to their respective controls. When keeping the most stringent p-value (adj-p value < 0.05) we could only compare the mHP-cCOC in the D2 SPNs of the NAc. By this comparison we obtain only 2 common genes in mHP and cCOC: Rangap1 (RAN GTPase activating protein 1) and Tuba1b (tubulin, alpha 1B). Both genes are down-regulated.

To gain insight into the biological significance of this correlated regulation of gene expression we performed a gene ontology analysis on the genes in common between the different treatments. We found an enrichment in genes connected to “microtubules” (Adj p-value 0.0044) and “axones” (Adj p-value 0.00054) among those commonly regulated in cCoc and mHP indicating their possible contribution to the spine changes induced by both treatments. Our behavioural results showed that only the mHP mice continued to work for pellets when the caloric restriction was over. Our results indicate that cocaine and conditioning for HP food share some commonly regulated genes in the D2 SPNs in the NAc.

The comparison of the other regions-treatment-types of neurons showed a number of genes in common between the different treatments. However, it did not show any precise scheme of co-regulation or anti-regulation of the common genes, except for the PFC in which we found the tendency of anti-regulation of the gene expression over the comparisons cocaine-yoked and co-regulation in the comparison cocaine-learning for standard food.

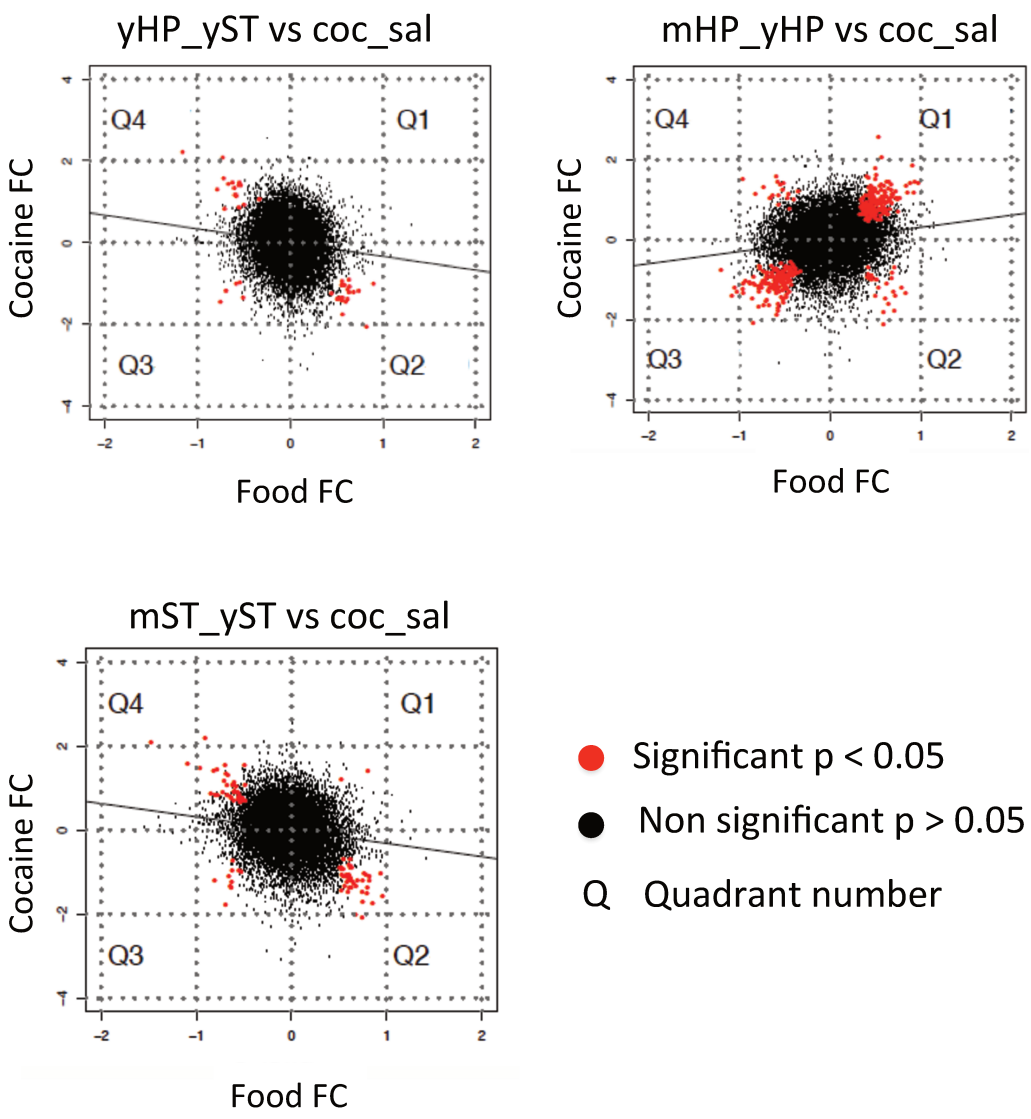

Figure 35: **Comparison of the effects of operant conditioning, food type and chronic cocaine treatment on the transcriptional profiles of D2-NAc-SPNs**.

Different groups of BAC-TRAP mice were subjected to operant training for standard (ST) or highly palatable (HP) food or to chronic cocaine treatment. Controls were yoked mice for each type of food and mice injected with vehicle for the cocaine group. Fold changes (FC) of the genes regulated in the D2 SPNs of the NAc by the different treatments is indicated.

Green= similar regulation as compared to cCOC.

Red= opposite regulation as compared to cCOC

Nucleus accumbens		
Genes increased in the NAc D1 neurons		
mHP-yHP	yHP-yST	mST-yST
Adam17, Arhgap24, Bcap31, Btaf1, C2cd2, Cep162, Clip2, Cmbl, Crtac1,Cryz, Cstf2t,Cux2, Cyp2j9, Ddx5, Ednrb,Ehmt1, Fam198a, Galnt18, Gfra1, Gja1, Gpr165, Gpr26, Gprasp1, Lats2, Mthfd1, Nfkbie, Ngb, Phip, Phlpp1, Pkib, Ppap2b, Prkcq, Rdx, Scnm1, Slc17a6, Slc6a11, Snapc1, Stac, Szt2, Timp3, Wdr11	5330434G04Rik, 6030419C18Rik, Acot3, Adam12, Bmi1, Btbd3, Cdh2, Cntn3, Dnlz, Ext2, Filip1l, Gal3st3,Grem2, Ids, Insc, Kcnd3, Klf3, Lmcd1, Lmln, Lrp3, Megf8, Mlec, Nkain1, Nptn, Pcdhb13, Pcdhgb1, Peak1, Prkaca, Reep1, Rnf10, Samd4b, Setbp1, Skap2, Slc11a2, Slc7a1, Sptlc1, Tmeff2, Tmem47, Tmem62, Tmsb10, Tor1aip1, Zfhx2, Zfp385b, Znrf3	2810025M15Rik, 4932438A13Rik, 6030419C18Rik, Adcy1, Brk1, Ccdc130, Ccdc176, Cdh2, Clstn3, Cnpy3, Csmd3, Dll1, Ebf3, Ext2, Fam195b, Fdps, Flrt3, Fmnl1, Gabrb3, Gpm6a, Gpm6b, Hcn1, Ide, Kcnd3, Klf3, Mansc1, Mical2, Mlf2, Nfkbie, Nptn, Nrsn2, Pclo, Pisd, Pkig, Plxna4, Plxnd1, Ptpra, Reep5, Rpsa, Rtn3, Sh3bgrl3, Sptlc1, Ssr4, Tacr3, Tbc1d25, Tmem131, Tmem47, Tmsb10, Tspan7, Txndc12, Wdr83
Genes decreased in the NAc D1 neurons		
mHP-yHP	yHP-yST	mST-yST
3110035E14Rik,4930451G09Rik 5330434G04Rik,Aff3, Atp6v1g2 Bmi1,Cck, Cobl, Dok5, Dusp14, Etl4, Fam124a, Fezf2, Fmnl1 Gal3st3, Grem2, Grik3, Lrp3, Lypd6b, Mfsd9, Nkain1 Nlrp6, Nrep,Nrgn,Preb ,Ptpn3 Rab26, Rhou, Runx2, Samd4b Samd9l, Scmh1, Serinc5, Setbp1	1700003M02Rik, 2410015M20Rik, Arpc3 Bcap31, Btaf1, C2cd2, Cdkn2d, Clip2, Cmbl, Ehmt1, Fam101b Fam198a, Fus, Galnt18 Gpr165, Gprasp1, Lamtor4, Mthfd1, Nbl1, Ngb, Pfkl, Phip Phlpp1, Pkib, Plcg1, Ppp1ca Rab11fip4, Sepw1, Snca Snf8, Snrnp70, Snx31,	1700003M02Rik 4930539E08Rik, Adam17 Aldh5a1, Cep97, Clip2 Cryz, Exoc8, Fam198a Fbxo10, Fgd6, Foxn3, Glra3 Igsf10, Mir6236 Msi2 Nek10, Ppp1ca, Ppp1r3c Prkar2b, Rab11fip4, Sephs1 Tbc1d31, Timm17b, Ube2g2 Zc3hav1l, Zfp191

Skap2, Taf10, Tmco6, Tmem62 Tmsb10, Tnrc6c, Tor1aip1 Zfhx2, Zfp385b	Swi5 Szt2, Timm17b, Tmem59. Ube2g2, Wdr11, Zcchc12 Zfp191, Znhit1	
Genes increased in the Nac D2 neurons		
mHP-yHP	yHP-yST	mST-yST
1500011K16Rik, 4930430F08Rik, 8030462N17Rik, A230072C01Rik, A830018L16Rik, Acad11, Acbd5, Acyp2, Adk, Aff2, AI987944, Ano3, Arid5a, Arl6, Atf2, Atp11c, Atxn3, AU041133, AW549877, Azin1, B3gat2, Bbs5, BC029722, Bet1, Bmi1, Bmpr1a, Bola3, Bzw1, C030023E24Rik, Capza2, Cldnd1, Cnep1r1, Cnot6, Col12a1, Copa, Dazl, Dctn6, Dgkb, Dmtf1, Dnajc19, Dynll1, Eml5, Epyc, Fam188a, Fancg, Fgd6, Fgf14, Fign, Fktn, Fpgt, Fundc1, Fzd3, Gabra3, Gabra4, Gabrb3, Galnt13, Gm10754, Gm12657, Gm5141, Gmfb, Gpm6a, Gpr52, Gprasp2, Grm5, Gtf2a2, Gtf2h1, Gtpbp10, Gucy1a2, Hace1, Hdgfrp3, Hs2st1, Impad1, Ivns1abp, Izumo4, Kansl1l, Kcnab1, Kcnc2, Kdsr, Kitl, Klhdc1, Klhl13, Lamtor3, Lin7c, Lmo3, Lpl, Lrrc58, Lyrm7, Magef1, Mal2, Mbnl1, Mbnl2, Mettl9, Mme, Mtpn, Mzt1, Naa20, Napepld, Ndufc1, Neto1, Nkrf, Nnat, Otud4, Pex7, Phex, Pias2, Pkia, Plcxd2, Pnpla8, Ppp3r1, Pptc7, Prkar2b, Prrx1, Qser1, Qsox2, Rab10, Rabl2, Rassf4,	Ank1, Calb2, Cep57l1, Csmd2, Frmpd1, Lrrc75b, Lsg1, Ntng1, Pcbd1, Pcx, Psd2, Rassf4, Scml4, Triobp, Tshz2, Tyw3, Vwa5b2, Zc3h3, Zim1	Ank1, Apod, Blcap, C130046K22Rik, Csmd2, Disp2, Dscam, Dync1h1, Fam188b, Fkbp4, Fmnl1, Fndc1, Frem3, Fzd1, Gabrd, Gak, Gse1, Iglon5, Kif21b, Klhdc8a, Klhl21, Lars2, Lrp1, Lrrc75b, Mapk8ip3, Pcbd1, Prkcd, Psd2, Pygb, Rapgef1, Rassf4, Rtl1, Sfmbt2, Shank3, Sox10, Sparc, Tln1, Tmem214, Triobp, Tshz2, Vwa5b2, Zc3h3, Zfat, Zfp423, Zfp521, Zim1

Rc3h2, Rfx4, Rgs7bp, Rrm2b, Sema3a, Slc35a5, Slc35d1, Smc5, Smim15, Sncb, Snhg1, Snhg20, Snhg6, Sox2, Sparc, Spock3, Stk32b, Stx7, Styx, Svip, Synpr, Taf9b, Tceanc, Tceb1, Tcf4, Tfb2m, Timm9, Tmed7, Tmem126a, Tmem161b, Tmem184c, Tmem258, Tmem68, Tmx3, Tox2, Trhr, Ube2d1, Ube2g1, Vma21, Zbtb18, Zbtb6, Zc3h11a, Zc4h2, Zfp157, Zfp26, Zfp280d, Zfp386, Zfp40, Zfp446, Zfp518a, Zfp709, Zfp882, Zfp97, Zkscan8		

Genes decreased in the NAc D2 neurons		
mHP-yHP	yHP-yST	mST-yST
1500009C09Rik, 2900079G21Rik, 8430419L09Rik, A430005L14Rik, Adgra1, Akr1b10, Aldh2, Ankfn1, Ankrd13d, Apc2, Arhgap33, Arhgef15, Atp1a3, Atp5a1, Avpi1, Bcl9l, Bloc1s3, Bsn, Caskin1, Ccdc85b, Ccdc88c, Cdk18, Cep170b, Cic, Cit, Clstn1, Cntn2, Cpne7, Cyhr1, Dctn1, Ddx56, Dennd4b, Dgcr2, Dhcr24, Dido1, Dmrtc1a, Dnajb2, Dnlz, Dos, Dpysl5, E130307A14Rik, Eef2, Elp3, Emd, Epn2, Fasn, Fbxw8, Fkbp4, Flii, Fmnl1, Ftsj2, Gabbr2, Gabrd, Gdi1, Gga2, Gm29766, Gm6682, Got1, Hapln4, Hdac11, Hmbs, Ints1, Irf2bp1, Klhl21, Ldoc1l, Letm1, Lrrc59, Lrrc75b, Lsg1, Madd, Magee1, Mapk8ip3, Mast3, Mboat7, Mdh2, Med15, Micall1, Mir6240, Mkrn1, Mlec, Mpp2, Mrps23, Mrps6, Myo18a, Nacc1, Ncor2, Ndrg2, Ndufa9, Neu1, Nfya, Nkd1, Nsmce1, Nwd2, Ogdh, Paf1, Pcdhga7, Pcx, Pdf, Pdzd4, Pelp1, Pgk1, Pgs1, Pink1, Pkm, Plekhm1, Pnmal2, Pnpla6, Poc1a, Ppard, Prkar1b, Prpf19, Prr14, Ptpn1, R74862, Rangap1, Rnf41, Rnft2, Rpp25, Rps10, Rptor, Rusc1, Rusc2, Rxra, Safb2, Sall2, Setd1b, Sh2d3c, Slc39a7, Slmo2, Smarca4, Spag7, Spock2, Ssrp1, Stk11, Svop, Syngr1, Taf10, Tbc1d16, Tmem191c, Trim46, Trp53rka, Tuba1a, Tuba1b,	3110035E14Rik, 5530601H04Rik, A230072C01Rik, Actr6, Alox12b, Art3, B2m, Bok, Cercam, Drd2, Faap24, Gm7120, Gng11, Gpc4, Ifih1, Neurod2, Nr4a2, Palm3, Pigc, Ptpn3, Slc17a7, Tmco5	3110035E14Rik, 4930447M23Rik, 5530601H04Rik, 6820408C15Rik, Actr6, Aph1c, B2m, Bok, Cabyr, Cetn3, Eny2, Ets1, Faap24, Fam103a1, Fundc1, Gm7120, Gng10, Gng11, Gpc4, Gtf2h1, H3f3a, Hat1, Id3, Ifih1, Igbp1, Lmo4, Lsm8, Mfn2, Micu3, Mpc1, Mrps33, Mzt1, Neurod2, Nfib, Npy, Nr4a2, Ptpru, Rbm41, Rheb, Rnf219, Sap30, Slc17a7, Snrnp27, Stmn1, Tmco5, Txndc17, Uqcrb

Tuba1c, Tuba4a, Tubb3, Tubb4b, Tubg2, Uap1l1, Ube3b, Urgcp, Usp35, Vat1l, Vprbp, Vwa5b2, Wdr46, Wfs1, Zc3h3, Zfp423, Zfp428, Zfp622, Zfp740, Zmiz2, Zswim3		
Dorsal striatum		
Genes increased in the DS D1 neurons		
mHP-yHP	yHP-yST	mST-yST
Aldh1a1, Cadm3, Cd200, Cgn, Dio2, Dner, Endod1, Entpd1, Faah, Grem2, Itga5, Klhdc8a, Lhx2, Lsamp, Mrgpre, Nacc2, Nell1, Nrp2, Pea15a, Pkib, Plcb4, Plce1, Ptprv, Slc16a1, Slc41a3, Slitrk6, Sulf1, Ubr2, Unc5c, Vsnl1, Wfs1	Adamts17, Aldh1a1, Arhgap24, Atp10a, BC051142, Caprin2, Cd200, Coprs, Dio2, Dner, Faah, Kndc1, Lef1, Mt2, Oprl1, Pkib, Rgs6, Slc17a6	4930429F24Rik, A230070E04Rik, Ank2, Bdnf, Calcoco1, Casc4, Cat, Cd274, Cep95, Chst2, Ckap4, Dhdh, Fstl1, Gabrg3, Gm14164, Iars, Igsf11, Inhba, Klf7, L1cam, Mt2, Mxra8, Napepld, Nop56, Npy2r, Ntng1, Omg, Oprl1, Prrc2c,

		Ptrf, Pura, Rasa2, Rorb, Scaf4, Slc30a2, Slk, Sowaha, Sqle, Tanc1, Tcf7l2, Tmem229a, Vsnl1, Zfp839, Znrf2
Genes decreased in the DS D1 neurons		
mHP-yHP	yHP-yST	mST-yST
5830454E08Rik, Ccdc12, Cops5, Erh, Hinfp, Kif23, Lsm10, Nyx, Pkig, Polr2c, Preb, Prkar2a, Rarb, Rhobtb2, Rxrg, Slc25a16, St5, Ung, Usf2, Zscan20	Alox12b, Arhgap29, Lars2, Nyx, Postn, Rps21	2310039H08Rik, Ap1s1, Copz1, Cox6b1, D8Ertd738e, Eef1e1, Eif3k, Elof1, Fis1, Gmpr, Grcc10, Klhdc9, Lamtor2, Lars2, Mrpl37, Mrps34, Ndufb7, Opa3, Oprd1, Pin1, Prss36, Rab1b, Rabep2, Romo1, Rplp1, Rplp2, Rps21, Rps5, Timm13, Tomm6, Trappc4, Uqcr11, Uqcrq, Vti1b
Genes increased in the DS D2 neurons		
mHP-yHP	yHP-yST	mST-yST
0610007P14Rik, Aamp, Atxn7, Bckdha, Chrna7, Ctsf, D230025D16Rik, Ddr1, Dok4, Ephb2, Fam102a, Fam60a, Fam78a, Farsa, Gramd1a, Lipe, Mcrs1, Mdga1, Mrps11, Prmt1, Rnf144a, S100a10, Slc35e4, Slc8a3, Spry4, Tcaf1, Ttc28, Zfp532, Zfp677, Zfp710	Abi3bp, Adsl, Ankrd49, Apool, Asah2, Asb13, Asxl3, Atg4c, Ccdc34, Cd24a, Cd59a, Cep112, Cfap97, Ciao1, Coch, Coq5, Ctage5, Ctxn2, Cys1, Ddx50, Degs1, Dhfr, Dleu2, Dnajb11, Doc2b, Ebag9, Efr3a, Fabp5, Fam193a, Fbxo47, Gad2, Gfra2, Gm20063, Gng5, Golim4, Hectd2, Hnrnpm, Ift74, Klf5, Klhl1, Lamp5, Lpcat2, Lrp8, Lrrcc1, Maf, Mark3, Mettl15, Mrto4, Nbr1, Ndn, Pan3, Pfkfb3, Plp1, Ptcd2, Slc4a10, Sox2ot, Srfbp1, Stc1, Toporsos, Txndc17, Ube2f, Wdr1, Yipf4, Zfp426, Zfp86	Coch, Irf2

Genes decreased in the DS D2 neurons		
mHP-yHP	yHP-yST	mST-yST
Abi3bp, Adsl, Ankrd49, Apbb1ip, Asxl3, Ccdc167, Ccdc34, Cd24a, Cd274, Cd59a, Ciart, Ctxn2, Degs1, Dhfr, Dkk3, Efr3a, Fabp5, Fhl4, Gab3, Gad2, Gfra2, Gm20063, Gng5, Ift74, Lpcat2, Lrp8, Mark3, Mettl15, Mrto4, Ndn, Oxld1, Pan3, Pex2, Pfkfb3, Plp1, Ptcd2, Shtn1, Toporsos, Txndc17, Ube2f, Wsb1, Yipf4, Zfp867	0610007P14Rik, Aamp, Aifm3, Atp2b4, Atxn7, Bckdha, Chrna7, Ctsf, D230025D16Rik, Ddr1, Dok4, Ercc4, Fam102a, Fam60a, Fam78a, Farsa, Fsd1, Gmppa, Gramd1a, Hivep1, Lipe, Mafk, Mcrs1, Mdga1, Mrps11, Pagr1a, Pdcd11, Prmt1, Rnf112, Rnf144a, S100a1, S100a10, Slc35e4, Slc45a1, Slc8a3, Spry4, Tcaf1, Tube1, Usp29, Wdr74, Xpo4, Zfp532, Zfp646, Zfp710	Gnb4, Hnrnpdl, Neurod6
Prefrontal cortex		
Genes increased in the PFC D1 neurons		
mHP-yHP	yHP-yST	mST-yST
1700003M07Rik, A730056A06Rik, Acot1, Adcy5, Agps, Arhgdib, Ccdc166, Ccnc, Cdh13, Cfdp1, Cmpk1, Dgkb, Dph6, Filip1l, Gabarapl2, Gfra1, Gfra2, Gnal, H2afy, Ide, Idi1, Irf2bp1, Klf9, Lamtor5, Lppr5, Lrrc3b, Lrrtm4, Marcks, Mettl16, Naa20, Nr4a2, Omg, Pbx3, Pdcd5, Pde1c, Prpf19, Scg2, Sema5a, Sema5b, Serpina3n, Shisa6, Slc4a10, Snrnp27, Snrpd1, Snx31, Srgap1, Stk24, Theg, Ttc7b, Vbp1, Vdac1, Yipf1	Abca1, Adam21, Arl6ip5, Bhlhe40, Clstn3, Dlgap2, Dopey2, Efna3, Elovl2, Epha3, Fam171a1, Fkbp1b, Gramd1b, Hcfc1, Kcng3, Kcnh1, Marf1, Neurl1b, Nmi, Ntrk3, Oasl2, Pde3b, Pomt2, Ppt2, Prdm16, Pxn, Rasl10b, Scrt1, Sh3bp4, Shank1, Sipa1l3, Syt17, Tnk2, Ust	Acly, Actn2, Adam1a, Akap9, Ank2, Arhgap20, Arl6ip5, Bcl9, Bsn, Camk2a, Camsap3, Cd47, Cgref1, Cnksr2, Cul9, Dopey2, Erdr1, Fam193a, Fam65a, Gm15800, Gpr155, Gpr25, Hcfc1, Kcnh1, Kif5a, Krcc1, Krt1, Ldlrad3, Lppr5, Lrrc7, Lrtm2, Map3k12, Mapre3, Mest, Micall1, Msc, Ncam1, Nedd4, Neo1, Ntrk3, Oasl2, Pde1c, Phc1, Phf24, Pik3r4, Pkp1, Plk5, Prdm8, Raly, Rasgrf1, Rasl10b, Setd5, Shank1, Sipa1l3, Snrpd3, Sowaha, Speg, Srpk1, Strip2, Syn3, Syt5, Ttc7b, Zfp39

Genes decreased in the PFC D1 neurons		
mHP-yHP	yHP-yST	mST-yST
A330040F15Rik, Abca1, Abhd2, Akap8l, Bhlhe40, Clstn3, Cmc2, Deaf1, Dlk2, Eif2b2, Eml2, Hsf4, Kcnq3, Marf1, Oasl2, Pla2g16, Pnpla3, Pomt2, Ppm1m, Ptrf, Pxn, Rab11fip4, Rab1b, Rell2, Rgmb, Rplp1, Rpph1, Sf3a2, Stom, Thap7, Tmem185b, Tnnc1, Zc3h3	9530082P21Rik, Aen, Arhgdib, Atg3, Bloc1s2, Cdk5rap1, Cfdp1, Clybl, Cmpk1, Dars2, Dtl, Eif4e2, Elavl2, Erich1, Erich6, Filip1l, Gabarapl2, Gfra1, Ide, Lsm5, Magee1, Mcts2, Mdga1, Mettl16, Ndufa9, Pdcd5, Pex13, Ppp1r2, Scgn, Sema5b, Srp9, Tbp, Terf2, Tmem242, Ube2z, Usp27x, Vsnl1, Zfp664	Arfgap2, Arl2bp, Cdhr1, Cdk5rap3, Cox4i1, Dars2, Diras1, Efhd2, Eif4e2, Eno3, Gm14295, Golga7b, Gtf2h4, Hace1, Hsf1, Mrps18a, Mydgf, Myl12b, Ndufb8, Nr1h2, Nsg1, Parl, Pfdn5, Pfkl, Polr2h, Ppm1m, Rps13, Sae1, Smim7, Swi5, Tmem234, Tmem242, Umad1, Zfp664

Table1: Genes commonly regulated between cocaine treatment and operant training for food. In green the genes similarly regulated, in red the genes oppositely regulated.

- Discussion -

In the first part of the introduction of this thesis I reviewed the anatomy of the basal ganglia (BG), a large collection of subcortical nuclei interconnected with the cerebral cortex, thalamus, and brainstem. The striatum is the major entry structure of BG. The striatum is characterized by a complex intrinsic organization related to the segregation of its neurons in two different populations expressing either of the two types of DA receptors, D1 and D2. The D1 and D2 SPNs closely correspond to the direct and indirect projection pathways in the DS, although this correlation is much less straightforward in the NAc, especially in its shell part. In addition other subdivisions of the striatum are well described and correspond to important anatomical and functional differences, including the patch/matrix organization of the striatum and the multiple subdivisions of the NAc shell. Several studies have already addressed some of the differences in transcriptional profiles that underlie this anatomical complexity. For example it has been shown that D1 and D2 neurons have strikingly different transcriptional profiles (Lobo et al., 2007; Guez-Barber et al., 2011; Guez-Barber et al., 2012; Heiman et al., 2008). In addition, some of the differences between striosomes and matrix have been identified, including 60 genes specifically enriched in one or the other compartment (reviewed in Crittenden and Graybel 2011).

In the first part of this thesis we used the BAC-TRAP system to isolate currently translated mRNA from identified D1 and D2 cell populations (Heiman et al. 2008) in the DA and NAc and D1 cells in the PFC.

A first point concerned the comparison between the D1 SPNs and the D1 PFC neurons which share the expression of D1 receptors. Our analysis showed that 5481 transcripts are differentially enriched in D1 SPNs and D1 pyramidal neurons. This result is not surprising if we consider that D1 SPNs and D1 pyramidal neurons are respectively GABAergic and glutamatergic neurons.

We then confirmed that D1 and D2 SPNs are characterized by different transcriptional profiles. We found more than 700 hundreds transcripts being differentially expressed between D1 and D2 in the DS and between D1 and D2 in NAc (adj p-value < 0.05, reads > 30). Most of these genes are expressed in the two populations of neurons but are more expressed in one population or the other, and very few are significantly expressed only in D1 or in D2 neurons.

For the first time we specifically compared the genes expressed in D1 and D2 neurons in the DS and in the NAc, and reciprocally the differences between the NAc

and the DS in D1 and D2 neurons. Interestingly we observed that the differences between the DS and the NAc, within D1 or D2 neurons, are as big as the difference that we could find between D1 and D2. By crossing our data sets we also identified a group of genes common to D1 and D2 and enriched in the NAc or the DS. In absence of anatomical borders, the only criterion used for distinguishing NAc and DS is the regional distribution of the inputs coming from the afferent regions. Here we provided a novel criterion to distinguish these two regions and a novel level of description of the two types of neurons.

In a very recent paper Gokce and coll. (Gokce O., et al; 2016) used FACS-based single-cell RNA sequencing to study the whole striatal cell diversity. This paper confirmed most of the data already reported in literature, and showed that the D1 and the D2 neurons could be divided in 2 additional subpopulations that express a gradient of transcriptional states that could explain the patch matrix organization of the striatum. Interestingly, the genes that the authors have chosen as defining the opposite gradient of expression in the two SPNs populations correspond to some of the genes that we identified as highly enriched in the NAc (Wfs1-Crym) or the DS (Cnr1). Further analysis will be needed to determine whether the gradient observed in this paper correlates with the patch matrix organization and the dorsoventral gradient.

In relation with the anatomical organization of the inputs converging to the striatum and on the basis of multiple functional studies, the NAc has been associated to the motivation-related processes (Lobo and Nestler 2011), while the DS is implicated in motor behaviour, associative learning, and habits formation (Albin et al., 1989; Chang et al., 2002; Balleine et al., 2007 Graybiel et al., 2008). As a prelude to testing the biological relevance of the genes that we found to be enriched in D1 and D2 neurons in the DS and in the NAc, we performed an upstream analysis. The analysis showed that different chemicals or transcription factors are predicted to regulate specific sets of genes in the D1 or the D2 neurons depending on their location in the NAc or the DS. Among these different upstream regulators, we found that prostaglandin E2 (PGE2) was the only compound predicted to be a possible positive regulator of the genes expressed in both D1 and D2 neurons in the DS. Therefore, we chose it as a possible target to study the effects of its manipulation on striatal function. Prostaglandins (PGs) are a family of lipid mediators involved in a

plethora of processes including vascular homeostasis, inflammation, and reproduction (Narumiya et al., 1999). We showed that chronic infusion of a non-selective agonist of PGE2 receptors elicits an improvement of the mice performance in the rotarod and in reversal learning, two behaviours specifically mediated by dorsal striatum. This result agrees with the previous studies showing that PGE2 amplifies both the D1 and the D2 signalling pathways (Kitaoka S. et al., 2007) and supports the finding of PGE2 as a key upstream regulator from our transcriptional analysis. It will be important to determine whether some of the target genes enriched in DS that led to the identification of PGE2 were modified by the agonist treatment. These analyses are in progress.

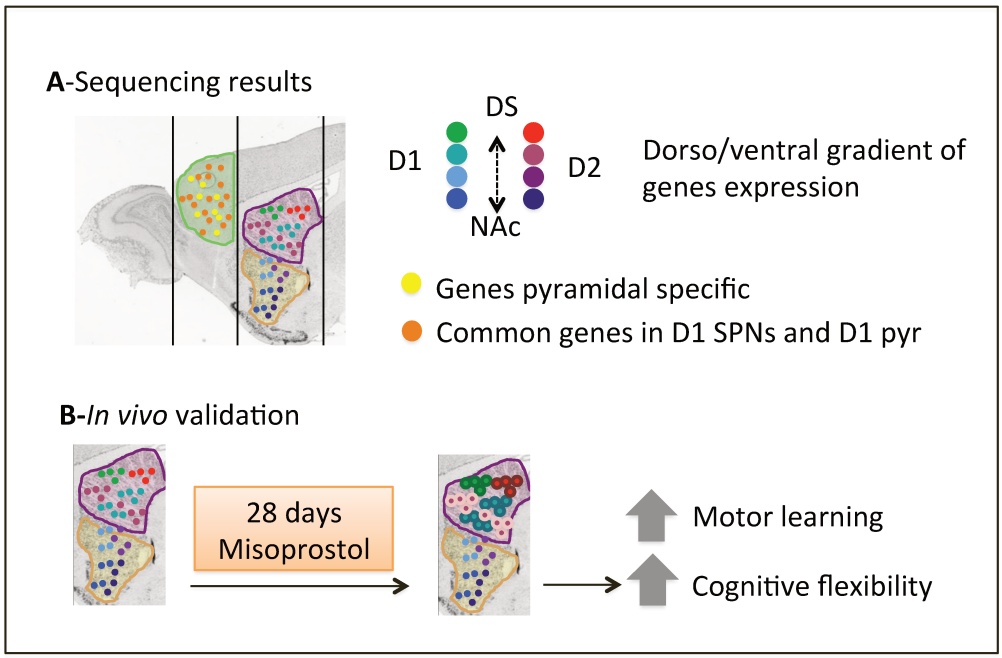

Figure 36: **Graphical conclusion aim -1**

In the second part of my thesis we provide a cell-type specific study of the transcriptional effects of operant conditioning for food. Prior studies of transcriptional mechanisms of operant learning for natural reward focused primarily on identifying individual candidate genes or microarray profiling of a single region with the principal aim of measuring consequences of frustrated expected reward on the regulation of gene expression (Martín-García E. 2015). Here we used a combination of behavioural and genome-wide approaches to study the effects of the operant learning for standard and highly palatable food in D1 and D2 SPNs of the

NAc and DS and in D1 pyramidal neurons of the PFC. Furthermore the presence of yoked controls allowed the analysis of the effects of the same food availability without operant conditioning but all other conditions (i.e. food deprivation, exposure to operant cages, manipulations…) being identical. The rewarding effects of a stimulus can be measured by the willingness of the subject to work in order to gain the access to it. In this framework, it has been known for more than a century that the responses to stimuli that produce positive effects are likely to be repeated again (E.L. Thorndike 1898). The idea that behavioural responses can be a direct measure of the rewarding properties of a certain object is the basis of the theory of reinforcement initially proposed by Skinner in 1938. A form of operant training was also used in the studies of Olds and Milner in 1954 to investigate the responses to intracranial self-stimulation, leading to the discovery of brain reward systems. Operant training is still one of the paradigms mainly used in measuring the rewarding properties of an object. In agreement with previous studies (Balleine and Killcross 1994, and Guegan T et AL., 2012), we observed that food palatability strongly increases the positive pokes in the operant behaviour. However, while most of the previous studies used a longer training paradigm, we obtained a stable operant response after only 2 weeks of training in order to get access to relatively early molecular brain alterations. Indeed the mice trained with highly palatable food worked sensibly more than those trained for standard food (figure 16, results section 2).

Different studies have already shown that striatum and PFC play a central in mediating the effects of reward. The DA released by the DA neurons of the VTA modulates the D1 and D2 SPNs activity in the striatum, and the D1 pyramidal neurons in the PFC. A DA increase has been reported in the NAc after both drugs (Di Chiara G., 1992) and natural reward (Hernandez L., 1988, Hajnal A., 2001). We reasoned that – as for the drugs of abuse – the increase of DA induced by highly palatable food could regulate the structural plasticity in the areas targeted by the VTA projection. Therefore we measured the spine density induced by our training paradigm in PFC, DS and NAc. From this series of experiment we could study both the effect of the training and of the food on spine formation. Concerning the training, we obtained an increase of spines only in the mice trained with highly palatable food. This is in agreement with the previous results reported in literature (Guegan T et al., 2012). However here we report that the training for highly palatable food increases the spine number in PFC, NAc and DS, while the non-contingent presentation of

highly palatable food has the same effect only in the NAc. The spine increase in the DS agrees with humans imaging studies in which this region has been reported to be activated in response to food (Small DM, 2003). The increase in spines in NAc seems related more to the highly palatable food itself rather than to the learning for the highly palatable food. Hence, we obtain an increase of the spine density also in the control mice that have been show to do not learn during the operant training. This result is in agreement with the increased spine density in the yoked mice reported in the mesocorticolimbic system in response to a psychostimulant (Russo et al., 2010). In particular, the increase of spines in the yoked mice in the NAc is not surprising in given the fact that the NAc is the region traditionally considered associated with the primary reinforcing effect of drugs (Di Chiara et al. 2004; Wise 2004; Ikemoto et al. 2005; Wise 2008). It is important to mention that at the same time our results are in contrast with those of Guegan and collaborators (2012). In their work, no spine induction was observed in yoked mice. This discrepancy might be due to the different length of the operant training (15 days vs 41 days), as well as to the fact that we did not use any progressive ratio at the end of the experiment and that we waited 24 h before sacrificing mice after the last training session. Concerning the PFC the increase of dendritic spines in the master highly palatable food group is in agreement with recent work that demonstrated with completely different approaches a role for D1-type dopamine receptor-expressing neurons in the medial prefrontal cortex (mPFC) in the regulation of feeding (Land BB 2014). Food intake increased the activity of D1 neurons of the mPFC in mice, and optogenetic stimulation of D1 neurons increased feeding. Conversely, inhibition of D1 neurons decreases intake (Land BB 2014). The analysis of the structural plasticity induced by highly palatable food is still in progress, in particular the morphology of the spines. Additional experiments would be useful to test some of the points discussed above. For instance, an interesting experiment would be to distinguish between D1 and D2 by using a transgenic line expressing GFP under the control of the promoter of DA receptors and perform spine quantification with an appropriate technique such as gene gun labelling with DiI. This would allow to define which cells are responsive to highly palatable food conditioning, and test whether the increase in spine density in the DS is due to a neuroadaptation of the D2 neurons as in the case of the drugs of abuse (Porrino, Daunais 2004, Smith, & Nader, 2004). This type of experiment would also allow to better correlate the structural plasticity that we observed with the data that

we obtained from sequencing (see below). Another potentially interesting experiment would be to analyse the dendritic spines of the mice in the 3 regions just after the learning phase. This would allow to see which differences exist between the synaptic structures induced by the 2 different phases of the training, and to check if, as for cocaine self-administration, the NAc is the most involved structure during the first phase of training.

Several studies have already shown that drugs of abuse are able to induce long-lasting modifications in gene expression. Such modifications might underlie some aspects of addictive behaviour and require changes in gene transcription. We investigated whether highly palatable food could also induce long-lasting modifications in gene expression. We found that transcriptional changes induced by highly palatable food conditioning were mainly taking place in the D2 neurons, in the DS and to a lesser extent in the NAc. This result might seem surprising, as D1 neurons appear to be primary targets for rewarding stimuli such as cocaine (e.g. Pascoli&Luscher 2012). However it is in agreement with several other work using completely different approaches and readouts, which showed the importance of the D2 neurons in both obesity and drug addiction **(ref)**. Indeed, a clear common feature between drugs of abuse and obesity is the lower availability of the D2 receptors within the striatum. Human imaging studies have established that less D2 receptor are available in the striatum of obese relative to lean individuals (Stice E, 2008; Wang GJ, 2001, Barnard ND.; 2009) as well as in addicted individual compared to controls (Asensio S, 2010; Volkow ND., 1993). Importantly, in both the obese (Stice E, 2008; Wang GJ, 2001, Barnard ND; 2009) and drug-dependent population, (Noble EP, 2000; Lawford BR, 2000) an over representation of individuals harbouring the TaqIA A1 allele has been observed, which results in ~30–40 % reduction in striatal D2Rs (Stice E., 2010; Jönsson EG., 1999). In rodents, a lot of work has already been done for the elucidation of the role of D2 neurons in the context of drugs of abuse. For instance, it has been showed that impulsivity is associated to the prediction of cocaine intake and to the lower availability of D2/3 DA receptors in the ventral striatum (Dalley et al., 2007). It has been proposed that drug exposure would be able to induce plasticity in D2 neurons, possibly diminishing their activity and facilitating inflexible, compulsive-like drug-taking behaviour, which in rodents can be measured by the presentation of a progressive ratio schedule. Consistently Alvarez and co-workers have shown that the synaptic strengthening in the D2 SPNs in the NAc was

inversely correlated with the emergence of compulsive-like cocaine responding in mice with a history of self-administration (Bock R., 2013). Moreover, DREADD-mediated inhibition of D2 SPNs increases the compulsive like response to cocaine, while their optical stimulation decreases it (Bock R., 2013). These observations suggest a clear link between the D2 neurons and the appearance of the compulsivity. It raises on the other hand the question of whether the D2 neurons have a similar role in the consumption of highly palatable food. Indeed, the knockdown of striatal D2-receptor, using a lentiviral vector, accelerates the emergence of compulsive-like consumption of calorically dense, palatable but not standard food (Johnson PM., 2010). These results suggest that the activation of the D2 neurons during the training for highly palatable food could have similar functional consequences as their activation in response to cocaine. Compulsivity could perhaps arise from the sensitization of the DA fibres that have been already excited by the reward. Sensitization has been linked to a faster formation of habits, which according to the work of Everitt's group, would be associated with a greater activation of the DS (Johnson & Kenny 2010). In this perspective, the identification of the neurons in which synaptic density is altered by highly palatable food would be useful to determine if, as for drugs, the structural plasticity is taking place mainly in the D2 neurons. A deep analysis of the transcriptional profile that we obtained after the training for the highly palatable food is still in progress. The ensemble of results that we report provides a strong base for a deeper analysis of the response of the DA SPNs in to the highly palatable food.

We started an in vivo validation of our results by genetically knocking down one of the genes regulated in the D2 neurons in both NAc and DS. Norbin (encoded by the Ncdn gene) was up-regulated by the learning for HP food in the DS while it was down-regulated in the NAc. In line with the general hypothesis that a certain regulation of the gene is related to the facilitation of a certain behavioural output, we observed two different behavioural effects of the norbin-KO that correlated with the differential regulation of the expression of this gene in NAc and DS. As already explained our training paradigm encompassed two different phases: a learning phase in which animals are under food restriction, and an *ad libitum* phase in the established. According to the view of "dorsalization" of the striatal function in the paradigms in which a reward is associated to a cue, we might speculate that the first phase of operant training would be more associated to the activation of the nucleus

accumbens, while the second phase would be more associated to the activation of the DS. The norbin-ko mice showed an amelioration of the behaviour during the learning phase and an impairment during the *ad libitum* phase, in which mice worked at the same rate for HP food as those trained with standard food. This result was particularly clear when mice were presented with a PR schedule (figure 21B-D). Importantly, it is possible to contextualize these results with the reported norbin functions, and with the different inputs and outputs of the NAc and DS. Norbin or neurochondrin is a 75 kDa protein that interacts with 3 important modulators of the striatal function that could be potentially involved in the behavioural effects we observed in the norbin KO mice: GluR5 (Wang H. et al., 2009), MCHR1 (melanin concentrating hormone) (Francke F., 2006) and CaMKII (Dateki M, et al., 2005).

Norbin has been shown to inhibit MCHR-induced G protein activation and downstream calcium influx. By binding to MCHR1, norbin sterically competes with the binding of G-proteins to the receptor and thereby inhibits G protein-coupled transduction (Francke F., 2006). The NAc is the only region of the striatum innervated by the melanin-concentrating hormone (MCH) producing neurons. As discussed in the introduction of this thesis, MCH neurons have been implicated in the homeostatic regulation of feeding: intracerebroventricular injections of the peptide increase feeding and body weight in rodents, and MCH mRNA levels are increased by food deprivation (Qu D., 1996); mice lacking MCH neurons (Alon, T. et al., 2006) or the MCH gene (Shimada, M. 1998) are hypophagic and lean. On the other hand the overexpression of MCH results in hyperphagia, resistance to insulin and obesity (Ludwig, D.S., 2001). We found that norbin is down-regulated specifically by highly palatable food in the NAc during the first phase of conditioning. We could speculate that this down-regulation is a homeostatic response to HP food, since norbin is a negative regulator of the MCHR. The down-regulation of norbin would lead to an increased MCHR activity facilitating the feeding behaviour. The same idea could explain the effects of the norbin KO during this phase. The combination of the normal overproduction of MCH in fasted mice, with the increased activity of the MCHR due to the loss of the negative regulation exerted by norbin could explain the facilitation of the feeding behaviour that we obtained with the norbin-ko mice.

As mentioned above, mGluR5 is another important partner interacting with norbin. In 2009, Wang and co-workers showed that norbin increases the synaptic surface localization of mGluR5 and positively regulates mGluR5 signalling. Furthermore, in the hippocampus, the genetic deletion of norbin attenuates mGluR5-dependent stable changes in synaptic function measured as long-term depression (LTD) or long-term potentiation (LTP) of synaptic transmission. In the striatum, excitatory synaptic inputs from cortical neurons can undergo mGluR5-dependent LTD (reviewed in Lüscher C, Huber KM, 2010). Such cortico-striatal afferents impinge on both D1 and D2 SPNs. Both D1 and D2 are able to express forms of mGluR5-LTD (Calabresi et al., 1997); however a striking difference between the 2 types of neurons consists in the fact that while the LTD in the D1 is blocked by the activation of the D1 receptor, in the D2 neurons it is induced by the D2 activation (Kreitzer and Malenka, 2007; Shen et al., 2009). In the D2 neurons of the indirect pathway of the DS, LTD is initiated by a high frequency stimulation, which leads to postsynaptic activation (Choi and Lovinger, 1997). The postsynaptic activation triggers the production of an endocannabinoid retrograde messenger – most probably anandamide – that binds to the presynaptic cannabinoid 1 receptor (CB1) and triggers the presynaptic expression of LTD (Genderman et al., 2002). This phenomenon is referred to as mGluRs-LTD. Importantly, it has been demonstrated that this mechanism takes place only when the D2 activation is induced (Kreitzer and Malenka, 2007;); thus, logically in normal conditions mGluR-LTD will be induced in the D2 neurons of the DS only in the case of a concomitant activation of both the glutamatergic afferences from the prefrontal cortex and the DA fibres arising from the midbrain. SPNs have been shown to express a higher-level of mGluR5 compared to mGluR1, however, a genetic model that clearly links this form of LTD to mGluR1 or mGlur5 is not yet available. Given this background, we could speculate that the absence of norbin from the DS would correlate with a decreased expression of mGluR5 at synapses. This down-regulation of mGluR5 would prevent the production of the endocannabinoid messenger, the activation of the CB1R, and lastly the presynaptic plasticity. In support to this hypothesis CBR1-KO mice showed the same phenotype as we observed with the norbin-KO mice when presented to a progressive ratio schedule for obtaining highly palatable food (Guegan T et al, 2012).

It has been published that norbin-ko mice show a lower preference for sucrose (Wang H. et al., 2015). However the long term implication of the loss of sucrose preference has not been explored. Because we already proved that it is possible to induce obesity by using our highly palatable isocaloric pellets, we are currently performing an obesity experiment with the norbin-ko mice, to check if Ncdn is implicated in the obesity development.

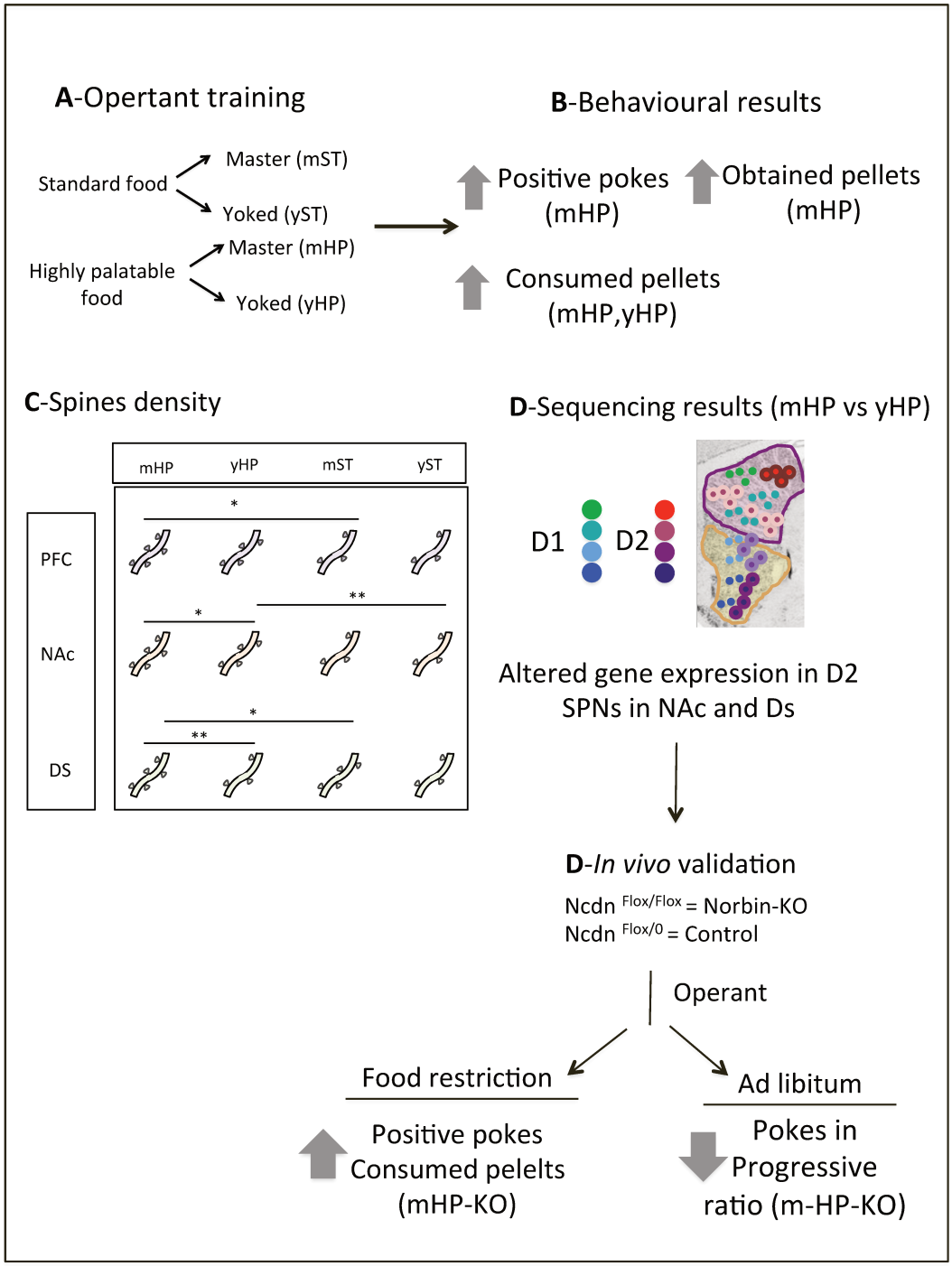

Figure 37 **Graphical conclusion aim-2.**

In the third part of my thesis we used a chronic regimen of cocaine injections to analyze the structural plasticity induced by cocaine administration as well as the influence of cocaine on the transcriptional profiles in identified neuronal populations in the NAc, DS, and PFC.

We found that in our conditions, chronic cocaine administration triggered an increase of dendritic spines in the NAc as compared to vehicle-treated controls. This result confirms previous studies reporting that cocaine and other drugs of abuse produce persistent changes in the structure of dendrites and dendritic spines in D1 and D2 SPNs in the NAc (Lee et al., 2006; Li et al., 2012; Zhang et al., 2012). We also confirmed (Dobi A. et al., 2011) that in the NAc, chronic cocaine administration triggered an increase of the spine head area, suggesting a general increase of the area available for the synaptic contact after cocaine administration.

Correlating with this persistent increase of spines in the NAc our sequencing data showed that for both D1 and D2 SPNs, the NAc is the region in which the largest number of genes was altered by cocaine administration. Interestingly, the GO analysis on the genes regulated by cocaine in the NAc showed a major enrichment in genes related to synaptic and structural plasticity, and to actin cytoskeleton remodelling. For example, chronic cocaine administration induced an up-regulation of the cordon-bleu WH2 repeat gene, Cobl. WH2 Cobl binds to actin to promote actin filament formation. It therefore has a role in neuronal morphogenesis, dendrite formation, and dendritic arborisation (Ahuja R. et al., 2007). This effect is in line with the observation that chronic cocaine administration reduces the activity of Rac1, leading to the intensification of the polymerization rate of filamentous actin in the NAc (Dietz MD et al., 2012).

Interestingly we did not observe any cocaine-mediated induction of spines in the DS and PFC. This observation could be explained by the fact that the PFC and DS are more associated to habit formation (reviewed in Everitt & Robbins, 2005). Since in our protocol we passively stimulate the reward system, not implying any learning or habit formation, we might not be sufficient to engage a major involvement of the DS and a de novo synthesis of spine formation. Accordingly with this result, we were not able to observe any significant change in gene expression neither in D1 or D2 SPNs in the DS. However, it is important to note that we could observe changes in the spine morphology. An increase in the neck length in the DS and in minor extend

in the PFC have been observed in mice injected with cocaine compared to their vehicle-injected controls. Although the mechanism through which spine shape affect its function is not fully understood yet, morphology does play a role, as long and thin necks prevent the diffusion of calcium, whereas shorter and thicker necks allow for better diffusional coupling with the dendrite (Majewska et al., 2000; Holthoff et al., 2002; Sabatini et al., 2002; Korkotian et al., 2004; Noguchi et al., 2005). Furthermore It was shown that reduction of the spine neck length after synaptic potentiation mediates enhanced electric coupling between the spine and the dendrite, thereby increasing the influence of the potentiated spine on the dendritic and somatic membrane potential (Araya et al., 2014; Tønnesen et al., 2014). However, the morphological changes that are associated with synaptic modulation could just be a secondary effect of altered actin dynamics required to more directly modulate synapse functioning or actin-based transport.

The cell population specific RNA sequencing in the NAc, DS and PFC, showed that several transcript are differentially regulated by repeated cocaine administration. Within the striatum, the majority of the changes were taking place in the NAc for both the D1 and the D2 SPNs in which 136 and 72 transcripts were differentially regulated, respectively. Importantly, among these transcripts we identified some genes that have been already described as regulated by cocaine. Although it is often complicated to make a direct comparison of data across drug administration experiments from published studies due to the differences in strain background, cocaine doses and assay sensitivity, we were able to identify various genes that have been already reported to be affected by cocaine administration. Importantly, our experimental approach provides information in which neurons and which sub-region of the striatum those genes are expressed. Examples of those genes are Crtac1, Etv5, Tbr1, Dusp3, Plcg1 Txndc13, Epdr1, Snapc3 (Heiman et al., 2008) (up in NAc D1), Nfib (Feng et al.; 2014) (up in D1 NAc). Unc5b, Gna12 and Ttbk1 (Heiman et al., 2008) (up in NAc D2). GO analysis in the NAc -D1 neurons showed an enrichment of genes implicated in the regulation of synaptic and structural plasticity. Indeed, we found some genes that have been already implicated with those processes. One interesting gene is homer2, up regulated in D1 SNPs of the NAc. The homers isoforms interact with the mGluR1 receptor to induce LTD and have already been implicated in synaptic plasticity induced by cocaine stimulation. Disrupting the interaction between homer and mGluR1 has opposite effects depending on the

location of the manipulation. The homer-mGlur1 connection disruption in the VTA, induces a plasticity response to a single injection of cocaine in the NAc comparable to the synaptic adaptations that are normally obtained by chronic cocaine injections. Interestingly, the opposite is true in the NAc, where mGluR1 is a positive modulator of synaptic plasticity (Knoflach et al., 2001; Mameli et al., 2009). Indeed, the up-regulation of Homer2 in the NAc could contribute to the synaptic plasticity linked to the mGluR1 receptor.

Another interesting example of a regulated gene is Grin3a, which was down-regulated after 7 days in the D1 neurons of the NAc. Grin3A is a gene coding for the semi-Ca2+-impermeable NMDARs subunit GluN3A. As Homer, GluN3A has a central role in the plasticity induced by cocaine. In the VTA a single cocaine injection is able to induce a considerable potentiation of the excitatory synaptic transmission in the DA neurons of the VTA, due to the increase of the AMPAR/NMDAR ratio (Ungless et al., 2001). It has been shown that the increase in the ratio is due to an increase of the AMPAR-dependent currents, related to the insertion of the Ca2+-permeable Glu2A subunit and to the reduction of the NMDAR-dependent currents, related to the insertion of the semi-Ca2+-impermeable NMDARs containing GluN3A (Mameli et al., 2011, Yuan et al., 2013). Unlike in the VTA, multiple non-contingent doses of cocaine administration are required to elicit synaptic plasticity in excitatory synapses in the NAc (Thomas et al., 2001) and to reduce the AMPA/NMDRA ration (Thomas et al., 2001; Beurrier and Malenka, 2002; Thomas et al., 2008). It could be argued that the down-regulation of the expression of Grin3A in the NAc could be related to an increased permeability of NMDA receptors to Ca2+ in the D1 neurons, contributing to the decrease of the AMPAR/NMDAR ratio and to the cocaine-induced synaptic plasticity in the NAc. Our cell-specific RNA sequencing confirmed that the PFC is a region clearly receptive to cocaine stimulation. We identified a number of genes regulated by chronic cocaine in the D1 pyramidal neurons of the PFC.

We (WCGNA) approach to construct a gene coexpression network of the D1 neurons in NAc and PFC in response to cocaine, to identify candidate genes more involved in the instauration of the modification induced by chronic cocaine exposure. The GO on the modules more related to the cocaine treatment showed an enrichment of genes involved in the structural plasticity for the NAc and in the epigenetic regulation of the DNA for the PFC. Different studies suggest that the PFC underlies

the relapse triggered by drugs. Human's neuroimaging studies show that both cocaine and cocaine-paired cues activate PFC in cocaine addicts (Breiter et al., 1997; Childress et al., 1999; Grant et al., 1996). Consistently, reports from animal studies in rats showed that cocaine-seeking is associated with changes in the expression of Fos, and γ protein kinase C, a plasticity-regulated gene, in the PFC (Ciccocioppo, Sanna, & Weiss, 2001; Neisewander et al., 2000; Thomas & Everitt, 2001). Because the drug-relapse is one of the effects of the long-lasting modifications induced by cocaine, we could hypothesize that the enrichment in epigenetic regulators that we found in the PFC, could be the prelude to another wave of modification of gene expression involved in the instauration of more stable mechanisms of relapse. The network analysis on the modules whose clusterization was more related to the cocaine stimulation identified the transcriptional networks more responsive to the cocaine induction as well as key driver genes forming the major nodes of the network. Ultimately, these types of analysis are the prelude to the identification hubs genes that may play an important role in the transcriptional response to cocaine. A logical follow up of this work would be to study the modulation of the most connected candidate hub genes and the study of their targeted deletion on cocaine-induced behaviours.

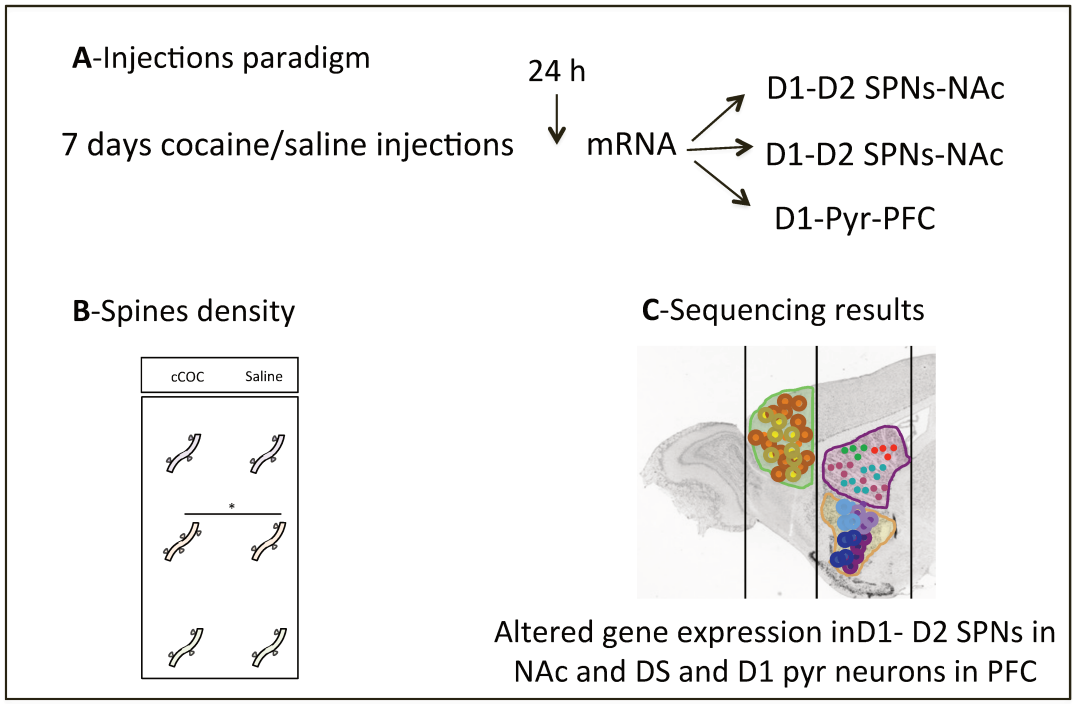

Figure 38 **Graphical conclusion aim-3**

Lastly, we compared the effects of operant conditioning and those of cocaine administration on the structural plasticity and the transcription.

The NAc is the only region in which we found an increase of spine density after both non-contingent presentation of HP food and chronic cocaine administration. The increase in spine number in both cocaine and yHP is in line with the finding that both sweets (Hajnal A., 2001) and cocaine (Wise and Rompre, 1989) induce an activation of the NAc, especially in the shell subregion (Di Chiara and Imperato, 1988). In particular it has been demonstrated that DA release in the NAc increases in response to unexpected food (Norgren, et al. 2006). Moreover, it is important to observe that those results correlate well with our gene expression data in which we observed that both cocaine and learning for highly palatable food induce an alteration of the gene expression within the NAc. Of note, only the learning for the highly palatable food has an effect on the gene expression within the DS.

We identified common sets of regulated genes in all the comparisons, however we mainly focused on the D2 neurons of the NAc, being the only population in which significant changes were occurring in both operant training for highly palatable food and cocaine treatment. Depending on the type of conditioning, some genes were regulated in the same direction compared to cocaine exposure (mHP vs cCOC), and some in the opposite direction (yHP vs cCOC and mST vs cCOC). All the comparisons were obtained by setting the threshold to a nominal p-value of 0.05. By setting the threshold to an adj p-value of 0.05, we could find only 2 genes in common between cocaine and training for highly palatable food in the NAc D2 SPNs: Rangap1 (RAN GTPase activating protein 1) and Tuba1b (tubulin, alpha 1B). Both genes are commonly down regulated by cocaine and training for highly palatable food. The common regulation of the Tuba1b codes for the tubulin alpha 1B; tubulin is the major component of the microtubules. Rangap1 is a protein that associates with the nuclear pore complex and participates in the regulation of nuclear transport by interacting with the Ras-related nuclear protein 1 (RAN) and by regulating the guanosine triphosphate (GTP)-binding and exchange. When binding to RAN, Rangap1 induces its conversion to the putatively inactive GDP-bound state. Although this protein has never been directly investigated in response to cocaine or food reward, it has been found associated to other types of addiction such as alcohol (Marballi et al. 2016; Sikela et al. 2006). This comparison thus provides interesting

novel information on the similarities and differences between various types of recruitment of the reward systems. They may provide clues for future investigation of pathological consequences of their dysregulation in the context of drug addiction and eating disorders.

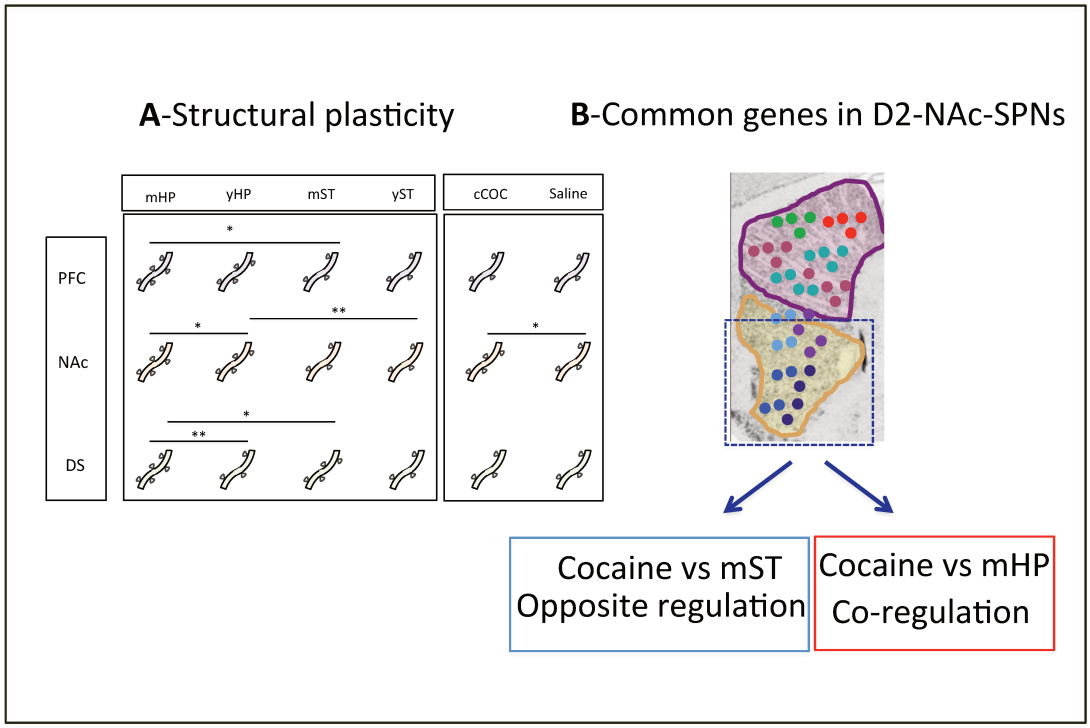

Figure 39 **Graphical conclusion of the comparison of the transcriptional effects of the operant training for food and the chronic cocaine injections.**

- Bibliography -

-

Acevedo, Bianca P, Arthur Aron, Helen E Fisher, and Lucy L Brown. 2012. "Neural Correlates of Long-Term Intense Romantic Love." *Social cognitive and affective neuroscience* 7(2): 145–59. http://www.ncbi.nlm.nih.gov/pubmed/21208991.

Adamantidis, Antoine R et al. 2007. "Neural Substrates of Awakening Probed with Optogenetic Control of Hypocretin Neurons." *Nature* 450(7168): 420–24. http://www.ncbi.nlm.nih.gov/pubmed/17943086.

Adams, David H, Glen R Hanson, and Kristen A Keefe. 2003. "Distinct Effects of Methamphetamine and Cocaine on Preprodynorphin Messenger RNA in Rat Striatal Patch and Matrix." *Journal of neurochemistry* 84(1): 87–93. http://www.ncbi.nlm.nih.gov/pubmed/12485404.

Ade, Kristen K, Megan J Janssen, Pavel I Ortinski, and Stefano Vicini. 2008. "Differential Tonic GABA Conductances in Striatal Medium Spiny Neurons." *The Journal of neuroscience : the official journal of the Society for Neuroscience* 28(5): 1185–97. http://www.ncbi.nlm.nih.gov/pubmed/18234896.

Ahrén, B. 2000. "Autonomic Regulation of Islet Hormone Secretion--Implications for Health and Disease." *Diabetologia* 43(4): 393–410. http://www.ncbi.nlm.nih.gov/pubmed/10819232.

Ahuja, Rashmi et al. 2007. "Cordon-Bleu Is an Actin Nucleation Factor and Controls Neuronal Morphology." *Cell* 131(2): 337–50. http://www.ncbi.nlm.nih.gov/pubmed/17956734.

Albanese, Alberto, and Diego Minciacchi. 1983. "Organization of the Ascending Projections from the Ventral Tegmental Area: A Multiple Fluorescent Retrograde Tracer Study in the Rat." *The Journal of Comparative Neurology* 216(4): 406–20. http://doi.wiley.com/10.1002/cne.902160406.

Albert, P R, K A Neve, J R Bunzow, and O Civelli. 1990. "Coupling of a Cloned Rat Dopamine-D2 Receptor to Inhibition of Adenylyl Cyclase and Prolactin Secretion." *The Journal of biological chemistry* 265(4): 2098–2104. http://www.ncbi.nlm.nih.gov/pubmed/1688845.

Albertson, Dawn N, Carl J Schmidt, Gregory Kapatos, and Michael J Bannon. 2006. "Distinctive Profiles of Gene Expression in the Human Nucleus Accumbens Associated with Cocaine and Heroin Abuse." *Neuropsychopharmacology*. http://www.nature.com/doifinder/10.1038/sj.npp.1301089.

Albin, R L, A B Young, and J B Penney. 1989. "The Functional Anatomy of Basal Ganglia Disorders." *Trends in neurosciences* 12(10): 366–75. http://www.ncbi.nlm.nih.gov/pubmed/2479133.

Alcaro, Antonio, Robert Huber, and Jaak Panksepp. 2007. "Behavioral Functions of the Mesolimbic Dopaminergic System: An Affective Neuroethological Perspective." *Brain research reviews* 56(2): 283–321. http://www.ncbi.nlm.nih.gov/pubmed/17905440.

Alexander, G E, M R DeLong, and P L Strick. 1986. "Parallel Organization of Functionally Segregated Circuits Linking Basal Ganglia and Cortex." *Annual Review of Neuroscience* 9(1): 357–81. http://www.annualreviews.org/doi/10.1146/annurev.ne.09.030186.002041.

Alheid, G F, and L Heimer. 1988. "New Perspectives in Basal Forebrain Organization of Special Relevance for Neuropsychiatric Disorders: The Striatopallidal, Amygdaloid, and Corticopetal Components of Substantia Innominata." *Neuroscience* 27(1): 1–39. http://www.ncbi.nlm.nih.gov/pubmed/3059226.

Alon, Tamar, and Jeffrey M Friedman. 2006. "Late-Onset Leanness in Mice with Targeted Ablation of Melanin Concentrating Hormone Neurons." *The Journal of neuroscience : the official journal of the Society for Neuroscience* 26(2): 389–97. http://www.ncbi.nlm.nih.gov/pubmed/16407534.

ANAND, B K, and J R BROBECK. 1951. "Hypothalamic Control of Food Intake in Rats and Cats." *The Yale journal of biology and medicine* 24(2): 123–40. http://www.ncbi.nlm.nih.gov/pubmed/14901884.

Anthony, Todd E et al. 2014. "Control of Stress-Induced Persistent Anxiety by an Extra-Amygdala Septohypothalamic Circuit." *Cell* 156(3): 522–36. http://www.ncbi.nlm.nih.gov/pubmed/24485458.

Araya, Roberto, Tim P Vogels, and Rafael Yuste. 2014. "Activity-Dependent Dendritic Spine Neck Changes Are Correlated with Synaptic Strength." *Proceedings of the National Academy of Sciences of the United States of America* 111(28): E2895–2904. http://www.ncbi.nlm.nih.gov/pubmed/24982196.

Aron, Adam R, and Russell A Poldrack. 2006. "Cortical and Subcortical Contributions to Stop Signal Response Inhibition: Role of the Subthalamic Nucleus." *The Journal of neuroscience : the official journal of the Society for Neuroscience* 26(9): 2424–33. http://www.ncbi.nlm.nih.gov/pubmed/16510720.

Asensio, Samuel et al. 2010. "Altered Neural Response of the Appetitive Emotional System in Cocaine Addiction: An fMRI Study." *Addiction biology* 15(4): 504–16. http://www.ncbi.nlm.nih.gov/pubmed/20579005

Atalayer, Deniz. 2013. "Anorexia of Aging and Gut Hormones." *Aging and Disease* 04(05): 264–75. http://www.aginganddisease.org/AD-abstract-Atalayer.htm.

Avena, Nicole M., Pedro Rada, and Bartley G. Hoebel. 2008. "Evidence for

Sugar Addiction: Behavioral and Neurochemical Effects of Intermittent, Excessive Sugar Intake." *Neuroscience and Biobehavioral Reviews* 32(1): 20–39.

Babits, Réka, Balázs Szőke, Péter Sótonyi, and Bence Rácz. 2016. "Food Restriction Modifies Ultrastructure of Hippocampal Synapses." *Hippocampus* 26(4): 437–44. http://www.ncbi.nlm.nih.gov/pubmed/26386363.

Balleine, B, and S Killcross. 1994. "Effects of Ibotenic Acid Lesions of the Nucleus Accumbens on Instrumental Action." *Behavioural brain research* 65(2): 181–93. http://www.ncbi.nlm.nih.gov/pubmed/7718151.

Balleine, Bernard W, Mauricio R Delgado, and Okihide Hikosaka. 2007. "The Role of the Dorsal Striatum in Reward and Decision-Making." *The Journal of neuroscience : the official journal of the Society for Neuroscience* 27(31): 8161–65. http://www.ncbi.nlm.nih.gov/pubmed/17670959.

Balleine, Bernard W, and John P O'Doherty. 2010. "Human and Rodent Homologies in Action Control: Corticostriatal Determinants of Goal-Directed and Habitual Action." *Neuropsychopharmacology : official publication of the American College of Neuropsychopharmacology* 35(1): 48–69. http://www.ncbi.nlm.nih.gov/pubmed/19776734.

Bannister, A J, and T Kouzarides. "The CBP Co-Activator Is a Histone Acetyltransferase." *Nature* 384(6610): 641–43. http://www.ncbi.nlm.nih.gov/pubmed/8967953.

Barnard, Neal D et al. 2009. "D2 Dopamine Receptor Taq1A Polymorphism, Body Weight, and Dietary Intake in Type 2 Diabetes." *Nutrition (Burbank, Los Angeles County, Calif.)* 25(1): 58–65. http://www.ncbi.nlm.nih.gov/pubmed/18834717.

Barrot, Michel et al. 2002. "CREB Activity in the Nucleus Accumbens Shell Controls Gating of Behavioral Responses to Emotional Stimuli." *Proceedings of the National Academy of Sciences of the United States of America* 99(17): 11435–40. http://www.ncbi.nlm.nih.gov/pubmed/12165570.

Beckstead, R M, V B Domesick, and W J Nauta. 1979. "Efferent Connections of the Substantia Nigra and Ventral Tegmental Area in the Rat." *Brain research* 175(2): 191–217. http://www.ncbi.nlm.nih.gov/pubmed/314832.

Belin, David, Aude Belin-Rauscent, Jennifer E Murray, and Barry J Everitt. 2013. "Addiction: Failure of Control over Maladaptive Incentive Habits." *Current opinion in neurobiology* 23(4): 564–72. http://www.ncbi.nlm.nih.gov/pubmed/23452942.

Bellone, Camilla, and Christian Lüscher. 2006. "Cocaine Triggered AMPA Receptor Redistribution Is Reversed in Vivo by mGluR-Dependent Long-Term Depression." *Nature neuroscience* 9(5): 636–41.

http://www.ncbi.nlm.nih.gov/pubmed/16582902.

Bennett, B D, and J P Bolam. 1993. "Characterization of Calretinin-Immunoreactive Structures in the Striatum of the Rat." *Brain research* 609(1-2): 137–48. http://www.ncbi.nlm.nih.gov/pubmed/8508297.

Bennett, B D, and J P Bolam. 1994. "Synaptic Input and Output of Parvalbumin-Immunoreactive Neurons in the Neostriatum of the Rat." *Neuroscience* 62(3): 707–19. http://www.ncbi.nlm.nih.gov/pubmed/7870301.

Berendse, H W, Y Galis-de Graaf, and H J Groenewegen. 1992. "Topographical Organization and Relationship with Ventral Striatal Compartments of Prefrontal Corticostriatal Projections in the Rat." *The Journal of comparative neurology* 316(3): 314–47. http://www.ncbi.nlm.nih.gov/pubmed/1577988.

Berk, M L, and J A Finkelstein. 1982. "Efferent Connections of the Lateral Hypothalamic Area of the Rat: An Autoradiographic Investigation." *Brain research bulletin* 8(5): 511–26. http://www.ncbi.nlm.nih.gov/pubmed/6811106.

Bernardis, L L, and L L Bellinger. 1993. "The Lateral Hypothalamic Area Revisited: Neuroanatomy, Body Weight Regulation, Neuroendocrinology and Metabolism." *Neuroscience and biobehavioral reviews* 17(2): 141–93. http://www.ncbi.nlm.nih.gov/pubmed/8515901.

Berridge, C W, S J Bolen, M S Manley, and S L Foote. 1996. "Modulation of Forebrain Electroencephalographic Activity in Halothane-Anesthetized Rat via Actions of Noradrenergic Beta-Receptors within the Medial Septal Region." *The Journal of neuroscience : the official journal of the Society for Neuroscience* 16(21): 7010–20. http://www.ncbi.nlm.nih.gov/pubmed/8824337.

Berthoud, Hans-Rudolf. 2007. "Interactions between The 'cognitive' and 'metabolic' brain in the Control of Food Intake." *Physiology & behavior* 91(5): 486–98. http://www.ncbi.nlm.nih.gov/pubmed/17307205.

Bertran-Gonzalez, Jesus, Denis Hervé, Jean-Antoine Girault, and Emmanuel Valjent. 2010. "What Is the Degree of Segregation between Striatonigral and Striatopallidal Projections?" *Frontiers in neuroanatomy* 4. http://www.ncbi.nlm.nih.gov/pubmed/20953289.

Betley, J Nicholas, Zhen Fang Huang Cao, Kimberly D Ritola, and Scott M Sternson. 2013. "Parallel, Redundant Circuit Organization for Homeostatic Control of Feeding Behavior." *Cell* 155(6): 1337–50. http://www.ncbi.nlm.nih.gov/pubmed/24315102.

Beurrier, Corinne, and Robert C Malenka. 2002. "Enhanced Inhibition of Synaptic Transmission by Dopamine in the Nucleus Accumbens during Behavioral Sensitization to Cocaine." *The Journal of neuroscience : the official journal of the Society for Neuroscience* 22(14): 5817–22.

http://www.ncbi.nlm.nih.gov/pubmed/12122043.

Beutler, Lisa R et al. 2011. "Severely Impaired Learning and Altered Neuronal Morphology in Mice Lacking NMDA Receptors in Medium Spiny Neurons." *PloS one* 6(11): e28168. http://www.ncbi.nlm.nih.gov/pubmed/22132236.

Bevan, M D, and J P Bolam. 1995. "Cholinergic, GABAergic, and Glutamate-Enriched Inputs from the Mesopontine Tegmentum to the Subthalamic Nucleus in the Rat." *The Journal of neuroscience : the official journal of the Society for Neuroscience* 15(11): 7105–20. http://www.ncbi.nlm.nih.gov/pubmed/7472465.

Bevan, M D, P A Booth, S A Eaton, and J P Bolam. 1998. "Selective Innervation of Neostriatal Interneurons by a Subclass of Neuron in the Globus Pallidus of the Rat." *The Journal of neuroscience : the official journal of the Society for Neuroscience* 18(22): 9438–52. http://www.ncbi.nlm.nih.gov/pubmed/9801382.

Bevan, M D, A R Crossman, and J P Bolam. 1994. "Neurons Projecting from the Entopeduncular Nucleus to the Thalamus Receive Convergent Synaptic Inputs from the Subthalamic Nucleus and the Neostriatum in the Rat." *Brain research* 659(1-2): 99–109. http://www.ncbi.nlm.nih.gov/pubmed/7529649.

Bevan, Mark D., Nicholas E. Hallworth, and Jérôme Baufreton. 2007. "GABAergic Control of the Subthalamic Nucleus." In , 173–88. http://linkinghub.elsevier.com/retrieve/pii/S0079612306600101.

Bibb, J A et al. 2001. "Effects of Chronic Exposure to Cocaine Are Regulated by the Neuronal Protein Cdk5." *Nature* 410(6826): 376–80. http://www.ncbi.nlm.nih.gov/pubmed/11268215.

Bittencourt, J C et al. 1992. "The Melanin-Concentrating Hormone System of the Rat Brain: An Immuno- and Hybridization Histochemical Characterization." *The Journal of comparative neurology* 319(2): 218–45. http://www.ncbi.nlm.nih.gov/pubmed/1522246.

Björklund, Anders, and Stephen B Dunnett. 2007. "Dopamine Neuron Systems in the Brain: An Update." *Trends in neurosciences* 30(5): 194–202. http://www.ncbi.nlm.nih.gov/pubmed/17408759.

Blank, T et al. 1997. "The Phosphoprotein DARPP-32 Mediates cAMP-Dependent Potentiation of Striatal N-Methyl-D-Aspartate Responses." *Proceedings of the National Academy of Sciences of the United States of America* 94(26): 14859–64. http://www.ncbi.nlm.nih.gov/pubmed/9405704.

Bock, Roland et al. 2013. "Strengthening the Accumbal Indirect Pathway

Promotes Resilience to Compulsive Cocaine Use." *Nature neuroscience* 16(5): 632–38. http://www.ncbi.nlm.nih.gov/pubmed/23542690.

Bolam, J P, J F Powell, J Y Wu, and A D Smith. 1985. "Glutamate Decarboxylase-Immunoreactive Structures in the Rat Neostriatum: A Correlated Light and Electron Microscopic Study Including a Combination of Golgi Impregnation with Immunocytochemistry." *The Journal of comparative neurology* 237(1): 1–20. http://www.ncbi.nlm.nih.gov/pubmed/4044888.

Bolam, J P, B H Wainer, and A D Smith. 1984. "Characterization of Cholinergic Neurons in the Rat Neostriatum. A Combination of Choline Acetyltransferase Immunocytochemistry, Golgi-Impregnation and Electron Microscopy." *Neuroscience* 12(3): 711–18. http://www.ncbi.nlm.nih.gov/pubmed/6382048.

Brakeman, P R et al. 1997. "Homer: A Protein That Selectively Binds Metabotropic Glutamate Receptors." *Nature* 386(6622): 284–88. http://www.ncbi.nlm.nih.gov/pubmed/9069287.

Breiter, H C et al. 1997. "Acute Effects of Cocaine on Human Brain Activity and Emotion." *Neuron* 19(3): 591–611. http://www.ncbi.nlm.nih.gov/pubmed/9331351.

BRIESE, E, and J OLDS. 1964. "REINFORCING BRAIN STIMULATION AND MEMORY IN MONKEYS." *Experimental neurology* 10: 493–508. http://www.ncbi.nlm.nih.gov/pubmed/14239736.

Broberger, C, L De Lecea, J G Sutcliffe, and T Hökfelt. 1998. "Hypocretin/orexin- and Melanin-Concentrating Hormone-Expressing Cells Form Distinct Populations in the Rodent Lateral Hypothalamus: Relationship to the Neuropeptide Y and Agouti Gene-Related Protein Systems." *The Journal of comparative neurology* 402(4): 460–74. http://www.ncbi.nlm.nih.gov/pubmed/9862321.

Brown, Juliette A, Hillary L Woodworth, and Gina M Leinninger. 2015. "To Ingest or Rest? Specialized Roles of Lateral Hypothalamic Area Neurons in Coordinating Energy Balance." *Frontiers in systems neuroscience* 9: 9. http://www.ncbi.nlm.nih.gov/pubmed/25741247.

Brown, L L et al. 1979. "A Direct Role of Dopamine in the Rat Subthalamic Nucleus and an Adjacent Intrapeduncular Area." *Science (New York, N.Y.)* 206(4425): 1416–18. http://www.ncbi.nlm.nih.gov/pubmed/505015.

Cachope, Roger et al. 2012. "Selective Activation of Cholinergic Interneurons Enhances Accumbal Phasic Dopamine Release: Setting the Tone for Reward Processing." *Cell Reports* 2(1): 33–41. http://dx.doi.org/10.1016/j.celrep.2012.05.011.

Cai, X J et al. 1999. "Hypothalamic Orexin Expression: Modulation by Blood Glucose and Feeding." *Diabetes* 48(11): 2132–37.

http://www.ncbi.nlm.nih.gov/pubmed/10535445.

Calabresi, P, A Pisani, D Centonze, and G Bernardi. 1997. "Role of Dopamine Receptors in the Short- and Long-Term Regulation of Corticostriatal Transmission." *Nihon shinkei seishin yakurigaku zasshi = Japanese journal of psychopharmacology* 17(2): 101–4. http://www.ncbi.nlm.nih.gov/pubmed/9201731.

Carlezon, W A et al. 1998. "Regulation of Cocaine Reward by CREB." *Science (New York, N.Y.)* 282(5397): 2272–75. http://www.ncbi.nlm.nih.gov/pubmed/9856954.

Carlezon, William A, Ronald S Duman, and Eric J Nestler. 2005. "The Many Faces of CREB." *Trends in neurosciences* 28(8): 436–45. http://www.ncbi.nlm.nih.gov/pubmed/15982754.

Carr, D B, and S R Sesack. 2000. "Projections from the Rat Prefrontal Cortex to the Ventral Tegmental Area: Target Specificity in the Synaptic Associations with Mesoaccumbens and Mesocortical Neurons." *The Journal of neuroscience : the official journal of the Society for Neuroscience* 20(10): 3864–73. http://www.ncbi.nlm.nih.gov/pubmed/10804226.

Cazorla, Maxime et al. 2014. "Dopamine D2 Receptors Regulate the Anatomical and Functional Balance of Basal Ganglia Circuitry." *Neuron* 81(1): 153–64. http://www.ncbi.nlm.nih.gov/pubmed/24411738.

Cenci, M Angela, Veronica Francardo, Sean S O'Sullivan, and Hanna S Lindgren. 2015. "Rodent Models of Impulsive-Compulsive Behaviors in Parkinson's Disease: How Far Have We Reached?" *Neurobiology of disease* 82: 561–73. http://www.ncbi.nlm.nih.gov/pubmed/26325219.

Centonze, Diego et al. 2003. "Dopamine, Acetylcholine and Nitric Oxide Systems Interact to Induce Corticostriatal Synaptic Plasticity." *Reviews in the neurosciences* 14(3): 207–16. http://www.ncbi.nlm.nih.gov/pubmed/14513864.

Cepeda, Carlos et al. 2008. "Differential Electrophysiological Properties of Dopamine D1 and D2 Receptor-Containing Striatal Medium-Sized Spiny Neurons." *The European journal of neuroscience* 27(3): 671–82. http://www.ncbi.nlm.nih.gov/pubmed/18279319.

Chang, J-Y et al. 2002. "Neuronal Responses in the Frontal Cortico-Basal Ganglia System during Delayed Matching-to-Sample Task: Ensemble Recording in Freely Moving Rats." *Experimental brain research* 142(1): 67–80. http://www.ncbi.nlm.nih.gov/pubmed/11797085.

Chen, Andrew C H et al. 2002. "Potentially Functional Polymorphism in the Promoter Region of Prodynorphin Gene May Be Associated with Protection

against Cocaine Dependence or Abuse." *American journal of medical genetics* 114(4): 429–35. http://www.ncbi.nlm.nih.gov/pubmed/11992566.

Di Chiara, G. 1992. "Reinforcing Drug Seeking." *Trends in pharmacological sciences* 13(12): 428–29. http://www.ncbi.nlm.nih.gov/pubmed/1293867.

Di Chiara, Gaetano et al. 2004. "Dopamine and Drug Addiction: The Nucleus Accumbens Shell Connection." *Neuropharmacology* 47: 227–41. http://linkinghub.elsevier.com/retrieve/pii/S0028390804002199.

Choi, S, and D M Lovinger. 1997. "Decreased Frequency but Not Amplitude of Quantal Synaptic Responses Associated with Expression of Corticostriatal Long-Term Depression." *The Journal of neuroscience : the official journal of the Society for Neuroscience* 17(21): 8613–20. http://www.ncbi.nlm.nih.gov/pubmed/9334432.

Chuhma, Nao, Kenji F Tanaka, René Hen, and Stephen Rayport. 2011. "Functional Connectome of the Striatal Medium Spiny Neuron." *The Journal of neuroscience : the official journal of the Society for Neuroscience* 31(4): 1183–92. http://www.ncbi.nlm.nih.gov/pubmed/21273403.

Di Ciano, Patricia, and Barry J Everitt. 2004. "Direct Interactions between the Basolateral Amygdala and Nucleus Accumbens Core Underlie Cocaine-Seeking Behavior by Rats." *The Journal of neuroscience : the official journal of the Society for Neuroscience* 24(32): 7167–73. http://www.ncbi.nlm.nih.gov/pubmed/15306650.

Ciccocioppo, R, P P Sanna, and F Weiss. 2001. "Cocaine-Predictive Stimulus Induces Drug-Seeking Behavior and Neural Activation in Limbic Brain Regions after Multiple Months of Abstinence: Reversal by D(1) Antagonists." *Proceedings of the National Academy of Sciences of the United States of America* 98(4): 1976–81. http://www.ncbi.nlm.nih.gov/pubmed/11172061.

Clegg, Deborah J, Ellen L Air, Stephen C Woods, and Randy J Seeley. 2002. "Eating Elicited by Orexin-A, but Not Melanin-Concentrating Hormone, Is Opioid Mediated." *Endocrinology* 143(8): 2995–3000. http://www.ncbi.nlm.nih.gov/pubmed/12130565.

Colby, Christina R et al. 2003. "Striatal Cell Type-Specific Overexpression of DeltaFosB Enhances Incentive for Cocaine." *The Journal of neuroscience : the official journal of the Society for Neuroscience* 23(6): 2488–93. http://www.ncbi.nlm.nih.gov/pubmed/12657709.

Cole, R L, C Konradi, J Douglass, and S E Hyman. 1995. "Neuronal Adaptation to Amphetamine and Dopamine: Molecular Mechanisms of Prodynorphin Gene Regulation in Rat Striatum." *Neuron* 14(4): 813–23.

http://www.ncbi.nlm.nih.gov/pubmed/7718243.

Collin, Maria et al. 2003. "Plasma Membrane and Vesicular Glutamate Transporter mRNAs/proteins in Hypothalamic Neurons That Regulate Body Weight." *The European journal of neuroscience* 18(5): 1265–78. http://www.ncbi.nlm.nih.gov/pubmed/12956725.

Comings, D E et al. 1997. "Cannabinoid Receptor Gene (CNR1): Association with I.v. Drug Use." *Molecular psychiatry* 2(2): 161–68. http://www.ncbi.nlm.nih.gov/pubmed/9106242.

Cooke, Jennifer H et al. 2009. "Peripheral and Central Administration of Xenin and Neurotensin Suppress Food Intake in Rodents." *Obesity (Silver Spring, Md.)* 17(6): 1135–43. http://www.ncbi.nlm.nih.gov/pubmed/19214175.

Corbett, D, and R A Wise. 1979. "Intracranial Self-Stimulation in Relation to the Ascending Noradrenergic Fiber Systems of the Pontine Tegmentum and Caudal Midbrain: A Moveable Electrode Mapping Study." *Brain research* 177(3): 423–36. http://www.ncbi.nlm.nih.gov/pubmed/497844.

Corvol, J C et al. 2001. "Galpha(olf) Is Necessary for Coupling D1 and A2a Receptors to Adenylyl Cyclase in the Striatum." *Journal of neurochemistry* 76(5): 1585–88. http://www.ncbi.nlm.nih.gov/pubmed/11238742.

Costantini, F, and E Lacy. 1981. "Introduction of a Rabbit Beta-Globin Gene into the Mouse Germ Line." *Nature* 294(5836): 92–94. http://www.ncbi.nlm.nih.gov/pubmed/6945481.

Cragg, Stephanie J et al. 2004. "Synaptic Release of Dopamine in the Subthalamic Nucleus." *The European journal of neuroscience* 20(7): 1788–1802. http://www.ncbi.nlm.nih.gov/pubmed/15380000.

Crittenden, Jill R, and Ann M Graybiel. 2011a. "Basal Ganglia Disorders Associated with Imbalances in the Striatal Striosome and Matrix Compartments." *Frontiers in neuroanatomy* 5: 59. http://www.ncbi.nlm.nih.gov/pubmed/21941467.

Crittenden, Jill R., and Ann M. Graybiel. 2011b. "Basal Ganglia Disorders Associated with Imbalances in the Striatal Striosome and Matrix Compartments." *Frontiers in Neuroanatomy* 5..

Dalley, Jeffrey W et al. 2007. "Nucleus Accumbens D2/3 Receptors Predict Trait Impulsivity and Cocaine Reinforcement." *Science (New York, N.Y.)* 315(5816): 1267–70. http://www.ncbi.nlm.nih.gov/pubmed/17332411.

Dateki, Minori et al. 2005. "Neurochondrin Negatively Regulates CaMKII Phosphorylation, and Nervous System-Specific Gene Disruption Results in Epileptic Seizure." *The Journal of biological chemistry* 280(21): 20503–8. http://www.ncbi.nlm.nih.gov/pubmed/15790563.

Davis, Jon F, Derrick L Choi, Deborah J Clegg, and Stephen C Benoit. 2011. "Signaling through the Ghrelin Receptor Modulates Hippocampal Function and Meal Anticipation in Mice." *Physiology & behavior* 103(1): 39–43. http://www.ncbi.nlm.nih.gov/pubmed/21036184.

Davis, Margaret I, and Henry L Puhl. 2011. "Nr4a1-eGFP Is a Marker of Striosome-Matrix Architecture, Development and Activity in the Extended Striatum." *PloS one* 6(1): e16619. http://www.ncbi.nlm.nih.gov/pubmed/21305052.

Day, Michelle et al. 2006. "Selective Elimination of Glutamatergic Synapses on Striatopallidal Neurons in Parkinson Disease Models." *Nature neuroscience* 9(2): 251–59. http://www.ncbi.nlm.nih.gov/pubmed/16415865.

Deniau, J M, and G Chevalier. 1984. "Synaptic Organization of the Basal Ganglia: An Electroanatomical Approach in the Rat." *Ciba Foundation symposium* 107: 48–63. http://www.ncbi.nlm.nih.gov/pubmed/6094126.

Deniau, J M, P Mailly, N Maurice, and S Charpier. 2007. "The Pars Reticulata of the Substantia Nigra: A Window to Basal Ganglia Output." *Progress in brain research* 160: 151–72. http://www.ncbi.nlm.nih.gov/pubmed/17499113.

Descarries, L, V Gisiger, and M Steriade. 1997. "Diffuse Transmission by Acetylcholine in the CNS." *Progress in neurobiology* 53(5): 603–25. http://www.ncbi.nlm.nih.gov/pubmed/9421837.

Deschênes, M, J Bourassa, V D Doan, and A Parent. 1996. "A Single-Cell Study of the Axonal Projections Arising from the Posterior Intralaminar Thalamic Nuclei in the Rat." *The European journal of neuroscience* 8(2): 329–43. http://www.ncbi.nlm.nih.gov/pubmed/8714704.

Dietz, David M et al. 2012. "Rac1 Is Essential in Cocaine-Induced Structural Plasticity of Nucleus Accumbens Neurons." *Nature Neuroscience* 15(6): 891–96. http://www.nature.com/doifinder/10.1038/nn.3094.

Difiglia, M, P Pasik, and T Pasik. 1982. "A Golgi and Ultrastructural Study of the Monkey Globus Pallidus." *The Journal of comparative neurology* 212(1): 53–75. http://www.ncbi.nlm.nih.gov/pubmed/7174908.

Dobi, Alice et al. 2011. "Cocaine-Induced Plasticity in the Nucleus Accumbens Is Cell Specific and Develops without Prolonged Withdrawal." *The Journal of neuroscience : the official journal of the Society for Neuroscience* 31(5): 1895–1904. http://www.ncbi.nlm.nih.gov/pubmed/21289199.

Douglass, J, A A McKinzie, and P Couceyro. 1995. "PCR Differential Display Identifies a Rat Brain mRNA That Is Transcriptionally Regulated by Cocaine and Amphetamine." *The Journal of neuroscience : the official journal of the Society for Neuroscience* 15(3 Pt 2): 2471–81.

http://www.ncbi.nlm.nih.gov/pubmed/7891182.

Doyle, Joseph P et al. 2008. "Application of a Translational Profiling Approach for the Comparative Analysis of CNS Cell Types." *Cell* 135(4): 749–62. http://www.ncbi.nlm.nih.gov/pubmed/19013282.

Eblen, F, and A M Graybiel. 1995. "Highly Restricted Origin of Prefrontal Cortical Inputs to Striosomes in the Macaque Monkey." *The Journal of neuroscience : the official journal of the Society for Neuroscience* 15(9): 5999–6013. http://www.ncbi.nlm.nih.gov/pubmed/7666184.

Ehrich, Jonathan M, Paul E M Phillips, and Charles Chavkin. 2014. "Kappa Opioid Receptor Activation Potentiates the Cocaine-Induced Increase in Evoked Dopamine Release Recorded in Vivo in the Mouse Nucleus Accumbens." *Neuropsychopharmacology : official publication of the American College of Neuropsychopharmacology* 39(13): 3036–48. http://www.ncbi.nlm.nih.gov/pubmed/24971603.

Elias, C F et al. 1998. "Chemically Defined Projections Linking the Mediobasal Hypothalamus and the Lateral Hypothalamic Area." *The Journal of comparative neurology* 402(4): 442–59. http://www.ncbi.nlm.nih.gov/pubmed/9862320.

Emmert-Buck, M R et al. 1996. "Laser Capture Microdissection." *Science (New York, N.Y.)* 274(5289): 998–1001. http://www.ncbi.nlm.nih.gov/pubmed/8875945.

English, Daniel F et al. 2012. "GABAergic Circuits Mediate the Reinforcement-Related Signals of Striatal Cholinergic Interneurons." *Nature neuroscience* 15(1): 123–30. http://www.ncbi.nlm.nih.gov/pubmed/22158514.

Epstein, Leonard H, Jennifer L Temple, James N Roemmich, and Mark E Bouton. 2009. "Habituation as a Determinant of Human Food Intake." *Psychological review* 116(2): 384–407. http://www.ncbi.nlm.nih.gov/pubmed/19348547.

Erlanson-Albertsson, Charlotte. 2005. "How Palatable Food Disrupts Appetite Regulation." *Basic & clinical pharmacology & toxicology* 97(2): 61–73. http://www.ncbi.nlm.nih.gov/pubmed/15998351.

Ersche, K. D. et al. 2012. "Abnormal Brain Structure Implicated in Stimulant Drug Addiction." *Science* 335(6068): 601–4. http://www.sciencemag.org/cgi/doi/10.1126/science.1214463.

Espina, Virginia et al. 2006. "Laser-Capture Microdissection." *Nature protocols* 1(2): 586–603. http://www.ncbi.nlm.nih.gov/pubmed/17406286.

Everitt, Barry J et al. 2008. "Review. Neural Mechanisms Underlying the Vulnerability to Develop Compulsive Drug-Seeking Habits and Addiction." *Philosophical transactions of the Royal Society of London. Series B, Biological*

sciences 363(1507): 3125–35.
http://www.pubmedcentral.nih.gov/articlerender.fcgi?artid=2607322&tool=pmcentrez&rendertype=abstract.

Everitt, Barry J, and Trevor W Robbins. 2005. "Neural Systems of Reinforcement for Drug Addiction: From Actions to Habits to Compulsion." *Nature neuroscience* 8(11): 1481–89.
http://www.ncbi.nlm.nih.gov/pubmed/16251991.

Exley, R, and S J Cragg. 2008. "Presynaptic Nicotinic Receptors: A Dynamic and Diverse Cholinergic Filter of Striatal Dopamine Neurotransmission." *British journal of pharmacology* 153 Suppl: S283–97.
http://www.ncbi.nlm.nih.gov/pubmed/18037926.

Feng, Jian et al. 2014. "Chronic Cocaine-Regulated Epigenomic Changes in Mouse Nucleus Accumbens." *Genome biology* 15(4): R65.
http://www.ncbi.nlm.nih.gov/pubmed/24758366.

Fink-Jensen, A, and J D Mikkelsen. 1991. "A Direct Neuronal Projection from the Entopeduncular Nucleus to the Globus Pallidus. A PHA-L Anterograde Tracing Study in the Rat." *Brain research* 542(1): 175–79.
http://www.ncbi.nlm.nih.gov/pubmed/1647254.

Flaherty, A W, and A M Graybiel. 1994. "Input-Output Organization of the Sensorimotor Striatum in the Squirrel Monkey." *The Journal of neuroscience : the official journal of the Society for Neuroscience* 14(2): 599–610.
http://www.ncbi.nlm.nih.gov/pubmed/7507981.

Floresco, S B, C R Yang, A G Phillips, and C D Blaha. 1998. "Basolateral Amygdala Stimulation Evokes Glutamate Receptor-Dependent Dopamine Efflux in the Nucleus Accumbens of the Anaesthetized Rat." *The European journal of neuroscience* 10(4): 1241–51. http://www.ncbi.nlm.nih.gov/pubmed/9749778.

Francke, Felix et al. 2006. "Interaction of Neurochondrin with the Melanin-Concentrating Hormone Receptor 1 Interferes with G Protein-Coupled Signal Transduction but Not Agonist-Mediated Internalization." *The Journal of biological chemistry* 281(43): 32496–507.
http://www.ncbi.nlm.nih.gov/pubmed/16945926.

Freund, T F, Z Maglóczky, I Soltész, and P Somogyi. 1986. "Synaptic Connections, Axonal and Dendritic Patterns of Neurons Immunoreactive for Cholecystokinin in the Visual Cortex of the Cat." *Neuroscience* 19(4): 1133–59.
http://www.ncbi.nlm.nih.gov/pubmed/3029625.

Fuchs, R. A. 2006. "Different Neural Substrates Mediate Cocaine Seeking after Abstinence versus Extinction Training: A Critical Role for the Dorsolateral Caudate-Putamen." *Journal of Neuroscience* 26(13): 3584–88.
http://www.jneurosci.org/cgi/doi/10.1523/JNEUROSCI.5146-05.2006.

Fujishige, K, J Kotera, and K Omori. 1999. "Striatum- and Testis-Specific

Phosphodiesterase PDE10A Isolation and Characterization of a Rat PDE10A." *European journal of biochemistry / FEBS* 266(3): 1118–27. http://www.ncbi.nlm.nih.gov/pubmed/10583409.

Fujiyama, Fumino et al. 2006. "Difference in Organization of Corticostriatal and Thalamostriatal Synapses between Patch and Matrix Compartments of Rat Neostriatum." *The European journal of neuroscience* 24(10): 2813–24. http://www.ncbi.nlm.nih.gov/pubmed/17156206.

Fujiyama, Fumino et al. 2006. 2011. "Exclusive and Common Targets of Neostriatofugal Projections of Rat Striosome Neurons: A Single Neuron-Tracing Study Using a Viral Vector." *The European journal of neuroscience* 33(4): 668–77. http://www.ncbi.nlm.nih.gov/pubmed/21314848.

Gaiteri, C et al. 2014. "Beyond Modules and Hubs: The Potential of Gene Coexpression Networks for Investigating Molecular Mechanisms of Complex Brain Disorders." *Genes, brain, and behavior* 13(1): 13–24. http://www.ncbi.nlm.nih.gov/pubmed/24320616.

Gangarossa, Giuseppe et al. 2013. "Distribution and Compartmental Organization of GABAergic Medium-Sized Spiny Neurons in the Mouse Nucleus Accumbens." *Frontiers in Neural Circuits* 7. http://journal.frontiersin.org/article/10.3389/fncir.2013.00022/abstract.

Garavan, H et al. 2000. "Cue-Induced Cocaine Craving: Neuroanatomical Specificity for Drug Users and Drug Stimuli." *The American journal of psychiatry* 157(11): 1789–98. http://www.ncbi.nlm.nih.gov/pubmed/11058476.

Gelernter, J, H R Kranzler, S L Satel, and P A Rao. 1994. "Genetic Association between Dopamine Transporter Protein Alleles and Cocaine-Induced Paranoia." *Neuropsychopharmacology : official publication of the American College of Neuropsychopharmacology* 11(3): 195–200. http://www.ncbi.nlm.nih.gov/pubmed/7865100.

Gerfen, C R. 1989. "The Neostriatal Mosaic: Striatal Patch-Matrix Organization Is Related to Cortical Lamination." *Science (New York, N.Y.)* 246(4928): 385–88. http://www.ncbi.nlm.nih.gov/pubmed/2799392.

Gerfen, C R. 1989. "The Neostriatal Mosaic: Compartmentalization of Corticostriatal Input and Striatonigral Output Systems." *Nature* 311(5985): 461–64. http://www.ncbi.nlm.nih.gov/pubmed/6207434.

Gerfen, C R, K G Baimbridge, and J J Miller. 1985. "The Neostriatal Mosaic: Compartmental Distribution of Calcium-Binding Protein and Parvalbumin in the Basal Ganglia of the Rat and Monkey." *Proceedings of the National Academy of Sciences of the United States of America* 82(24): 8780–84. http://www.ncbi.nlm.nih.gov/pubmed/3909155.

Gerfen, C R, M Herkenham, and J Thibault. 1987. "The Neostriatal Mosaic: II. Patch- and Matrix-Directed Mesostriatal Dopaminergic and Non-Dopaminergic

Systems." *The Journal of neuroscience : the official journal of the Society for Neuroscience* 7(12): 3915–34. http://www.ncbi.nlm.nih.gov/pubmed/2891799.

Gerfen, C R, and W S Young. 1988. "Distribution of Striatonigral and Striatopallidal Peptidergic Neurons in Both Patch and Matrix Compartments: An in Situ Hybridization Histochemistry and Fluorescent Retrograde Tracing Study." *Brain research* 460(1): 161–67. http://www.ncbi.nlm.nih.gov/pubmed/2464402.

Gertler, Tracy S, C Savio Chan, and D James Surmeier. 2008. "Dichotomous Anatomical Properties of Adult Striatal Medium Spiny Neurons." *The Journal of neuroscience : the official journal of the Society for Neuroscience* 28(43): 10814–24. http://www.ncbi.nlm.nih.gov/pubmed/18945889.

Ghazalpour, Anatole et al. 2006. "Integrating Genetic and Network Analysis to Characterize Genes Related to Mouse Weight." *PLoS genetics* 2(8): e130. http://www.ncbi.nlm.nih.gov/pubmed/16934000.

Giménez-Amaya, J M, and A M Graybiel. 1991. "Modular Organization of Projection Neurons in the Matrix Compartment of the Primate Striatum." *The Journal of neuroscience : the official journal of the Society for Neuroscience* 11(3): 779–91. http://www.ncbi.nlm.nih.gov/pubmed/1705968.

Gokce, Ozgun et al. 2016. "Cellular Taxonomy of the Mouse Striatum as Revealed by Single-Cell RNA-Seq." *Cell reports* 16(4): 1126–37. http://www.ncbi.nlm.nih.gov/pubmed/27425622.

Gong, Shiaoching et al. 2003. "A Gene Expression Atlas of the Central Nervous System Based on Bacterial Artificial Chromosomes." *Nature* 425(6961): 917–25. http://www.ncbi.nlm.nih.gov/pubmed/14586460.

Gordon, J W, and F H Ruddle. 1981. "Integration and Stable Germ Line Transmission of Genes Injected into Mouse Pronuclei." *Science (New York, N.Y.)* 214(4526): 1244–46. http://www.ncbi.nlm.nih.gov/pubmed/6272397.

Gossen, M et al. 1995. "Transcriptional Activation by Tetracyclines in Mammalian Cells." *Science (New York, N.Y.)* 268(5218): 1766–69. http://www.ncbi.nlm.nih.gov/pubmed/7792603.

Gossen, M, and H Bujard. 1992. "Tight Control of Gene Expression in Mammalian Cells by Tetracycline-Responsive Promoters." *Proceedings of the National Academy of Sciences of the United States of America* 89(12): 5547–51. http://www.ncbi.nlm.nih.gov/pubmed/1319065.

Grande, Cristina et al. 2004. "Chronic Treatment with Atypical Neuroleptics Induces Striosomal FosB/DeltaFosB Expression in Rats." *Biological psychiatry* 55(5): 457–63. http://www.ncbi.nlm.nih.gov/pubmed/15023572.

Grant, S et al. 1996. "Activation of Memory Circuits during Cue-Elicited Cocaine Craving." *Proceedings of the National Academy of Sciences of the United*

States of America 93(21): 12040–45.
http://www.ncbi.nlm.nih.gov/pubmed/8876259.

Graybiel, A M, T Aosaki, A W Flaherty, and M Kimura. 1994. "The Basal Ganglia and Adaptive Motor Control." *Science (New York, N.Y.)* 265(5180): 1826–31. http://www.ncbi.nlm.nih.gov/pubmed/8091209.

Graybiel, A M, and T L Hickey. 1982. "Chemospecificity of Ontogenetic Units in the Striatum: Demonstration by Combining [3H]thymidine Neuronography and Histochemical Staining." *Proceedings of the National Academy of Sciences of the United States of America* 79(1): 198–202.
http://www.ncbi.nlm.nih.gov/pubmed/6172791.

Graybiel, A M, R Moratalla, and H A Robertson. 1990. "Amphetamine and Cocaine Induce Drug-Specific Activation of the c-Fos Gene in Striosome-Matrix Compartments and Limbic Subdivisions of the Striatum." *Proceedings of the National Academy of Sciences of the United States of America* 87(17): 6912–16.
http://www.ncbi.nlm.nih.gov/pubmed/2118661.

Graybiel, A. M., and C. W. Ragsdale. 1978. "Histochemically Distinct Compartments in the Striatum of Human, Monkeys, and Cat Demonstrated by Acetylthiocholinesterase Staining." *Proceedings of the National Academy of Sciences* 75(11): 5723–26.
http://www.pnas.org/cgi/doi/10.1073/pnas.75.11.5723.

Griffond, B et al. 1999. "Insulin-Induced Hypoglycemia Increases Preprohypocretin (Orexin) mRNA in the Rat Lateral Hypothalamic Area." *Neuroscience letters* 262(2): 77–80.
http://www.ncbi.nlm.nih.gov/pubmed/10203235.

Groenewegen, H J, and H W Berendse. 1994. "The Specificity of the 'Nonspecific' Midline and Intralaminar Thalamic Nuclei." *Trends in neurosciences* 17(2): 52–57. http://www.ncbi.nlm.nih.gov/pubmed/7512768.

Groenewegen, H J, C I Wright, A V Beijer, and P Voorn. 1999. "Convergence and Segregation of Ventral Striatal Inputs and Outputs." *Annals of the New York Academy of Sciences* 877: 49–63.
http://www.ncbi.nlm.nih.gov/pubmed/10415642.

Grove, E A. 1988. "Efferent Connections of the Substantia Innominata in the Rat." *The Journal of comparative neurology* 277(3): 347–64.
http://www.ncbi.nlm.nih.gov/pubmed/2461973
.

Grueter, Brad A et al. 2013. "ΔFosB Differentially Modulates Nucleus Accumbens Direct and Indirect Pathway Function." *Proceedings of the National Academy of Sciences of the United States of America* 110(5): 1923–28.
http://www.ncbi.nlm.nih.gov/pubmed/23319622

.

Guegan, Thomas et al. 2013. "Operant Behavior to Obtain Palatable Food Modifies Neuronal Plasticity in the Brain Reward Circuit." *European neuropsychopharmacology : the journal of the European College of Neuropsychopharmacology* 23(2): 146–59. http://www.ncbi.nlm.nih.gov/pubmed/22612989.

Guez-Barber, Danielle et al. 2011. "FACS Identifies Unique Cocaine-Induced Gene Regulation in Selectively Activated Adult Striatal Neurons." *The Journal of neuroscience : the official journal of the Society for Neuroscience* 31(11): 4251–59. http://www.ncbi.nlm.nih.gov/pubmed/21411666.

Guez-Barber, Danielle et al. 2012a. "FACS Purification of Immunolabeled Cell Types from Adult Rat Brain." *Journal of Neuroscience Methods* 203(1): 10–18. http://linkinghub.elsevier.com/retrieve/pii/S0165027011005206.

Guindalini, Camila et al. 2006. "A Dopamine Transporter Gene Functional Variant Associated with Cocaine Abuse in a Brazilian Sample." *Proceedings of the National Academy of Sciences of the United States of America* 103(12): 4552–57. http://www.ncbi.nlm.nih.gov/pubmed/16537431.

Guyenet, P G, and G K Aghajanian. 1978. "Antidromic Identification of Dopaminergic and Other Output Neurons of the Rat Substantia Nigra." *Brain research* 150(1): 69–84. http://www.ncbi.nlm.nih.gov/pubmed/78748.

Haber, S N, J L Fudge, and N R McFarland. 2000. "Striatonigrostriatal Pathways in Primates Form an Ascending Spiral from the Shell to the Dorsolateral Striatum." *The Journal of neuroscience : the official journal of the Society for Neuroscience* 20(6): 2369–82. http://www.ncbi.nlm.nih.gov/pubmed/10704511.

Hajnal, A, and R Norgren. 2001. "Accumbens Dopamine Mechanisms in Sucrose Intake." *Brain research* 904(1): 76–84. http://www.ncbi.nlm.nih.gov/pubmed/11516413.

Han, Dawn D, and Howard H Gu. 2006. "Comparison of the Monoamine Transporters from Human and Mouse in Their Sensitivities to Psychostimulant Drugs." *BMC pharmacology* 6: 6. http://www.ncbi.nlm.nih.gov/pubmed/16515684.

Hanley, J J, and J P Bolam. 1997. "Synaptology of the Nigrostriatal Projection in Relation to the Compartmental Organization of the Neostriatum in the Rat." *Neuroscience* 81(2): 353–70. http://www.ncbi.nlm.nih.gov/pubmed/9300427.

Harbers, K, D Jähner, and R Jaenisch. "Microinjection of Cloned Retroviral Genomes into Mouse Zygotes: Integration and Expression in the Animal." *Nature* 293(5833): 540–42. http://www.ncbi.nlm.nih.gov/pubmed/7197324.

Harris, Glenda C, Mathieu Wimmer, and Gary Aston-Jones. 2005. "A Role for

Lateral Hypothalamic Orexin Neurons in Reward Seeking." *Nature* 437(7058): 556–59. http://www.ncbi.nlm.nih.gov/pubmed/16100511.

Harthoorn, Lucien F, Arseni Sañé, Micha Nethe, and Joop J Van Heerikhuize. 2005. "Multi-Transcriptional Profiling of Melanin-Concentrating Hormone and Orexin-Containing Neurons." *Cellular and molecular neurobiology* 25(8): 1209–23. http://www.ncbi.nlm.nih.gov/pubmed/16388333.

Haynes, Andrea C et al. 2002. "Anorectic, Thermogenic and Anti-Obesity Activity of a Selective Orexin-1 Receptor Antagonist in Ob/ob Mice." *Regulatory peptides* 104(1-3): 153–59. http://www.ncbi.nlm.nih.gov/pubmed/11830290.

Hayward, Michael D, John E Pintar, and Malcolm J Low. 2002. "Selective Reward Deficit in Mice Lacking Beta-Endorphin and Enkephalin." *The Journal of neuroscience : the official journal of the Society for Neuroscience* 22(18): 8251–58. http://www.ncbi.nlm.nih.gov/pubmed/12223579.

Hazrati, L N, A Parent, S Mitchell, and S N Haber. 1990. "Evidence for Interconnections between the Two Segments of the Globus Pallidus in Primates: A PHA-L Anterograde Tracing Study." *Brain research* 533(1): 171–75. http://www.ncbi.nlm.nih.gov/pubmed/2085730.

HEBB, C O. 1957. "Biochemical Evidence for the Neural Function of Acetylcholine." *Physiological reviews* 37(2): 196–220. http://www.ncbi.nlm.nih.gov/pubmed/13441423.

Heiman, Myriam et al. 2008. "A Translational Profiling Approach for the Molecular Characterization of CNS Cell Types." *Cell* 135(4): 738–48.

Herkenham, M, and C B Pert. 1981. "Mosaic Distribution of Opiate Receptors, Parafascicular Projections and Acetylcholinesterase in Rat Striatum." *Nature* 291(5814): 415–18. http://www.ncbi.nlm.nih.gov/pubmed/6165892.

Hernandez-Lopez, S et al. 2000. "D2 Dopamine Receptors in Striatal Medium Spiny Neurons Reduce L-Type Ca2+ Currents and Excitability via a Novel PLC[beta]1-IP3-Calcineurin-Signaling Cascade." *The Journal of neuroscience : the official journal of the Society for Neuroscience* 20(24): 8987–95. http://www.ncbi.nlm.nih.gov/pubmed/11124974.

Hernandez, L, and B G Hoebel. 1988. "Food Reward and Cocaine Increase Extracellular Dopamine in the Nucleus Accumbens as Measured by Microdialysis." *Life sciences* 42(18): 1705–12. http://www.ncbi.nlm.nih.gov/pubmed/3362036.

Herrera, Carolina Gutierrez et al. 2016. "Hypothalamic Feedforward Inhibition of Thalamocortical Network Controls Arousal and Consciousness." *Nature neuroscience* 19(2): 290–98. http://www.ncbi.nlm.nih.gov/pubmed/26691833.

Hervé, D et al. 1993. "G(olf) and Gs in Rat Basal Ganglia: Possible Involvement of G(olf) in the Coupling of Dopamine D1 Receptor with Adenylyl Cyclase." *The Journal of neuroscience : the official journal of the Society for Neuroscience* 13(5): 2237–48. http://www.ncbi.nlm.nih.gov/pubmed/8478697.

Hess, Martin E, and Jens C Brüning. 2014. "Obesity: The Need to Eat--Overruling the Homeostatic Control of Feeding." *Nature reviews. Endocrinology* 10(1): 5–6. http://www.ncbi.nlm.nih.gov/pubmed/24275739.

Hetherington, A. W., and S. W. Ranson. 1940. "Hypothalamic Lesions and Adiposity in the Rat." *The Anatomical Record* 78(2): 149–72. http://doi.wiley.com/10.1002/ar.1090780203.

Heusner, Carrie L, Lisa R Beutler, Carolyn R Houser, and Richard D Palmiter. 2008. "Deletion of GAD67 in Dopamine Receptor-1 Expressing Cells Causes Specific Motor Deficits." *Genesis (New York, N.Y. : 2000)* 46(7): 357–67. http://www.ncbi.nlm.nih.gov/pubmed/18615733.

Holt, D J, A M Graybiel, and C B Saper. 1997. "Neurochemical Architecture of the Human Striatum." *The Journal of comparative neurology* 384(1): 1–25. http://www.ncbi.nlm.nih.gov/pubmed/9214537.

Holthoff, Knut, and David Tsay. 2002. "Calcium Dynamics in Spines: Link to Synaptic Plasticity." *Experimental physiology* 87(6): 725–31. http://www.ncbi.nlm.nih.gov/pubmed/12530404.

Hope, B, B Kosofsky, S E Hyman, and E J Nestler. 1992. "Regulation of Immediate Early Gene Expression and AP-1 Binding in the Rat Nucleus Accumbens by Chronic Cocaine." *Proceedings of the National Academy of Sciences of the United States of America* 89(13): 5764–68. http://www.ncbi.nlm.nih.gov/pubmed/1631058
.

Hope, B T et al. 1994. "Induction of a Long-Lasting AP-1 Complex Composed of Altered Fos-like Proteins in Brain by Chronic Cocaine and Other Chronic Treatments." *Neuron* 13(5): 1235–44. http://www.ncbi.nlm.nih.gov/pubmed/7946359
.

Hopf, F Woodward et al. 2003. "Cooperative Activation of Dopamine D1 and D2 Receptors Increases Spike Firing of Nucleus Accumbens Neurons via G-Protein Betagamma Subunits." *The Journal of neuroscience : the official journal of the Society for Neuroscience* 23(12): 5079–87. http://www.ncbi.nlm.nih.gov/pubmed/12832531.

Huang, Yanhua H. et al. 2009. "In Vivo Cocaine Experience Generates Silent Synapses." *Neuron* 63(1): 40–47. http://linkinghub.elsevier.com/retrieve/pii/S0896627309004607.

Hyman, Steven E. 2005. "Addiction: A Disease of Learning and Memory." *The American journal of psychiatry* 162(8): 1414–22.

http://www.ncbi.nlm.nih.gov/pubmed/16055762.

Ibáñez-Sandoval, Osvaldo et al. 2011. "A Novel Functionally Distinct Subtype of Striatal Neuropeptide Y Interneuron." *The Journal of neuroscience : the official journal of the Society for Neuroscience* 31(46): 16757–69. http://www.ncbi.nlm.nih.gov/pubmed/22090502.

Íbias, Javier, Miguel Miguéns, and Ricardo Pellón. 2016. "Effects of Dopamine Agents on a Schedule-Induced Polydipsia Procedure in the Spontaneously Hypertensive Rat and in Wistar Control Rats." *Journal of psychopharmacology (Oxford, England)*. http://www.ncbi.nlm.nih.gov/pubmed/27296274.

Ikemoto, Satoshi, Mei Qin, and Zhong-Hua Liu. 2005. "The Functional Divide for Primary Reinforcement of D-Amphetamine Lies between the Medial and Lateral Ventral Striatum: Is the Division of the Accumbens Core, Shell, and Olfactory Tubercle Valid?" *The Journal of neuroscience : the official journal of the Society for Neuroscience* 25(20): 5061–65. http://www.ncbi.nlm.nih.gov/pubmed/15901788.

Imperato, A, and G Di Chiara. 1988. "Effects of Locally Applied D-1 and D-2 Receptor Agonists and Antagonists Studied with Brain Dialysis." *European journal of pharmacology* 156(3): 385–93. http://www.ncbi.nlm.nih.gov/pubmed/2905668.

Ito, R et al. 2000. "Dissociation in Conditioned Dopamine Release in the Nucleus Accumbens Core and Shell in Response to Cocaine Cues and during Cocaine-Seeking Behavior in Rats." *The Journal of neuroscience : the official journal of the Society for Neuroscience* 20(19): 7489–95. http://www.ncbi.nlm.nih.gov/pubmed/11007908.

Ito, Rutsuko, Jeffrey W Dalley, Trevor W Robbins, and Barry J Everitt. 2002. "Dopamine Release in the Dorsal Striatum during Cocaine-Seeking Behavior under the Control of a Drug-Associated Cue." *The Journal of neuroscience : the official journal of the Society for Neuroscience* 22(14): 6247–53. http://www.ncbi.nlm.nih.gov/pubmed/12122083.

Ito, Rutsuko, Trevor W Robbins, and Barry J Everitt. 2004. "Differential Control over Cocaine-Seeking Behavior by Nucleus Accumbens Core and Shell." *Nature neuroscience* 7(4): 389–97. http://www.ncbi.nlm.nih.gov/pubmed/15034590

Izzo, P N, and J P Bolam. 1988. "Cholinergic Synaptic Input to Different Parts of Spiny Striatonigral Neurons in the Rat." *The Journal of comparative neurology* 269(2): 219–34. http://www.ncbi.nlm.nih.gov/pubmed/3281983.

Jackson, M E, A S Frost, and B Moghaddam. 2001. "Stimulation of Prefrontal Cortex at Physiologically Relevant Frequencies Inhibits Dopamine Release in the Nucleus Accumbens." *Journal of neurochemistry* 78(4): 920–23.

http://www.ncbi.nlm.nih.gov/pubmed/11520912.

Jarosz, Patricia A, May T Dobal, Feleta L Wilson, and Cheryl A Schram. 2007. "Disordered Eating and Food Cravings among Urban Obese African American Women." *Eating behaviors* 8(3): 374–81. http://www.ncbi.nlm.nih.gov/pubmed/17606235.

Joel, D, and I Weiner. 1994. "The Organization of the Basal Ganglia-Thalamocortical Circuits: Open Interconnected rather than Closed Segregated." *Neuroscience* 63(2): 363–79. http://www.ncbi.nlm.nih.gov/pubmed/7891852.

Johannessen, Mona, and Ugo Moens. 2007. "Multisite Phosphorylation of the cAMP Response Element-Binding Protein (CREB) by a Diversity of Protein Kinases." *Frontiers in bioscience : a journal and virtual library* 12: 1814–32. http://www.ncbi.nlm.nih.gov/pubmed/17127423.

Johnson, Paul M, and Paul J Kenny. 2010. "Dopamine D2 Receptors in Addiction-like Reward Dysfunction and Compulsive Eating in Obese Rats." *Nature neuroscience* 13(5): 635–41. http://www.ncbi.nlm.nih.gov/pubmed/20348917.

Jönsson, E G et al. 1999. "Polymorphisms in the Dopamine D2 Receptor Gene and Their Relationships to Striatal Dopamine Receptor Density of Healthy Volunteers." *Molecular psychiatry* 4(3): 290–96. http://www.ncbi.nlm.nih.gov/pubmed/10395223.

Jordi, Emmanuelle et al. 2013. "Differential Effects of Cocaine on Histone Posttranslational Modifications in Identified Populations of Striatal Neurons." *Proceedings of the National Academy of Sciences of the United States of America* 110(23): 9511–16. http://www.ncbi.nlm.nih.gov/pubmed/23690581.

Karnani, Mahesh M, Gábor Szabó, Ferenc Erdélyi, and Denis Burdakov. 2013. "Lateral Hypothalamic GAD65 Neurons Are Spontaneously Firing and Distinct from Orexin- and Melanin-Concentrating Hormone Neurons." *The Journal of physiology* 591(4): 933–53. http://www.ncbi.nlm.nih.gov/pubmed/23184514
.

Kaufman, Marc J. 1998. "Cocaine-Induced Cerebral Vasoconstriction Detected in Humans With Magnetic Resonance Angiography." *JAMA* 279(5): 376. http://jama.jamanetwork.com/article.aspx?doi=10.1001/jama.279.5.376.

Kawaguchi, Y. 1993. "Physiological, Morphological, and Histochemical Characterization of Three Classes of Interneurons in Rat Neostriatum." *The Journal of neuroscience : the official journal of the Society for Neuroscience* 13(11): 4908–23. http://www.ncbi.nlm.nih.gov/pubmed/7693897.

Kawaguchi, Y, T Aosaki, and Y Kubota. 1997. "Cholinergic and GABAergic Interneurons in the Striatum." *Nihon shinkei seishin yakurigaku zasshi =*

Japanese journal of psychopharmacology 17(2): 87–90. http://www.ncbi.nlm.nih.gov/pubmed/9201728.

Kawaguchi, Y, C J Wilson, and P C Emson. 1990. "Projection Subtypes of Rat Neostriatal Matrix Cells Revealed by Intracellular Injection of Biocytin." *The Journal of neuroscience : the official journal of the Society for Neuroscience* 10(10): 3421–38. http://www.ncbi.nlm.nih.gov/pubmed/1698947.

Kebabian, J W, and P Greengard. 1971. "Dopamine-Sensitive Adenyl Cyclase: Possible Role in Synaptic Transmission." *Science (New York, N.Y.)* 174(4016): 1346–49. http://www.ncbi.nlm.nih.gov/pubmed/4332627.

Kelz, M B et al. 1999. "Expression of the Transcription Factor deltaFosB in the Brain Controls Sensitivity to Cocaine." *Nature* 401(6750): 272–76. http://www.ncbi.nlm.nih.gov/pubmed/10499584.

Kempadoo, Kimberly A et al. 2013. "Hypothalamic Neurotensin Projections Promote Reward by Enhancing Glutamate Transmission in the VTA." *The Journal of neuroscience : the official journal of the Society for Neuroscience* 33(18): 7618–26. http://www.ncbi.nlm.nih.gov/pubmed/23637156.

Kenny, Paul J. 2011. "Reward Mechanisms in Obesity: New Insights and Future Directions." *Neuron* 69(4): 664–79. http://www.ncbi.nlm.nih.gov/pubmed/21338878.

Kent, J L, C B Pert, and M Herkenham. 1981. "Ontogeny of Opiate Receptors in Rat Forebrain: Visualization by in Vitro Autoradiography." *Brain research* 254(4): 487–504. http://www.ncbi.nlm.nih.gov/pubmed/6272946.

Kim, Daehwan et al. 2013. "TopHat2: Accurate Alignment of Transcriptomes in the Presence of Insertions, Deletions and Gene Fusions." *Genome Biology* 14(4): R36. http://genomebiology.biomedcentral.com/articles/10.1186/gb-2013-14-4-r36.

Kim, Eun Ran, Arnold Leckstrom, and Tooru M Mizuno. 2008. "Impaired Anorectic Effect of Leptin in Neurotensin Receptor 1-Deficient Mice." *Behavioural brain research* 194(1): 66–71. http://www.ncbi.nlm.nih.gov/pubmed/18639588.

Kincaid, A E, and C J Wilson. 1996. "Corticostriatal Innervation of the Patch and Matrix in the Rat Neostriatum." *The Journal of comparative neurology* 374(4): 578–92. http://www.ncbi.nlm.nih.gov/pubmed/8910736.

Kita, H. 1993. "GABAergic Circuits of the Striatum." *Progress in brain research* 99: 51–72. http://www.ncbi.nlm.nih.gov/pubmed/8108557.

Kita, H, and S T Kitai. 1994. "The Morphology of Globus Pallidus Projection Neurons in the Rat: An Intracellular Staining Study." *Brain research* 636(2): 308–19. http://www.ncbi.nlm.nih.gov/pubmed/8012814.

Kita, H, T Kosaka, and C W Heizmann. 1990. “Parvalbumin-Immunoreactive Neurons in the Rat Neostriatum: A Light and Electron Microscopic Study.” *Brain research* 536(1-2): 1–15. http://www.ncbi.nlm.nih.gov/pubmed/2085740.

Kita, H, and Y Oomura. 1981. “Reciprocal Connections between the Lateral Hypothalamus and the Frontal Complex in the Rat: Electrophysiological and Anatomical Observations.” *Brain research* 213(1): 1–16. http://www.ncbi.nlm.nih.gov/pubmed/6165439.

Kita, Hitoshi. 2007. “Globus Pallidus External Segment.” *Progress in brain research* 160: 111–33. http://www.ncbi.nlm.nih.gov/pubmed/17499111.

Kitai, S T, and J M Deniau. 1981. “Cortical Inputs to the Subthalamus: Intracellular Analysis.” *Brain research* 214(2): 411–15. http://www.ncbi.nlm.nih.gov/pubmed/7237177.

Kitaoka, S. et al. 2007. “Prostaglandin E2 Acts on EP1 Receptor and Amplifies Both Dopamine D1 and D2 Receptor Signaling in the Striatum.” *Journal of Neuroscience* 27(47): 12900–907. http://www.jneurosci.org/cgi/doi/10.1523/JNEUROSCI.3257-07.2007.

Knoflach, F et al. 2001. “Positive Allosteric Modulators of Metabotropic Glutamate 1 Receptor: Characterization, Mechanism of Action, and Binding Site.” *Proceedings of the National Academy of Sciences of the United States of America* 98(23): 13402–7. http://www.ncbi.nlm.nih.gov/pubmed/11606768.

Koós, T, and J M Tepper. 1999. “Inhibitory Control of Neostriatal Projection Neurons by GABAergic Interneurons.” *Nature neuroscience* 2(5): 467–72. http://www.ncbi.nlm.nih.gov/pubmed/10321252.

Koós, Tibor, and James M Tepper. 2002. “Dual Cholinergic Control of Fast-Spiking Interneurons in the Neostriatum.” *The Journal of neuroscience : the official journal of the Society for Neuroscience* 22(2): 529–35. http://www.ncbi.nlm.nih.gov/pubmed/11784799.

Koos, Tibor, James M Tepper, and Charles J Wilson. 2004. “Comparison of IPSCs Evoked by Spiny and Fast-Spiking Neurons in the Neostriatum.” *The Journal of neuroscience : the official journal of the Society for Neuroscience* 24(36): 7916–22. http://www.ncbi.nlm.nih.gov/pubmed/15356204.

van der Kooy, D, and G Fishell. 1987. “Neuronal Birthdate Underlies the Development of Striatal Compartments.” *Brain research* 401(1): 155–61. http://www.ncbi.nlm.nih.gov/pubmed/3028569.

Korkotian, Eduard, David Holcman, and Menahem Segal. 2004. “Dynamic Regulation of Spine-Dendrite Coupling in Cultured Hippocampal Neurons.” *The*

European journal of neuroscience 20(10): 2649–63. http://www.ncbi.nlm.nih.gov/pubmed/15548208.

Kreitzer, Anatol C. 2009. "Physiology and Pharmacology of Striatal Neurons." *Annual review of neuroscience* 32: 127–47. http://www.ncbi.nlm.nih.gov/pubmed/19400717.

Kreitzer, Anatol C, and Robert C Malenka. 2007. "Endocannabinoid-Mediated Rescue of Striatal LTD and Motor Deficits in Parkinson's Disease Models." *Nature* 445(7128): 643–47. http://www.ncbi.nlm.nih.gov/pubmed/17287809.

Kriaucionis, Skirmantas, and Nathaniel Heintz. 2009. "The Nuclear DNA Base 5-Hydroxymethylcytosine Is Present in Purkinje Neurons and the Brain." *Science (New York, N.Y.)* 324(5929): 929–30. http://www.ncbi.nlm.nih.gov/pubmed/19372393.

Kubota, Y, and Y Kawaguchi. 2000. "Dependence of GABAergic Synaptic Areas on the Interneuron Type and Target Size." *The Journal of neuroscience : the official journal of the Society for Neuroscience* 20(1): 375–86. http://www.ncbi.nlm.nih.gov/pubmed/10627614.

Kubota, Y, S Mikawa, and Y Kawaguchi. 1993. "Neostriatal GABAergic Interneurones Contain NOS, Calretinin or Parvalbumin." *Neuroreport* 5(3): 205–8. http://www.ncbi.nlm.nih.gov/pubmed/7507722.

Kullmann, Dimitri M, and Karri P Lamsa. 2007. "Long-Term Synaptic Plasticity in Hippocampal Interneurons." *Nature reviews. Neuroscience* 8(9): 687–99. http://www.ncbi.nlm.nih.gov/pubmed/17704811.

Kupchik, Yonatan M et al. 2015. "Coding the Direct/indirect Pathways by D1 and D2 Receptors Is Not Valid for Accumbens Projections." *Nature neuroscience* 18(9): 1230–32. http://www.ncbi.nlm.nih.gov/pubmed/26214370.

Kuzhikandathil, E V, W Yu, and G S Oxford. 1998. "Human Dopamine D3 and D2L Receptors Couple to Inward Rectifier Potassium Channels in Mammalian Cell Lines." *Molecular and cellular neurosciences* 12(6): 390–402. http://www.ncbi.nlm.nih.gov/pubmed/9888991.

Kwok, R P et al. 1994. "Nuclear Protein CBP Is a Coactivator for the Transcription Factor CREB." *Nature* 370(6486): 223–26. http://www.ncbi.nlm.nih.gov/pubmed/7913207.

Kyosseva, S V, S M Owens, A D Elbein, and C N Karson. 2001. "Differential and Region-Specific Activation of Mitogen-Activated Protein Kinases Following Chronic Administration of Phencyclidine in Rat Brain." *Neuropsychopharmacology : official publication of the American College of Neuropsychopharmacology* 24(3): 267–77. http://www.ncbi.nlm.nih.gov/pubmed/11166517.

Luscher, Christian, and Kimberly M. Huber. 2010. "Group 1 mGluR-Dependent Synaptic Long-Term Depression: Mechanisms and Implications for Circuitry and Disease." *Neuron* 65(4): 445–59. http://dx.doi.org/10.1016/j.neuron.2010.01.016.

Lacey, C J et al. 2005. "GABA(B) Receptors at Glutamatergic Synapses in the Rat Striatum." *Neuroscience* 136(4): 1083–95. http://www.ncbi.nlm.nih.gov/pubmed/16226840.

Lambot, Laurie et al. 2016. "Striatopallidal Neuron NMDA Receptors Control Synaptic Connectivity, Locomotor, and Goal-Directed Behaviors." *The Journal of neuroscience : the official journal of the Society for Neuroscience* 36(18): 4976–92. http://www.ncbi.nlm.nih.gov/pubmed/27147651.

Lammel, Stephan, Daniela I Ion, Jochen Roeper, and Robert C Malenka. 2011. "Projection-Specific Modulation of Dopamine Neuron Synapses by Aversive and Rewarding Stimuli." *Neuron* 70(5): 855–62. http://www.ncbi.nlm.nih.gov/pubmed/21658580.

Land, Benjamin B et al. 2014. "Medial Prefrontal D1 Dopamine Neurons Control Food Intake." *Nature neuroscience* 17(2): 248–53. http://www.ncbi.nlm.nih.gov/pubmed/24441680.

Laque, Amanda et al. 2013. "Leptin Receptor Neurons in the Mouse Hypothalamus Are Colocalized with the Neuropeptide Galanin and Mediate Anorexigenic Leptin Action." *American journal of physiology. Endocrinology and metabolism* 304(9): E999–1011. http://www.ncbi.nlm.nih.gov/pubmed/23482448.

Lattemann, Dianne Figlewicz. 2008. "Endocrine Links between Food Reward and Caloric Homeostasis." *Appetite* 51(3): 452–55. http://www.ncbi.nlm.nih.gov/pubmed/18638514.

Lavoie, B, Y Smith, and A Parent. 1989. "Dopaminergic Innervation of the Basal Ganglia in the Squirrel Monkey as Revealed by Tyrosine Hydroxylase Immunohistochemistry." *The Journal of comparative neurology* 289(1): 36–52. http://www.ncbi.nlm.nih.gov/pubmed/2572613.

Lawford, B R et al. 2000. "The D(2) Dopamine Receptor A(1) Allele and Opioid Dependence: Association with Heroin Use and Response to Methadone Treatment." *American journal of medical genetics* 96(5): 592–98. http://www.ncbi.nlm.nih.gov/pubmed/11054765
.

Lee, Brian R et al. 2013. "Maturation of Silent Synapses in Amygdala-Accumbens Projection Contributes to Incubation of Cocaine Craving." *Nature neuroscience* 16(11): 1644–51.

http://www.ncbi.nlm.nih.gov/pubmed/24077564
.

Lee, K.-W. et al. 2006. "Cocaine-Induced Dendritic Spine Formation in D1 and D2 Dopamine Receptor-Containing Medium Spiny Neurons in Nucleus Accumbens." *Proceedings of the National Academy of Sciences* 103(9): 3399–3404. http://www.pnas.org/cgi/doi/10.1073/pnas.0511244103.

Lee, Ko-Woon et al. 2002. "Impaired D2 Dopamine Receptor Function in Mice Lacking Type 5 Adenylyl Cyclase." *The Journal of neuroscience : the official journal of the Society for Neuroscience* 22(18): 7931–40. http://www.ncbi.nlm.nih.gov/pubmed/12223546.

Lehrmann, Elin et al. 2006. "Transcriptional Changes Common to Human Cocaine, Cannabis and Phencyclidine Abuse." *PloS one* 1: e114. http://www.ncbi.nlm.nih.gov/pubmed/17205118.

Lein, Ed S et al. 2007. "Genome-Wide Atlas of Gene Expression in the Adult Mouse Brain." *Nature* 445(7124): 168–76. http://www.ncbi.nlm.nih.gov/pubmed/17151600.

Leinninger, Gina M et al. 2011. "Leptin Action via Neurotensin Neurons Controls Orexin, the Mesolimbic Dopamine System and Energy Balance." *Cell metabolism* 14(3): 313–23. http://www.ncbi.nlm.nih.gov/pubmed/21907138.

Lenoir, Magalie, Fuschia Serre, Lauriane Cantin, and Serge H Ahmed. 2007. "Intense Sweetness Surpasses Cocaine Reward." *PloS one* 2(8): e698. http://www.ncbi.nlm.nih.gov/pubmed/17668074.

Letchworth, S R et al. 2001. "Progression of Changes in Dopamine Transporter Binding Site Density as a Result of Cocaine Self-Administration in Rhesus Monkeys." *The Journal of neuroscience : the official journal of the Society for Neuroscience* 21(8): 2799–2807. http://www.ncbi.nlm.nih.gov/pubmed/11306632.

Lévesque, M, and A Parent. "Axonal Arborization of Corticostriatal and Corticothalamic Fibers Arising from Prelimbic Cortex in the Rat." *Cerebral cortex (New York, N.Y. : 1991)* 8(7): 602–13. http://www.ncbi.nlm.nih.gov/pubmed/9823481.

Lewkowski, Maxim D, Blaine Ditto, Marios Roussos, and Simon N Young. 2003. "Sweet Taste and Blood Pressure-Related Analgesia." *Pain* 106(1-2): 181–86. http://www.ncbi.nlm.nih.gov/pubmed/14581126.

Li, Juan et al. 2012. "Cocaine-Induced Dendritic Remodeling Occurs in Both D1 and D2 Dopamine Receptor-Expressing Neurons in the Nucleus Accumbens." *Neuroscience letters* 517(2): 118–22. http://www.ncbi.nlm.nih.gov/pubmed/22561554.

Liu, F C, and A M Graybiel. 1992. "Heterogeneous Development of Calbindin-D28K Expression in the Striatal Matrix." *The Journal of comparative neurology* 320(3): 304–22. http://www.ncbi.nlm.nih.gov/pubmed/1351896.

Liu, S, and S L Borgland. 2015. "Regulation of the Mesolimbic Dopamine Circuit by Feeding Peptides." *Neuroscience* 289: 19–42. http://www.ncbi.nlm.nih.gov/pubmed/25583635.

Lobo, Mary Kay et al. 2007. "Genetic Control of Instrumental Conditioning by Striatopallidal Neuron-Specific S1P Receptor Gpr6." *Nature neuroscience* 10(11): 1395–97. http://www.ncbi.nlm.nih.gov/pubmed/17934457.

Lobo, Mary Kay, and Eric J Nestler. 2011. "The Striatal Balancing Act in Drug Addiction: Distinct Roles of Direct and Indirect Pathway Medium Spiny Neurons." *Frontiers in neuroanatomy* 5: 41.

Love, Michael I, Wolfgang Huber, and Simon Anders. 2014. "Moderated Estimation of Fold Change and Dispersion for RNA-Seq Data with DESeq2." *Genome Biology* 15(12): 550. http://genomebiology.biomedcentral.com/articles/10.1186/s13059-014-0550-8.

Ludwig, D S et al. 2001. "Melanin-Concentrating Hormone Overexpression in Transgenic Mice Leads to Obesity and Insulin Resistance." *The Journal of clinical investigation* 107(3): 379–86. http://www.ncbi.nlm.nih.gov/pubmed/11160162.

Luk, K C, and A F Sadikot. 2001. "GABA Promotes Survival but Not Proliferation of Parvalbumin-Immunoreactive Interneurons in Rodent Neostriatum: An in Vivo Study with Stereology." *Neuroscience* 104(1): 93–103. http://www.ncbi.nlm.nih.gov/pubmed/11311534.

Lundblad, J R et al. 1995. "Adenoviral E1A-Associated Protein p300 as a Functional Homologue of the Transcriptional Co-Activator CBP." *Nature* 374(6517): 85–88. http://www.ncbi.nlm.nih.gov/pubmed/7870179.

Lüscher, Christian, and Vincent Pascoli. 2012. "[Optogenetic Reversal of Cocaine-Evoked Synaptic Potentiation Normalizes Behavioural Sensitization]." *Médecine sciences : M/S* 28(4): 353–55. http://www.ncbi.nlm.nih.gov/pubmed/22549856.

Lutter, Michael, and Eric J Nestler. 2009. "Homeostatic and Hedonic Signals Interact in the Regulation of Food Intake." *The Journal of nutrition* 139(3): 629–32. http://www.ncbi.nlm.nih.gov/pubmed/19176746.

Ma, Yao-Ying et al. 2014. "Bidirectional Modulation of Incubation of Cocaine Craving by Silent Synapse-Based Remodeling of Prefrontal Cortex to Accumbens Projections." *Neuron* 83(6): 1453–67. http://www.ncbi.nlm.nih.gov/pubmed/25199705.

Macintosh, F C. 1941. "The Distribution of Acetylcholine in the Peripheral and the Central Nervous System." *The Journal of physiology* 99(4): 436–42. http://www.ncbi.nlm.nih.gov/pubmed/16995263.

Mahler, Stephen V, Kyle S Smith, and Kent C Berridge. 2007. "Endocannabinoid Hedonic Hotspot for Sensory Pleasure: Anandamide in Nucleus Accumbens Shell Enhances 'Liking' of a Sweet Reward." *Neuropsychopharmacology : official publication of the American College of Neuropsychopharmacology* 32(11): 2267–78. http://www.ncbi.nlm.nih.gov/pubmed/17406653.

Majewska, A, A Tashiro, and R Yuste. 2000. "Regulation of Spine Calcium Dynamics by Rapid Spine Motility." *The Journal of neuroscience : the official journal of the Society for Neuroscience* 20(22): 8262–68. http://www.ncbi.nlm.nih.gov/pubmed/11069932.

Maldonado-Irizarry, C S, C J Swanson, and A E Kelley. 1995. "Glutamate Receptors in the Nucleus Accumbens Shell Control Feeding Behavior via the Lateral Hypothalamus." *The Journal of neuroscience : the official journal of the Society for Neuroscience* 15(10): 6779–88. http://www.ncbi.nlm.nih.gov/pubmed/7472436.

Malenka, Robert C, and Mark F Bear. 2004. "LTP and LTD: An Embarrassment of Riches." *Neuron* 44(1): 5–21. http://www.ncbi.nlm.nih.gov/pubmed/15450156.

Mameli, Manuel et al. 2009. "Cocaine-Evoked Synaptic Plasticity: Persistence in the VTA Triggers Adaptations in the NAc." *Nature neuroscience* 12(8): 1036–41. http://www.ncbi.nlm.nih.gov/pubmed/19597494.

Mameli, Manuel, Bénédicte Balland, Rafael Luján, and Christian Lüscher. 2007. "Rapid Synthesis and Synaptic Insertion of GluR2 for mGluR-LTD in the Ventral Tegmental Area." *Science (New York, N.Y.)* 317(5837): 530–33. http://www.ncbi.nlm.nih.gov/pubmed/17656725.

Marballi, K. et al. 2016. "Alcohol Consumption Induces Global Gene Expression Changes in VTA Dopaminergic Neurons." *Genes, Brain and Behavior* 15(3): 318–26. http://doi.wiley.com/10.1111/gbb.12266.

Martín-García, Elena et al. 2015. "Frustrated Expected Reward Induces Differential Transcriptional Changes in the Mouse Brain." *Addiction biology* 20(1): 22–37. http://www.ncbi.nlm.nih.gov/pubmed/25288320.

Mash, D C et al. 2000. "Serotonin Transporters Upregulate with Chronic Cocaine Use." *Journal of chemical neuroanatomy* 20(3-4): 271–80. http://www.ncbi.nlm.nih.gov/pubmed/11207425.

Matamales, Miriam et al. 2009. "Striatal Medium-Sized Spiny Neurons: Identification by Nuclear Staining and Study of Neuronal Subpopulations in BAC

Transgenic Mice." *PloS one* 4(3): e4770. http://www.ncbi.nlm.nih.gov/pubmed/19274089.

Mattiace, L A et al. "Mesostriatal Projections in BALB/c and CBA Mice: A Quantitative Retrograde Neuroanatomical Tracing Study." *Brain research bulletin* 23(1-2): 61–68. http://www.ncbi.nlm.nih.gov/pubmed/2478265.

Mayford, M et al. 1996. "Control of Memory Formation through Regulated Expression of a CaMKII Transgene." *Science (New York, N.Y.)* 274(5293): 1678–83. http://www.ncbi.nlm.nih.gov/pubmed/8939850.

McBride, W J, J M Murphy, and S Ikemoto. 1999. "Localization of Brain Reinforcement Mechanisms: Intracranial Self-Administration and Intracranial Place-Conditioning Studies." *Behavioural brain research* 101(2): 129–52. http://www.ncbi.nlm.nih.gov/pubmed/10372570.

McClung, Colleen A, and Eric J Nestler. 2003. "Regulation of Gene Expression and Cocaine Reward by CREB and DeltaFosB." *Nature neuroscience* 6(11): 1208–15. http://www.ncbi.nlm.nih.gov/pubmed/14566342.

Miura, Masami et al. 2007. "Compartment-Specific Modulation of GABAergic Synaptic Transmission by Mu-Opioid Receptor in the Mouse Striatum with Green Fluorescent Protein-Expressing Dopamine Islands." *The Journal of neuroscience : the official journal of the Society for Neuroscience* 27(36): 9721–28. http://www.ncbi.nlm.nih.gov/pubmed/17804632.

Montemurro, D G, and J A STEVENSON. 1957. "Adipsia Produced by Hypothalamic Lesions in the Rat." *Canadian journal of biochemistry and physiology* 35(1): 31–37. http://www.ncbi.nlm.nih.gov/pubmed/13396659.

Moon Edley, S, and M Herkenham. 1984. "Comparative Development of Striatal Opiate Receptors and Dopamine Revealed by Autoradiography and Histofluorescence." *Brain research* 305(1): 27–42. http://www.ncbi.nlm.nih.gov/pubmed/6331599.

Moore, R Y, A E Halaris, and B E Jones. 1978. "Serotonin Neurons of the Midbrain Raphe: Ascending Projections." *The Journal of comparative neurology* 180(3): 417–38. http://www.ncbi.nlm.nih.gov/pubmed/77865.

Moratalla, R et al. 1992. "Differential Vulnerability of Primate Caudate-Putamen and Striosome-Matrix Dopamine Systems to the Neurotoxic Effects of 1-Methyl-4-Phenyl-1,2,3,6-Tetrahydropyridine." *Proceedings of the National Academy of Sciences of the United States of America* 89(9): 3859–63. http://www.ncbi.nlm.nih.gov/pubmed/1570304.

Moratalla, R, M Vallejo, B Elibol, and A M Graybiel. 1996. "D1-Class Dopamine Receptors Influence Cocaine-Induced Persistent Expression of Fos-Related Proteins in Striatum." *Neuroreport* 8(1): 1–5. http://www.ncbi.nlm.nih.gov/pubmed/9051741.

Moriguchi, T et al. 1999. “Neurons Containing Orexin in the Lateral Hypothalamic Area of the Adult Rat Brain Are Activated by Insulin-Induced Acute Hypoglycemia.” *Neuroscience letters* 264(1-3): 101–4. http://www.ncbi.nlm.nih.gov/pubmed/10320024.

Morton, G. J., and M. W. Schwartz. 2011. “Leptin and the Central Nervous System Control of Glucose Metabolism.” *Physiological Reviews* 91(2): 389–411. http://physrev.physiology.org/cgi/doi/10.1152/physrev.00007.2010.

Moulédous, Lionel et al. 2003. “Proteomic Analysis of Immunostained, Laser-Capture Microdissected Brain Samples.” *Electrophoresis* 24(1-2): 296–302. http://www.ncbi.nlm.nih.gov/pubmed/12652601.

Muñoz-Manchado, A B et al. 2016. “Novel Striatal GABAergic Interneuron Populations Labeled in the 5HT3a(EGFP) Mouse.” *Cerebral cortex (New York, N.Y. : 1991)* 26(1): 96–105. http://www.ncbi.nlm.nih.gov/pubmed/25146369.

Murase, S et al. 1993. “Prefrontal Cortex Regulates Burst Firing and Transmitter Release in Rat Mesolimbic Dopamine Neurons Studied in Vivo.” *Neuroscience letters* 157(1): 53–56. http://www.ncbi.nlm.nih.gov/pubmed/7901810.

Murray, Jennifer E, Barry J Everitt, and David Belin. 2012. “N-Acetylcysteine Reduces Early- and Late-Stage Cocaine Seeking without Affecting Cocaine Taking in Rats.” *Addiction biology* 17(2): 437–40. http://www.ncbi.nlm.nih.gov/pubmed/21521427.

Muschamp, John W et al. 2011. “Activation of CREB in the Nucleus Accumbens Shell Produces Anhedonia and Resistance to Extinction of Fear in Rats.” *The Journal of neuroscience : the official journal of the Society for Neuroscience* 31(8): 3095–3103. http://www.ncbi.nlm.nih.gov/pubmed/21414930.

Nakamura, G R et al. 1992. “Monoclonal Antibodies to the Extracellular Domain of HIV-1IIIB gp160 That Neutralize Infectivity, Block Binding to CD4, and React with Diverse Isolates.” *AIDS research and human retroviruses* 8(11): 1875–85. http://www.ncbi.nlm.nih.gov/pubmed/1283308.

Nakanishi, H, H Kita, and S T Kitai. 1987. “Intracellular Study of Rat Substantia Nigra Pars Reticulata Neurons in an in Vitro Slice Preparation: Electrical Membrane Properties and Response Characteristics to Subthalamic Stimulation.” *Brain research* 437(1): 45–55. http://www.ncbi.nlm.nih.gov/pubmed/3427482.

Nambu, A, M Takada, M Inase, and H Tokuno. 1996. “Dual Somatotopical Representations in the Primate Subthalamic Nucleus: Evidence for Ordered but Reversed Body-Map Transformations from the Primary Motor Cortex and the

Supplementary Motor Area." *The Journal of neuroscience : the official journal of the Society for Neuroscience* 16(8): 2671–83. http://www.ncbi.nlm.nih.gov/pubmed/8786443.

Narumiya, S, Y Sugimoto, and F Ushikubi. 1999. "Prostanoid Receptors: Structures, Properties, and Functions." *Physiological reviews* 79(4): 1193–1226. http://www.ncbi.nlm.nih.gov/pubmed/10508233.

NAUTA, W J. 1958. "Hippocampal Projections and Related Neural Pathways to the Midbrain in the Cat." *Brain : a journal of neurology* 81(3): 319–40. http://www.ncbi.nlm.nih.gov/pubmed/13596467.

Neisewander, J L et al. 2000. "Fos Protein Expression and Cocaine-Seeking Behavior in Rats after Exposure to a Cocaine Self-Administration Environment." *The Journal of neuroscience : the official journal of the Society for Neuroscience* 20(2): 798–805. http://www.ncbi.nlm.nih.gov/pubmed/10632609.

Nelson, Alexandra B. et al. 2014. "Striatal Cholinergic Interneurons Drive GABA Release from Dopamine Terminals." *Neuron* 82(1): 63–70. http://linkinghub.elsevier.com/retrieve/pii/S0896627314000543.

Nestler, E J, M Barrot, and D W Self. 2001. "DeltaFosB: A Sustained Molecular Switch for Addiction." *Proceedings of the National Academy of Sciences of the United States of America* 98(20): 11042–46. http://www.ncbi.nlm.nih.gov/pubmed/11572966.

Nestler, Eric J. 2008. "Review. Transcriptional Mechanisms of Addiction: Role of DeltaFosB." *Philosophical transactions of the Royal Society of London. Series B, Biological sciences* 363(1507): 3245–55. http://www.ncbi.nlm.nih.gov/pubmed/18640924.

Nicola, Saleem M. 2007. "The Nucleus Accumbens as Part of a Basal Ganglia Action Selection Circuit." *Psychopharmacology* 191(3): 521–50. http://www.ncbi.nlm.nih.gov/pubmed/16983543.

Nieh, Edward H et al. 2015. "Decoding Neural Circuits That Control Compulsive Sucrose Seeking." *Cell* 160(3): 528–41. http://www.ncbi.nlm.nih.gov/pubmed/25635460.

Nieuwenhuys, R, L M Geeraedts, and J G Veening. 1982. "The Medial Forebrain Bundle of the Rat. I. General Introduction." *The Journal of comparative neurology* 206(1): 49–81. http://www.ncbi.nlm.nih.gov/pubmed/6124562.

Nishi, Akinori et al. 2008. "Distinct Roles of PDE4 and PDE10A in the Regulation of cAMP/PKA Signaling in the Striatum." *The Journal of neuroscience : the official journal of the Society for Neuroscience* 28(42): 10460–71.

http://www.ncbi.nlm.nih.gov/pubmed/18923023.

Noble, E P et al. 1993. "Allelic Association of the D2 Dopamine Receptor Gene with Cocaine Dependence." *Drug and alcohol dependence* 33(3): 271–85. http://www.ncbi.nlm.nih.gov/pubmed/8261891.

Noble, E P et al. 2000. "Addiction and Its Reward Process through Polymorphisms of the D2 Dopamine Receptor Gene: A Review." *European psychiatry : the journal of the Association of European Psychiatrists* 15(2): 79–89. http://www.ncbi.nlm.nih.gov/pubmed/10881203.

Noguchi, Jun, Masanori Matsuzaki, Graham C R Ellis-Davies, and Haruo Kasai. 2005. "Spine-Neck Geometry Determines NMDA Receptor-Dependent Ca2+ Signaling in Dendrites." *Neuron* 46(4): 609–22. http://www.ncbi.nlm.nih.gov/pubmed/15944129.

Norgren, R, A Hajnal, and S S Mungarndee. 2006. "Gustatory Reward and the Nucleus Accumbens." *Physiology & behavior* 89(4): 531–35. http://www.ncbi.nlm.nih.gov/pubmed/16822531.

Norrholm, S D et al. 2003. "Cocaine-Induced Proliferation of Dendritic Spines in Nucleus Accumbens Is Dependent on the Activity of Cyclin-Dependent Kinase-5." *Neuroscience* 116(1): 19–22. http://www.ncbi.nlm.nih.gov/pubmed/12535933.

O'Connor, Eoin C. et al. 2015. "Accumbal D1R Neurons Projecting to Lateral Hypothalamus Authorize Feeding." *Neuron* 88(3): 553–64.

OLDS, J, and P MILNER. 1954. "Positive Reinforcement Produced by Electrical Stimulation of Septal Area and Other Regions of Rat Brain." *Journal of comparative and physiological psychology* 47(6): 419–27. http://www.ncbi.nlm.nih.gov/pubmed/13233369.

Olson, L, A Seiger, and K Fuxe. 1972. "Heterogeneity of Striatal and Limbic Dopamine Innervation: Highly Fluorescent Islands in Developing and Adult Rats." *Brain research* 44(1): 283–88. http://www.ncbi.nlm.nih.gov/pubmed/4403485.

Parent, A, and Y Smith. 1987. "Organization of Efferent Projections of the Subthalamic Nucleus in the Squirrel Monkey as Revealed by Retrograde Labeling Methods." *Brain research* 436(2): 296–310. http://www.ncbi.nlm.nih.gov/pubmed/3435830.

Pert, C B, M J Kuhar, and S H Snyder. 1976. "Opiate Receptor: Autoradiographic Localization in Rat Brain." *Proceedings of the National Academy of Sciences of the United States of America* 73(10): 3729–33. http://www.ncbi.nlm.nih.gov/pubmed/185626.

Petryszyn, Sarah, Jean-Martin Beaulieu, André Parent, and Martin Parent. 2014. "Distribution and Morphological Characteristics of Striatal Interneurons Expressing Calretinin in Mice: A Comparison with Human and Nonhuman Primates." *Journal of chemical neuroanatomy* 59-60: 51–61. http://www.ncbi.nlm.nih.gov/pubmed/24960462.

Pfaus, J G, G Damsma, D Wenkstern, and H C Fibiger. 1995. "Sexual Activity Increases Dopamine Transmission in the Nucleus Accumbens and Striatum of Female Rats." *Brain research* 693(1-2): 21–30. http://www.ncbi.nlm.nih.gov/pubmed/8653411.

Polli, J W, and R L Kincaid. 1994. "Expression of a Calmodulin-Dependent Phosphodiesterase Isoform (PDE1B1) Correlates with Brain Regions Having Extensive Dopaminergic Innervation." *The Journal of neuroscience : the official journal of the Society for Neuroscience* 14(3 Pt 1): 1251–61. http://www.ncbi.nlm.nih.gov/pubmed/8120623.

Porrino, Linda J, James B Daunais, Hilary R Smith, and Michael A Nader. 2004. "The Expanding Effects of Cocaine: Studies in a Nonhuman Primate Model of Cocaine Self-Administration." *Neuroscience & Biobehavioral Reviews* 27(8): 813–20. http://linkinghub.elsevier.com/retrieve/pii/S0149763403001416.

Prensa, L, J M Giménez-Amaya, and A Parent. 1999. "Chemical Heterogeneity of the Striosomal Compartment in the Human Striatum." *The Journal of comparative neurology* 413(4): 603–18. http://www.ncbi.nlm.nih.gov/pubmed/10495446.

Qu, D et al. 1996. "A Role for Melanin-Concentrating Hormone in the Central Regulation of Feeding Behaviour." *Nature* 380(6571): 243–47. http://www.ncbi.nlm.nih.gov/pubmed/8637571.

Quarta, Davide, and Ilse Smolders. 2014. "Rewarding, Reinforcing and Incentive Salient Events Involve Orexigenic Hypothalamic Neuropeptides Regulating Mesolimbic Dopaminergic Neurotransmission." *European Journal of Pharmaceutical Sciences* 57: 2–10. http://linkinghub.elsevier.com/retrieve/pii/S0928098714000232.

Ragsdale, C W, and A M Graybiel. 1990. "A Simple Ordering of Neocortical Areas Established by the Compartmental Organization of Their Striatal Projections." *Proceedings of the National Academy of Sciences of the United States of America* 87(16): 6196–99. http://www.ncbi.nlm.nih.gov/pubmed/1696719.

Raju, Dinesh V et al. 2006. "Differential Synaptology of vGluT2-Containing Thalamostriatal Afferents between the Patch and Matrix Compartments in Rats." *The Journal of comparative neurology* 499(2): 231–43. http://www.ncbi.nlm.nih.gov/pubmed/16977615.

Rasmussen, Erin B, and Sally L Huskinson. 2008. "Effects of Rimonabant on Behavior Maintained by Progressive Ratio Schedules of Sucrose Reinforcement in Obese Zucker (Fa/fa) Rats." *Behavioural pharmacology* 19(7): 735–42. http://www.ncbi.nlm.nih.gov/pubmed/18797250.

Redish, A David. 2004. "Addiction as a Computational Process Gone Awry." *Science (New York, N.Y.)* 306(5703): 1944–47. http://www.ncbi.nlm.nih.gov/pubmed/15591205.

Redish, A David, Steve Jensen, and Adam Johnson. 2008. "A Unified Framework for Addiction: Vulnerabilities in the Decision Process." *The Behavioral and brain sciences* 31(4): 415–37; discussion 437–87. http://www.ncbi.nlm.nih.gov/pubmed/18662461.

Reid, M S, and S P Berger. 1996. "Evidence for Sensitization of Cocaine-Induced Nucleus Accumbens Glutamate Release." *Neuroreport* 7(7): 1325–29. http://www.ncbi.nlm.nih.gov/pubmed/8817559.

Reith, M E, B E Meisler, and A Lajtha. 1985. "Locomotor Effects of Cocaine, Cocaine Congeners, and Local Anesthetics in Mice." *Pharmacology, biochemistry, and behavior* 23(5): 831–36. http://www.ncbi.nlm.nih.gov/pubmed/2417262.

Renthal, William et al. 2009. "Genome-Wide Analysis of Chromatin Regulation by Cocaine Reveals a Role for Sirtuins." *Neuron* 62(3): 335–48. http://www.ncbi.nlm.nih.gov/pubmed/19447090.

Ribak, C E, J E Vaughn, and E Roberts. 1979. "The GABA Neurons and Their Axon Terminals in Rat Corpus Striatum as Demonstrated by GAD Immunocytochemistry." *The Journal of comparative neurology* 187(2): 261–83. http://www.ncbi.nlm.nih.gov/pubmed/226567.

Richard, Denis, Benjamin Guesdon, and Elena Timofeeva. 2009. "The Brain Endocannabinoid System in the Regulation of Energy Balance." *Best practice & research. Clinical endocrinology & metabolism* 23(1): 17–32. http://www.ncbi.nlm.nih.gov/pubmed/19285258.

Ritz, M C, E J Cone, and M J Kuhar. 1990. "Cocaine Inhibition of Ligand Binding at Dopamine, Norepinephrine and Serotonin Transporters: A Structure-Activity Study." *Life sciences* 46(9): 635–45. http://www.ncbi.nlm.nih.gov/pubmed/2308472.

Roberts, D C, and G F Koob. 1982. "Disruption of Cocaine Self-Administration Following 6-Hydroxydopamine Lesions of the Ventral Tegmental Area in Rats." *Pharmacology, biochemistry, and behavior* 17(5): 901–4. http://www.ncbi.nlm.nih.gov/pubmed/6817350.

Robinson, T E, and B Kolb. 1997. “Persistent Structural Modifications in Nucleus Accumbens and Prefrontal Cortex Neurons Produced by Previous Experience with Amphetamine.” *The Journal of neuroscience : the official journal of the Society for Neuroscience* 17(21): 8491–97. http://www.ncbi.nlm.nih.gov/pubmed/9334421.

Robison, Alfred J et al. 2013. “Behavioral and Structural Responses to Chronic Cocaine Require a Feedforward Loop Involving ΔFosB and Calcium/calmodulin-Dependent Protein Kinase II in the Nucleus Accumbens Shell.” *The Journal of neuroscience : the official journal of the Society for Neuroscience* 33(10): 4295–4307.

Root, David H, Roberto I Melendez, Laszlo Zaborszky, and T Celeste Napier. 2015. “The Ventral Pallidum: Subregion-Specific Functional Anatomy and Roles in Motivated Behaviors.” *Progress in neurobiology* 130: 29–70. http://www.ncbi.nlm.nih.gov/pubmed/25857550.

Rosin, Diane L et al. 2003. “Hypothalamic Orexin (Hypocretin) Neurons Express Vesicular Glutamate Transporters VGLUT1 or VGLUT2.” *The Journal of comparative neurology* 465(4): 593–603. http://www.ncbi.nlm.nih.gov/pubmed/12975818.

Rymar, Vladimir V, Rachel Sasseville, Kelvin C Luk, and Abbas F Sadikot. 2004. “Neurogenesis and Stereological Morphometry of Calretinin-Immunoreactive GABAergic Interneurons of the Neostriatum.” *The Journal of comparative neurology* 469(3): 325–39. http://www.ncbi.nlm.nih.gov/pubmed/14730585.

Sabatini, Bernardo L, Thomas G Oertner, and Karel Svoboda. 2002. “The Life Cycle of Ca(2+) Ions in Dendritic Spines.” *Neuron* 33(3): 439–52. http://www.ncbi.nlm.nih.gov/pubmed/1832230.

Saka, E, B Elibol, S Erdem, and T Dalkara. 1999. “Compartmental Changes in Expression of c-Fos and FosB Proteins in Intact and Dopamine-Depleted Striatum after Chronic Apomorphine Treatment.” *Brain research* 825(1-2): 104–14. http://www.ncbi.nlm.nih.gov/pubmed/10216178.

Sakurai, T. 1999. “Orexins and Orexin Receptors: Implication in Feeding Behavior.” *Regulatory peptides* 85(1): 25–30. http://www.ncbi.nlm.nih.gov/pubmed/10588447.

Salamone, J D et al. 1993. “The Role of Brain Dopamine in Response Initiation: Effects of Haloperidol and Regionally Specific Dopamine Depletions on the Local Rate of Instrumental Responding.” *Brain research* 628(1-2): 218–26. http://www.ncbi.nlm.nih.gov/pubmed/8313150.

Salamone, J D, M J Zigmond, and E M Stricker. 1990. “Characterization of the Impaired Feeding Behavior in Rats given Haloperidol or Dopamine-Depleting Brain Lesions.” *Neuroscience* 39(1): 17–24. http://www.ncbi.nlm.nih.gov/pubmed/2128534.

Salinas, Armando G, Margaret I Davis, David M Lovinger, and Yolanda Mateo. 2016. "Dopamine Dynamics and Cocaine Sensitivity Differ between Striosome and Matrix Compartments of the Striatum." *Neuropharmacology* 108: 275–83. http://www.ncbi.nlm.nih.gov/pubmed/27036891.

Salzmann, Julie et al. 2003. "Importance of ERK Activation in Behavioral and Biochemical Effects Induced by MDMA in Mice." *British journal of pharmacology* 140(5): 831–38. http://www.ncbi.nlm.nih.gov/pubmed/14517176.

Saper, Clifford B., Thomas C. Chou, and Joel K. Elmquist. 2002. "The Need to Feed." *Neuron* 36(2): 199–211. http://www.sciencedirect.com/science/article/pii/S0896627302009698.

Saunders, Arpiar et al. 2015. "A Direct GABAergic Output from the Basal Ganglia to Frontal Cortex." *Nature* 521(7550): 85–89. http://www.ncbi.nlm.nih.gov/pubmed/25739505.

Schroeder, Jason P et al. 2008. "Cue-Induced Reinstatement of Alcohol-Seeking Behavior Is Associated with Increased ERK1/2 Phosphorylation in Specific Limbic Brain Regions: Blockade by the mGluR5 Antagonist MPEP." *Neuropharmacology* 55(4): 546–54. http://www.ncbi.nlm.nih.gov/pubmed/18619984.

Schwartz, Bryan G, Shereif Rezkalla, and Robert A Kloner. 2010. "Cardiovascular Effects of Cocaine." *Circulation* 122(24): 2558–69. http://www.ncbi.nlm.nih.gov/pubmed/21156654.

See, R E, J C Elliott, and M W Feltenstein. 2007. "The Role of Dorsal vs Ventral Striatal Pathways in Cocaine-Seeking Behavior after Prolonged Abstinence in Rats." *Psychopharmacology* 194(3): 321–31. http://www.ncbi.nlm.nih.gov/pubmed/17589830.

Sharp, B M et al. 2011. "Gene Expression in Accumbens GABA Neurons from Inbred Rats with Different Drug-Taking Behavior." *Genes, brain, and behavior* 10(7): 778–88. http://www.ncbi.nlm.nih.gov/pubmed/21745336.

Shaywitz, A J, and M E Greenberg. 1999. "CREB: A Stimulus-Induced Transcription Factor Activated by a Diverse Array of Extracellular Signals." *Annual review of biochemistry* 68: 821–61. http://www.ncbi.nlm.nih.gov/pubmed/10872467.

Shen, Hai-Ying, and Jiang-Fan Chen. 2009. "Adenosine A(2A) Receptors in Psychopharmacology: Modulators of Behavior, Mood and Cognition." *Current neuropharmacology* 7(3): 195–206. http://www.ncbi.nlm.nih.gov/pubmed/20190961.

Shiflett, Michael W, Robert A Brown, and Bernard W Balleine. 2010. "Acquisition and Performance of Goal-Directed Instrumental Actions Depends

on ERK Signaling in Distinct Regions of Dorsal Striatum in Rats." *The Journal of neuroscience : the official journal of the Society for Neuroscience* 30(8): 2951–59. http://www.ncbi.nlm.nih.gov/pubmed/20181592.

Shimada, M et al. 1998. "Mice Lacking Melanin-Concentrating Hormone Are Hypophagic and Lean." *Nature* 396(6712): 670–74. http://www.ncbi.nlm.nih.gov/pubmed/9872314.

Shuen, Jessica A, Meng Chen, Bernd Gloss, and Nicole Calakos. 2008. "Drd1a-tdTomato BAC Transgenic Mice for Simultaneous Visualization of Medium Spiny Neurons in the Direct and Indirect Pathways of the Basal Ganglia." *The Journal of neuroscience : the official journal of the Society for Neuroscience* 28(11): 2681–85. http://www.ncbi.nlm.nih.gov/pubmed/18337395.

Sikela, James M. et al. 2006. "DNA Microarray and Proteomic Strategies for Understanding Alcohol Action." *Alcoholism: Clinical and Experimental Research* 30(4): 700–708. http://doi.wiley.com/10.1111/j.1530-0277.2006.00081.x.

Small, Dana M, Marilyn Jones-Gotman, and Alain Dagher. 2003. "Feeding-Induced Dopamine Release in Dorsal Striatum Correlates with Meal Pleasantness Ratings in Healthy Human Volunteers." *NeuroImage* 19(4): 1709–15. http://www.ncbi.nlm.nih.gov/pubmed/12948725.

Smith, Y et al. 1994. "Synaptic Relationships between Dopaminergic Afferents and Cortical or Thalamic Input in the Sensorimotor Territory of the Striatum in Monkey." *The Journal of comparative neurology* 344(1): 1–19. http://www.ncbi.nlm.nih.gov/pubmed/7914894.

Smith, Y, and J P Bolam. 1989. "Neurons of the Substantia Nigra Reticulata Receive a Dense GABA-Containing Input from the Globus Pallidus in the Rat." *Brain research* 493(1): 160–67. http://www.ncbi.nlm.nih.gov/pubmed/2476197.

Snyder, G L, A A Fienberg, R L Huganir, and P Greengard. 1998. "A dopamine/D1 Receptor/protein Kinase A/dopamine- and cAMP-Regulated Phosphoprotein (Mr 32 kDa)/protein Phosphatase-1 Pathway Regulates Dephosphorylation of the NMDA Receptor." *The Journal of neuroscience : the official journal of the Society for Neuroscience* 18(24): 10297–303. http://www.ncbi.nlm.nih.gov/pubmed/9852567.

Soghomonian, J J, L Descarries, and K C Watkins. 1989. "Serotonin Innervation in Adult Rat Neostriatum. II. Ultrastructural Features: A Radioautographic and Immunocytochemical Study." *Brain research* 481(1): 67–86. http://www.ncbi.nlm.nih.gov/pubmed/2706468.

Spanagel, R, A Herz, and T S Shippenberg. 1992. "Opposing Tonically Active Endogenous Opioid Systems Modulate the Mesolimbic Dopaminergic Pathway." *Proceedings of the National Academy of Sciences of the United States of America*

89(6): 2046–50. http://www.ncbi.nlm.nih.gov/pubmed/1347943.

Spano, P F et al. 1978. "Interaction of Metergoline with Striatal Dopamine System." *Life sciences* 23(24): 2383–91. http://www.ncbi.nlm.nih.gov/pubmed/745518.

Stamatakis, Alice M et al. 2013. "A Unique Population of Ventral Tegmental Area Neurons Inhibits the Lateral Habenula to Promote Reward." *Neuron* 80(4): 1039–53. http://www.ncbi.nlm.nih.gov/pubmed/24267654.

Stice, E, S Spoor, C Bohon, and D M Small. 2008. "Relation between Obesity and Blunted Striatal Response to Food Is Moderated by TaqIA A1 Allele." *Science (New York, N.Y.)* 322(5900): 449–52. http://www.ncbi.nlm.nih.gov/pubmed/18927395.

Stoof, J C, and J W Kebabian. 1981. "Opposing Roles for D-1 and D-2 Dopamine Receptors in Efflux of Cyclic AMP from Rat Neostriatum." *Nature* 294(5839): 366–68. http://www.ncbi.nlm.nih.gov/pubmed/6273735.

Stratford, T R, and A E Kelley. 1997. "GABA in the Nucleus Accumbens Shell Participates in the Central Regulation of Feeding Behavior." *The Journal of neuroscience : the official journal of the Society for Neuroscience* 17(11): 4434–40. http://www.ncbi.nlm.nih.gov/pubmed/9151760.

Surmeier, D J et al. 1995. "Modulation of Calcium Currents by a D1 Dopaminergic Protein Kinase/phosphatase Cascade in Rat Neostriatal Neurons." *Neuron* 14(2): 385–97. http://www.ncbi.nlm.nih.gov/pubmed/7531987.

Surmeier, D James. 2007. "Calcium, Ageing, and Neuronal Vulnerability in Parkinson's Disease." *The Lancet. Neurology* 6(10): 933–38. http://www.ncbi.nlm.nih.gov/pubmed/17884683.

Suzuki, Keisuke, Channa N Jayasena, and Stephen R Bloom. 2012. "Obesity and Appetite Control." *Experimental diabetes research* 2012: 824305. http://www.ncbi.nlm.nih.gov/pubmed/22899902.

Taber, M T, and H C Fibiger. 1995. "Electrical Stimulation of the Prefrontal Cortex Increases Dopamine Release in the Nucleus Accumbens of the Rat: Modulation by Metabotropic Glutamate Receptors." *The Journal of neuroscience : the official journal of the Society for Neuroscience* 15(5 Pt 2): 3896–3904. http://www.ncbi.nlm.nih.gov/pubmed/7751954.

Tennyson, V M et al. 1972. "The Developing Neostriatum of the Rabbit: Correlation of Fluorescence Histochemistry, Electron Microscopy, Endogenous Dopamine Levels, and (3 H)dopamine Uptake." *Brain research* 46: 251–85. http://www.ncbi.nlm.nih.gov/pubmed/4635366.

Tepper, James M, Fatuel Tecuapetla, Tibor Koós, and Osvaldo Ibáñez-Sandoval. 2010. "Heterogeneity and Diversity of Striatal GABAergic

Interneurons." *Frontiers in neuroanatomy* 4: 150. http://www.ncbi.nlm.nih.gov/pubmed/21228905.

Thomas, M J, C Beurrier, A Bonci, and R C Malenka. 2001. "Long-Term Depression in the Nucleus Accumbens: A Neural Correlate of Behavioral Sensitization to Cocaine." *Nature neuroscience* 4(12): 1217–23. http://www.ncbi.nlm.nih.gov/pubmed/11694884.

Thompson, R H, N S Canteras, and L W Swanson. 1996. "Organization of Projections from the Dorsomedial Nucleus of the Hypothalamus: A PHA-L Study in the Rat." *The Journal of comparative neurology* 376(1): 143–73. http://www.ncbi.nlm.nih.gov/pubmed/8946289.

Thorndike, Edward L. 1898. "Animal Intelligence: An Experimental Study of the Associative Processes in Animals." *The Psychological Review: Monograph Supplements* 2(4): i – 109. http://doi.apa.org/getdoi.cfm?doi=10.1037/h0092987.

Thornton-Jones, Zoë D, Steven P Vickers, and Peter G Clifton. 2005. "The Cannabinoid CB1 Receptor Antagonist SR141716A Reduces Appetitive and Consummatory Responses for Food." *Psychopharmacology* 179(2): 452–60. http://www.ncbi.nlm.nih.gov/pubmed/15821957.

Threlfell, Sarah et al. 2012. "Striatal Dopamine Release Is Triggered by Synchronized Activity in Cholinergic Interneurons." *Neuron* 75(1): 58–64.

Tong, Z Y, P G Overton, and D Clark. 1996. "Stimulation of the Prefrontal Cortex in the Rat Induces Patterns of Activity in Midbrain Dopaminergic Neurons Which Resemble Natural Burst Events." *Synapse (New York, N.Y.)* 22(3): 195–208. http://www.ncbi.nlm.nih.gov/pubmed/9132987.

Tonini, Raffaella et al. 2006. "ERK-Dependent Modulation of Cerebellar Synaptic Plasticity after Chronic Delta9-Tetrahydrocannabinol Exposure." *The Journal of neuroscience : the official journal of the Society for Neuroscience* 26(21): 5810–18. http://www.ncbi.nlm.nih.gov/pubmed/16723539.

Tønnesen, Jan, Gergely Katona, Balázs Rózsa, and U Valentin Nägerl. 2014. "Spine Neck Plasticity Regulates Compartmentalization of Synapses." *Nature neuroscience* 17(5): 678–85. http://www.ncbi.nlm.nih.gov/pubmed/24657968.

Ulery-Reynolds, P G et al. 2009. "Phosphorylation of DeltaFosB Mediates Its Stability in Vivo." *Neuroscience* 158(2): 369–72. http://www.ncbi.nlm.nih.gov/pubmed/19041372.

Ungless, M A, J L Whistler, R C Malenka, and A Bonci. 2001. "Single Cocaine Exposure in Vivo Induces Long-Term Potentiation in Dopamine Neurons." *Nature* 411(6837): 583–87. http://www.ncbi.nlm.nih.gov/pubmed/11385572.

Unzai, Tomo, Eriko Kuramoto, Takeshi Kaneko, and Fumino Fujiyama. 2015.

"Quantitative Analyses of the Projection of Individual Neurons from the Midline Thalamic Nuclei to the Striosome and Matrix Compartments of the Rat Striatum." *Cerebral cortex (New York, N.Y. : 1991)*.

Valjent, Emmanuel et al. 2004. "Addictive and Non-Addictive Drugs Induce Distinct and Specific Patterns of ERK Activation in Mouse Brain." *The European journal of neuroscience* 19(7): 1826–36. http://www.ncbi.nlm.nih.gov/pubmed/15078556.

Valjent, Emmanuel et al. 2004. 2009. "Looking BAC at Striatal Signaling: Cell-Specific Analysis in New Transgenic Mice." *Trends in neurosciences* 32(10): 538–47. http://www.ncbi.nlm.nih.gov/pubmed/19765834.

Vanderschuren, L. J. M. J. 2005. "Involvement of the Dorsal Striatum in Cue-Controlled Cocaine Seeking." *Journal of Neuroscience* 25(38): 8665–70. http://www.jneurosci.org/cgi/doi/10.1523/JNEUROSCI.0925-05.2005.

Veening, J G, F M Cornelissen, and P A Lieven. 1980. "The Topical Organization of the Afferents to the Caudatoputamen of the Rat. A Horseradish Peroxidase Study." *Neuroscience* 5(7): 1253–68. http://www.ncbi.nlm.nih.gov/pubmed/7402468.

Volkow, N D et al. 1993. "Decreased Dopamine D2 Receptor Availability Is Associated with Reduced Frontal Metabolism in Cocaine Abusers." *Synapse (New York, N.Y.)* 14(2): 169–77. http://www.ncbi.nlm.nih.gov/pubmed/8101394.

Voorn, Pieter et al. 2004. "Putting a Spin on the Dorsal-Ventral Divide of the Striatum." *Trends in neurosciences* 27(8): 468–74. http://www.ncbi.nlm.nih.gov/pubmed/15271494.

Walters, Carrie L., Yuo-Chen Kuo, and Julie A. Blendy. 2003. "Differential Distribution of CREB in the Mesolimbic Dopamine Reward Pathway." *Journal of Neurochemistry* 87(5): 1237–44. http://doi.wiley.com/10.1046/j.1471-4159.2003.02090.x.

Wang, G J et al. 2001. "Brain Dopamine and Obesity." *Lancet (London, England)* 357(9253): 354–57. http://www.ncbi.nlm.nih.gov/pubmed/11210998.

Wang, Hong et al. 2009. "Norbin Is an Endogenous Regulator of Metabotropic Glutamate Receptor 5 Signaling." *Science (New York, N.Y.)* 326(5959): 1554–57. http://www.ncbi.nlm.nih.gov/pubmed/20007903.

Wang, Hong et al 2015. "Norbin Ablation Results in Defective Adult Hippocampal Neurogenesis and Depressive-like Behavior in Mice." *Proceedings of the National Academy of Sciences of the United States of America* 112(31): 9745–50. http://www.ncbi.nlm.nih.gov/pubmed/26195764.

Wassum, K M, S B Ostlund, N T Maidment, and B W Balleine. 2009. "Distinct Opioid Circuits Determine the Palatability and the Desirability of Rewarding Events." *Proceedings of the National Academy of Sciences of the United States of America* 106(30): 12512–17. http://www.ncbi.nlm.nih.gov/pubmed/19597155.

Watabe-Uchida, Mitsuko et al. 2012. "Whole-Brain Mapping of Direct Inputs to Midbrain Dopamine Neurons." *Neuron* 74(5): 858–73. http://www.ncbi.nlm.nih.gov/pubmed/22681690.

Watt, Alanna J et al. 2004. "A Proportional but Slower NMDA Potentiation Follows AMPA Potentiation in LTP." *Nature neuroscience* 7(5): 518–24. http://www.ncbi.nlm.nih.gov/pubmed/15048122.

Werme, Martin et al. 2002. "Delta FosB Regulates Wheel Running." *The Journal of neuroscience : the official journal of the Society for Neuroscience* 22(18): 8133–38. http://www.ncbi.nlm.nih.gov/pubmed/12223567.

Whitelaw, R B, A Markou, T W Robbins, and B J Everitt. 1996. "Excitotoxic Lesions of the Basolateral Amygdala Impair the Acquisition of Cocaine-Seeking Behaviour under a Second-Order Schedule of Reinforcement." *Psychopharmacology* 127(3): 213–24. http://www.ncbi.nlm.nih.gov/pubmed/8912399.

Wickman, K D et al. 1994. "Recombinant G-Protein Beta Gamma-Subunits Activate the Muscarinic-Gated Atrial Potassium Channel." *Nature* 368(6468): 255–57. http://www.ncbi.nlm.nih.gov/pubmed/8145826.

Wilson, Charles J. 2007. "GABAergic Inhibition in the Neostriatum." *Progress in brain research* 160: 91–110. http://www.ncbi.nlm.nih.gov/pubmed/17499110.

Wilson, Stephen J, Michael A Sayette, Mauricio R Delgado, and Julie A Fiez. 2008. "Effect of Smoking Opportunity on Responses to Monetary Gain and Loss in the Caudate Nucleus." *Journal of abnormal psychology* 117(2): 428–34. http://www.ncbi.nlm.nih.gov/pubmed/18489219.

Winn, P, V J Brown, and W L Inglis. 1997. "On the Relationships between the Striatum and the Pedunculopontine Tegmental Nucleus." *Critical reviews in neurobiology* 11(4): 241–61. http://www.ncbi.nlm.nih.gov/pubmed/9336713.

Wise, R A, and P P Rompre. 1989. "Brain Dopamine and Reward." *Annual Review of Psychology* 40(1): 191–225. http://www.annualreviews.org/doi/10.1146/annurev.ps.40.020189.001203.

Wise, Roy A. 2004. "Dopamine, Learning and Motivation." *Nature Reviews Neuroscience* 5(6): 483–94. http://www.nature.com/doifinder/10.1038/nrn1406.

Wise, Roy A. 2008. "Dopamine and Reward: The Anhedonia Hypothesis 30 Years on." *Neurotoxicity Research* 14(2-3): 169–83. http://link.springer.com/10.1007/BF03033808.

Wu, Zhaofei et al. 2015. "GABAergic Projections from Lateral Hypothalamus to Paraventricular Hypothalamic Nucleus Promote Feeding." *The Journal of neuroscience : the official journal of the Society for Neuroscience* 35(8): 3312–18. http://www.ncbi.nlm.nih.gov/pubmed/25716832.

Yager, L M, A F Garcia, A M Wunsch, and S M Ferguson. 2015. "The Ins and Outs of the Striatum: Role in Drug Addiction." *Neuroscience* 301: 529–41. http://www.ncbi.nlm.nih.gov/pubmed/26116518.

Yamamoto, T, R Matsuo, Y Kiyomitsu, and R Kitamura. 1989. "Response Properties of Lateral Hypothalamic Neurons during Ingestive Behavior with Special Reference to Licking of Various Taste Solutions." *Brain research* 481(2): 286–97. http://www.ncbi.nlm.nih.gov/pubmed/2720381.

Yang, Bao-Zhu et al. 2008. "Haplotypic Variants in DRD2, ANKK1, TTC12, and NCAM1 Are Associated with Comorbid Alcohol and Drug Dependence." *Alcoholism, clinical and experimental research* 32(12): 2117–27. http://www.ncbi.nlm.nih.gov/pubmed/18828801.

Yang, X W, P Model, and N Heintz. 1997. "Homologous Recombination Based Modification in Escherichia Coli and Germline Transmission in Transgenic Mice of a Bacterial Artificial Chromosome." *Nature biotechnology* 15(9): 859–65. http://www.ncbi.nlm.nih.gov/pubmed/9306400.

Yasukawa, T, T Kita, Y Xue, and H Kita. 2004. "Rat Intralaminar Thalamic Nuclei Projections to the Globus Pallidus: A Biotinylated Dextran Amine Anterograde Tracing Study." *The Journal of comparative neurology* 471(2): 153–67. http://www.ncbi.nlm.nih.gov/pubmed/14986309.

Yin, Henry H, Barbara J Knowlton, and Bernard W Balleine. 2004. "Lesions of Dorsolateral Striatum Preserve Outcome Expectancy but Disrupt Habit Formation in Instrumental Learning." *The European journal of neuroscience* 19(1): 181–89. http://www.ncbi.nlm.nih.gov/pubmed/14750976.

in, Henry H, Barbara J Knowlton, and Bernard W Balleine. 2006. "Inactivation of Dorsolateral Striatum Enhances Sensitivity to Changes in the Action-Outcome Contingency in Instrumental Conditioning." *Behavioural brain research* 166(2): 189–96. http://www.ncbi.nlm.nih.gov/pubmed/16153716.

You, Z B, T M Tzschentke, E Brodin, and R A Wise. 1998. "Electrical Stimulation of the Prefrontal Cortex Increases Cholecystokinin, Glutamate, and Dopamine Release in the Nucleus Accumbens: An in Vivo Microdialysis Study in Freely Moving Rats." *The Journal of neuroscience : the official journal of the Society for Neuroscience* 18(16): 6492–6500. http://www.ncbi.nlm.nih.gov/pubmed/9698337.

Yuan, Tifei et al. 2013. "Expression of Cocaine-Evoked Synaptic Plasticity by GluN3A-Containing NMDA Receptors." *Neuron* 80(4): 1025–38. http://linkinghub.elsevier.com/retrieve/pii/S0896627313007095.

Yuferov, Vadim et al. 2003. "Differential Gene Expression in the Rat Caudate Putamen After 'binge' cocaine Administration: Advantage of Triplicate Microarray Analysis." *Synapse (New York, N.Y.)* 48(4): 157–69. http://www.ncbi.nlm.nih.gov/pubmed/12687634.

Zahm, D S. 2000. "An Integrative Neuroanatomical Perspective on Some Subcortical Substrates of Adaptive Responding with Emphasis on the Nucleus Accumbens." *Neuroscience and biobehavioral reviews* 24(1): 85–105. http://www.ncbi.nlm.nih.gov/pubmed/10654664.

Zahm, D S, and J S Brog. 1992. "On the Significance of Subterritories in The 'accumbens' part of the Rat Ventral Striatum." *Neuroscience* 50(4): 751–67. http://www.ncbi.nlm.nih.gov/pubmed/1448200.

Zahm, D S, E Williams, and C Wohltmann. 1996. "Ventral Striatopallidothalamic Projection: IV. Relative Involvements of Neurochemically Distinct Subterritories in the Ventral Pallidum and Adjacent Parts of the Rostroventral Forebrain." *The Journal of comparative neurology* 364(2): 340–62. http://www.ncbi.nlm.nih.gov/pubmed/8788254.

Zhou, F M, Y Liang, and J A Dani. 2001. "Endogenous Nicotinic Cholinergic Activity Regulates Dopamine Release in the Striatum." *Nature neuroscience* 4(12): 1224–29. http://www.ncbi.nlm.nih.gov/pubmed/11713470.

Zhuang, X, L Belluscio, and R Hen. 2000. "G(olf)alpha Mediates Dopamine D1 Receptor Signaling." *The Journal of neuroscience : the official journal of the Society for Neuroscience* 20(16): RC91. http://www.ncbi.nlm.nih.gov/pubmed/10924528.

Ziegler, Dana R, William E Cullinan, and James P Herman. 2002. "Distribution of Vesicular Glutamate Transporter mRNA in Rat Hypothalamus." *The Journal of comparative neurology* 448(3): 217–29. http://www.ncbi.nlm.nih.gov/pubmed/12115705.

Zubieta, J K et al. 1996. "Increased Mu Opioid Receptor Binding Detected by PET in Cocaine-Dependent Men Is Associated with Cocaine Craving." *Nature medicine* 2(11): 1225–29. http://www.ncbi.nlm.nih.gov/pubmed/8898749.

- Annexes -

NAc-D2-SPNs: mHP vs yHP

Gene	GeneDescription	FC	padj_YasRef
Abca1	ATP-binding cassette, sub-family A (ABC1), member 1	2.41	0.002
Ednrb	endothelin receptor type B	2.38	0.01
Pigf	phosphatidylinositol glycan anchor biosynthesis, class F	2.20	0.01
Megf10	multiple EGF-like-domains 10	2.16	0.01
Acer3	alkaline ceramidase 3	2.13	0.01
Mthfd2l	methylenetetrahydrofolate dehydrogenase (NADP+ dependent) 2-like	2.13	0.02
Zfp459	zinc finger protein 459	2.09	0.03
Pde3b	phosphodiesterase 3B, cGMP-inhibited	2.04	0.03
Zfp873	zinc finger protein 873	2.03	0.01
Trim59	tripartite motif-containing 59	2.02	0.01
Gm10033	predicted gene 10033	2.02	0.02
Cbln4	cerebellin 4 precursor protein	1.96	0.01
A230072C01Rik	RIKEN cDNA A230072C01 gene	1.96	0.00
Zfp758	zinc finger protein 758	1.94	0.01
Rasgrp3	RAS, guanyl releasing protein 3	1.93	0.03
Cenpw	centromere protein W	1.92	0.05
Snhg6	small nucleolar RNA host gene 6	1.90	0.03
Rian	RNA imprinted and accumulated in nucleus	1.90	0.00
BC029722	cDNA sequence BC029722	1.89	0.04
Tspan6	tetraspanin 6	1.89	0.03
Gpr165	G protein-coupled receptor 165	1.88	0.02
Gm16532	NA	1.88	0.04
March1	membrane-associated ring finger (C3HC4) 1	1.88	0.00
AU041133	expressed sequence AU041133	1.87	0.03
Ddx59	DEAD (Asp-Glu-Ala-Asp) box polypeptide 59	1.87	0.03
Uvssa	UV stimulated scaffold protein A	1.86	0.05
Plp1	proteolipid protein (myelin) 1	1.83	0.01
Tmem229a	transmembrane protein 229A	1.83	0.03
Crim1	cysteine rich transmembrane BMP regulator 1 (chordin like)	1.83	0.01
Zfp932	zinc finger protein 932	1.82	0.02
Rdx	Radixin	1.82	0.01
Kantr	Kdm5c adjacent non-coding transcript	1.81	0.02
Vps13a	vacuolar protein sorting 13A (yeast)	1.80	0.00
Epyc	Epiphycan	1.80	0.04
Zfp72	zinc finger protein 72	1.79	0.03
Tmem161b	transmembrane protein 161B	1.79	0.03
Itgbl1	integrin, beta-like 1	1.77	0.04
Mbip	MAP3K12 binding inhibitory protein 1	1.77	0.04
Lipo1	lipase, member O1	1.76	0.03
Ptprz1	protein tyrosine phosphatase, receptor type Z, polypeptide 1	1.76	0.05

Cetn4	centrin 4	1.76	0.03
Fbxo8	F-box protein 8	1.74	0.02
Arl6ip6	ADP-ribosylation factor-like 6 interacting protein 6	1.72	0.03
Tuba1a	tubulin, alpha 1°	0.58	0.01
Wdr46	WD repeat domain 46	0.58	0.03
Cry2	cryptochrome 2 (photolyase-like)	0.58	0.00
Eif2b5	eukaryotic translation initiation factor 2B, subunit 5 epsilon	0.57	0.02
Egln2	egl-9 family hypoxia-inducible factor 2	0.57	0.04
9530082P21Rik	RIKEN cDNA 9530082P21 gene	0.57	0.01
Gtpbp1	GTP binding protein 1	0.57	0.04
Agap2	ArfGAP with GTPase domain, ankyrin repeat and PH domain 2	0.57	0.04
Ogfod2	2-oxoglutarate and iron-dependent oxygenase domain containing 2	0.57	0.03
Nfya	nuclear transcription factor-Y alpha	0.56	0.03
Dnajb1	DnaJ heat shock protein family (Hsp40) member B1	0.56	0.03
Fam213b	family with sequence similarity 213, member B	0.56	0.01
Dusp26	dual specificity phosphatase 26 (putative)	0.56	0.01
Eif6	eukaryotic translation initiation factor 6	0.56	0.03
Mau2	MAU2 sister chromatid cohesion factor	0.56	0.02
Hdac5	histone deacetylase 5	0.56	0.03
Trmt61a	tRNA methyltransferase 61A	0.56	0.01
Polm	polymerase (DNA directed), mu	0.56	0.05
Cep170b	centrosomal protein 170B	0.56	0.00
Gga2	golgi associated, gamma adaptin ear containing, ARF binding protein 2	0.56	0.01
R74862	expressed sequence R74862	0.55	0.03
Usp5	ubiquitin specific peptidase 5 (isopeptidase T)	0.55	0.03
Commd9	COMM domain containing 9	0.55	0.04
Hras	Harvey rat sarcoma virus oncogene	0.55	0.02
Tars2	threonyl-tRNA synthetase 2, mitochondrial (putative)	0.55	0.05
Cct7	chaperonin containing Tcp1, subunit 7 (eta)	0.55	0.01
Ttll12	tubulin tyrosine ligase-like family, member 12	0.55	0.03
Shf	Src homology 2 domain containing F	0.55	0.04
Puf60	poly-U binding splicing factor 60	0.54	0.01
Ppp1r12c	protein phosphatase 1, regulatory (inhibitor) subunit 12C	0.54	0.00
Ftsj2	FtsJ RNA methyltransferase homolog 2 (E. coli)	0.54	0.03
Gabrd	gamma-aminobutyric acid (GABA) A receptor, subunit delta	0.54	0.03
Ubxn1	UBX domain protein 1	0.54	0.00
Ier5	immediate early response 5	0.53	0.01
Dohh	deoxyhypusine hydroxylase/monooxygenase	0.53	0.03
Micall1	microtubule associated monooxygenase, calponin and LIM domain containing -like 1	0.52	0.03
Gnl1	guanine nucleotide binding protein-like 1	0.52	0.00
Tab1	TGF-beta activated kinase 1/MAP3K7 binding protein 1	0.52	0.03
Bloc1s3	biogenesis of lysosomal organelles complex-1, subunit 3	0.51	0.03
Klhl21	kelch-like 21	0.51	0.01
Zfp622	zinc finger protein 622	0.51	0.01

Ip6k1	inositol hexaphosphate kinase 1	0.51	0.00
Nsmce1	NSE1 homolog, SMC5-SMC6 complex component	0.51	0.00
Pomt2	protein-O-mannosyltransferase 2	0.50	0.03
Dalir	DNMT1 associated long intergenic non-coding RNA	0.50	0.03
Znhit2	zinc finger, HIT domain containing 2	0.49	0.00
Mir6240	microRNA 6240	0.49	0.03
Rdh13	retinol dehydrogenase 13 (all-trans and 9-cis)	0.49	0.01
Lrrc10b	leucine rich repeat containing 10B	0.49	0.00
Map2k3	mitogen-activated protein kinase kinase 3	0.48	0.03
Pex11b	peroxisomal biogenesis factor 11 beta	0.48	0.00
Stk11	serine/threonine kinase 11	0.48	0.00
D8Ertd82e	DNA segment, Chr 8, ERATO Doi 82, expressed	0.48	0.02
Rnft2	ring finger protein, transmembrane 2	0.47	0.00
Timm50	translocase of inner mitochondrial membrane 50	0.47	0.02
Cep250	centrosomal protein 250	0.47	0.00
Ccdc88c	coiled-coil domain containing 88C	0.43	0.00

Table 2: **Genes differentially expressed in D2-SPNs-NAc. Comparison mHP vs yHP.**

Genes are ranked by FC. In blue the genes up-regulated and in orange the genes down-regulated. A total of 238 genes is differentially regulated in this comparison. Genes have been ranked by FC and only the top 100 are shown.

DS-D2-SPNs: mHP vs yHP

Gzsene	GeneDescription	FC	padj.YasRef
Fam219aos	family with sequence similarity 219, member A, opposite strand	16.37	3.26425E-17
Rn45s	45S pre-ribosomal RNA	5.11	2.11396E-08
Klhl3	kelch-like 3	4.96	8.13402E-05
Hexa	hexosaminidase A	4.91	2.47775E-07
Gan	giant axonal neuropathy	4.84	0.000211404
Mark4	MAP/microtubule affinity regulating kinase 4	4.72	1.51768E-06
Flywch1	FLYWCH-type zinc finger 1	4.56	2.12127E-05
Shank3	SH3/ankyrin domain gene 3	4.53	5.01391E-12
Elfn2	leucine rich repeat and fibronectin type III, extracellular 2	4.32	6.72258E-07
Lrrc20	leucine rich repeat containing 20	4.25	3.27268E-07
Plxnb1	plexin B1	4.16	0.001333197
Ttbk1	tau tubulin kinase 1	3.93	5.09917E-05
Mdga1	MAM domain containing glycosylphosphatidylinositol anchor 1	3.79	0.00290457
Hist1h1c	histone cluster 1, H1c	3.78	0.002545121
Nynrin	NYN domain and retroviral integrase containing	3.76	0.00299932
Syt2	synaptotagmin II	3.72	3.53229E-05
Adgrb2	adhesion G protein-coupled receptor B2	3.69	0.000224395
Gabrd	gamma-aminobutyric acid (GABA) A receptor, subunit delta	3.68	3.11338E-07
Ppp4c	protein phosphatase 4, catalytic subunit	3.68	0.000593609
Szt2	seizure threshold 2	3.67	0.00222907
Clip2	CAP-GLY domain containing linker protein 2	3.67	0.001335102
Dcaf15	DDB1 and CUL4 associated factor 15	3.64	0.004362427
Fam110a	family with sequence similarity 110, member A	3.63	0.004121029
Hdac4	histone deacetylase 4	3.62	3.98685E-05
Ppt2	palmitoyl-protein thioesterase 2	3.62	0.002476795
Diras1	DIRAS family, GTP-binding RAS-like 1	3.60	4.44554E-06

Zfp53	zinc finger protein 53	3.60	0.00350017
Tmem132a	transmembrane protein 132A	3.59	0.000502964
Sdc4	syndecan 4	3.58	0.004042935
Chrna7	cholinergic receptor, nicotinic, alpha polypeptide 7	3.56	0.003743727
Mtg2	mitochondrial ribosome associated GTPase 2	3.54	0.005362114
Mpzl1	myelin protein zero-like 1	3.54	0.004114135
Rrp9	RRP9, small subunit (SSU) processome component, homolog (yeast)	3.51	0.002540436
Arvcf	armadillo repeat gene deleted in velo-cardio-facial syndrome	3.50	0.001335102
Tmed1	transmembrane emp24 domain containing 1	3.49	0.005406983
Sptbn4	spectrin beta, non-erythrocytic 4	3.45	0.000224441
Dapk3	death-associated protein kinase 3	3.45	0.004982914
Ubb	ubiquitin B	3.43	5.62754E-05
Zfp628	zinc finger protein 628	3.39	0.004777811
Adora2a	adenosine A2a receptor	3.38	4.30641E-06
Palm	paralemmin	3.34	0.00036648
Clcn6	chloride channel, voltage-sensitive 6	3.30	0.000567585
Adam11	a disintegrin and metallopeptidase domain 11	3.27	0.00174131
Ccdc106	coiled-coil domain containing 106	3.24	0.000440033
Rnd2	Rho family GTPase 2	3.23	0.008744221
Haghl	hydroxyacylglutathione hydrolase-like	3.21	0.009816539
Evl	Ena-vasodilator stimulated phosphoprotein	3.21	5.31718E-05
Pdgfra	platelet derived growth factor receptor, alpha polypeptide	3.20	0.010221858
Alg5	asparagine-linked glycosylation 5 (dolichyl-phosphate beta-glucosyltransferase)	3.20	0.007482699
Trim25	tripartite motif-containing 25	3.20	0.011144877
Zdhhc1	zinc finger, DHHC domain containing 1	3.18	0.006942311
Hspbp1	HSPA (heat shock 70kDa) binding protein, cytoplasmic cochaperone 1	3.16	0.000295487
Slc35e4	solute carrier family 35, member E4	3.16	0.011838974
Pcnxl3	NA	3.15	5.74691E-05
Cntfr	ciliary neurotrophic factor receptor	3.14	0.008037254
Fbxl	F-box and leucine-rich repeat protein 19	3.14	0.0018667

19			36
Sept5	septin 5	3.08	3.24208E-05
Dlgap3	discs, large (Drosophila) homolog-associated protein 3	3.08	1.62951E-05
Fbxw8	F-box and WD-40 domain protein 8	3.07	0.008686492
Lars2	leucyl-tRNA synthetase, mitochondrial	3.06	0.000101477
Stub1	STIP1 homology and U-Box containing protein 1	3.06	0.014058231
Hmgxb3	HMG box domain containing 3	3.06	0.000279469
Gpr6	G protein-coupled receptor 6	3.04	0.000302502
Tspan12	tetraspanin 12	3.04	0.007915795
Arl4c	ADP-ribosylation factor-like 4C	3.03	0.003743727
Evi5l	ecotropic viral integration site 5 like	3.03	0.002479062
Ppp1ca	protein phosphatase 1, catalytic subunit, alpha isoform	3.03	0.000299358
Rpap1	RNA polymerase II associated protein 1	3.01	0.006979397
Pfkl	phosphofructokinase, liver, B-type	3.01	0.00290457
Sema6b	sema domain, transmembrane domain (TM), and cytoplasmic domain, (semaphorin) 6B	3.00	0.002700009
Slc38a10	solute carrier family 38, member 10	3.00	0.004777811
Slc22a15	solute carrier family 22 (organic anion/cation transporter), member 15	2.98	0.016288435
Scaf1	SR-related CTD-associated factor 1	2.98	0.000283471
Ints1	integrator complex subunit 1	2.96	0.000358555
Bad	BCL2-associated agonist of cell death	2.96	0.007482699
Mark2	MAP/microtubule affinity regulating kinase 2	2.96	3.3524E-05
Nat6	N-acetyltransferase 6	2.95	0.006979397
Zdhhc18	zinc finger, DHHC domain containing 18	2.94	0.002775462
Adamts20	a disintegrin-like and metallopeptidase (reprolysin type) with thrombospondin type 1 motif, 20	0.34	0.019988959
1810022K09Rik	RIKEN cDNA 1810022K09 gene	0.34	2.12127E-05
Samd15	sterile alpha motif domain containing 15	0.33	0.000171905
Smim11	small integral membrane protein 11	0.33	5.42098E-05
Ankrd44	ankyrin repeat domain 44	0.33	0.013199187
Rnf207	ring finger protein 207	0.33	0.005808285
Gbp7	guanylate binding protein 7	0.33	0.0135417

Table 3: **Genes differentially expressed in D2-SPNs-DS. Comparison mHP vs yHP.**

Genes are ranked by FC. In blue the genes up-regulated and in orange the genes down-regulated. A1139 genes are differentially regulated in this comparison. Genes have been ranked by FC and only the top 100 are shown

			37
A830011K09Rik	RIKEN cDNA A830011K09 gene	0.33	0.001363379
B830017H08Rik	RIKEN cDNA B830017H08 gene	0.33	0.014481006
3110009E18Rik	RIKEN cDNA 3110009E18 gene	0.32	0.009631735
Usp27x	ubiquitin specific peptidase 27, X chromosome	0.32	3.11338E-07
Nudt7	nudix (nucleoside diphosphate linked moiety X)-type motif 7	0.32	0.005095843
A630089N07Rik	RIKEN cDNA A630089N07 gene	0.32	0.005808285
Anxa10	annexin A10	0.32	0.01153025
Plekhf2	pleckstrin homology domain containing, family F (with FYVE domain) member 2	0.32	0.000937724
Gm5	predicted gene 5	0.31	0.010777295
Plekha2	pleckstrin homology domain-containing, family A (phosphoinositide binding specific) member 2	0.31	0.001409622
Nexn	nexilin	0.30	3.11338E-07
Arhgef28	Rho guanine nucleotide exchange factor (GEF) 28	0.29	0.002545121
Uqcrb	ubiquinol-cytochrome c reductase binding protein	0.27	4.81159E-08
Krt20	keratin 20	0.20	0.000174421
Dkk2	dickkopf WNT signaling pathway inhibitor 2	0.20	0.000127554

NAc-D1-SPNs: cCOC vs cSAL

Gene	GeneDescription	FC	padj.Sal_as_ref
Medag	mesenteric estrogen dependent adipogenesis	1.55	0.002286943
Ttc9b	tetratricopeptide repeat domain 9B	1.55	4.93731E-05
Prss12	protease, serine 12 neurotrypsin (motopsin)	1.54	4.93731E-05
Lypd6b	LY6/PLAUR domain containing 6B	1.51	0.003853639
Mapk11	mitogen-activated protein kinase 11	1.45	0.01404397
Sla	src-like adaptor	1.45	0.010026 47
Stx1a	syntaxin 1A (brain)	1.45	0.008697229
Homer2	homer scaffolding protein 2	1.42	0.010027 68
Bdnf	brain derived neurotrophic factor	1.41	0.008697229
Fkbp1b	FK506 binding protein 1b	1.41	0.016869798
Dlx1as	distal-less homeobox 1, antisense	1.41	0.030020 41
Art3	ADP-ribosyltransferase 3	1.41	0.030020 41
Nov	nephroblastoma overexpressed gene	1.41	0.016869798
Fam101b	family with sequence similarity 101, member B	1.41	0.010027 68
Etl4	enhancer trap locus 4	1.41	0.009227473
Rai14	retinoic acid induced 14	1.40	0.018838327
Nfix	nuclear factor I/X	1.40	0.018838327
Nfib	nuclear factor I/B	1.40	0.035357879
Slc30a3	solute carrier family 30 (zinc transporter), member 3	1.39	0.010027 68
Mir6236	microRNA 6236	1.38	0.044132181
Fmnl1	formin-like 1	1.37	0.018838327
Mpped1	metallophosphoesterase domain containing 1	1.36	0.008697229
S100a16	S100 calcium binding protein A16	1.34	0.030693779
3110035E14Rik	RIKEN cDNA 3110035E14 gene	1.33	0.030020 41
Mical2	microtubule associated monooxygenase, calponin and LIM domain containing 2	1.32	0.030020 41
Samd9l	sterile alpha motif domain containing 9-like	1.32	0.035357879

Hs3st2	heparan sulfate (glucosamine) 3-O-sulfotransferase 2	1.32	0.029563628
Zeb2	zinc finger E-box binding homeobox 2	1.32	0.049589542
1700001L19Rik	RIKEN cDNA 1700001L19 gene	1.31	0.038100668
Clic5	chloride intracellular channel 5	1.31	0.040591801
Etv5	ets variant 5	1.30	0.016869798
Tbr1	T-box brain gene 1	1.30	0.040399834
Dusp3	dual specificity phosphatase 3 (vaccinia virus phosphatase VH1-related)	1.29	0.000457112
1110008P14Rik	RIKEN cDNA 1110008P14 gene	1.28	0.018580153
Cobl	cordon-bleu WH2 repeat	1.28	0.047061011
Fxyd7	FXYD domain-containing ion transport regulator 7	1.28	0.029563628
Plcg1	phospholipase C, gamma 1	1.28	0.012755386
Satb2	special AT-rich sequence binding protein 2	1.28	0.019788027
Nnat	neuronatin	1.27	0.024590203
Arap2	ArfGAP with RhoGAP domain, ankyrin repeat and PH domain 2	1.26	0.049065375
Hmgcs1	3-hydroxy-3-methylglutaryl-Coenzyme A synthase 1	1.25	0.044692 78
Snapc3	small nuclear RNA activating complex, polypeptide 3	1.25	0.021887316
Htra4	HtrA serine peptidase 4	1.24	0.035357879
Ivns1abp	influenza virus NS1A binding protein	1.24	0.040399834
Rxrg	retinoid X receptor gamma	1.24	0.008942949
Rnf166	ring finger protein 166	1.24	0.019788027
Snrnp70	small nuclear ribonucleoprotein 70 (U1)	1.23	0.030693779
Hpca	hippocalcin	1.22	0.016869798
Zfhx2	zinc finger homeobox 2	1.21	0.030693779
Figf	c-fos induced growth factor	1.21	0.040399834
Mark1	MAP/microtubule affinity regulating kinase 1	1.21	0.019788027
Scmh1	sex comb on midleg homolog 1	1.19	0.048406056
Rogdi	rogdi homolog	1.19	0.030020 41
Tmsb10	thymosin, beta 10	1.19	0.042748232
Myl6	myosin, light polypeptide 6, alkali, smooth muscle and non-muscle	1.18	0.035357879
Rps15	ribosomal protein S15	1.1	0.040591

		8	801
Tubb5	tubulin, beta 5 class I	1.18	0.02565196
Glul	glutamate-ammonia ligase (glutamine synthetase)	0.83	0.029563628
Pttg1ip	pituitary tumor-transforming 1 interacting protein	0.81	0.048081035
Trank1	tetratricopeptide repeat and ankyrin repeat containing 1	0.81	0.018838327
Yipf6	Yip1 domain family, member 6	0.80	0.046757918
Clcn4-2	NA	0.80	0.04469278
Tcerg1l	transcription elongation regulator 1-like	0.80	0.01002768
Isl1	ISL1 transcription factor, LIM/homeodomain	0.79	0.030693779
M6pr	mannose-6-phosphate receptor, cation dependent	0.79	0.040399834
Ppp1r15b	protein phosphatase 1, regulatory (inhibitor) subunit 15b	0.79	0.049589542
Tmeff2	transmembrane protein with EGF-like and two follistatin-like domains 2	0.79	0.018838327
Epdr1	ependymin related protein 1 (zebrafish)	0.78	0.03002041
Cers6	ceramide synthase 6	0.78	0.046757918
Eogt	EGF domain-specific O-linked N-acetylglucosamine (GlcNAc) transferase	0.78	0.040399834
2410089E03Rik	RIKEN cDNA 2410089E03 gene	0.78	0.016869798
Tmx4	thioredoxin-related transmembrane protein 4	0.78	0.049065375
Glce	glucuronyl C5-epimerase	0.78	0.043879334
Zmat4	zinc finger, matrin type 4	0.77	0.040591801
Tmem9b	TMEM9 domain family, member B	0.77	0.030347263
Foxn3	forkhead box N3	0.77	0.042509847
Abcg1	ATP-binding cassette, sub-family G (WHITE), member 1	0.77	0.03002041
Ostm1	osteopetrosis associated transmembrane protein 1	0.77	0.030853639
Sgce	sarcoglycan, epsilon	0.77	0.026636535
Rasgrf2	RAS protein-specific guanine nucleotide-releasing factor 2	0.76	0.037132581
Fat3	FAT atypical cadherin 3	0.76	0.019788027
Cadm2	cell adhesion molecule 2	0.76	0.040591801
Lamp5	lysosomal-associated membrane protein family, member 5	0.76	0.035357879
Robo1	roundabout guidance receptor 1	0.75	0.040748312
Acvr2a	activin receptor IIA	0.75	0.037132581

Lgals8	lectin, galactose binding, soluble 8	0.75	0.047244426
Cdh4	cadherin 4	0.75	0.034275493
Apmap	adipocyte plasma membrane associated protein	0.75	0.01404397
Edil3	EGF-like repeats and discoidin I-like domains 3	0.75	0.018838327
Dock7	dedicator of cytokinesis 7	0.75	0.019788027
Pcdh19	protocadherin 19	0.75	0.019788027
Ncam2	neural cell adhesion molecule 2	0.75	0.017068437
Tspan2	tetraspanin 2	0.74	0.01002768
Dpy19l4	dpy-19-like 4 (C. elegans)	0.74	0.048406056
Atp1b2	ATPase, Na+/K+ transporting, beta 2 polypeptide	0.74	0.03002041
Fam126a	family with sequence similarity 126, member A	0.74	0.024180704
Tmem260	transmembrane protein 260	0.74	0.019788027
Lpl	lipoprotein lipase	0.74	0.003718394
Sema6a	sema domain, transmembrane domain (TM), and cytoplasmic domain, (semaphorin) 6A	0.74	0.033111974
Dab2	disabled 2, mitogen-responsive phosphoprotein	0.74	0.03002041
Gpr149	G protein-coupled receptor 149	0.74	0.045922701
Gpr101	G protein-coupled receptor 101	0.73	0.040399834
Crh	corticotropin releasing hormone	0.73	0.049065375
Ddc	dopa decarboxylase	0.73	0.044132181
Sox1	SRY (sex determining region Y)-box 1	0.73	0.001212425
Rprm	reprimo, TP53 dependent G2 arrest mediator candidate	0.73	0.018838327
Nos1	nitric oxide synthase 1, neuronal	0.73	0.002380169
Slc7a5	solute carrier family 7 (cationic amino acid transporter, y+ system), member 5	0.73	0.04469278
Adgrg1	adhesion G protein-coupled receptor G1	0.73	0.042509847
Tacr3	tachykinin receptor 3	0.73	0.035935828
Lats2	large tumor suppressor 2	0.73	0.046146269
Ell3	elongation factor RNA polymerase II-like 3	0.73	0.043891178
Zfp566	zinc finger protein 566	0.72	0.016490949
Sgcd	sarcoglycan, delta (dystrophin-associated glycoprotein)	0.72	0.046146269
Grid2	glutamate receptor, ionotropic, delta 2	0.7	0.027157

		2	627
Mrap2	melanocortin 2 receptor accessory protein 2	0.72	0.008942949
Htr4	5 hydroxytryptamine (serotonin) receptor 4	0.72	0.042509847
Ggh	gamma-glutamyl hydrolase	0.72	0.040399834
Gm5607	predicted gene 5607	0.71	0.003853639
Crtac1	cartilage acidic protein 1	0.71	0.03002041
Ret	ret proto-oncogene	0.71	0.015340045
Vimp	VCP-interacting membrane protein	0.71	0.008697229
Tmem255a	transmembrane protein 255A	0.71	0.008697229
Pcdhb13	protocadherin beta 13	0.69	0.008942949
Prkg2	protein kinase, cGMP-dependent, type II	0.69	0.008697229
Gabrg1	gamma-aminobutyric acid (GABA) A receptor, subunit gamma 1	0.69	0.004050778
Scn5a	sodium channel, voltage-gated, type V, alpha	0.69	0.01404397
Grin3a	glutamate receptor ionotropic, NMDA3A	0.69	0.00257267
Tmbim1	transmembrane BAX inhibitor motif containing 1	0.68	0.011278383
Prok2	prokineticin 2	0.68	0.012385433
Mrgpre	MAS-related GPR, member E	0.68	0.010027 68
Dock5	dedicator of cytokinesis 5	0.68	0.008697229
Mob3c	MOB kinase activator 3C	0.67	0.00125961
Pkib	protein kinase inhibitor beta, cAMP dependent, testis specific	0.67	0.008697229
Sfrp1	secreted frizzled-related protein 1	0.62	0.000457112
Prkcq	protein kinase C, theta	0.55	3.28505E-07

Table 4: **Genes differentially expressed in D1-SPNs-NAc. Comparison cCOC vs cSAL.**

Genes are ranked by FC. In blue the genes up-regulated and in orange the genes down-regulated. A total of 136 genes is differentially regulated in this comparison.

NAc-D2-SPNs: cCOC vs cSAL

Gene	GeneDescription	FC	padj.Sal_as_ref
Tmem258	transmembrane protein 258	5.89	6.00215E-05
Slc17a7	solute carrier family 17 (sodium-dependent inorganic phosphate cotransporter), member 7	4.61	0.013022793
Nr4a2	nuclear receptor subfamily 4, group A, member 2	4.22	0.003302259
Gpr6	G protein-coupled receptor 6	4.19	0.011289848
Gm10754	predicted gene 10754	4.13	6.51512E-05
Phf1	PHD finger protein 1	3.75	0.027168272
AU041133	expressed sequence AU041133	3.65	0.045636507
Ankk1	ankyrin repeat and kinase domain containing 1	3.58	0.025524648
Mphosph6	M phase phosphoprotein 6	3.57	0.025052909
Gtpbp10	GTP-binding protein 10 (putative)	3.46	0.045636507
Banf1	barrier to autointegration factor 1	3.14	0.029799287
Eny2	enhancer of yellow 2 homolog (Drosophila)	2.95	0.001839411
Tfb2m	transcription factor B2, mitochondrial	2.93	0.02434075
Adk	adenosine kinase	2.83	0.003169207
Nfyb	nuclear transcription factor-Y beta	2.68	0.037484956
A230072C01Rik	RIKEN cDNA A230072C01 gene	2.67	0.037050423
Ndufa1	NADH dehydrogenase (ubiquinone) 1 alpha subcomplex, 1	2.57	0.037050423
Nabp2	nucleic acid binding protein 2	2.57	0.003258462
Etaa1	Ewing tumor-associated antigen 1	2.54	0.049709916
Lpl	lipoprotein lipase	2.53	0.010282836
Exd2	exonuclease 3'-5' domain containing 2	2.49	0.018390888
l7Rn6	lethal, Chr 7, Rinchik 6	2.38	0.007700951
Tmem64	transmembrane protein 64	2.29	0.025052909
Atf1	activating transcription factor 1	2.23	0.025052909
Tubb2a	tubulin, beta 2A class IIA	0.48	0.011289848
Hid1	HID1 domain containing	0.48	0.045636507

Mast2	microtubule associated serine/threonine kinase 2	0.47	0.04677021
Rn45s	45S pre-ribosomal RNA	0.45	0.04136511
Tuba1b	tubulin, alpha 1B	0.44	0.034394321
Acin1	apoptotic chromatin condensation inducer 1	0.44	0.025052909
Rangap1	RAN GTPase activating protein 1	0.43	0.007700951
Zmiz2	zinc finger, MIZ-type containing 2	0.42	0.016503336
Ttbk1	tau tubulin kinase 1	0.41	0.04318843
Sf3b4	splicing factor 3b, subunit 4	0.41	0.025052909
Zranb1	zinc finger, RAN-binding domain containing 1	0.40	0.047293606
Lars2	leucyl-tRNA synthetase, mitochondrial	0.38	0.022947484
Ntng1	netrin G1	0.37	0.000824059
Mapk8ip3	mitogen-activated protein kinase 8 interacting protein 3	0.37	0.011289848
Tmem130	transmembrane protein 130	0.37	0.037050423
Prox1	prospero homeobox 1	0.35	0.011966739
Dpysl3	dihydropyrimidinase-like 3	0.35	0.006990386
Osbp	oxysterol binding protein	0.34	0.037613439
Rptor	regulatory associated protein of MTOR, complex 1	0.33	0.025052909
Gemin5	gem (nuclear organelle) associated protein 5	0.33	0.04677021
Tcf7l2	transcription factor 7 like 2, T cell specific, HMG box	0.33	6.00215E-05
Fam43a	family with sequence similarity 43, member A	0.33	0.016503336
Trf	transferrin	0.31	0.006164536
Gbf1	golgi-specific brefeldin A-resistance factor 1	0.30	8.33494E-05
Psd2	pleckstrin and Sec7 domain containing 2	0.30	0.000691819
Gna12	guanine nucleotide binding protein, alpha 12	0.29	0.037094527
Fasn	fatty acid synthase	0.29	0.006164536
Plekhg1	pleckstrin homology domain containing, family G (with RhoGef domain) member 1	0.29	0.00343472
Ddx56	DEAD (Asp-Glu-Ala-Asp) box polypeptide 56	0.27	0.022787696
Unc5b	unc-5 netrin receptor B	0.27	0.004764402
Anapc7	anaphase promoting complex subunit 7	0.26	0.001839411
Htr7	5-hydroxytryptamine (serotonin) receptor 7	0.2	0.02505290

		6	9
Plxna1	plexin A1	0.25	0.022947484
Fzd1	frizzled class receptor 1	0.25	0.022947484
Mdga1	MAM domain containing glycosylphosphatidylinositol anchor 1	0.24	0.02434075
Ret	ret proto-oncogene	0.24	0.016503336
Vwa5b2	von Willebrand factor A domain containing 5B2	0.24	0.003258462
Stk32b	serine/threonine kinase 32B	0.23	0.012397409
Lig1	ligase I, DNA, ATP-dependent	0.23	0.003169207
Pxdc1	PX domain containing 1	0.22	0.01459616
Cpne9	copine family member IX	0.22	0.013022793
Ltbp4	latent transforming growth factor beta binding protein 4	0.21	0.003399898
Adam17	a disintegrin and metallopeptidase domain 17	0.20	0.003258462
Smyd1	SET and MYND domain containing 1	0.15	0.000824059
Pcid2	PCI domain containing 2	0.14	9.71639E-05
Cbln1	cerebellin 1 precursor protein	0.13	6.00215E-05
Aard	alanine and arginine rich domain containing protein	0.12	6.00215E-05

Table 5: **Genes differentially expressed in D2-SPNs-NAc. Comparison cCOC vs cSAL.**

Genes are ranked by FC. In blue the genes up-regulated and in orange the genes down-regulated. A total of 71 genes is differentially regulated in this comparison.

PFC-D1 neurons: cCOC vs cSAL

Gene	GeneDescription	FC	padj.Sal_as_ref
Lamtor2	late endosomal/lysosomal adaptor, MAPK and MTOR activator 2	1,58	0,002521517
Fam219aos	family with sequence similarity 219, member A, opposite strand	1,47	0,02465952
Bag2	BCL2-associated athanogene 2	1,45	0,01796564
Vps72	vacuolar protein sorting 72 (yeast)	1,44	0,031045264
Dtl	denticleless E3 ubiquitin protein ligase	1,44	0,015036231
Mvd	mevalonate (diphospho) decarboxylase	1,42	0,023667547
Eif4e2	eukaryotic translation initiation factor 4E member 2	1,40	0,020998051
Gabarapl2	gamma-aminobutyric acid (GABA) A receptor-associated protein-like 2	1,39	0,02465952
Nop16	NOP16 nucleolar protein	1,37	0,031045264
Sepw1	selenoprotein W, muscle 1	1,36	0,000310082
Cebpg	CCAAT/enhancer binding protein (C/EBP), gamma	1,33	0,029458364
Srsf1	serine/arginine-rich splicing factor 1	1,33	0,010276304
Phpt1	phosphohistidine phosphatase 1	1,33	0,017025231
Eif4a2	eukaryotic translation initiation factor 4A2	1,32	0,023667547
Fubp3	far upstream element (FUSE) binding protein 3	1,31	0,048820458
Gpatch2l	G patch domain containing 2 like	1,31	0,038101141
Stx1a	syntaxin 1A (brain)	1,30	0,039684259
Fam168b	family with sequence similarity 168, member B	1,29	0,043798585
Diras1	DIRAS family, GTP-binding RAS-like 1	1,27	0,038101141
Eid1	EP300 interacting inhibitor of differentiation 1	1,24	0,038313817
Hpca	hippocalcin	0,81	0,027136366

Slc25a22	solute carrier family 25 (mitochondrial carrier, glutamate), member 22	0,80	0,048828265
Phf24	PHD finger protein 24	0,80	0,036872072
Fgf13	fibroblast growth factor 13	0,79	0,032829691
Crebbp	CREB binding protein	0,79	0,023667547
Pde4b	phosphodiesterase 4B, cAMP specific	0,79	0,049160668
Git1	G protein-coupled receptor kinase-interactor 1	0,79	0,032577826
Dgkb	diacylglycerol kinase, beta	0,79	0,03402363
Fbxl16	F-box and leucine-rich repeat protein 16	0,78	0,032577826
Ncoa6	nuclear receptor coactivator 6	0,78	0,032814611
Ablim2	actin-binding LIM protein 2	0,78	0,032829691
Vsnl1	visinin-like 1	0,78	0,044859251
Ttc7b	tetratricopeptide repeat domain 7B	0,78	0,044717358
Fam65a	family with sequence similarity 65, member A	0,78	0,032577826
Syn1	synapsin I	0,78	0,01796564
Acly	ATP citrate lyase	0,78	0,023667547
Nono	non-POU-domain-containing, octamer binding protein	0,77	0,03205232
Srcin1	SRC kinase signaling inhibitor 1	0,77	0,023667547
Nefl	neurofilament, light polypeptide	0,77	0,023667547
Dlgap2	discs, large (Drosophila) homolog-associated protein 2	0,77	0,032814611
Adrbk1	adrenergic receptor kinase, beta 1	0,76	0,019927032
H2afy	H2A histone family, member Y	0,76	0,032814611
Sowaha	sosondowah ankyrin repeat domain family member A	0,76	0,019927032
Smad3	SMAD family member 3	0,75	0,038101141

Skiv2l	superkiller viralicidic activity 2-like (S. cerevisiae)	0,75	0,032829691
Ppp1r9b	protein phosphatase 1, regulatory subunit 9B	0,75	0,032814611
Xab2	XPA binding protein 2	0,75	0,023667547
Wipf3	WAS/WASL interacting protein family, member 3	0,75	0,014638109
Jph4	junctophilin 4	0,74	0,038101141
Zfp574	zinc finger protein 574	0,74	0,02465952
Adora1	adenosine A1 receptor	0,74	0,025954243
E130309D02Rik	RIKEN cDNA E130309D02 gene	0,74	0,02465952
Cdh13	cadherin 13	0,74	0,038101141
Ube2r2	ubiquitin-conjugating enzyme E2R 2	0,73	0,01796564
Tatdn2	TatD DNase domain containing 2	0,73	0,038101141
Sh2d5	SH2 domain containing 5	0,73	0,023667547
Rnf10	ring finger protein 10	0,72	0,015036231
Pcid2	PCI domain containing 2	0,72	0,031045264
Kif5a	kinesin family member 5A	0,72	2,38145E-05
Ppp1r16b	protein phosphatase 1, regulatory (inhibitor) subunit 16B	0,71	0,01796564
Slc39a6	solute carrier family 39 (metal ion transporter), member 6	0,71	0,010276304
Xrcc3	X-ray repair complementing defective repair in Chinese hamster cells 3	0,71	0,043155519
Necab3	N-terminal EF-hand calcium binding protein 3	0,71	0,010276304
Ntng1	netrin G1	0,71	0,032814611
Ppm1d	protein phosphatase 1D magnesium-dependent, delta isoform	0,71	0,011076225
C1ql3	C1q-like 3	0,70	0,010276304
Adcy5	adenylate cyclase 5	0,70	0,023667547

Taf5l	TATA-box binding protein associated factor 5 like	0,69	0,011076225
Pura	purine rich element binding protein A	0,69	0,010276304
Dok5	docking protein 5	0,68	0,015036231
Fto	fat mass and obesity associated	0,68	0,001922995
Calcoco1	calcium binding and coiled coil domain 1	0,67	0,000310082
Sema5b	Semaphoring 5B	0,67	0,010980648
Car12	carbonic anhydrase 12	0,65	0,001199925
Snrpd3	small nuclear ribonucleoprotein D3	0,57	2,38145E-05

Table 6: Genes differentially expressed in D2-SPNs-NAc. Comparison cCOC vs cSAL.

Genes are ranked by FC. In blue the genes up-regulated and in orange the genes down-regulated. A total of 71 genes is differentially regulated in this comparison.

EJN European Journal of Neuroscience

FENS Federation of European Neuroscience Societies

European Journal of Neuroscience, Vol. 39, pp. 1234–1244, 2014 doi:10.1111/ejn.12506

TECHNICAL SPOTLIGHT
Fluorescence-activated sorting of fixed nuclei: a general method for studying nuclei from specific cell populations that preserves post-translational modifications

Lucile Marion-Poll,[1,2,3] Enrica Montalban,[1,2,3] Annie Munier,[2,4] Denis Hervé[1,2,3] and Jean-Antoine Girault[1,2,3]
[1]Inserm UMR-S 839, Paris, France
[2]Université Pierre & Marie Curie, Sorbonne Universités, Paris, France
[3]Institut du Fer à Moulin, Paris, France
[4]Cell Imaging and Flow Cytometry Facility, IFR83 Paris, France

Keywords: epigenetics, histone modifications, flow cytometry, fluorescence-activated cell sorting, formaldehyde fixation, nuclear purification

Abstract

Long-lasting brain alterations that underlie learning and memory are triggered by synaptic activity. How activity can exert long-lasting effects on neurons is a major question in neuroscience. Signalling pathways from cytoplasm to nucleus and the resulting changes in transcription and epigenetic modifications are particularly relevant in this context. However, a major difficulty in their study comes from the cellular heterogeneity of brain tissue. A promising approach is to directly purify identified nuclei. Using mouse striatum we have developed a rapid and efficient method for isolating cell type-specific nuclei from fixed adult brain (fluorescence-activated sorting of fixed nuclei; FAST-FIN). Animals are quickly perfused with a formaldehyde fixative that stops enzymatic reactions and maintains the tissue in the state it was at the time of death, including nuclear localisation of soluble proteins such as GFP and differences in nuclear size between cell types. Tissue is subsequently dissociated with a Dounce homogeniser and nuclei prepared by centrifugation in an iodixanol density gradient. The purified fixed nuclei can then be immunostained with specific antibodies and analysed or sorted by flow cytometry. Simple criteria allow distinction of neurons and non-neuronal cells. Immunolabelling and transgenic mice that express fluorescent proteins can be used to identify specific cell populations, and the nuclei from these populations can be efficiently isolated, even rare cell types such as parvalbumin-expressing interneurons. FAST-FIN allows the preservation and study of dynamic and labile post-translational protein modifications. It should be applicable to other tissues and species, and allow study of DNA and its modifications.

Introduction

In the brain, long-lasting alterations that underlie learning and memory require modifications in gene expression. Specific signalling pathways triggered by synaptic activity converge on the nucleus where they can modify gene expression and other nuclear functions (Jordan & Kreutz, 2009; Matamales & Girault, 2011). Differentiated cell phenotypes result from specific patterns of gene expression, while long-lasting changes in cellular properties involve gene transcription regulation. In addition to the interplay of numerous transcription factors, epigenetic marks, including histone and DNA modifications, as well as non-coding RNAs, play a crucial role in transcription regulation (Borrelli *et al.*, 2008; Meaney & Ferguson-Smith, 2010). Epigenetic marks are characteristic of cell types and their modifications may provide further traces of the cell history. In neurons, it has been proposed that epigenetic modifications contribute to long-lasting alterations reflecting environmental stimuli (Zhang & Meaney, 2010). All these processes can be altered in neurological and psychiatric disorders (Telese *et al.*, 2013).

Tissue heterogeneity, however, makes the study of nuclear signalling particularly challenging, as relevant changes occur only in a fraction of specific cells. Therefore it is critical to design methods to selectively study nuclei of interest. Laser capture allows microdissection of specific cell types, including, in principle, their nuclei (Cheng *et al.*, 2013), but generally yields low amounts of material. Cell-sorting has been used to recover specific neuronal or glial populations from brain tissue (Lobo *et al.*, 2006; Guez-Barber *et al.*, 2012), but this approach is limited by the difficulty and time required to dissociate adult brain, with the risk of biochemical reactions altering observed responses. A more promising approach is the direct purification of nuclei. Nuclei can be purified from post-fixed brain tissues (Herculano-Houzel & Lent, 2005; Jiang *et al.*, 2008; Collins *et al.*, 2010; Okada *et al.*, 2011; Young *et al.*, 2012). These methods do not prevent alterations before fixation, a problem particularly serious with labile modifications such as protein phosphorylation and contamination with cellular debris is very high. As commonly used fluorescent proteins can leak out of nuclei before

Correspondence: Dr J.-A. Girault, [3]Institut du Fer à Moulin, as above.
E-mail: jean-antoine.girault@inserm.fr

Received 30 October 2013, revised 2 January 2014, accepted 8 January 2014

fixation, elegant approaches using specific tagging of nuclear proteins that allows affinity-purification of nuclei (Deal & Henikoff, 2011; Steiner *et al.*, 2012) or their fluorescence-activated sorting (Jiang *et al.*, 2008; Kriaucionis & Heintz, 2009) have been recently developed. However, these methods require the production of specific transgenic lines and the proposed protocols do not fully preserve labile modifications.

To overcome these difficulties we have developed a methodology (fluorescence-activated sorting of fixed nuclei; FAST-FIN) to prepare, stain, and analyse or sort by flow cytometry specific nuclei from fixed tissue. Although we have set up this method using mouse striatum as a model tissue, it should have general applicability.

Materials and methods

Animals

We used C57Bl/6J (Janvier, Le Genest Saint Isle, France) and mutant adult male (unless otherwise indicated) mice. *Drd1*::EGFP (enhanced green fluorescent protein under the control of dopamine D1a receptor promoter) and *drd2*::EGFP transgenic mice were generated by GENSAT (Gene Expression Nervous System Atlas; Gong *et al.*, 2003) and *drd1a*::tdTomato, produced by N. Calakos, Duke University Medical Center (Shuen *et al.*, 2008) were obtained from the Jackson lab. In these latter mice the transgene is inserted into the X chromosome and in hemizigous females tdTomato is expressed in about half of the D1R-positive cells due to X chromosome inactivation. In contrast, in males all the D1R-positive cells express tdTomato. *Pvalb*::Cre mice, expressing the Cre recombinase under the control of the parvalbumin promoter (Hippenmeyer *et al.*, 2005), crossed with RCE:LoxP reporter mice expressing EGFP under the control of promoter sequences of the Rosa locus (Sousa *et al.*, 2009) were provided by Jean-Christophe Poncer, Institut du Fer à Moulin, Paris. Animals were housed in a 12-h light–dark cycle, in stable conditions of temperature, with food and water *ad libitum*. All the experiments were in accordance with the European Communities Council Directive of 24 November 1986 (86/609/EEC) and approved by the Comité d'éthique pour l'expérimentation animale Charles Darwin (Paris, France).

Drugs

Cocaine hydrochloride (Cooper, Melun, France) was dissolved in 0.9% (wt/vol) NaCl solution (saline) at 2 mg/mL and injected i.p. (10 mL/kg).

Antibodies

The primary antibodies used with their corresponding final concentrations were the following: $acH4K_5$ rabbit IgG (Merck-Millipore, Billerica MA, USA; ref. 07–327, 156 ng/mL), CNPase (Abcam; ref. ab6319; 625 ng/mL), DARPP-32 rabbit IgG (Cell Signaling, Danvers MA, USA; ref. 2306; 156 ng/mL), me_3H3K_9 rabbit IgG (Abcam, ref. ab8898; 625 ng/mL), methyl CpG binding domain protein 2 (MBD2) rabbit IgG (Sigma-Aldrich, Saint-Quentin Fallavier, France; ref. M7318; 313 ng/mL), methyl CpG-binding protein 2 (MeCP2) rabbit IgG (Sigma-Aldrich, ref. HPA001341; 625 ng/mL), NeuN mouse IgG1 (Merck-Millipore; ref. MAB377; 625 ng/mL), phospho-extracellular signal-regulated kinase (pERK) mouse IgG (Cell Signaling; ref. 5726; 313 ng/mL), phospho-mitogen- and stress-activated protein kinase 1 (pMSK1) rabbit IgG (Cell Signaling; ref. 9595; 39 ng/mL). For the study of phosphorylation, we added to all the solutions from homogenisation onwards a cocktail of five phosphatase inhibitors (Merck Millipore): imidazole, 2 mM; NaF, 1 mM; Na_2MoO_4, 1.15 mM; Na_3VO_4, 1 mM; and sodium tartrate, 4 mM. The primary isotype controls were: mouse IgG (Abcam; ref. ab37355), mouse IgG1 (Abcam; ref. ab91353) and rabbit IgG (Abcam; ref. ab37415). The secondary antibodies and their corresponding dilutions were the following: anti-rabbit allophycocyanin (APC)-conjugated (Abcam, ref. ab130805, 1 : 500) and anti-mouse phycoerythrin (PE)-conjugated (Abcam, ref. ab7003, 1 : 400). For *drd1a*::EGFP mice that express less EGFP, we incubated the nuclei with a fluorescein isothiocyanate (FITC)-conjugated anti-GFP antibody (Abcam; ref. ab6662; 625 ng/mL).

Fixation

Animals were quickly and deeply anesthetised with 500 mg/kg pentobarbital (Sanofi-Aventis, France) i.p. and perfused transcardially with 4% (wt/vol) formaldehyde in PBS (pH 7.4) at 20 mL/min at room temperature for precisely 5 min. The brain regions of interest were dissected before being dipped into the homogenisation solution which contained a formaldehyde-neutralising chemical NH_4^+ (50 mM NH_4Cl; see below), exactly 9 min after the perfusion had begun. Excess of fixation would induce more nuclei loss during homogenisation especially from neurons (which have bigger nuclei) whereas insufficient fixation would result in more protein leakage. For quantitative studies it is really critical to respect identical fixation duration for each sample.

Tissue dissociation

Cross-linked tissue was homogenised in 2-mL Dounce homogeniser (Dominique Dutscher, Brumath, France) containing 1 mL of solution (in mM: sucrose, 50; KCl, 25; $MgCl_2$, 5; NH_4Cl, 50; and Tris, pH 7.4, 120). Twenty-five strokes of pestle A (clearance 76–127 μm) followed by 25 strokes of pestle B (clearance 12–63 μm) were applied gently to avoid damage to nuclei.

Nuclei purification

The considerable amount of debris from a cross-linked dissociated tissue makes nuclei purification essential. Previous work used filtration and myelin removal beads (Collins *et al.*, 2010; Bonn *et al.*, 2012), but this resulted in a substantial loss of material. We opted for an iodixanol (Optiprep™; Sigma Aldrich) discontinuous density gradient, which yielded a very good purity nuclear fraction with little nuclei loss. For optimisation, Hoechst-stained fractions with various iodixanol concentrations were verified by observation with a fluorescence microscope. As fixed glial nuclei had a slightly lower density than fixed neuronal nuclei, any variation in the gradient could lead to a relative enrichment of one cell type vs. the other. The iodixanol gradient solutions were prepared as follows: five volumes of Optiprep containing 60% (wt/vol) iodixanol were mixed with one volume of 150 mM KCl, 30 mM $MgCl_2$ and 120 mM Tris, pH 7.4. This 50% iodixanol solution was then further diluted to make two solutions of different densities (containing 22% and 43% of iodixanol, respectively) using 250 mM sucrose, 25 mM KCl, 5 mM $MgCl_2$ and 20 mM Tris, pH 7.4, as a diluent.

After homogenisation, the solutions containing brain extracts were transferred into Eppendorf tubes to be centrifuged at 2000 ***g*** for 5 min. The supernatant was completely replaced by 1 mL of the 22% iodixanol solution and the pellet was resuspended by pipetting up and

down 15 times to ensure proper dissociation of the material. After that, a 43%–22% iodixanol gradient was prepared in centrifuge tubes compatible with swinging buckets (rotor TI-SW60; Beckman Coulter, Villepinte, France), 22% iodixanol was carefully layered onto 500 μL of the 43% iodixanol solution, and the homogenate was added on top. This preparation was centrifuged at 10 000 ***g*** for 30 min at 4 °C. Given their density the nuclei accumulate between the 22% and the 43% iodixanol layers. This interface was collected and diluted 1 : 2 with the resuspension solution [in mM: sucrose, 250; KCl, 25; $MgCl_2$, 5; and Tris, 20; with 1% (wt/vol) BSA, pH 7.4], the nuclei were collected by centrifugation at 10 000 ***g*** for 10 min and resuspended in the same solution to remove iodixanol.

Nuclear preparation for flow cytometry

For all the following steps, nuclei were kept in the resuspension solution described above, with the indicated supplements. Every time the solution had to be changed, the nuclei were collected by a 5-min centrifugation at 2000 ***g*** and resuspended thereafter (except for consecutive washes). DNA was labelled using 0.2 μg/mL Hoechst 33258 and incubated for 20 min at 4 °C. Subsequent wash was necessary as we observed that a too-strong Hoechst labelling can blur the GFP signal. For immunolabelling, nuclei were permeabilised with 0.1% (vol/vol) Triton X-100 for 10 min and the nuclear suspensions were aliquoted for incubation with different antibodies. A minimum of 5000 nuclei of the population of interest per aliquot was generally required to obtain a reliable signal. Nuclei were incubated with primary antibodies overnight at 4 °C and then washed twice before incubation with the secondary antibody (1 h) and washed twice again.

Antibody titration and isotype controls

For every sample labelling, a control experiment was carried out in parallel with a nonspecific antibody of the same isotype at the corresponding final concentration and with the secondary antibody, to reveal background fluorescence. For each primary antibody, several dilutions were tested (serial two-fold dilutions) and the final fluorescence intensity was compared to the labelling with the nonspecific isotype control. The highest specific signal with the best signal-to-noise ratio was determined and used to choose the optimal dilution.

Flow cytometry analysis

All the acquisitions were done using a MACSQuant VYB (Miltenyi Biotec, Bergisch Gladbach, Germany) flow cytometer analyser. The Hoechst fluorescence was collected with a 450/50 nm filter (405 nm laser), GFP/FITC with a 525/50 nm filter (488 nm laser), PE with a 586/15 nm filter (561 nm laser), tdTomato with a 615/20 nm filter (561 nm laser) and APC with a 661/20 nm filter (561 nm laser). For quantitative analysis of the signal, the population of interest was gated, then the mean and median intensity of fluorescence of each channel were given by the MACSQuant software (Miltenyi Biotec, Germany). The background fluorescence, given by the isotype control, was subtracted for each labelling.

Fluorescence-activated nuclei sorting

Sorting was done at the Cell Imaging and Flow Cytometry facility of the IFR83 (Paris, France). We used a Moflo XDP (Beckman Coulter) flow cytometry sorter, equipped with a 70-μm nozzle. We collected Hoechst fluorescence with a 355-nm laser and 450/60-nm filter, and GFP fluorescence with a 488-nm laser and 530/40-nm filter.

Microscopy

A DM600 fluorescence microscope (Leica) was used for image acquisition, with a 10 × objective. It was carried out at the Institut du Fer à Moulin Imaging Facility.

Results

Preparation quality and gating strategy

Most of our experiments were performed using mouse striatum as starting material. The general procedure used is summarised in Fig. 1. We first examined a scatter plot of the particles in the nuclear fraction (Fig. 2A) in which each 'event' (debris or nucleus) is plotted as a single dot whose coordinates (forward scatter and side scatter) are respectively correlated with the volume of the particle and its inner complexity. To distinguish the isolated nuclei from the various debris and aggregated nuclei we plotted the intensity of the side scatter as a function of the Hoechst DNA labelling (Fig. 2B). On this plot the population of nuclei singlets can be easily distinguished from the debris which contain no DNA and the doublets that have twice the Hoechst labelling intensity. The cloud for singlet nuclei was clearly the most visible and contained the majority of the events (Fig. 2B). Large quantities of myelin debris are generated when brain tissue is dissociated, making flow cytometry analysis difficult (Young *et al.*, 2012). This contamination could have been particularly problematic in the striatum which is crossed by numerous myelinated fibre tracts responsible for its striate appearance. Our iodixanol gradient protocol, however, allowed removal of most of the debris and clean nuclear preparations were obtained (Fig. 2B). We then plotted the area vs. the height of the peak of Hoechst signal for all the events containing DNA (Fig. 2C). This plot allowed an accurate selection of nuclei singlets. As the tissue was fixed with formaldehyde before dissociation, it could have been expected to deliver a larger proportion of nuclei multiplets, yet between 85 and 95% of the nuclei events were singlets in our protocol, as compared

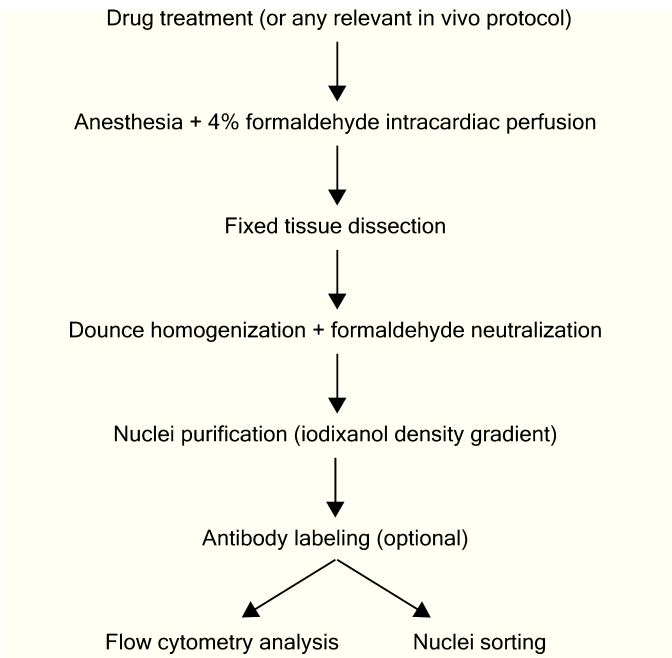

FIG. 1. Outline of the FAST-FIN procedure.

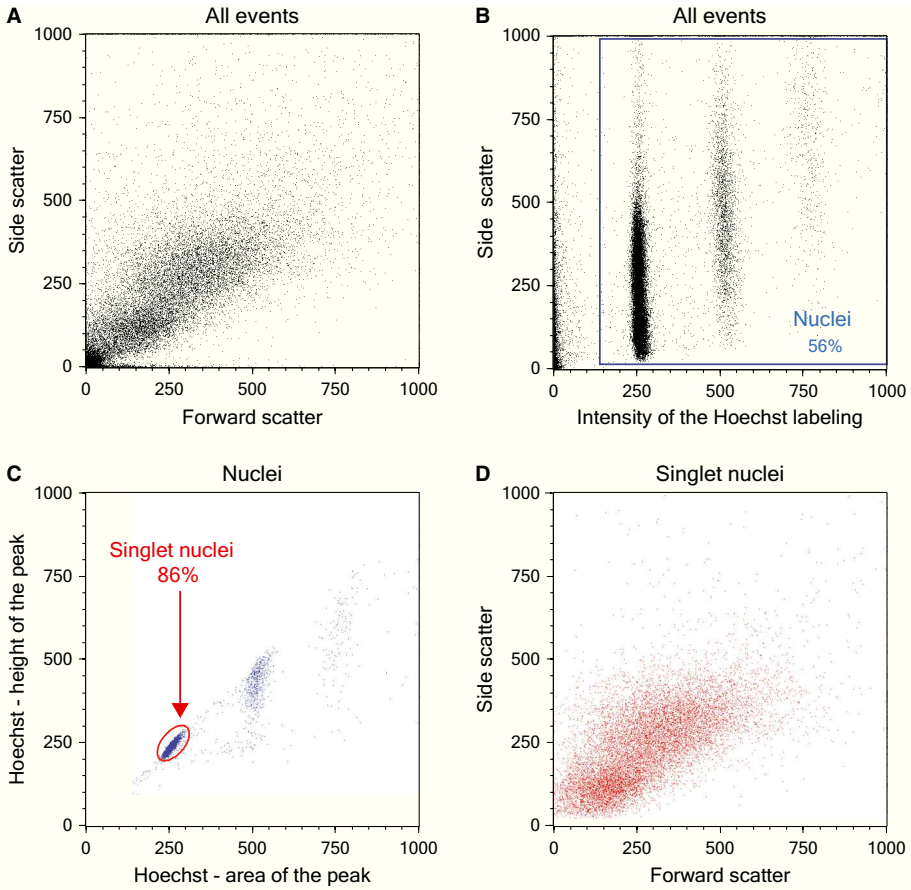

FIG. 2. Flow cytometry characterisation of purified nuclei and gating strategy. (A) Scatter dot plot (Forward Scatter, Side Scatter) of all recorded events from a nuclear preparation made with the FAST-FIN protocol. (B) Dot plot of the side scatter as a function of the Hoechst fluorescence intensity (area of the fluorescence peak), for all the events. The blue rectangle defines the events considered as Hoechst-positive (in this case 56% of total events), including nuclei singlets and multiplets. (C) Dot plot of the height of the fluorescence peak as a function of the area of the peak, for each event from the previously selected population (nuclei). Nuclei singlets are circled in red and represent in this example 86% of the total Hoechst-positive events. (D) Scatter dot plot (Forward Scatter, Side Scatter) of the nuclei singlets only.

to ~ 95% in the absence of fixation (data not shown). On the Hoechst plot (Fig. 2C), some events had twice the area and twice the height as singlets, corresponding to what is commonly considered to be cells in G2M phase, when analysing entire cells. However, sorting and observation under the microscope of these events only revealed nuclei doublets (data not shown). We then selected by gating only the singlet nuclei (Fig. 2D). We obtained ~ 1.2 million singlets from the two striata of a mouse. Comparison of the raw (Fig. 2A) and gated (Fig. 2D) plots of the same analysis shows our protocol yielded a very clean nuclei preparation. The gating strategy allowed us to perform further analysis without interference from debris or multiplets and was used for all subsequent analyses.

Neuronal and glial nuclei differ by size

When singlet nuclei from mouse striatum were shown in a scatter plot, we observed a broad distribution that could contain several populations of nuclei (Fig. 3A). To determine the position of the nuclei from various cell types in this cloud we used Neuronal Nuclei (NeuN) antibodies that react with a nuclear epitope present in most neuronal populations (Mullen *et al.*, 1992), later identified as the splicing factor Fox-3 (Kim *et al.*, 2009). NeuN labelling (Fig. 3B) revealed that non-neuronal (presumably mostly glial) cells were not more numerous than neurons in the mouse striatum, contrary to a common belief but in accordance with previous studies (Herculano-Houzel & Lent, 2005; Matamales & Girault, 2011; Jordi *et al.*, 2013). Actually, in our experiments the proportion of neuronal to non-neuronal nuclei in the mouse striatum was close to a 1 : 1 ratio with slightly more neuronal nuclei (Fig. 3C). FAST-FIN does not favour either neurons or glia, as NeuN staining performed on nuclei preparations without fixation led to similar ratios (52% of neurons; data not shown). Moreover, we observed that the population with higher scatter values consisted of neurons (NeuN+), whereas the other population was NeuN-negative (Fig. 3D). This finding was in agreement with histochemical studies showing that nuclei of striatal neurons are larger than those of glial cells (Matamales *et al.*, 2009). Furthermore, as background fluorescence was consistently lower in glial nuclei it was possible to distinguish neuronal nuclei from glial nuclei without any labelling, simply by combining scatter and background fluorescence plots (Fig. 3E and F), providing a simple means of identifying these two populations in our experimental conditions, without specific labelling.

Fixation preserved size and prevented soluble proteins from leaking out of the nucleus

FAST-FIN includes an early formaldehyde fixation by intracardiac perfusion and we optimised this essential step to prevent proteins

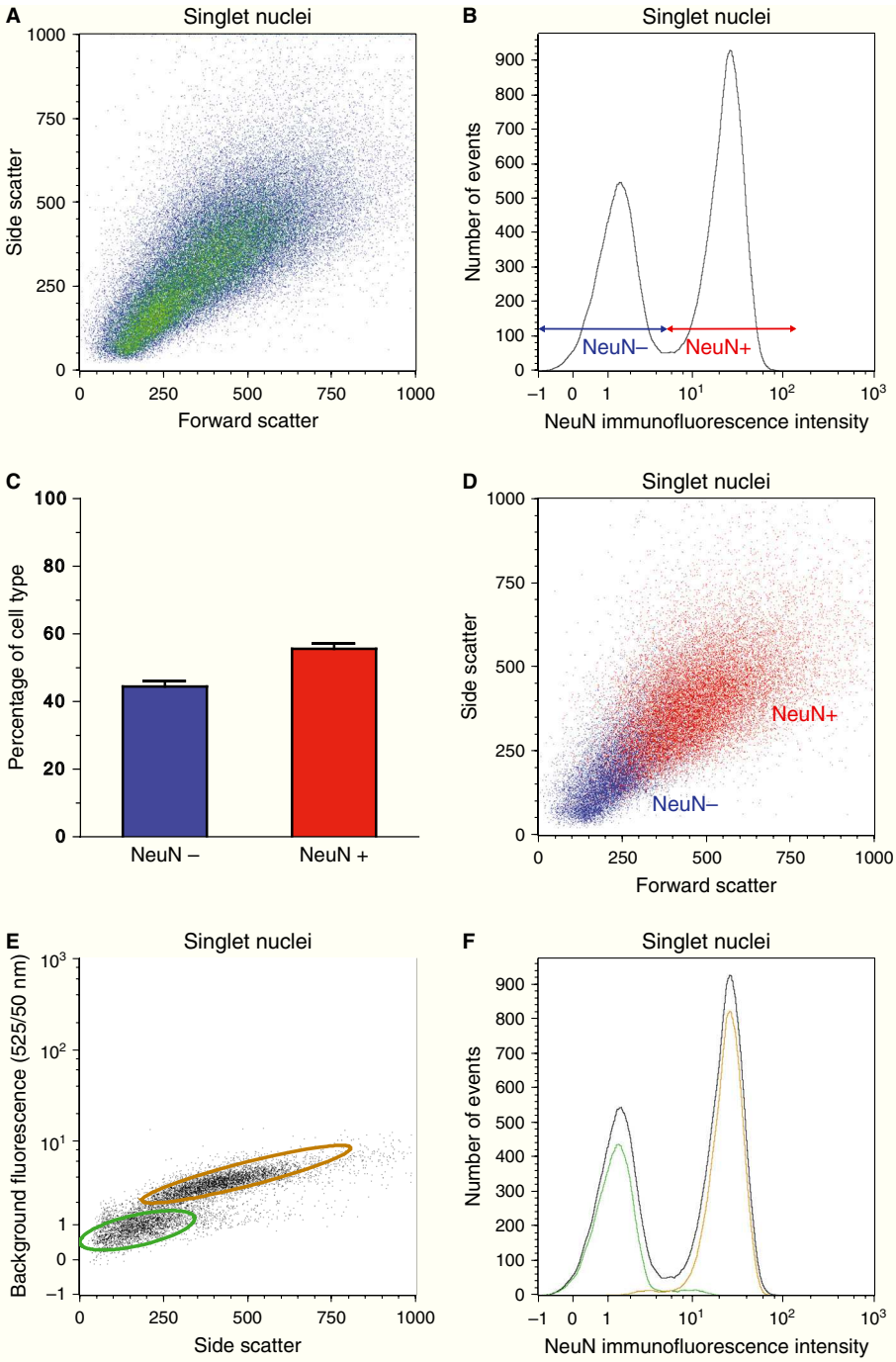

FIG. 3. Neuronal and non-neuronal nuclei differ by simple flow cytometry parameters. (A) Scatter density plot of all the singlet nuclei. Blue dots correspond to sparse events whereas green and yellow dots indicate increasingly higher densities of events. (B) Histogram of the frequencies of measured fluorescence intensity values. NeuN immunolabelling was revealed using a phycoerythrin-conjugated secondary antibody. (C) Estimate of the proportion of NeuN-positive nuclei. Data are means + SEM (n = 4 mice). (D) Scatter dot plot of the nuclei singlets, as in (A), in which NeuN-positive events are coloured in red whereas NeuN-negative events are in blue. This staining allows clear the identification of the two populations in (A). (E) Density plot of the background fluorescence (a channel with no labelling, here with a 525/50 nm filter and a 488 nm laser) as a function of the side scatter. The population with the lowest Side Scatter and background fluorescence is circled in green and the other population is circled in orange. (F) Superimposition of histograms of frequencies of measured fluorescence intensity values. NeuN labelling was revealed with a phycoerythrin-conjugated secondary antibody (as in B). All the nuclei singlets are plotted in black, whereas the two populations selected in (E) are plotted in green and orange, respectively.

from leaking out of the nucleus without preventing tissue dissociation and nuclear preparation. For example, GFP, a very commonly used protein, is present in both the nucleus and the cytoplasm when not fused to any other proteins. To test whether some GFP would remain in the nucleus without fixation and evaluate the importance of the fixation step, we carried out the same protocol with or without formaldehyde fixation, using transgenic mice which express GFP under the control of the D2R promoter (*drd2*::EGFP). In these

mice > 40% of neurons are expected to be GFP-positive (Matamales *et al.*, 2009). Without fixation we could not distinguish any GFP-positive population (Fig. 4A), whereas with fixation (Fig. 4B) we could discriminate three peaks, the most intense corresponding to GFP-positive neurons and the two others to glia and GFP-negative neurons (as identified by their background fluorescence, as shown above; see Fig. 3E). Moreover, the difference in nuclear size between neurons and glia was lost without fixation (Fig. 4C and D). Thus, unlike other approaches in which the material is not cross-linked or is cross-linked at a later stage after tissue dissociation or nuclei separation, FAST-FIN prevents leakage out of the nucleus of proteins that are not anchored to the nuclear matrix or DNA and preserves nuclear size.

Estimate of the abundance of specific subpopulations among glial or neuronal cells

We then investigated various cell populations among glia and neurons using immunolabelling. We first used 2′, 3′-cyclic nucleotide 3′-phosphodiesterase (CNPase) to identify oligodendrocytes (Braun & Barchi, 1972; Sheedlo & Sprinkle, 1983). A control with a non-immune antibody of the same isotype (isotype control) allowed in each experiment evaluation of the non-specific background fluorescence (Fig. 5A). CNPase-positive singlet nuclei displayed a low side scatter (Fig. 5B), in accordance with the above observation that glial nuclei have a lower side scatter than neurons (Fig. 3). Interestingly, the CNPase-positive events had the largest side scatter among those ascribed to non-neuronal nuclei (Fig. 5B). Based on parallel NeuN labelling we found that, in the mouse striatum, more than half of the glial nuclei were CNPase-positive and thus were derived from oligodendrocytes (Fig. 5C).

The vast majority of striatal neurons are medium-sized spiny neurons (MSNs) that are GABAergic efferent neurons (Kreitzer, 2009). To identify these neurons we used antibodies to dopamine- and cAMP-regulated phosphoprotein of 32 kDa [DARPP-32, protein phosphatase 1, regulatory (inhibitor) subunit 1B, PPP1R1B], a protein highly enriched in MSNs (Ouimet *et al.*, 1984) that shuttles between nucleus and cytoplasm (Stipanovich *et al.*, 2008). As compared to isotype control, the DARPP-32 labelling gave a specific signal (Fig. 5D and E). DARPP-32-positive singlets had a relatively large side scatter (Fig. 5E) and were included in the large nuclei population (see Fig. 3). As DARPP-32 leaks out of the nucleus in the absence of fixation as readily as GFP (our unpublished observations) the good labelling observed in our conditions

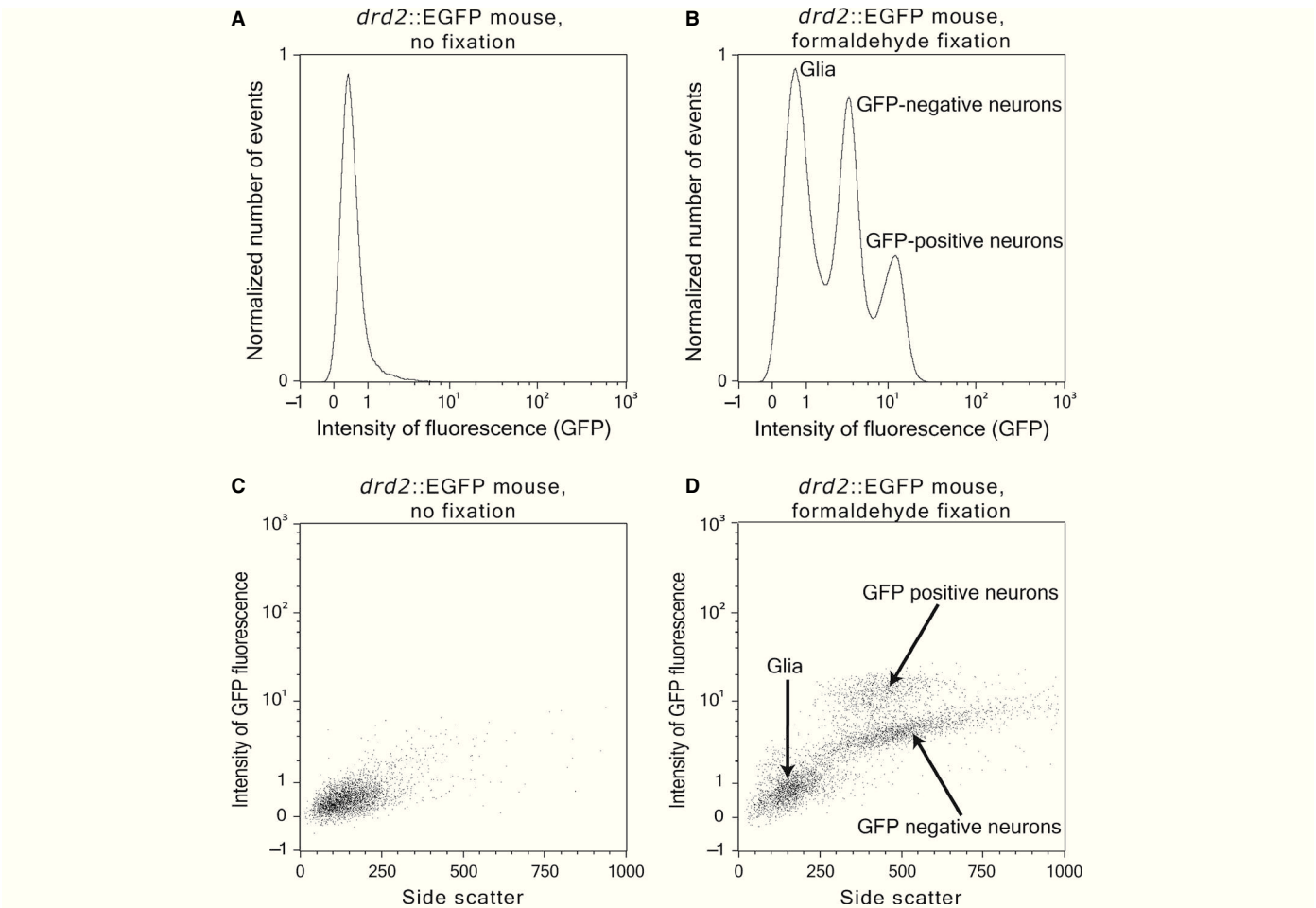

FIG. 4. Fixation preserves size and prevents soluble proteins from leaking out of the nucleus. Nuclei preparations from *drd2*::EGFP mice, without (A and C) or with (B and D) formaldehyde fixation by intracardiac perfusion. (A and B) Histograms of the frequencies of measured flurorescence intensity values (525/50 nm), normalised to the area under the curve. (C and D) Dot plots of nuclei singlets according to their side scatter and their fluorescence intensity (525/50 nm). In nuclei preparation from fixed brain tissue (B and D) it is easy to recognise distinct nuclear populations which were identified as 'glial' and 'neuronal' nuclei as in Fig. 3.

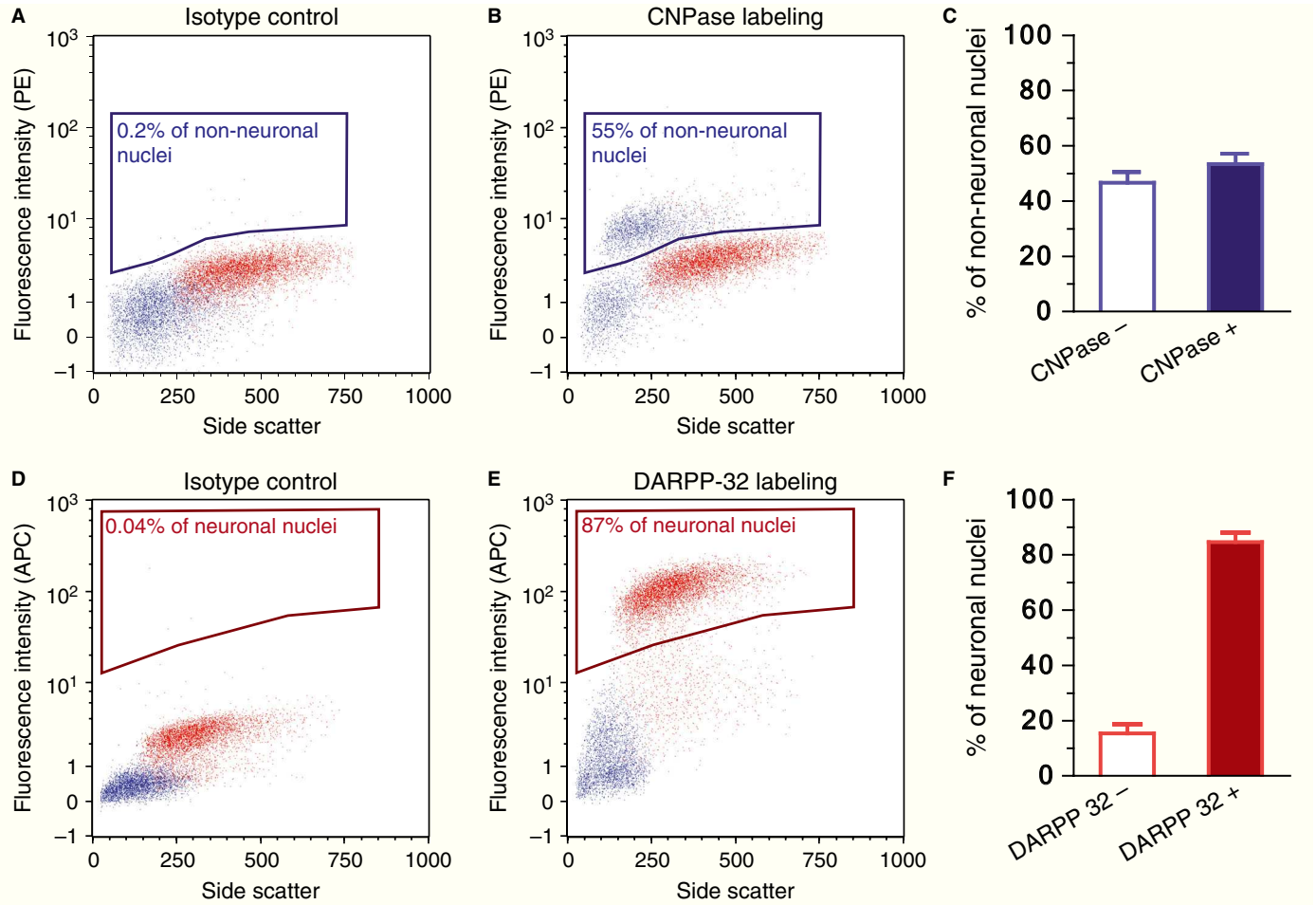

FIG. 5. Selective analysis of glial and neuronal subtypes nuclei. Dot plots of nuclei singlet events according to their side scatter and their fluorescence intensity at (A and B) 586/15 nm or (D and E) 661/20 nm. In all plots non-neuronal and neuronal nuclei were identified according to their side scatter and background fluorescence as in Fig. 3E and plotted in blue and red, respectively. (A) Labelling with a mouse IgG1 primary isotype control and a PE-conjugated secondary antibody. (B) Labelling of nuclei singlets from the same animal with a CNPase primary antibody. (C) Estimate of the proportion of CNPase-positive nuclei among non-neuronal nuclei, mean + SEM (n = 4 mice). (D) Labelling with a rabbit IgG primary isotype control and an APC-conjugated secondary antibody. (E) Labelling of nuclei singlets from the same animal, with a DARPP-32 primary antibody. (F) Estimate of the proportion of DARPP-32-positive nuclei among neuronal nuclei; mean + SEM (n = 4 mice).

demonstrates the efficacy of our fixation protocol. In our analysis 85% of the neuronal nuclei were DARPP-32-positive (Fig. 5F). Comparison of the proportion of DARPP-32-positive neuronal nuclei with FAST-FIN is compatible with the percentage observed by immunohistochemistry taking into account perikarya, as not all MSNs contain nuclear DARPP-32 (Ouimet *et al.*, 1998; Matamales *et al.*, 2009).

Selectively expressed GFP and Tomato fluorescent proteins allow distinguishing nuclei from the two types of MSNs

The dorsolateral and ventromedial regions of the striatum receive dopaminergic inputs from the substantia nigra pars compacta and the ventral tegmental area, respectively (Voorn *et al.*, 2004). MSNs are divided into two populations according to their projections and the type of dopamine receptors they express (Gerfen *et al.*, 1990). Striatonigral MSNs express dopamine D1 receptors (D1R), whereas striatopallidal MSNs express D2R. Fluorescent proteins such as GFP or Tomato are present in nuclei but in the absence of fixation leak out during nuclear preparation, as they are not fused to any resident nuclear protein. We took advantage of our protocol in which the nuclear localisation of proteins is preserved by fixation to identify the two populations of MSNs with these markers. We used transgenic mice carrying a bacterial artificial chromosome expressing EGFP under the control of either the D1R promoter (*Drd1a::*EGFP) or the D2R promoter (*Drd2::*EGFP; Gong *et al.*, 2003) or tdTomato under the control of the D1R promoter (*Drd1a*::tdTomato; Shuen *et al.*, 2008), as well as double transgenic mice (*Drd2::*EGFP × *Drd1a*::tdTomato). In wild-type mice a dot plot using emission fluorescence for EGFP (525/50 nm) and tdTomato (615/20 nm) showed the background level of fluorescence (Fig. 6A). All events were close to the diagonal, with two dot clouds corresponding to glial cells and neurons (Fig. 6A), as identified on the scatter plot (not shown). In *Drd2::*EGFP mice, a population of events with a strong signal at 525/50 nm was detected (Fig. 6B), whereas in *Drd1a*::tdTomato mice a population with a strong signal at 615/20 nm was apparent (Fig. 6C). The tdTomato-positive (Fig. 6C) and EGFP-positive (Fig. 6B) nuclei were very well separated and in double-mutant mice, carrying the two types of transgenes, the two populations could easily be identified simultaneously (Fig. 6D). Using *Drd1a::*EGFP and *Drd2::*EGFP transgenic mice, the proportions of D1R- and D2R-positive

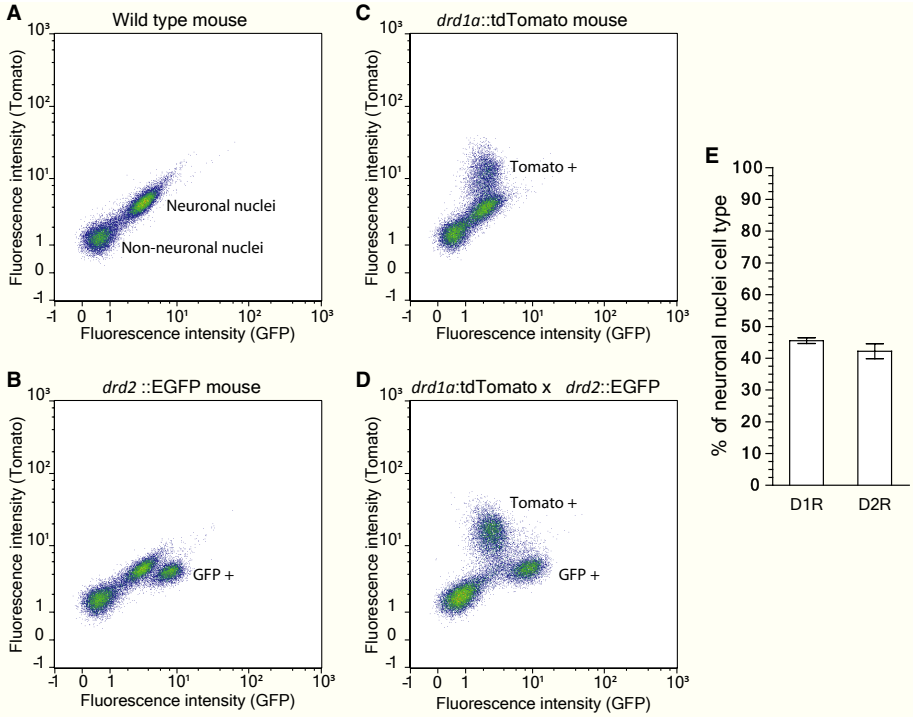

FIG. 6. Selective analysis of medium-sized spiny neuron subtypes in transgenic mice expressing EGFP and tdTomato fluorescent proteins. Density plots using emission fluorescence for EGFP (525/50 nm) and tdTomato (615/20 nm). (A) Nuclei singlets from a wild-type animal (background fluorescence). Neuronal and non-neuronal nuclei were identified as in Fig. 3E and were clearly distinguished by their background fluorescence. (B) Nuclei singlets from a *drd2*::EGFP mouse. (C) Nuclei singlets from a *drd1a*::tdTomato female mouse (see Materials and Methods for explanation of male–female differences). (D) Nuclei singlets from a *drd1a*::tdTomato *drd2*::EGFP double transgenic male mouse. (E) Proportion of EGFP-positive nuclei among neuronal nuclei from *drd1a*::EGFP mice (n = 8) and *drd2*::EGFP mice (n = 4). Data are means ± SEM.

nuclei were 46% and 42% of the neuronal nuclei, respectively (Fig. 6E), identified on side scatter vs. background fluorescence plots.

Comparison of nuclear signalling events between glial and neuronal nuclei

One of the aims of FAST-FIN being to study nuclear signalling events in specific nuclear populations, we first examined the differences between nuclei of neuronal and glial origin for a number of markers of interest. We examined two histone post-translational modifications which have been previously reported to be important in the striatum, acetylH4K5 and tri-methylH3K9, respectively associated with active and silent chromatin regions (Brami-Cherrier *et al.*, 2005; Maze *et al.*, 2010; Jordi *et al.*, 2013). These two modifications were more abundant in neuronal than in non-neuronal nuclei, with an eight-fold and a 100-fold enrichment, respectively (Fig. 7). We also examined the nuclear enrichment of two proteins, MeCP2 and MBD2, which interact with methylated DNA (Klose & Bird, 2006). The immunoreactivity for these proteins was ~ 10-fold higher in neuronal nuclei than in non-neuronal nuclei (Fig. 7). Finally we examined two phosphoproteins that have been shown to be important in nuclear signalling in striatal neurons, pERK and pMSK1 (Brami-Cherrier *et al.*, 2005; Bertran-Gonzalez *et al.*, 2008). The signals for these phosphoproteins were six- and 10-fold higher in neuronal than in non-neuronal nuclei, respectively (Fig. 7). In contrast, immunolabelling for CNPase was highly enriched in non-neuronal cells (Fig. 7). These results show that nuclear sorting allows a good preservation of post-translational modifications and a clear distinction between cell types.

Detection of signalling responses in nuclei of a specific MSN population

We then examined whether a drug-induced post-translational modification could be preserved in our experimental protocol. MSK1 is a nuclear protein kinase phosphorylated and activated by ERK in striatal nuclei following a single injection of cocaine, which mediates some of the long-lasting effects of this drug (Brami-Cherrier *et al.*, 2005; Bertran-Gonzalez *et al.*, 2008). We treated two groups of *drd1a*::GFP mice with either vehicle or 20 mg/kg cocaine 5 min before killing. The intensity of labelled nuclei in the ventral part of the striatum (the nucleus accumbens) was approximately three-fold increased in GFP-positive nuclei from cocaine-treated mice as compared to vehicle-treated controls, whereas no difference was observed in the rest of the neurons (Fig. 8). This result confirmed the applicability of FAST-FIN for studying acute signalling responses in subpopulations of nuclei.

Isolation of nuclei from a 'rare' cell population

In the striatum as in other brain regions interneurons are less numerous than principal cells and are divided in a variety of subpopulations. In spite of their relatively low number they play critical functional roles yet they are poorly studied from a biochemical or signalling standpoint due to the difficulty of isolating these cell types in sufficient numbers. We took advantage of the FAST-FIN protocol to select a subtype of nuclei from parvalbumin-expressing interneurons. We used transgenic mice that express EGFP in cells in which the parvalbumin promoter is active and purified nuclei from the striatum and hippocampus of these mice. Before sorting, only a few EGFP-positive

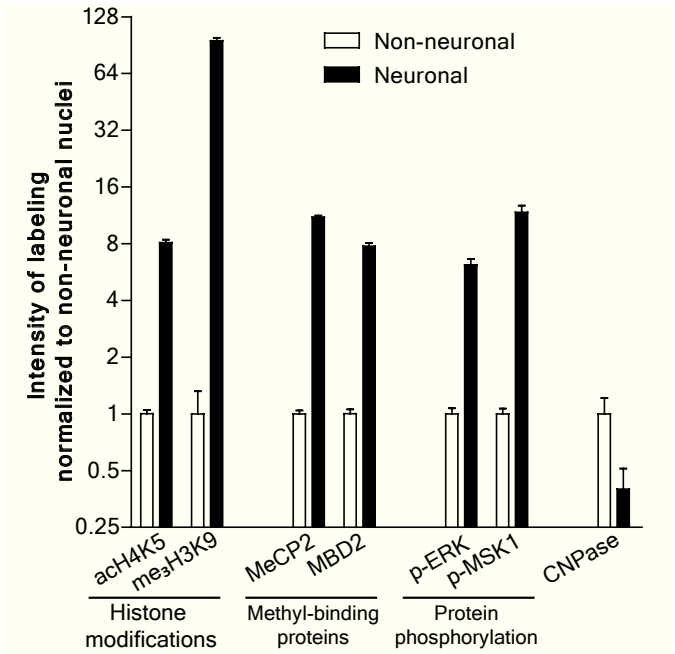

FIG. 7. Comparison of signalling markers between non-neuronal and neuronal nuclei. Flow cytometry analysis of nuclei immunostained for H4 acetyl-Lys5 (acH4K5), H3 trimethyl-Lys9 (me_3H3K9), MeCP2, MBD2, phospho-ERK1/2 (pERK) and phospho-Thr581-MSK1 (pMSK1). CNPase labelling was used as a control to show that labelling can also be stronger in non-neuronal than in neuronal nuclei. The amount of nuclear immunoreactivity was estimated as the median of the immunofluorescence intensity minus background. Neuronal and non-neuronal nuclei were identified according to their scatter plot as in Fig. 3E. Data are means + SEM plotted on a $\log_2$ scale (n = 8 mice).

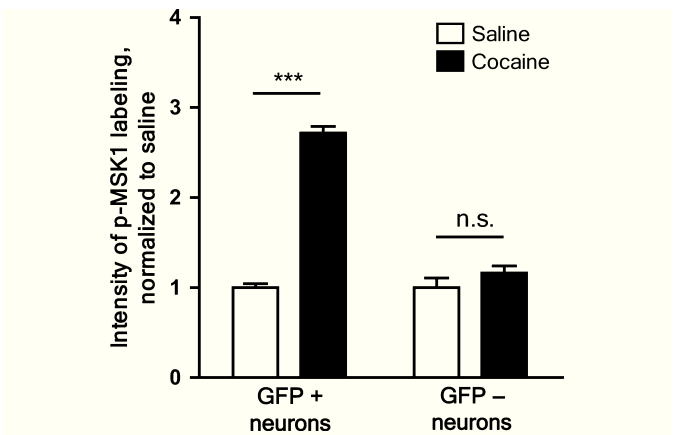

FIG. 8. Acute cocaine administration increased MSK1 phosphorylation specifically in D1R neurons of the nucleus accumbens. *drd1a*::GFP mice were injected with 20 mg/kg cocaine or vehicle, anesthetised with pentobarbital after 5 min and perfused with formaldehyde when reflexes were abolished (~ 2 min). Nucleus accumbens was dissected and nuclei preparations were labelled with phospho-Thr581-MSK1 and anti-GFP antibody. The amount of nuclear phosphoMSK1 was estimated as the geometric mean of the immunofluorescence intensity (661/20 nm, minus background) in GFP-positive and GFP-negative neuronal nuclei. Data are means + SEM of results from four saline- and three cocaine-treated mice. Two-way ANOVA: drug effect, $F_{(1,10)} = 135.5$, $P < 0.0001$; cell-type effect, $F_{(1,10)} = 92.9$, $P < 0.0001$; interaction, $F_{(1,10)} = 92.9$, $P < 0.0001$). Bonferoni *post hoc* test, ***$P < 0.001$; n.s., non-significant.

nuclei were detected among an overwhelming majority of negative nuclei (Fig. 9A). The GFP-positive nuclei corresponded to 0.6% and 1.2% of the total number of nuclei in these brain regions, respectively.

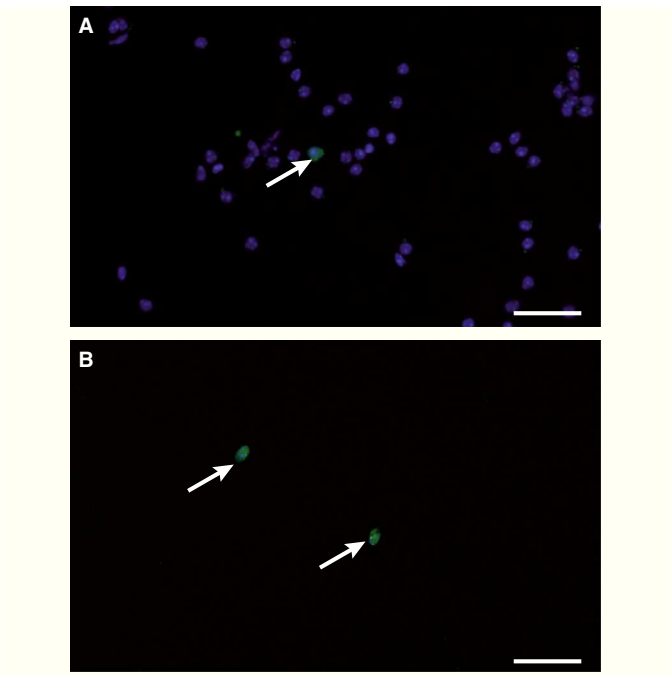

FIG. 9. Purification of nuclei from a rare striatal neuronal population, parvalbumin-expressing interneurons. Striatal nuclei from a double transgenic (*Pvalb*::Cre × RCE:LoxP) mouse, (A) before and (B) after FAST-FIN sorting gated as EGFP-positive nuclei singlets. Virtually all nuclei after sorting were EGFP-positive. Green channel, EGFP; blue channel, Hoechst. White arrows indicate EGFP-positive nuclei. Scale bars, 50 μm.

By fluorescence-activated sorting we were able to isolate ~ 5000 GFP-positive nuclei from the whole striata and ~ 10 000 from the hippocampi of one mouse. The obtained fraction contained GFP-positive nuclei singlets which appeared intact (Fig. 9B) and had a 97% purity, as determined by flow cytometry reanalysis. Thus FAST-FIN efficiently allowed purification of a rare population of neuronal nuclei from adult brain tissue.

Discussion

The FAST-FIN method proposed here allows immunolabelling and sorting of nuclei from fixed adult brain tissue. The characterisation of the obtained fractions shows that the contamination by debris is very low and that most nuclei are isolated (singlets), not attached to other nuclei (multiplets). This is very important when considering sorting by flow cytometry. The fast but not excessive fixation preserves the distinct characteristics of the nuclei, including shape, size and protein content. It is noteworthy that size and background intensity, although they are not specific by themselves, when combined allow a reliable distinction between nuclei from neuronal and non-neuronal cells with a flow cytometer, even without any labelling. Moreover, we designed the fixation and labelling steps of the FAST-FIN protocol as very similar to standard protocols extensively used in many laboratories for immunohistochemistry, which have been validated and applied to the study of numerous post-translational modifications. We were actually able to recover strong differences in histone modifications or protein phosphorylation between neurons and glia. We could also readily detect a previously characterised nuclear phosphorylation reaction in response to a pharmacological treatment, phosphorylation of MSK1 in response to cocaine (Brami-Cherrier *et al.*, 2005; Bertran-Gonzalez

et al., 2008). We were able to detect not only post-translational modifications of histones that are tightly linked to the chromatin but, importantly, also of proteins that are transiently present in the nucleus (DARPP-32, phospho-ERK1/2). Thus, FAST-FIN allows the quantitative study of very dynamic labile post-translational modifications of presumably any nuclear protein. All these characteristics distinguish the FAST-FIN protocol from previously used approaches that either did not preserve the initial state of the purified nuclei (i.e. preservation of labile proteins or post-translational modifications) and/or were too strongly fixed and highly contaminated with debris (Herculano-Houzel & Lent, 2005; Collins *et al.*, 2010; Okada *et al.*, 2011; Young *et al.*, 2012). The quality of the FAST-FIN protocol in adult mammalian brain is similar to that obtained with a different protocol adapted to drosophila embryos (Bonn *et al.*, 2012), which are, among other differences, devoid of myelin.

Recently transgenic mice have been developed that express EGFP fused to a ribosomal protein, L10a, which transiently accumulates in nucleoles before ribosomes are exported to the cytoplasm (Doyle *et al.*, 2008; Heiman *et al.*, 2008). These mice provide powerful tools for studying DNA methylation or hydroxy-methylation (Kriaucionis & Heintz, 2009), or histone post-translational modifications in specific nuclei populations (Jordi *et al.*, 2013). Similarly, EGFP-tagged histone allowed chromatin immunoprecipitation from purified nuclei (Jiang *et al.*, 2008). A limitation to these approaches is that they require the availability of the relevant transgenic mouse line. Using FAST-FIN, fluorescent proteins do not need to be fused to any resident nuclear protein and can be maintained in the nuclei during the whole process. This is a considerable advantage as it allows analysis or sorting of nuclei with the most commonly used reporter genes such as EGFP or tdTomato. We applied it to transgenic mice expressing EGFP or tdTomato under the control of promoters specific for either of the two populations of striatal MSNs. The resolution between negative and positive populations was high and resulted in proportions similar to those obtained by tissue section studies (Bertran-Gonzalez *et al.*, 2008; Matamales *et al.*, 2009). For quantitative studies, FAST-FIN allows the automatic study of all recovered nuclei in which fluorescence intensity can be quantitatively assessed, in contrast with histochemistry studies in which an arbitrary threshold is used and the number of cells counted is necessarily limited. Thus FAST-FIN quantification of a positive cell population can be faster, more accurate and more objective than microscopy. Combining fluorescent proteins with antibody labelling, we were able to separate D1R- and D2R-expressing MSNs and examine a signalling response specifically in one of these populations. We were also able to purify a rare population of neurons, parvalbumin-positive interneurons from the striatum or the hippocampus. This opens the possibility for molecular or epigenetic studies in low-abundance brain cell populations, provided a good marker is available.

A particularly interesting prospect for FAST-FIN is its possible application not only to histone post-translational modifications but also to DNA modifications which can be readily studied in fixed material. Therefore FAST-FIN is a simple method that should be useful for studying nuclear molecular markers, signalling events and epigenetic marks in specific neuronal populations, in response to physiological or chemical stimuli or in pathological conditions. In addition it should be applicable to other types of material in which it is important to identify specific nuclei populations, including in cancer. Sorting cells on simple gating parameters can already be useful but much broader applications can be envisaged based on the use of transgenic reporters and immunolabelling.

Acknowledgements

We thank Yohann Bertelle and Annie Rousseau for animal care, Mythili Savariradjane for assistance with the microscope, Patricia Gaspar for NeuN antibody and Jean-Christophe Poncer for PVCre::RCE mice, all from the Institut du Fer à Moulin. We are grateful to Paul Greengard (The Rockefeller University, New York) for initially providing the *drd1a*::EGFP and *drd2*::EGFP mice. The Cell Imaging and Flow Cytometry facility of the IFR83 (Paris, France) is supported by the Conseil Régional Ile-de-France. This work was supported by an ERC grant to J.A.G., E.M. was supported by the Marie Curie early training network N-Plast. The authors declare no competing interest.

Abbreviations

APC, allophycocyanin; CNPase, 2′,3′-cyclic-nucleotide 3′-phosphodiesterase; D1R, drd1a receptor; D2R, drd2 receptor; DARPP-32, protein phosphatase 1 regulatory subunit 1B; EGFP, enhanced green fluorescent protein; ERK, extracellular signal-regulated kinase; FAST-FIN, fluorescence activated sorting of fixed nuclei; FITC, fluorescein isothicyanate; MBD2, methyl CpG binding domain protein 2; MeCP2, methyl CpG-binding protein 2; MSK1, mitogen- and stress-activated protein kinase 1; MSN, medium-sized neuron; NeuN, neuronal nuclei (neuron-specific nuclear protein); PE, phycoerythrin.

References

Bertran-Gonzalez, J., Bosch, C., Maroteaux, M., Matamales, M., Herve, D., Valjent, E. & Girault, J.A. (2008) Opposing patterns of signaling activation in dopamine D1 and D2 receptor-expressing striatal neurons in response to cocaine and haloperidol. *J. Neurosci.*, **28**, 5671–5685.

Bonn, S., Zinzen, R.P., Perez-Gonzalez, A., Riddell, A., Gavin, A.C. & Furlong, E.E. (2012) Cell type-specific chromatin immunoprecipitation from multicellular complex samples using BiTS-ChIP. *Nat. Protoc.*, **7**, 978–994.

Borrelli, E., Nestler, E.J., Allis, C.D. & Sassone-Corsi, P. (2008) Decoding the epigenetic language of neuronal plasticity. *Neuron*, **60**, 961–974.

Brami-Cherrier, K., Valjent, E., Herve, D., Darragh, J., Corvol, J.C., Pages, C., Arthur, S.J., Girault, J.A. & Caboche, J. (2005) Parsing molecular and behavioral effects of cocaine in mitogen- and stress-activated protein kinase-1-deficient mice. *J. Neurosci.*, **25**, 11444–11454.

Braun, P.E. & Barchi, R.L. (1972) 2′,3′-cyclic nucleotide 3′-phosphodiesterase in the nervous system. Electrophoretic properties and developmental studies. *Brain Res.*, **40**, 437–444.

Cheng, L., Zhang, S., MacLennan, G.T., Williamson, S.R., Davidson, D.D., Wang, M., Jones, T.D., Lopez-Beltran, A. & Montironi, R. (2013) Laser-assisted microdissection in translational research: theory, technical considerations, and future applications. *Appl. Immunohistochem. M. M.*, **21**, 31–47.

Collins, C.E., Young, N.A., Flaherty, D.K., Airey, D.C. & Kaas, J.H. (2010) A rapid and reliable method of counting neurons and other cells in brain tissue: a comparison of flow cytometry and manual counting methods. *Front. Neuroanat.*, **4**, 5.

Deal, R.B. & Henikoff, S. (2011) The INTACT method for cell type-specific gene expression and chromatin profiling in *Arabidopsis thaliana*. *Nat. Protoc.*, **6**, 56–68.

Doyle, J.P., Dougherty, J.D., Heiman, M., Schmidt, E.F., Stevens, T.R., Ma, G., Bupp, S., Shrestha, P., Shah, R.D., Doughty, M.L., Gong, S., Greengard, P. & Heintz, N. (2008) Application of a translational profiling approach for the comparative analysis of CNS cell types. *Cell*, **135**, 749–762.

Gerfen, C.R., Engber, T.M., Mahan, L.C., Susel, Z., Chase, T.N., Monsma, F.J. Jr. & Sibley, D.R. (1990) D_1 and D_2 dopamine receptor-regulated gene expression of striatonigral and striatopallidal neurons. *Science*, **250**, 1429–1432.

Gong, S., Zheng, C., Doughty, M.L., Losos, K., Didkovsky, N., Schambra, U.B., Nowak, N.J., Joyner, A., Leblanc, G., Hatten, M.E. & Heintz, N. (2003) A gene expression atlas of the central nervous system based on bacterial artificial chromosomes. *Nature*, **425**, 917–925.

Guez-Barber, D., Fanous, S., Harvey, B.K., Zhang, Y., Lehrmann, E., Becker, K.G., Picciotto, M.R. & Hope, B.T. (2012) FACS purification of immunolabeled cell types from adult rat brain. *J. Neurosci. Meth.*, **203**, 10–18.

Heiman, M., Schaefer, A., Gong, S., Peterson, J.D., Day, M., Ramsey, K.E., Suarez-Farinas, M., Schwarz, C., Stephan, D.A., Surmeier, D.J., Greengard, P. & Heintz, N. (2008) A translational profiling approach for the molecular characterization of CNS cell types. *Cell*, **135**, 738–748.

Herculano-Houzel, S. & Lent, R. (2005) Isotropic fractionator: a simple, rapid method for the quantification of total cell and neuron numbers in the brain. *J. Neurosci.*, **25**, 2518–2521.

Hippenmeyer, S., Vrieseling, E., Sigrist, M., Portmann, T., Laengle, C., Ladle, D.R. & Arber, S. (2005) A developmental switch in the response of DRG neurons to ETS transcription factor signaling. *PLoS Biol.*, **3**, e159.

Jiang, Y., Matevossian, A., Huang, H.S., Straubhaar, J. & Akbarian, S. (2008) Isolation of neuronal chromatin from brain tissue. *BMC Neurosci.*, **9**, 42.

Jordan, B.A. & Kreutz, M.R. (2009) Nucleocytoplasmic protein shuttling: the direct route in synapse-to-nucleus signaling. *Trends Neurosci.*, **32**, 392–401.

Jordi, E., Heiman, M., Marion-Poll, L., Guermonprez, P., Cheng, S.K., Nairn, A.C., Greengard, P. & Girault, J.A. (2013) Differential effects of cocaine on histone posttranslational modifications in identified populations of striatal neurons. *Proc. Natl. Acad. Sci. USA*, **110**, 9511–9516.

Kim, K.K., Adelstein, R.S. & Kawamoto, S. (2009) Identification of neuronal nuclei (NeuN) as Fox-3, a new member of the Fox-1 gene family of splicing factors. *J. Biol. Chem.*, **284**, 31052–31061.

Klose, R.J. & Bird, A.P. (2006) Genomic DNA methylation: the mark and its mediators. *Trends Biochem. Sci.*, **31**, 89–97.

Kreitzer, A.C. (2009) Physiology and pharmacology of striatal neurons. *Annu. Rev. Neurosci.*, **32**, 127–147.

Kriaucionis, S. & Heintz, N. (2009) The nuclear DNA base 5-hydroxymethylcytosine is present in Purkinje neurons and the brain. *Science*, **324**, 929–930.

Lobo, M.K., Karsten, S.L., Gray, M., Geschwind, D.H. & Yang, X.W. (2006) FACS-array profiling of striatal projection neuron subtypes in juvenile and adult mouse brains. *Nat. Neurosci.*, **9**, 443–452.

Matamales, M. & Girault, J.A. (2011) Signaling from the cytoplasm to the nucleus in striatal medium-sized spiny neurons. *Front. Neuroanat.*, **5**, 37.

Matamales, M., Bertran-Gonzalez, J., Salomon, L., Degos, B., Deniau, J.M., Valjent, E., Herve, D. & Girault, J.A. (2009) Striatal medium-sized spiny neurons: identification by nuclear staining and study of neuronal subpopulations in BAC transgenic mice. *PLoS ONE*, **4**, e4770.

Maze, I., Covington, H.E. 3rd, Dietz, D.M., LaPlant, Q., Renthal, W., Russo, S.J., Mechanic, M., Mouzon, E., Neve, R.L., Haggarty, S.J., Ren, Y., Sampath, S.C., Hurd, Y.L., Greengard, P., Tarakhovsky, A., Schaefer, A. & Nestler, E.J. (2010) Essential role of the histone methyltransferase G9a in cocaine-induced plasticity. *Science*, **327**, 213–216.

Meaney, M.J. & Ferguson-Smith, A.C. (2010) Epigenetic regulation of the neural transcriptome: the meaning of the marks. *Nat. Neurosci.*, **13**, 1313–1318.

Mullen, R.J., Buck, C.R. & Smith, A.M. (1992) NeuN, a neuronal specific nuclear protein in vertebrates. *Development*, **116**, 201–211.

Okada, S., Saiwai, H., Kumamaru, H., Kubota, K., Harada, A., Yamaguchi, M., Iwamoto, Y. & Ohkawa, Y. (2011) Flow cytometric sorting of neuronal and glial nuclei from central nervous system tissue. *J. Cell. Physiol.*, **226**, 552–558.

Ouimet, C.C., Miller, P.E., Hemmings, H.C. Jr, Walaas, S.I. & Greengard, P. (1984) DARPP-32, a dopamine- and adenosine 3′:5′-monophosphate- regulated phosphoprotein enriched in dopamine-innervated brain regions. III Immunocytochemical localization. *J. Neurosci.*, **4**, 111–124.

Ouimet, C.C., Langley-Gullion, K.C. & Greengard, P. (1998) Quantitative immunocytochemistry of DARPP-32-expressing neurons in the rat caudatoputamen. *Brain Res.*, **808**, 8–12.

Sheedlo, H.J. & Sprinkle, T.J. (1983) The localization of 2′:3′-cyclic nucleotide 3′-phosphodiesterase in bovine cerebrum by immunofluorescence. *Brain Res.*, **288**, 330–333.

Shuen, J.A., Chen, M., Gloss, B. & Calakos, N. (2008) Drd1a-tdTomato BAC transgenic mice for simultaneous visualization of medium spiny neurons in the direct and indirect pathways of the basal ganglia. *J. Neurosci.*, **28**, 2681–2685.

Sousa, V.H., Miyoshi, G., Hjerling-Leffler, J., Karayannis, T. & Fishell, G. (2009) Characterization of Nk6–2-derived neocortical interneuron lineages. *Cereb. Cortex*, **19**(Suppl 1), i1–i10.

Steiner, F.A., Talbert, P.B., Kasinathan, S., Deal, R.B. & Henikoff, S. (2012) Cell-type-specific nuclei purification from whole animals for genome-wide expression and chromatin profiling. *Genome Res.*, **22**, 766–777.

Stipanovich, A., Valjent, E., Matamales, M., Nishi, A., Ahn, J.H., Maroteaux, M., Bertran-Gonzalez, J., Brami-Cherrier, K., Enslen, H., Corbille, A.G., Filhol, O., Nairn, A.C., Greengard, P., Herve, D. & Girault, J.A. (2008) A phosphatase cascade by which rewarding stimuli control nucleosomal response. *Nature*, **453**, 879–884.

Telese, F., Gamliel, A., Skowronska-Krawczyk, D., Garcia-Bassets, I. & Rosenfeld, M.G. (2013) "Seq-ing" insights into the epigenetics of neuronal gene regulation. *Neuron*, **77**, 606–623.

Voorn, P., Vanderschuren, L.J., Groenewegen, H.J., Robbins, T.W. & Pennartz, C.M. (2004) Putting a spin on the dorsal-ventral divide of the striatum. *Trends Neurosci.*, **27**, 468–474.

Young, N.A., Flaherty, D.K., Airey, D.C., Varlan, P., Aworunse, F., Kaas, J.H. & Collins, C.E. (2012) Use of flow cytometry for high-throughput cell population estimates in brain tissue. *Front. Neuroanat.*, **6**, 27.

Zhang, T.Y. & Meaney, M.J. (2010) Epigenetics and the environmental regulation of the genome and its function. *Annu. Rev. Psychol.*, **61**, 439–466. C431–433.